

2021

The role of autophagy in protecting periodontium integrity, and lipopolysaccharide-induced osteoclast differentiation

Grayson, Portia

<http://hdl.handle.net/10026.1/18188>

<http://dx.doi.org/10.24382/360>

University of Plymouth

All content in PEARL is protected by copyright law. Author manuscripts are made available in accordance with publisher policies. Please cite only the published version using the details provided on the item record or document. In the absence of an open licence (e.g. Creative Commons), permissions for further reuse of content should be sought from the publisher or author.

Copyright Statement

This copy of the thesis has been supplied on condition that anyone who consults it is understood to recognise that its copyright rests with its author and that no quotation from the thesis and no information derived from it may be published without the author's prior consent.



UNIVERSITY OF PLYMOUTH

THE ROLE OF AUTOPHAGY IN PROTECTING PERIODONTIUM INTEGRITY,
AND LIPOPOLYSACCHARIDE-INDUCED OSTEOCLAST DIFFERENTIATION

by

PORTIA GRAYSON

A thesis submitted to the University of Plymouth
in partial fulfilment for the degree of

DOCTOR OF PHILOSOPHY

School of Medicine and Dentistry

October 2021

Acknowledgments

I would like to thank my supervisory team, Dr Bing Hu, Professor Christopher Tredwin and Dr Louise Belfield. My sincere thanks also go to the collaborators for this project; Professor Kai Yang from Capital Medical University carried out the rat tooth movement experiment and provided me with FFPE samples for this work. Special thanks to Dr Yan Gao for all her help with the tooth movement paper, and to Ms Charlotte Illsley for carrying out some immunofluorescence staining for this project. Thanks also to Professor Stefan Scheming of Lund University who provided me with the human bone marrow cells which were essential for this work, and to Professor Alexander Zambon of the University of California for providing the Ki67 Fucci viral reporter system. My thanks also go to Professor Herbert Shea & Dr Alexander Poulin from École Polytechnique Fédérale de Lausanne for providing the cell stretching model and allowing me the opportunity to visit and work in their laboratory which was a valuable experience in my education.

I want to thank my fellow group members Jemma Walker, Donald Singer, Jon Davies, Chloe Bolton, Charlotte Illsley, Tulay Gulsen, Wai Ling Kok, Tracey Edwards, Yan Gao and Yuying Liu.

Special thanks to Jemma Walker and Tristan Maddick for painstakingly reading through drafts of this thesis. Last but not least I would like to thank my Grayson and Maddick family, especially my husband, parents and sister for supporting me in everything I do.

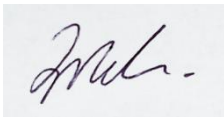
Author's Declaration

At no time during the registration for the degree of *Doctor of Philosophy* has the author been registered for any other University award without prior agreement of the Doctoral College Quality Sub-Committee.

Work submitted for this research degree at the University of Plymouth has not formed part of any other degree either at the University of Plymouth or at another establishment.

Word count of main body of thesis: 72,376

Signed:

A rectangular box containing a handwritten signature in black ink. The signature is cursive and appears to be 'M. L.' followed by a horizontal line.

Date: 21.10.2021

i. Abstract

The periodontium is a dynamic tissue that undergoes constant remodelling to maintain its structure and function. There is much evidence in the literature that autophagy can be activated by both mechanical stretching and inflammation, however the mechanisms involved are highly context dependant. Autophagy may also be important for bone remodelling in the oral cavity. Two scenarios where bone remodelling is key to the physiological outcome are orthodontic tooth movement and inflammatory-induced periodontal disease. This thesis aims to investigate the hypothesis that autophagy is involved in bone remodelling during orthodontic tooth movement and periodontal disease.

While the stem cells concerned in both osteogenesis and osteoclastogenesis are different, they both originate from the bone marrow, therefore the same primary human bone marrow cells containing the specific stem cell populations required for osteogenesis or osteoclastogenesis were used to establish *in vitro* models for mechanical strain and chronic inflammation, and the activation and differentiation of these bone marrow derived cells were analysed in response to the conditions created in these model systems.

Orthodontic tooth movement invokes constant mechanical force onto the periodontium, with tensile stretching force initiating osteogenesis. Mechanical strain is also linked to an increase in autophagy, a cellular degradation pathway that may be protective or can result in cell death.

The hypothesis was that cells exposed to tensile strain undergo an altered state of autophagic flux which contributes to osteogenesis. *In vivo* and *in vitro* models of tooth movement were used to analyse osteogenic and autophagy marker expression. Initially tensile strain was found to increase autophagy but decrease expression of osteogenic markers. However, by 24 hours there was a decrease in autophagy and osteogenesis marker expression was increased. Artificially activating autophagy in cells undergoing mechanical stretching resulted in enhanced Runt-

related transcription factor 2 (RUNX2) expression, a marker of osteogenic differentiation. Autophagy activation is perhaps a protective mechanism as an initial response to mechanical strain, after which osteogenesis may occur.

Patients undergoing orthodontic treatment are at risk of developing periodontitis, a chronic inflammatory disease caused by the presence of Gram-negative bacteria leading to inflammation of the periodontium. It is also clear that disease susceptibility and progression are affected by host factors, however the mechanisms behind this are unknown. Lipopolysaccharide (LPS) tolerance has been demonstrated in many chronic inflammatory diseases and may alleviate or exacerbate disease, but its role in periodontitis is not fully established. The hypothesis was that periodontitis results in LPS tolerance which affects osteoclastogenesis. Hyaluronan (HA) signalling was explored as a potential mechanism, as HA synthesis is upregulated in chronic inflammation. This thesis demonstrates that inflammatory monocytes increase HA synthesis in response to LPS, and that HA enhances differentiation of osteoclast precursors. However, LPS tolerance of inflammatory monocytes resulted in a rapid reduction in HA synthesis, which may be autophagy-dependant. This reduction in HA synthesis resulted in a reduction in osteoclast differentiation, which may explain why periodontal disease associated alveolar bone loss does not always occur to the same severity in different patients.

In conclusion, autophagy was found to have roles in the regulation of osteogenesis and osteoclastogenesis under tensile strain and chronic inflammation, respectively, and therefore may be an appropriate future target for pharmaceutical intervention.

Contents

Copyright Statement.....	1
Acknowledgments.....	3
Author’s Declaration.....	4
i. Abstract.....	5
ii. Abbreviations.....	12
iii. List of Tables.....	16
iv. List of Figures.....	17
1 Chapter 1: Literature Review.....	20
1.1 Overview.....	20
1.2 The Periodontium.....	21
1.2.1 Structure & Development.....	21
1.2.2 Remodelling.....	24
1.3 Cell Fate Determination.....	25
1.3.1 Mesenchymal Stem Cells.....	25
1.3.2 Osteogenesis.....	28
1.3.3 Haematopoietic Stem Cells.....	32
1.3.4 Osteoclastogenesis.....	36
1.4 Factors affecting Bone Remodelling.....	40
1.4.1 Mechanical Strain.....	41
1.4.2 Periodontitis.....	51
1.5 Autophagy.....	70

1.5.1	The Autophagy Pathway.....	70
1.5.2	Autophagy & Bone Remodelling	73
1.6	Aims	77
2	Chapter 2: Materials & Methods.....	80
2.1	Cell Culture	80
2.1.1	Maintenance.....	80
2.1.2	Osteogenesis Induction	81
2.1.3	Viral Infection	81
2.1.4	Cell Stretching.....	81
2.1.5	Cell Sorting.....	82
2.1.6	Osteoclastogenesis Induction.....	83
2.1.7	LPS Tolerance.....	83
2.2	RNA Analysis.....	84
2.2.1	RNA Extraction & Quantification	84
2.2.2	Reverse Transcription.....	85
2.2.3	Q-PCR.....	85
2.3	Protein Analysis	87
2.3.1	Protein Extraction & Quantification	87
2.3.2	Western Blotting.....	87
2.3.3	Flow Cytometry	89
2.3.4	Enzyme-Linked Immunosorbent Assay (ELISA)	91
2.3.5	Cell Fixation	92
2.3.6	Immunofluorescence.....	93

2.3.7	Tartrate-Resistant Acid Phosphatase (TRAP) Staining	96
2.4	<i>In vivo</i> Sample Processing & Analysis	97
2.4.1	Rat Tooth Movement Samples	97
2.4.2	H&E Staining.....	98
2.4.3	Immunofluorescence	98
3	Chapter 3: The role of Autophagy in the Periodontium during Experimental Orthodontic Tooth Movement	101
3.1	Introduction	101
3.2	Results.....	102
3.2.1	Tooth Movement <i>In Vivo</i>	102
3.2.2	Optimising an <i>In Vitro</i> Cell Stretching Model.....	109
3.2.3	Human Bone Marrow Cell Characterisation	124
3.2.4	Tooth Movement <i>In Vitro</i>	128
3.2.5	Autophagy Modulation using an <i>In Vitro</i> Stretching Model	132
4	Chapter 4: The Association of Autophagy with Osteoclastogenesis	137
4.1	Introduction	137
4.2	Results.....	138
4.2.1	Characterising hBMCs as cells capable of Osteoclast Differentiation	138
4.2.2	Determining the effects of LPS on Osteoclast Differentiation.....	139
4.2.3	LPS Tolerance	142
4.2.4	Determining the effects of Hyaluronan on the Differentiation of Osteoclast Precursors	155

4.2.5	Determining the effects of LPS and Hyaluronan treatment on the Differentiation of Osteoclast Precursors.....	157
4.2.6	Co-culturing Inflammatory Monocytes and Osteoclast Precursors	159
4.2.7	Determining the capability of THP1s to Differentiate to Osteoclasts in this Model 161	
5	Chapter 5: Discussion & Conclusions.....	163
5.1	Discussion	163
5.2	The role of Autophagy in the Periodontium during Experimental Orthodontic Tooth Movement	165
5.2.1	Tooth Movement <i>In Vivo</i>	165
5.2.2	Optimising an <i>In Vitro</i> Cell Stretching Model	171
5.2.3	Human Bone Marrow Cell Characterisation.....	172
5.2.4	Cell Stretching as an <i>In Vitro</i> Model of Tooth Movement.....	175
5.2.5	Future Work.....	183
5.3	The Association of Autophagy with Osteoclastogenesis in the Context of Periodontitis 186	
5.3.1	Characterising hBMCs as cells capable of Osteoclast Differentiation.....	186
5.3.2	Determining the effects of LPS on Osteoclast Differentiation	188
5.3.3	LPS Tolerance.....	189
5.3.4	Determining the effect of Hyaluronan on the Differentiation of Osteoclast Precursors.....	197
5.3.5	Determining the effects of LPS and Hyaluronan treatment on the Differentiation of Osteoclast Precursors.....	198
5.3.6	Co-culturing Inflammatory Monocytes and Osteoclast Precursors	199

5.3.7	Future Work	200
5.4	Concluding Remarks.....	203
6	References	205

ii. Abbreviations

Abbreviation	Definition
μM	Micro-molar
1x	Single exposure to LPS
2x	Multiple exposure to LPS
A20	Tumour necrosis factor alpha-induced protein 3
AMPK	AMP-activated protein kinase
AP-1	Activator protein 1
ATF4	Activating transcription factor 4
ATG3	Autophagy-related 3
ATG4B	Autophagy-related 4B
ATG5	Autophagy-related 5
ATG7	Autophagy-related 7
ATG10	Autophagy-related 10
ATG12	Autophagy-related 12
ATG13	Autophagy-related 13
ATG16L1	Autophagy-related 16 like 1
B220	Spice isoform of tyrosine phosphatase CD45
BCA	Bicinchoninic acid
BMP	Bone morphogenic protein
BSA	Bovine serum albumin
C3a	Complement component 3a
CD4	Cluster of differentiation 4
CD8	Cluster of differentiation 8
CD14	Cluster of differentiation 14
CD16	Cluster of differentiation 16
CD19	Cluster of differentiation 19
CD29	Cluster of differentiation 29
CD38	Cluster of differentiation 38
CD44	Cluster of differentiation 44
CD45	Cluster of differentiation 45
CD73	Cluster of differentiation 73
CD90	Cluster of differentiation 90
CD105	Cluster of differentiation 105
CD106	Cluster of differentiation 106
CD146	Cluster of differentiation 146
CD166	Cluster of differentiation 166
cDNA	Cellular deoxyribonucleic acid
C-FMS	Colony stimulating factor 1 receptor
cKit	KIT proto-oncogene receptor tyrosine kinase
Ct	Cycle threshold
DEPC	Diethyl pyricarbonate
Dlx5	Distal-less homeobox 5
DMEM	Dulbecco modified eagle's medium
DMEM-F12	Dulbecco modified eagle's medium/F12
DMP1	Dentin matrix acidic phosphoprotein 1

DMSO	Dimethyl sulfoxide
DNA	Deoxyribonucleic acid
<i>E.coli</i>	<i>Escherichia coli</i>
ECL	Enhanced chemiluminescence
EDTA	Ethylenediaminetetraacetic acid
ELISA	Enzyme-linked immunosorbent assay
ERK	Extracellular signal-related kinase
FAK	Protein tyrosine kinase 2
FBS	Foetal bovine serum
FFPE	Formalin fixed paraffin embedded
FGF	Fibroblast growth factor
FGFR2	Fibroblast growth factor receptor 2
FGFR3	Fibroblast growth factor receptor 3
FGF18	Fibroblast growth factor 18
FIP200	FAK family kinase-interacting protein of 200kDa
FOS	Fos proto-oncogene
GAPDH	Glyceraldehyde 3-phosphate dehydrogenase
GM-CSF	Granulocyte macrophage colony stimulating factor
H&E	Haematoxylin & eosin
HA	Hyaluronan
HARE	Hyaluronan receptor for endocytosis
HAS1	Hyaluronan synthase 1
HAS2	Hyaluronan synthase 2
HAS3	Hyaluronan synthase 3
hBMC	Human bone marrow cells
HBSS	Hank's balanced salt solution
HCl	Hydrochloric acid
HMW	High molecular weight
HOPs	Homotypic fusion and protein sorting
HRP	Horseshoe peroxidase
HSC	Haematopoietic stem cell
IF	Immunofluorescence
IFN γ	Interferon gamma
IFN β	Interferon beta
IGF1	Insulin-like growth factor 1
IgG	Immunoglobulin G
IgM	Immunoglobulin M
Ihh	Indian hedgehog
IL1 β	Interleukin 1 beta
IL4	Interleukin 4
IL6	Interleukin 6
IL8	Interleukin 8
IL10	Interleukin 10
IL12	Interleukin 12
IL13	Interleukin 13
IRAK-M	IL-1R-associated kinase-M
IRF3	Interferon regulatory factor 3
IRF5	Interferon regulatory factor 5

ISCT	International Society for Cellular Therapy
kDa	Kilodalton
Kdo	3-deoxy-D- <i>manno</i> -oct-2-ulosonic acid
LAMP1	Lysosomal-associated membrane protein 1
LBP	LPS binding protein
LC3	Microtubule-associated protein 1 light chain 3
LMW	Low molecular weight
LPS	Lipopolysaccharide
LRP5	LDL receptor related protein 5
M1	Classically activated macrophages
M2	Alternatively activated macrophages
MAC-1	Macrophage-1 antigen
MACS	Magnetic-activated cell sorting
MCP1	Monocyte chemoattractant protein 1
M-CSF	Macrophage colony-stimulating factor
MD2	Myeloid differentiation factor 2
Mef2	Myocyte enhancer factor-2
MES	2-(N-morpholino)ethanesulphonic acid
MOPS	3-(N-morpholino)propanesulfonic acid
Mreg	Regulatory macrophages
MSC	Mesenchymal stem cell
mTOR	Mammalian target of rapamycin
MyD88	Myeloid differentiation primary response gene 88
NCBI	National centre for biotechnology information
NFATC1	Nuclear factor of activated T Cells 1
NF- κ B	Nuclear factor kappa light chain enhancer of activated B cells
nM	Nanomolar
OCT	Optimal cutting temperature compound
OCT4	Octamer-binding transcription factor 4
OPG	Osteoprotegerin
OPGL	Osteoprotegerin ligand
Osx	Osterix
<i>P.gingivalis</i>	<i>Porphyromonas gingivalis</i>
p62	Protein 62
PAMPs	Pathogen associated molecular patterns
PBS	Phosphate buffered saline
PBS-T	Phosphate buffered saline & triton
PDL	Periodontal ligament
PDLSC	Periodontal ligament stem cell
PDMS	Polydimethylsiloxane
PE	Phosphatidylethanolamine
Pen-Strep	Penicillin-streptomycin-antimycotic
PFA	Paraformaldehyde
PI3K	Phosphoinositide 3-kinase
PIP2	Phosphatidylinositol 4,5-bisphosphate
PIP3	Phosphatidylinositol (3,4,5)-trisphosphate
PMA	Phorbol 12-myristate 13-acetate
PPAR γ	Peroxisome proliferator-activated receptor gamma

PVDF	Polyvinylidene fluoride
Q-PCR	Quantitative polymerase chain reaction
RAB7	Ras-related protein Rab 7
RANK	Receptor activator of nuclear factor kappa-B
RANKL	Receptor activator of nuclear factor kappa-B ligand
Ras	Ras proto-oncogene
RELM α	Resistin-like molecular alpha
RHAMM	Receptor for hyaluronan-mediated motility
RNA	Ribonucleic acid
RPMI	Roswell park memorial institute medium
RT-PCR	Reverse transcription polymerase chain reaction
RUNX2	Runt-related transcription factor 2
SARM	Sterile α and HEAT-armadillo motifs-containing protein
Sca-1	Stem cells antigen-1
SHIP-1	SH-2 containing inositol 5' polyphosphatase 1
Shn-3	Ethylene-responsive transcription factor SHINE 3
SLAM	Signalling lymphocyte activation molecule
SNARE	Soluble N-ethylmaleimide-sensitive factor activating protein receptor
SOCS-1	Suppressor of cytokine signalling 1
SOX2	Sry-box 2
SOX9	Sry-box 9
Stat1	Signal transducer and activator of transcription 1
TGF β	Transforming growth factor beta
THP1	Acute monocyte leukemic human cell line
TIR	Toll-interleukin 1
TIRAP	TIR domain-containing adaptor protein
TLR2	Toll-like receptor 2
TLR4	Toll-like receptor 4
TMB	3,3',5,5'-Tetramethylbenzidine
TNF α	Tumour necrosis factor alpha
Tollip	Toll-interacting protein
TRAF3	TNF receptor-associated factor 3
TRAF6	TNF receptor-associated factor 6
TRAM	TRIF-related adaptor molecule
TRAP	Tartrate-resistant acid phosphatase
TRIF	TIR domain-containing adaptor inducing IFN β
vegf	Transient Receptor Potential
TRPM7	Transient Receptor Potential Melastatin 7
Twist1/2	Twist-related protein 1/2
UCSC	University of California Santa Cruz
ULK1	Unc-51 like autophagy activating kinase
VEGF	Vascular endothelial growth factor
WWP1	WW domain containing protein 1

iii. List of Tables

<i>Table 1: The marker expression profile of MSCs</i>	26
<i>Table 2: Primers used for Q-PCR</i>	86
<i>Table 3: Antibodies used for Western Blotting</i>	89
<i>Table 4: Antibodies used for Immunofluorescence of fixed cells</i>	95
<i>Table 5: Antibodies used for immunofluorescence of FFPE tissue</i>	99
<i>Table 6: An overview of the work carried out with the EPFL stretching devices</i>	115

iv. List of Figures

<i>Figure 1: The structure of the periodontium</i>	21
<i>Figure 2: MSC differentiation</i>	27
<i>Figure 3: Osteoblast differentiation</i>	30
<i>Figure 4: HSC differentiation</i>	34
<i>Figure 5: Osteoclast differentiation</i>	38
<i>Figure 6: Orthodontic tooth movement causes bone remodelling</i>	41
<i>Figure 7: Mechanotransduction</i>	45
<i>Figure 8: Periodontitis</i>	52
<i>Figure 9: LPS chemical structure and location</i>	54
<i>Figure 10: LPS signalling</i>	57
<i>Figure 11: The molecular mechanisms behind LPS tolerance</i>	61
<i>Figure 12: Hyaluronan structure and synthesis</i>	63
<i>Figure 13: Hyaluronan signalling</i>	67
<i>Figure 14: The autophagy pathway</i>	71
<i>Figure 15: Tensile strain models of orthodontic tooth movement</i>	102
<i>Figure 16: H&E staining demonstrates a morphological change in the periodontium of rats exposed to tensile strain</i>	104
<i>Figure 17: Immunofluorescent staining for osteogenesis markers Osteopontin and DMP1 in the periodontium of rats exposed to tensile strain</i>	105
<i>Figure 18: Osteogenesis and autophagy marker expression of rat periodontiums exposed to tensile strain</i>	107
<i>Figure 19: Cytoskeletal changes in the periodontium of rats exposed to tensile strain, as determined by immunofluorescence</i>	109
<i>Figure 20: Brightfield images demonstrating the confluence and morphology of human periodontal ligament fibroblasts (HPLF) when cultured on LSR4305 Silbione or DC186 Sylgard PDMS compared to that of a plastic cell culture dish</i>	111
<i>Figure 21: Brightfield images demonstrating the confluence and morphology of HPLF cells cultured on the EPFL tester device compared to that of a plastic cell culture dish</i>	112

<i>Figure 22: An example set up of the EPFL stretching device</i>	113
<i>Figure 23: Brightfield images demonstrating issues with cell attachment on batch 3 EPFL devices</i>	117
<i>Figure 24: Brightfield images demonstrating the effects of washing EPFL devices with different solutions in order to remove the oil accumulated on the surface of the membranes</i>	118
<i>Figure 25: Confocal images demonstrating the imaging capabilities of hBMCs cultured on the EPFL stretching devices</i>	119
<i>Figure 26: Brightfield images demonstrating a white film that observed on batch 5 EPFL devices compared to the clarity of the batch 4 devices</i>	120
<i>Figure 27: Brightfield images of various defects observed in the Strex stretching device membranes</i>	122
<i>Figure 28: Representative brightfield images demonstrating the variation in the success of cell attachment within the same experiment</i>	123
<i>Figure 29: MSC and HSC marker expression of hBMCs, as determined by flow cytometry</i>	125
<i>Figure 30: Osteogenic differentiation of hBMCs</i>	127
<i>Figure 31: Autophagy expression in hBMCs undergoing osteogenic differentiation</i>	128
<i>Figure 32: Osteogenesis and autophagy marker expression of hBMCs exposed to constant tensile strain</i>	129
<i>Figure 33: Cytoskeletal changes in hBMCs exposed to constant tensile strain</i>	131
<i>Figure 34: Autophagy activation enhances osteogenic differentiation in response to tensile strain in vitro</i>	133
<i>Figure 35: Autophagy inhibition impedes osteogenic differentiation in response to tensile strain in vitro</i>	135
<i>Figure 36: Establishing an osteoclast differentiation protocol for hBMCs</i>	139
<i>Figure 37: The effect of LPS on osteoclast differentiation of hBMCs</i>	141
<i>Figure 38: Establishing an LPS tolerance protocol for THP1s</i>	143
<i>Figure 39: E.coli LPS tolerance of THP1 cells</i>	145
<i>Figure 40: Hyaluronan expression in THP1 cells tolerised to E.coli LPS</i>	147
<i>Figure 41: Autophagy expression in THP1s tolerised to E.coli LPS</i>	149
<i>Figure 42: Hyaluronan and autophagy expression in THP1 cells tolerised to E.coli LPS</i>	150
<i>Figure 43: P.gingivalis LPS tolerance of THP1 cells</i>	152

<i>Figure 44: Hyaluronan and autophagy expression in THP1 cells after multiple exposures to P.gingivalis LPS</i>	154
<i>Figure 45: The effect of hyaluronan on osteoclast differentiation</i>	156
<i>Figure 46: The effect of hyaluronan and LPS on osteoclast differentiation</i>	158
<i>Figure 47: Co-culturing osteoclast precursors with THP1 cells tolerised to E.coli LPS</i>	160
<i>Figure 48: Osteoclast differentiation of THP1 cells</i>	162

1 Chapter 1: Literature Review

1.1 Overview

The periodontium, consisting of the gingiva, periodontal ligament, cementum and alveolar bone, is constantly remodelled in order to maintain its integrity (Tomokiyo, Wada and Maeda, 2019). Remodelling of any tissue relies on the activation of specific stem cells and their differentiation to cell types specific to the tissue and need, therefore, an understanding of stem cell biology and the molecular mechanisms involved is required in order to discuss the remodelling of the periodontium. Bone homeostasis in particular relies on cycles of resorption and formation of new bone which are concerned with the differentiation of haematopoietic stem cells (HSCs) to osteoclasts for mesenchymal stem cells (MSCs) to osteoblasts, respectively (Crockett *et al.*, 2011).

Many factors can affect the integrity of bone and the periodontium in general, including that of orthodontic tooth movement or inflammatory diseases such as periodontitis (Krishnan and Davidovitch, 2006; Tomokiyo, Wada and Maeda, 2019).

In the case of orthodontics, remodelling of the periodontium is required in order for the teeth to be moved. However, these procedures are not without risks, including enamel demineralisation, root resorption, periodontal damage and relapse (Wishney, 2017). The ramifications of these risks on patient health are even more pressing when you consider the fact that orthodontic procedures have been increasing in popularity in recent years ('The number of adults seeking orthodontic treatment in the UK continues to rise', 2018). Further understanding the mechanisms behind strain-induced remodelling of the periodontium is required in order to attempt to reduce these risks and obtain better clinical outcomes for patients.

Periodontium remodelling may also be affected by disease. Periodontitis is an inflammatory disease that can result in the destruction of the periodontium and alveolar bone resorption (Hienz, Paliwal and Ivanovski, 2015). This not only affects the stability and function of the

periodontium itself, but can also cause systemic inflammation which is linked to widespread health concerns (Hayashi *et al.*, 2010). The destruction of the periodontium causes cells of the blood to come into contact with the inflamed tissue and the open air inside the oral cavity. Monocytes, macrophages and other inflammatory cells are then activated by exposure to bacteria and the inflamed tissue (Page *et al.*, 1997; Al-Qutub *et al.*, 2006). While the prevalence of periodontitis has risen in recent years, it is difficult to predict which patients are at risk of the disease, as it does not affect all patients with poor dental health (Al-Qutub *et al.*, 2006). It is thought that there are underlying mechanisms related to host immunity which affect the prevalence and progression of periodontitis, which need to be uncovered in order to understand and treat the disease effectively.

1.2 The Periodontium

1.2.1 Structure & Development

The periodontium consists of the alveolar bone, periodontal ligament (PDL), cementum and gingiva which provide structural and functional support to the teeth (*Figure 1*).

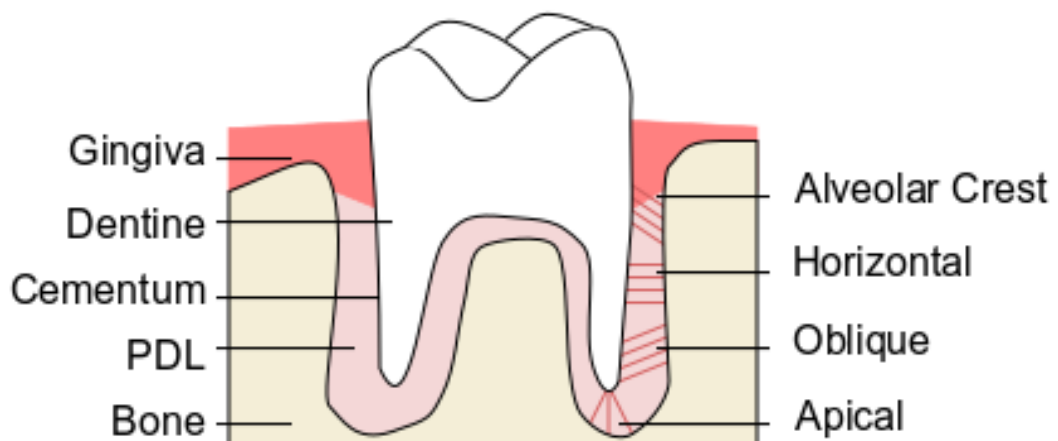


Figure 1: The structure of the periodontium and the orientation of the PDL fibre types (adapted by de Jong et al., 2017). PDL = periodontal ligament.

Gingival tissue consists of epithelial cells and fibroblasts and forms a barrier between the internal structures of the periodontium and the oral cavity. The sulcular and gingival epithelium are exposed to the oral cavity and protect the periodontium from microbial infection, while the

junctional epithelium directly attaches the tooth surface to the sulcular epithelium and the underlying PDL (Groeger and Meyle, 2019).

The PDL is a connective tissue which supports the tooth within the alveolar bone. The PDL is found in the space between the bone and tooth and provides shock absorption during biting. The fibres of the PDL consist mostly of collagen-I and -III, however oxytalan fibres formed from elastin are also present (Strydom *et al.*, 2012). Fibre organisation differs in separate areas of the periodontium, for instance horizontal fibres run perpendicular to the tooth root, while apical fibres are parallel to the root at the base of the tooth. The PDL is a highly vascularised and innervated tissue, which aids its nutritive and sensory functions, and contains many cell types including fibroblasts, which produce the extracellular matrix (ECM) that make up the PDL fibres (de Jong *et al.*, 2017). It also provides a niche for PDL stem cells (PDLSCs), which aid periodontal regeneration alongside stem cells from the bone marrow, found within the alveolar bone (Tomokiyo, Wada and Maeda, 2019; Trubiani *et al.*, 2019).

The PDL is connected to the alveolar process, the portion of bone containing the tooth sockets and alveolar crest, by attachment to the Volkmann canals within the bone (Nobuto *et al.*, 2003). PDL fibres are connected to the dentine via the cementum, a mineralised tissue formed along the dentine surface. PDL fibres develop initially from the cementum side of the PDL space, and extend to form Sharpey's fibres at the bone surface. These Sharpey's fibres, consisting mainly of collagen-I, are mineralised at the bone surface to anchor the PDL (de Jong *et al.*, 2017).

Cementum consists of both acellular and cellular components; the acellular mineralised tissue mainly consists of collagen fibres and hydroxyapatite, and physically attaches the PDL to the dentine (Yamamoto *et al.*, 2016). While the inner workings of the cementum are still unclear, it is thought that the cementoblasts found in the cellular component are similar to osteoblasts in their mesenchymal lineage and role in producing matrix (Bosshardt, 2005). However, unlike bone, cementum is not vascularised or innervated and has a low regenerative capacity (Foster, 2012).

The alveolar bone of the mandible and maxilla consists of trabecular and cortical bone, structured with an inner bone marrow compartment surrounded by mineralised osteoid (Nakamura, 2007). The mineralised portion of bone contains canaliculi, channels within the bone where interstitial fluid flows and osteocyte processes form a network of connected osteocytes and osteoblasts (Shapiro, 1988). The bone marrow is an innervated and highly vascularised environment, containing several cell populations including mesenchymal stem cells (MSCs), haematopoietic stem cells (HSCs), and cells of each of their respective lineages (Birbrair and Frenette, 2016). In this way, bone is vital to haematopoiesis, immunity, and the maintenance of its own and surrounding tissues. The craniofacial bones originate from cells of the neural crest, which form the bones of the face and anterior skull, while prechordal mesodermal cells produce the posterior skull (Berendsen and Olsen, 2015). The cells of the cementum and the PDL itself are also derived from stem cell populations, specifically dental follicle stem cells of mesenchymal origin (Yao *et al.*, 2008).

1.2.1.1 Bone Development

Skeletogenesis begins when MSCs migrate and condense at the site of future bone formation, which occurs around embryonic day 10.5 (E10.5) in humans. MSCs on the outside of the condensations remain undifferentiated, while those on the inside differentiate to chondrocytes to form cartilage, or osteoblasts to form bone (Hall and Miyake, 1992; Karsenty, Kronenberg and Settembre, 2009).

The majority of the skeleton is formed by endochondral ossification where cartilage is produced, mineralised, vascularised, and then remodelled as bone later in development (Karsenty, Kronenberg and Settembre, 2009) (Shum *et al.*, 2003; Shen, 2005). This is also the case for the development of the distal portions of the alveolar bone (Kjær and Bagheri, 1999; Parada and Chai, 2015). However, the majority of craniofacial bones are formed directly by intramembranous bone formation, when osteoblasts produce a matrix called osteoid which is

mineralised to form bone (Crockett *et al.*, 2011). The key molecular events involved in osteogenesis are discussed in section 1.3.2.2.

1.2.2 Remodelling

Throughout development remodelling of the alveolar bone occurs in order to form the socket and alveolar crest around the tooth (Parada and Chai, 2015). Postnatally, remodelling of the periodontium relies on the activation of stem cells from the bone marrow and PDL niches, however the exact contributions of each stem cell niche to periodontal regeneration are as yet unknown (Parada and Chai, 2015).

PDLSCs are a sub-set of MSCs that reside in the PDL space between the dentine and alveolar bone (Zhu and Liang, 2015). They have the capacity to differentiate to multiple lineages *in vitro*, including those of osteoblasts, adipocytes, cementoblasts, fibroblasts, myocytes and Schwann cells (Seo *et al.*, 2004; Osathanon *et al.*, 2013; Pelaez *et al.*, 2017). PDLSCs have comparable marker expression to other sub-sets of MSCs, including CD73, CD90 and CD105, and they share an immunomodulatory capacity with MSCs of the bone marrow (Wada *et al.*, 2009; Zhu and Liang, 2015). However, they differ from MSCs of other origins in their proliferative capacity *in vitro* and expression of certain markers involved in cell cycle regulation and stress response including an increase in CLPP, NQO1 and SCOT1 (Tomokiyo, Wada and Maeda, 2019; Trubiani *et al.*, 2019). Additionally, the regenerative contribution of PDLSCs comparable to other stem cell niches is not yet established in periodontal tissue (Parada and Chai, 2015).

The bone marrow contains both MSCs and HSCs which are the progenitors of osteoblasts, required for osteogenesis, and osteoclasts, specialised for bone resorption, respectively. These cells are known to contribute significantly to the remodelling of bones throughout the body, including that of the alveolar bone (Crockett *et al.*, 2011).

1.3 Cell Fate Determination

The integrity and regenerative capacity of the periodontium can be affected by many factors, including that of orthodontic tooth movement and periodontitis (Krishnan and Davidovitch, 2006; Tomokiyo, Wada and Maeda, 2019). In order to investigate how these events alter periodontal regeneration, there must first be an understanding of the stem cells involved and the molecular mechanisms behind alveolar bone remodelling.

1.3.1 Mesenchymal Stem Cells

1.3.1.1 Defining MSCs

Colony forming units (CFU) were first identified in the bone marrow and defined by their tri-lineage differentiation potential and adherence to plastic containers *in vitro* (Friedenstein, Chailakhjan and Lalykina, 1970; Friedenstein, Gorskaja and Kulagina, 1976). They originate from the mesoderm during development, hence MSCs, CFUs or stromal cells have since been identified in numerous other tissues including the peripheral blood, adipose tissue, vascular wall and dental pulp (Gronthos *et al.*, 2000; Hass *et al.*, 2011; Kramann *et al.*, 2016; Xu *et al.*, 2017).

In the early 2000s the international society for cellular therapy (ISCT) suggested a criteria to attempt to standardise the identification of these cells (Dominici *et al.*, 2006). Marker panels used to identify MSCs typically contain cell surface markers, including CD73, CD90, CD105, CD106 and Stro-1 (Simmons and Torok-Storb, 1991; Dominici *et al.*, 2006; Mabuchi *et al.*, 2013), intermediate filament proteins like vimentin (Bruno, Chiabotto and Camussi, 2014), and adhesion molecules such as integrins (integrin $\alpha 5\beta 1$) and cadherins (N-cadherin) (Goessler *et al.*, 2008; Aomatsu *et al.*, 2014; Zwolanek *et al.*, 2015). Positive markers for HSCs or their progenitors, for instance CD14, CD19 and CD45 are often used as negative MSC markers (Pittenger *et al.*, 1999; Colter *et al.*, 2000; Tare *et al.*, 2008). A selection of markers used for MSC identification has been collated in *Table 5*. It is also possible to distinguish between MSCs of different populations, for instance those of the dental pulp express higher levels of CD29 than bone marrow-derived MSCs (Ponnaiyan and Jegadeesan, 2014).

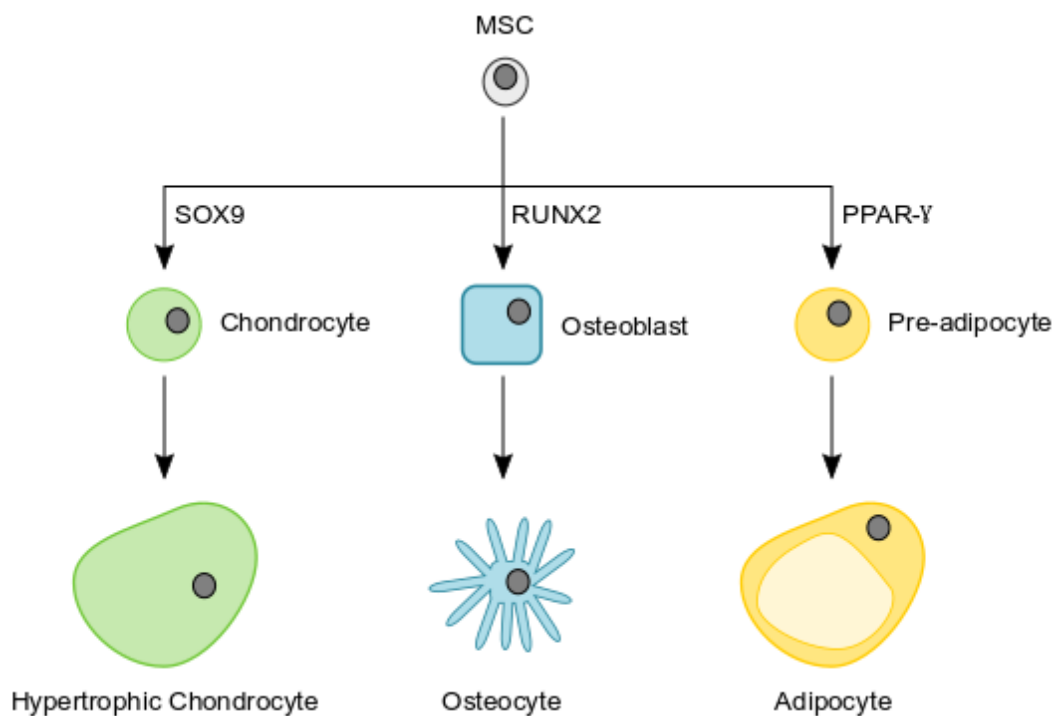
Marker	Expression	Details	References
CD14	Negative	Monocyte and macrophage marker (haematopoietic lineage)	<i>Pittenger et al., 1999, Colter et al., 2000</i>
CD19	Negative	B cell marker (haematopoietic lineage); specified by ISCT criteria	<i>Dominici et al., 2006, Tare et al., 2008</i>
CD29	Positive	Integrin β 1; cell-ECM adhesion protein	<i>Zwolanek et al., 2015, Tare et al., 2008</i>
CD44	Positive	Cell surface adhesion molecule	<i>Pittenger et al., 1999, Tare et al., 2008</i>
CD45	Negative	Leukocyte marker (haematopoietic lineage); specified by ISCT criteria	<i>Pittenger et al., 1999, Colter et al., 2000, Dominici et al., 2006</i>
CD73	Positive	Cell surface adhesion molecule; specified by ISCT criteria	<i>Pittenger et al., 1999, Dominici et al., 2006</i>
CD90	Positive	Cell surface protein; specified by ISCT criteria	<i>Pittenger et al., 1999, Dominici et al., 2006</i>
CD105	Positive	Cell surface TGF β receptor; specified by ISCT criteria	<i>Pittenger et al., 1999, Dominici et al., 2006</i>
CD106	Positive	Cell surface adhesion molecule	<i>Pittenger et al., 1999, Tare et al., 2008, Mabuchi et al., 2013</i>
CD146	Positive	Cell surface adhesion molecule	<i>Tare et al., 2008, Halfon et al., 2011</i>
CD166	Positive	Cell surface adhesion molecule	<i>Tare et al., 2008, Halfon et al., 2011</i>
Integrin α 5 β 1	Positive	Cell-ECM adhesion protein and fibronectin receptor	<i>Goessler et al., 2008</i>
N-Cadherin	Positive	Cell-cell adhesion protein	<i>Aomatsu et al., 2014</i>
Stro-1	Positive	Cell-surface trypsin-resistant antigen	<i>Simmons & Torok-Storb, 1991, Tare et al., 2008</i>
Vimentin	Positive	Mesenchyme marker	<i>Bruno, Chiabotto & Camussi, 2014</i>

Table 1: The marker expression profile of MSCs (adapted from Tare et al., 2008).

The ISCT criteria also states that MSCs should have the capability to be stimulated to differentiate to each of the classic lineages described by early papers investigating MSC differentiation: adipogenic, chondrogenic and osteogenic (Pittenger *et al.*, 1999). As such, these are the most extensively studied pathways of MSC differentiation and are thought of as the minimum differentiation requirement of suspected MSCs.

1.3.1.2 MSC Differentiation

MSCs may differentiate into a multitude of cell types in adult tissue, depending on the specific cues the cells receive (Nombela-Arrieta, Ritz and Silberstein, 2011). The classic differentiation lineages are to form osteoblasts for osteogenesis, adipocytes for adipogenesis, or chondrocytes for the production of cartilage (Figure 2), however MSCs also have the capacity for other lineages, such as those involved in tenogenesis and myogenesis (Kolf, Cho and Tuan, 2007).



*Figure 2: **MSC differentiation**; MSCs become activated and differentiate to specific lineages depending on the expression of key transcription factors. SOX9 causes chondrogenesis, RUNX2 causes osteogenesis and PPAR- γ causes adipogenesis (adapted from Long, 2012). MSC = mesenchymal stem cell, SOX9 = sry-box 9, RUNX2 = runt-related transcription factor 2, PPAR- γ = peroxisome proliferator-activated receptor gamma.*

MSC stemness is maintained by leukaemia inhibitory factor (LIF), fibroblast growth factor (FGF), particularly FGF2, and Wnt signalling. The actions of these proteins promote the expression of sry-box 2 (SOX2) and octamer-binding transcription factor 4 (OCT4), both of which are associated with pluripotency (Tsutsumi *et al.*, 2001; Jiang *et al.*, 2002; Boland *et al.*, 2004; Izadpanah *et al.*, 2006). Differentiation of MSCs is reliant on three master transcription factors; runt-related transcription factor-2 (RUNX2) for osteogenesis, peroxisome proliferator-activated receptor gamma (PPAR γ) for adipogenesis, or sry-box 9 (SOX9) for the chondrogenic lineage (Kolf, Cho and Tuan, 2007; Long, 2012; Chen *et al.*, 2016) (Bi *et al.*, 1999).

In vitro differentiation of MSCs to the osteogenic lineage is achieved through a well-established treatment protocol, using ascorbic acid, β -glycerol phosphate and dexamethasone (Jaiswal *et al.*, 1997; Peter *et al.*, 1998). Dexamethasone stimulates and enhances differentiation of MSCs, while ascorbic acid (vitamin C) is required for the production of collagen-I, the main component

of osteoid, and β -glycerol phosphate is involved in late stage differentiation and mineralisation (Song, Caplan and Dennis, 2009; Langenbach and Handschel, 2013; Yuasa *et al.*, 2015).

1.3.2 Osteogenesis

1.3.2.1 Defining Osteoblasts and Osteocytes

Osteoblasts are cuboidal cells of 20-30 μ M in size which are mostly found lining the periosteum and endosteum of the bone (Doherty *et al.*, 1995; Rutkovskiy, Stensl kken and Vaage, 2016).

Active osteoblasts are highly secretory and therefore contain large endoplasmic reticulum (ER) and Golgi complexes (Nakamura, 2007). The activation of MSCs to differentiate into osteoblasts is associated with many transcription factors, however RUNX2 is often used as a marker due to its role as the so-called master transcription factor of osteogenesis. RUNX2 not only has roles in the cell fate determination of MSCs to osteoblast and osteocyte lineages, but also in bone matrix deposition, which is the outcome of osteogenesis (Kolf, Cho and Tuan, 2007; Chen *et al.*, 2016).

Active osteoblasts are associated with osteoid production and mineralisation, which can be determined by staining for calcium deposits with alizarin red, 1,2-dihydroxyanthraquinone (Hoyte, 1960). Alkaline phosphatase is required for osteoid mineralisation and is therefore highly expressed in osteoblasts. It is often used as a histological marker of these cells, however this enzyme is also expressed in perivascular mesenchymal progenitor cells (Nakamura, 2007; Gerlach *et al.*, 2012).

After a period of active osteoid secretion and mineralisation, osteoblasts may further differentiate into osteocytes or they may become quiescent and are then referred to as bone lining cells. Both of these cell types can be distinguished from osteoblasts by their low alkaline phosphatase activity (Nakamura, 2007). Bone lining cells are flatter in shape and have less developed ER and Golgi as their secretory function is greatly reduced. Osteocytes are terminally differentiated cells of osteoblast-lineage that become embedded in the bone (Nakamura, 2007). They have a distinctive morphology with several cytoplasmic processes that connect via gap junctions to form a network with other osteocytes or osteoblasts on the bone surface. These

osteocyte processes possess a highly developed actin cytoskeleton, which is implicated in the role of these cells as mechanosensors (Nakamura, 2007). Mechanical strain that is propagated into the bone is thought to be sensed by disruption of this actin cytoskeleton, and the signal propagated across the network of osteocyte processes (Klein-Nulend, Bacabac and Bakker, 2012; Cowin and Cardoso, 2015). Osteocytes also contain mechanosensitive ion channels, which open on exposure to mechanical strain, and this flux of ions across gap junctions is thought confer mechanical signals through the network of osteocytes and to osteoblasts on the bone surface (Ypey *et al.*, 1992; Jørgensen *et al.*, 2003; Nakamura, 2007).

1.3.2.2 Osteoblast Differentiation

Expression of the RUNX2 transcription factor is necessary for the differentiation of MSCs to osteoblasts (Komori *et al.*, 1997; Otto *et al.*, 1997). SMAD-dependant transforming growth factor beta (TGF β) signalling and canonical Wnt signalling have been implicated in upregulating RUNX2 expression (Hill *et al.*, 2005; Chen, Deng and Li, 2012). Wnt signalling is particularly important to MSC fate determination, as it not only causes upregulation of RUNX2 but also downregulation of SOX9 to drive osteogenic differentiation (Komori *et al.*, 1997; Otto *et al.*, 1997; Rodda and McMahon, 2006; Kim *et al.*, 2013).

RUNX2 belongs to the Runt protein family which all share the Runt DNA-binding domain. RUNX2 binds and activates *Coll1 α 1*, *Bsp*, and *Bgp* genes, inducing the production of collagen-I, bone sialoprotein and osteocalcin, respectively (Ducy *et al.*, 1997). As osteoblasts differentiate they first upregulate their expression of TGF β receptors and osteopontin (Rutkovskiy, Stensløyken and Vaage, 2016). They also produce collagen-I, the major component of osteoid which is the unmineralized, organic component of bone (Murshed, 2018). Downstream of RUNX2, the Osterix (*Osx*) transcription factor is crucial for osteoblast differentiation. It contains a zinc-finger domain and interacts with nuclear factor of activated T Cells 1 (NFATC1) to activate further transcription of *Coll1 α 1* (Nakashima *et al.*, 2002; Koga *et al.*, 2005). Osteoblasts then begin to express alkaline phosphatase, the enzyme required for mineralisation of osteoid (Siffert, 1951),

and upregulate expression of calcium phosphatase, dentin matrix protein 1 (DMP1) and osteocalcin to aid mineralisation (Rutkovskiy, Stensl kken and Vaage, 2016). Osteocalcin also provides structural support to the new bone, being the second most abundant protein present in bone after collagen-I (Komori *et al.*, 1997) (Figure 3).

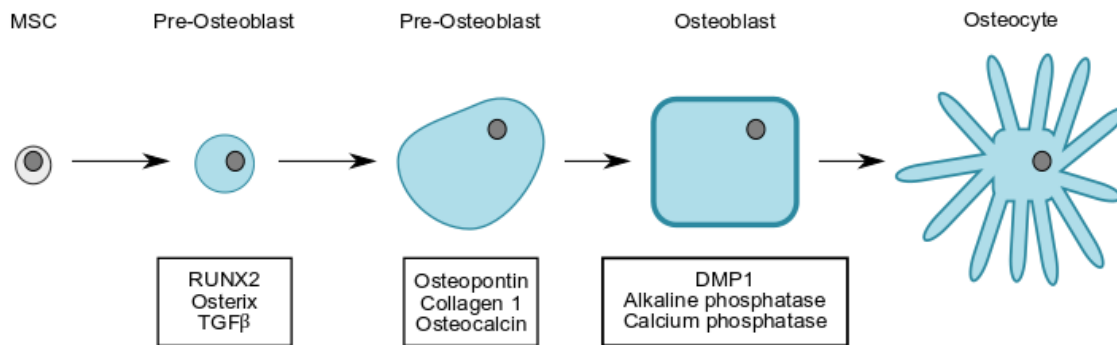


Figure 3: **Osteoblast differentiation**; MSCs differentiate to pre-osteoblasts, which highly express TGFβ and the RUNX2 and osterix transcription factors. This causes upregulated of osteopontin, osteocalcin and collagen-1 for the secretion of osteoid. Late stage osteoblasts express DMP1, alkaline phosphatase and calcium phosphatase, which aid in the mineralisation of osteoid. Some osteoblasts may further differentiate to osteocytes which are embedded in the bone (adapted from Rutkovskiy, Stensl kken & Vaage, 2016). MSC = mesenchymal stem cell, RUNX2 = runt-related transcription factor 2, TGFβ = transforming growth factor beta, DMP1 = dentin matrix protein 1.

Late stage differentiation of osteoblasts requires FGF18 signalling through FGFR2 and FGFR3, as seen with *fgf18* knockout mice whose osteoblast progenitors never fully mature (Ohbayashi *et al.*, 2002) (Lefebvre and Bhattaram, 2010). Osteoblast function relies on the expression of activating transcription factor 4 (ATF4), which stimulates amino acid import into osteoblasts to enhance the synthesis of collagen-I (Yang and Karsenty, 2004; Yang *et al.*, 2004).

Osteoblast differentiation and function is highly regulated to ensure controlled osteogenesis occurs only where needed. During development RUNX2 is negatively regulated by Twist1/2 interacting with its Runt DNA-binding domain (Bialek *et al.*, 2004). Postnatally, RUNX2 expression is tightly controlled by several factors. For instance, myocyte enhancer factor-2 (Mef2) and distal-less homeobox 5 (Dlx5) bind to an enhancer upstream of RUNX2 to prevent its activation and therefore regulate RUNX2 transcription (Kawane *et al.*, 2014). Ethylene-responsive transcription factor SHINE 3 (Shn-3) regulates RUNX2 activation by recruiting WW

domain containing protein 1 (WWP1), an E3 ligase, which works to degrade RUNX2 before it can be translocated to the nucleus. This was demonstrated in Shn-3 knockout mice which had accumulation of RUNX2 protein in osteoblasts causing upregulation of osteogenesis and increased bone mass (Jones, 2006). Additionally, signal transducer and activator of transcription 1 (Stat1) negatively regulates osteogenesis by preventing RUNX2 translocation to the nucleus which, as a transcription factor, is crucial for its function (Kim *et al.*, 2003; Karsenty, Kronenberg and Settembre, 2009).

Osteoblasts and osteocytes are also thought to have a role in bone resorption to some degree, as they produce collagenase and matrix metalloproteinase (MMP13) which degrade collagen in the bone and ECM (Sakamoto and Sakamoto, 1982; Nakamura *et al.*, 2004). This is thought to be a regulatory process, to supplement bone resorption by osteoclasts (Nakamura, 2007).

In fact, there are several instances of cross-talk between osteoblasts and osteoclasts demonstrated in the literature (Zhang *et al.*, 2003; Fuchs, Tumber and Guasch, 2004). Osteoblast and osteoclast interactions have been demonstrated via cell-cell contact and cytokine release (Chen *et al.*, 2018), for instance osteoblasts are known to secrete macrophage colony stimulating factor (M-CSF) and have receptor activator of nuclear factor NF- κ B ligand (RANKL) bound to their membrane; two key components in the differentiation of osteoclasts (Lacey *et al.*, 1994). Additionally, notch signalling causes osteoblasts to produce osteoprotegerin (OPG), a negative regulator of osteoclastogenesis (Bucay *et al.*, 1998; Engin *et al.*, 2008). Osteoclasts can also affect osteogenesis by producing complement component 3a (C3a), a protein involved in the complement inflammatory cascade which stimulates osteoblast differentiation (Matsuoka *et al.*, 2014). Tartrate-resistant acid phosphatase (TRAP), a marker of osteoclast function, may also be linked to osteogenesis regulation, as osteoblasts from TRAP knockout mice produced higher levels of osteogenesis proteins RUNX2 and osteocalcin, and had accelerated osteoid mineralisation compared to controls (Hayman, 2008). Additionally, osteoblasts on the inner

surface of bone maintain contact with quiescent HSCs, the progenitor cells of osteoclasts, until they begin to differentiate (Zhang *et al.*, 2003; Fuchs, Tumber and Guasch, 2004).

1.3.3 Haematopoietic Stem Cells

1.3.3.1 Defining HSCs

HSCs are a population of clonogenic cells able to give rise to all blood cell lineages (Eaves, 2015). They were first discovered in 1961 when bone marrow cells which had been injected into mice prior to exposure to radiation were found to be able to form colonies of cells in the spleen and survive the effects of the radiation, unlike controls (Till and McCulloch, 1961). Early work examining these spleen colony-forming-units, which are now thought to contain HSCs, found them to be a heterogeneous population of cells, some with the capacity to self-renew or to differentiate into a multitude of haematopoietic lineages (Siminovitch, McCulloch and Till, 1963).

Modern definitions of HSCs are more based on cell surface antigen expression. While there is some heterogeneity in HSCs *in vivo* (Uchida *et al.*, 1993; Sieburg *et al.*, 2006), generally HSCs are positive for stem cells antigen-1 (Sca-1) and also express low levels of CD90 which is lost in differentiated cells (Berman and Basch, 1985; Spangrude, Heimfeld and Weissman, 1988). cKit is critical for maintenance of HSCs, with loss-of-function mutations causing a decrease in HSC populations in mice (Sharma, Astle and Harrison, 2007). In 2005 a defining protocol was put forth which used a profile of signalling lymphocyte activation molecule (SLAM) family genes in an attempt to further define and purify HSCs and their progenitors (Kiel *et al.*, 2005). These SLAM codes are generally accepted as a good method of distinguishing HSCs from myeloid or macrophage, megakaryocyte, multipotent or lineage-restricted progenitors, with relatively few markers (Kiel *et al.*, 2005). Additionally, HSCs can be defined by their negative expression of a panel of differentiated cell markers, known as 'Lineage^{neg}'; these include MAC-1 for myelomonocytes, CD4 and CD8 for T cells, and B220, a splice isoform of CD45, for B cells (Spangrude, Heimfeld and Weissman, 1988).

HSCs are derived from the mesoderm, and initially reside in the aorto-gonado-mesonephros region of the embryo at E10.5 in mice. In adult tissue HSCs are primarily found in the bone marrow (Müller *et al.*, 1994; Medvinsky and Dzierzak, 1996) where they are thought to make up one in every ten thousand cells (Szilvassy *et al.*, 1990). When quiescent, adult HSCs reside in a hypoxic niche of the bone marrow, and if activated they re-join the cell cycle and either produce progeny to replenish the stem cell niche or differentiate (Nombela-Arrieta *et al.*, 2013).

1.3.3.2 HSC Differentiation

HSCs have the capacity to differentiate into all cells of the blood therefore any defects in HSC formation, self-renewal or differentiation may affect haematopoiesis and/or the immune response. The plasticity of HSCs decreases as they differentiate from short-term HSCs to multipotent progenitor cells, which each have a shorter capacity of self-renewal (Kondo *et al.*, 2003; Shizuru, Negrin and Weissman, 2005). HSCs may then differentiate into either common lymphoid progenitors or common myeloid progenitor cells (*Figure 4*). Lymphoid progenitors may further differentiate into Natural Killer (NK) cells, dendritic cells, B cells or T cells. Downstream of myeloid progenitors are erythrocytes and platelets (from megakaryocyte-erythroid progenitor cells), neutrophils, eosinophils and basophils (from myeloblasts), and macrophages (from monocytes) (Kawamoto *et al.*, 2010; Eaves, 2015; Hamey *et al.*, 2017). HSC differentiation to the monocyte lineage is required for the formation of osteoclasts.

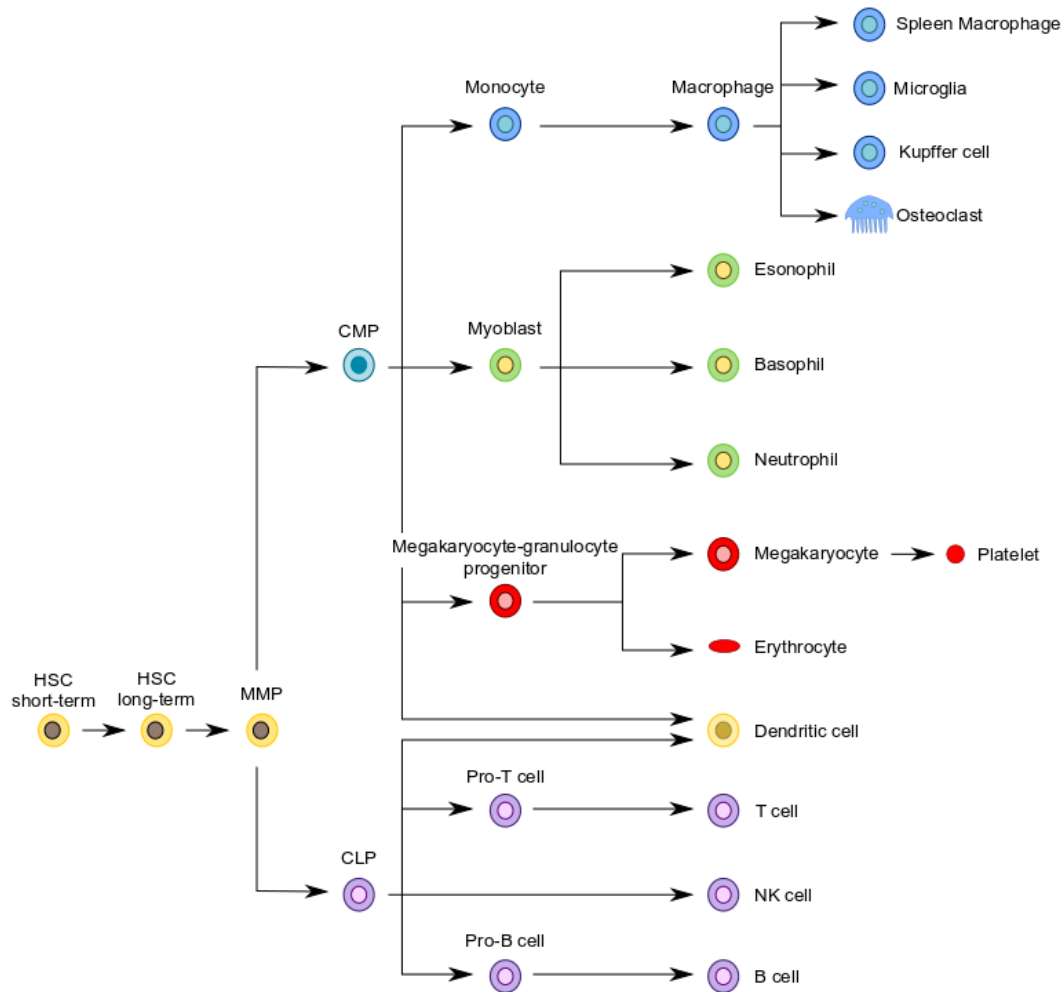


Figure 4: **HSC differentiation**; HSCs differentiate from long-term to short-term HSCs, then to MPPs, before either CLP or CMP cells. From these avenues they may further differentiate into many cell types in the blood and tissues. (adapted from Shizuru, Negrin & Weissman, 2005). HSC = haematopoietic stem cell, MPP = multipotent progenitor cell, CLP = common lymphoid progenitor, CMP = common myeloid progenitor.

Monocytes are a type of leukocyte with roles in innate and adaptive immunity, angiogenesis and tissue remodelling (Jakubzick, Randolph and Henson, 2017) that usually reside in the peripheral blood or the spleen (Swirski *et al.*, 2009).

The key marker for identifying monocytes and other myeloid progenitors is CD14, which is highly expressed on the plasma membrane and binds LPS in a complex with toll-like receptor 4 (TLR4) and myeloid differentiation factor 2 (MD2) to cause downstream upregulation of cytokines (Wright *et al.*, 1990; Lee *et al.*, 1992). There are two subtypes of monocytes based on their marker expression; classical monocytes strongly express CD14 and are negative for CD16 expression, while non-classical monocytes are positive for both CD14 and CD16. The classical

monocytes are the type most prevalent in humans (Passlick, Flieger and Ziegler-Heitbrock, 1989). Differentiation of HSCs to monocytes occurs in the bone marrow and is stimulated by M-CSF, after which monocytes are able to migrate to the bloodstream and to other tissues where they may differentiate to resident macrophages or dendritic cells (Stanley, Chen and Lin, 1978; Wiktor-Jedrzejczak and Gordon, 1996).

Macrophages are large leukocytes, approximately 20-50 μ M in diameter, that are involved in antigen presentation and phagocytosis of cells and pathogens (Tearney *et al.*, 2003). There are several sub-types of macrophages, which change type depending on the specific needs of the organism, in a process referred to as macrophage polarisation. Classically activated macrophages (M1) are inflammatory, and on the recognition of a potential threat, proliferation of M1 macrophages is strongly increased. There is some debate over the characterisation of other macrophages; some scholars designate alternatively-activated macrophages (M2) as being involved in wound-healing, while regulatory macrophages (Mreg) are anti-inflammatory to regulate immune response. However, others include anti-inflammatory macrophages under the M2 classification also (Murray *et al.*, 2014). Alternatively, macrophage polarisation has been described as a spectrum, rather than a set of distinct populations, which allows for greater flexibility in recognising and understanding their function (Mosser and Edwards, 2008). For instance, macrophages residing in adipose tissue are usually similar to the regulatory macrophages involved in wound healing, however they may become more M1-like in obese individuals (Lumeng, Bodzin and Saltiel, 2007).

Macrophage polarisation depends on many varied stimuli, including cytokines, growth factors and pathogen-associated molecular patterns (PAMPs). M1 macrophages are induced by cytokines such as interferon-gamma (IFN γ), granulocyte macrophage colony stimulating factor (GM-CSF), or exposure to PAMPs such as LPS (Verreck *et al.*, 2004; Martinez and Gordon, 2014; Murray *et al.*, 2014). They express the nuclear factor kappa light-chain enhancer of activated B cells (NF- κ B) transcription factor, which causes upregulation of tumour necrosis factor alpha

(TNF α) and IFN γ signalling, and downstream production of cytokines including IL1 β , IL6, IL8 and IL12 (Wang, Liang and Zen, 2014). M2 macrophages may be activated by IL4, IL13 or M-CSF and are responsible for the production of insulin-like growth factor 1 (IGF1) for fibroblast proliferation, and resistin-like molecule alpha (RELM α) which encourages further production of ECM components (Mosser and Edwards, 2008). Mregs are induced by the recognition of IL10, IgG complexes, glucocorticoids, or apoptotic cells. They result in the upregulation of anti-inflammatory cytokine IL10 and TGF β (Mantovani *et al.*, 2004; Martinez and Gordon, 2014).

Macrophage polarisation is relevant to osteoclast differentiation as osteoclasts also originate from the monocyte lineage. Therefore, if there are signals for macrophages to polarise to a specific phenotype, there may be fewer osteoclast precursors available to differentiate to active osteoclasts. An example of this is with IL4, which causes polarisation to M2 macrophages and inhibits osteoclast differentiation (Moreno *et al.*, 2003). However, the interplay between macrophage polarisation and osteoclast differentiation is not so straightforward; While the differentiation and polarisation of macrophages to the M1 phenotype may mean there are less pre-monocytes available to differentiate to osteoclasts, some inflammatory conditions are accompanied by bone loss. In fact, some papers designate RANKL-activated macrophages as an M1 phenotype, however these are distinct to LPS-induced M1 macrophages, both in their cytokine expression profiles and ability to differentiate to osteoclasts (Jeganathan *et al.*, 2014; Huang *et al.*, 2017).

1.3.4 Osteoclastogenesis

1.3.4.1 Defining Osteoclasts

Osteoclasts are large multi-nucleated cells involved in the resorption of mineralised tissue. They are essential for the development and maintenance of bone, and in the context of oral health specifically they allow for the modification of the alveolar bone seen in tooth eruption and orthodontic tooth movement (Okaji *et al.*, 2003; Holliday *et al.*, 2009; Wise, 2009).

Osteoclasts are structured with a clear zone anchoring the cell to the bone, and a ruffled border adjacent to the mineralised surface being resorbed (Nakamura, 2007). They are large cells, up to 100µM in length, with at least three nuclei but usually more (Kleinbans *et al.*, 2015). They are characterised as staining positive for tartrate-resistant acid phosphatase (TRAP) which was once used as a specific osteoclast marker in histology however it has also been found to be expressed by macrophages and osteoblasts (Hayman, 2008). Nevertheless, TRAP staining is still used as a method of identifying osteoclasts, alongside other characteristics such as nuclei number and the expression of markers including osteoclast-associated receptor (OSCAR), cathepsin K, integrin $\beta 3$ and calcitonin receptor (Arai *et al.*, 1999; Marino *et al.*, 2014; Tevlin *et al.*, 2014) (Lee, Goldring and Lorenzo, 1995).

Identifying active osteoclasts, either *in vivo* or *in vitro*, requires proof of resorption usually by measuring the size of resorption pits left behind in mineralised tissue (Vesprey and Yang, 2016). *In vitro* this may be set up by seeding osteoclasts onto a slice of dentine or bone. The pattern of pit resorption, either round or long, may also indicate differences in osteoclast activity (Merrild *et al.*, 2015). Once osteoclasts are deactivated they lose their distinctive ruffled border morphology and detach from the bone surface (Fukushima, Bekker and Gay, 1991).

1.3.4.2 Osteoclast Differentiation and Activation

Osteoclasts are formed from the differentiation of HSCs to the myeloid lineage, whereby osteoclast precursors fuse to form large, multinucleated cells (*Figure 5*) (Boyle, Simonet and Lacey, 2003). These osteoclast precursors express CD14 and receptor activator of nuclear factor NF- κ B (RANK) and are generally found in the bone marrow and peripheral blood (Matsuzaki *et al.*, 1998; Schlegel *et al.*, 2000), however may also be found in other areas of the body and different sub-sets may have different marker expression and differentiation potential. There is also some heterogeneity within osteoclast precursors of the same location, for instance cKit

positive bone marrow cells were found to have greater differentiation potential towards becoming osteoclasts than their cKit negative counterparts (Hayashi *et al.*, 1997).

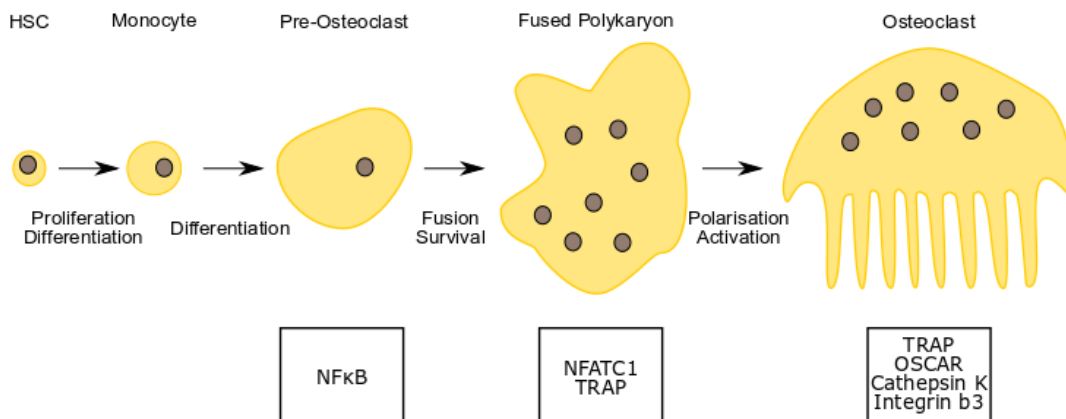


*Figure 5: **Osteoclast differentiation**; osteoclast precursor cells in the bone marrow differentiate into monocytes in response to M-CSF. Monocytes differentiate to osteoclasts with exposure to M-CSF and RANKL. Osteoclast precursor cells fuse to form multi-nucleated osteoclasts that are TRAP positive. Osteoclasts become polarised with a distinct morphology anchored to the bone surface. NFATC1 stimulates the activation of osteoclasts with the production of OSCAR and Cathepsin K (adapted from Boyle 2003 and Kim & Kim, 2016). HSC = haematopoietic stem cell, NF-κB = nuclear factor kappa light-chain enhancer of activated B cells, NFATC1 = nuclear factor of activated T Cells, TRAP = tartrate-resistant acid phosphatase, OSCAR = osteoclast-associated receptor.*

Two proteins essential for osteoclast differentiation are M-CSF and RANKL. The importance of M-CSF was discovered when an osteopetrosis mouse model, caused by M-CSF deficiency, was found to have decreased numbers of tissue-resident macrophages and osteoclasts compared to controls (Naito *et al.*, 1991). RANK knockout mice were also found to have severe osteopetrosis due to an absence of osteoclasts (Dougall *et al.*, 1999; Li *et al.*, 2000)

Stromal cells produce M-CSF which binds to colony stimulating factor 1 receptor (c-Fms) on osteoclast precursors, causing RANK to be expressed and promoting their proliferation and differentiation to macrophages (Arai *et al.*, 1999). RANKL is expressed on the osteoblast plasma membrane and on proteolytic cleavage is released into the microenvironment where it binds to its receptor, RANK (Lum *et al.*, 1999). This initiates the recruitment of osteoclast precursors and their adherence to bone, as well as cell fusion and differentiation to mature, multi-nucleated osteoclasts (Bucay *et al.*, 1998; Burgess *et al.*, 1999; O'Brien, Williams and Marshall, 2000; Kearns, Khosla and Kostenuik, 2008). Downstream of RANK activation, NF-κB and cFos are upregulated and NFATC1 is expressed, causing terminal differentiation of osteoclasts

(Takayanagi *et al.*, 2002; Asagiri *et al.*, 2005). NFATC1 is a transcription factor responsible for the expression of TRAP, OSCAR and cathepsin K, all of which are important to osteoclast function (Matsumoto *et al.*, 2004; K. Kim *et al.*, 2005; Y. Kim *et al.*, 2005). OSCAR is part of the leukocyte receptor complex family, and has roles in regulating the immune response, as well as propagating an activation signal in osteoclasts (Kim *et al.*, 2002). Cathepsin K is a protease that degrades collagen and bone matrix (Gelb *et al.*, 1996). One substrate of the TRAP enzyme is osteopontin, which is secreted by osteoblasts to encourage the adherence of osteoclasts to bone. TRAP dephosphorylates osteopontin which causes osteoclasts to detach from bone. In this way, TRAP may have a regulatory role in bone homeostasis (Ek-Rylander *et al.*, 1994).

There are several methods of differentiating osteoclast precursors to mature osteoclasts *in vitro*. The treatment of osteoclast precursor cells with M-CSF and RANKL seems to be the most common method. Generally, M-CSF is added first to stimulate macrophage differentiation, followed by the addition of RANKL to promote cell fusion and further differentiation to osteoclasts (Wani *et al.*, 1999; Cody *et al.*, 2011; Marino *et al.*, 2014). Alternatively, direct co-cultures of osteoblasts with HSCs have been shown to produce osteoclasts (Takahashi *et al.*, 1988). Prostaglandin E2 and vitamin D3 stimulate osteoblasts to produce M-CSF and RANKL, therefore are useful in stimulating osteoclast differentiation in cultures where osteoblasts are also present (Marino *et al.*, 2014). Seeding osteoclast precursors at a high density effectively increases the osteoclast yield *in vitro* (Tevlin *et al.*, 2014).

Negative regulation of osteoclastogenesis is necessary to prevent aberrant bone loss. One regulatory mechanism involves osteoprotegerin (OPG), which is produced by osteoblasts and acts to competitively bind RANKL to prevent downstream activation of RANK on osteoclast precursors (Bucay *et al.*, 1998). This process is tightly controlled by the production of OPG-ligand (OPGL), which binds to OPG in place of RANKL, negating the inhibitory effect on osteoclast production (Burgess *et al.*, 1999). In addition, active osteoclasts may be deactivated by increased cytoplasmic calcium, or recognition of the hormone calcitonin. This results in cytoskeleton

disruption and detachment of the osteoclast from the bone surface, effectively halting resorption (Holloway et al., 1997, Nakamura, 2007).

1.4 Factors affecting Bone Remodelling

Bone is constantly remodelled throughout life according to chemical and mechanical cues related to development and growth. This consists of a resorption phase where old bone is removed, followed by the formation of new bone. Maintaining bone homeostasis requires a tightly controlled balance of osteogenesis & osteoclastogenesis, and there are several clinical and pathological conditions that alter these processes in the periodontium and the skeleton as a whole. The two factors that are focused on in this thesis are mechanical strain and periodontitis, which are discussed in more detail in sections 1.4.1 and 1.4.2.

Other factors that are not discussed in this thesis but may still be pertinent to bone remodelling as a whole are:

- Mutations of genes involved in osteoblast or osteoclast differentiation and function eg. *RUNX2*, *Col1a1*, *Col1a2*, *BMP1*, *Wnt1*, *LRP5*, *RANK* and *Osteocalcin* (Kornak and Mundlos, 2003; Boudin and Van Hul, 2017).
- Deficiencies in certain vitamins and minerals eg. vitamin C is required for collagen production (Murad *et al.*, 1981), and vitamin D promotes osteoblast differentiation and expression of osteocalcin, osteonectin and alkaline phosphatase, which are all required for osteogenesis (Clarke, 2008). Calcium and calmodulin signalling regulate NFATC1 expression, and therefore have roles in regulating osteoclast activation (Kim and Kim, 2016).
- Hormonal changes, eg. oestrogen is thought to prevent apoptosis of osteocytes therefore deficiencies in oestrogen, as seen in menopause, reduce osteocyte number which effectively reduces their capacity to regulate osteogenesis (Plotkin *et al.*, 2005). Insufficient oestrogen levels lead to decreased OPG being produced and increased osteoclastogenesis as a result (Bucay *et al.*, 1998; Riggs, 2000).

1.4.1 Mechanical Strain

One factor which is of particular interest to the dental field is that of mechanical strain. It is well established that mechanical forces can affect bone mass and strength; Examples include tennis players which have larger bones in their playing arm, and bed-bound patients or astronauts who lose bone mass with lack of use or reduced gravity (Goodship *et al.*, 1998; Haapasalo *et al.*, 2000; Klein-Nulend *et al.*, 2003). However, much is still unknown about the exact effects these forces have on the cell and the molecular mechanisms involved.

Mechanical strain is utilised in several clinical scenarios to remodel bone, with one such method being in orthodontic treatments whereby the alveolar bone is remodelled to allow the teeth to be moved (Krishnan and Davidovitch, 2009). Orthodontic tooth movement utilises both tensile stretching and compression forces on different areas of the periodontium in order to remodel the alveolar bone (*Figure 6*). Broadly, the compression of one side of the periodontium causes bone resorption, while the constant tensile stretching of the bone and surrounding tissues on the side away from the direction of tooth movement stimulates osteogenesis (Krishnan and Davidovitch, 2009; Kitaura *et al.*, 2014).

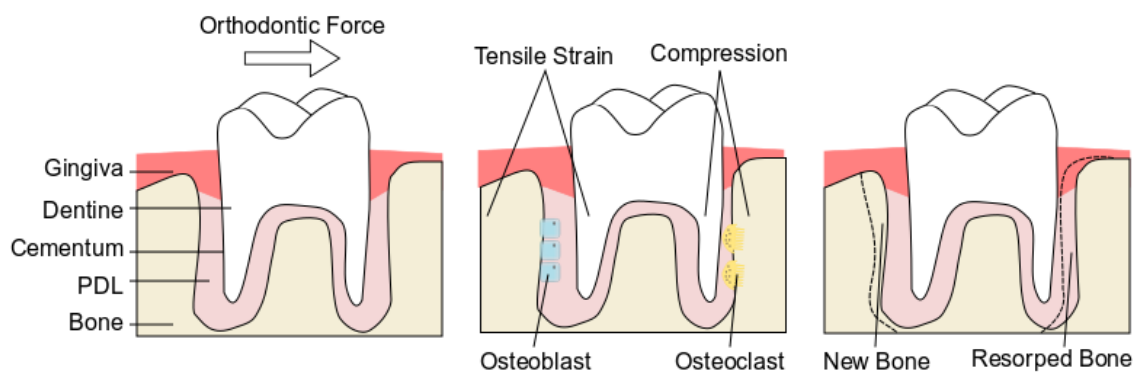


*Figure 6: Orthodontic tooth movement causes bone remodelling; Compression activates osteoclasts to resorb bone, while tensile strain activates osteogenesis and new bone is formed (adapted from Kitaura *et al.*, 2014). PDL = periodontal ligament.*

There is a rising demand for orthodontic treatments in the UK, especially in adult patients between 26-40 years of age ('The number of adults seeking orthodontic treatment in the UK

continues to rise', 2018). However, these procedures are not without their risks, including that of root resorption, enamel demineralisation, damage to the periodontium and an increase in the rate of caries which can compromise the stability and functionality of the periodontium, resulting in further health complications (Wishney, 2017). There is also the issue of relapse, where the teeth move back towards their original position after the orthodontic treatment has finished. While some studies have demonstrated a high percentage of relapse, it is dependent on many factors and therefore difficult to determine the risk to the individual patient (Little, Riedel and Artun, 1988; Littlewood, Kandasamy and Huang, 2017). Current clinical advice often involves the use of retention devices, that may be removeable or fixed retainers, however this requires a life-long commitment from the patient (Littlewood, Kandasamy and Huang, 2017). Even if the orthodontic procedure does not encounter these risks, they are still painful and take months or years to complete, therefore there is a demand for new molecular targets to reduce the time and cost as well as improve the clinical outcomes of orthodontic treatment.

Distraction surgery is another technique that uses mechanical forces to stimulate bone growth, and is used in many aspects of orthopaedic and craniomaxillofacial surgery. It consists of five stages; firstly, the bone is separated via an osteotomy and a distractor is surgically fitted across the gap. A latency period of 5-7 days allows for healing of the surgical site and for the distractor to become stable within the bone (McCarthy *et al.*, 2001). The distractor contains a screw that, when turned, increases the gap between the two sides of the bone, allowing for gradual separation in the distraction phase (Natu *et al.*, 2014). Initial wound healing mechanisms are employed, including the migration of inflammatory cells, and vascular endothelial growth factor (VEGF) initiates angiogenesis (Cano *et al.*, 2006). During the early stages of distraction osteogenesis, there is an increase in OPG, a negative regulator of osteoclastogenesis. Experiments using bisphosphonates have demonstrated that blocking osteoclastogenesis during distraction osteogenesis or fracture healing leads to increased bone mass, due to a delay in the onset of bone resorption (Smith *et al.*, 2004). However, measured osteoclast activity is required in order to remove the old bone and make way for osteogenesis. The mechanical strain

employed initiates osteoblast differentiation and osteogenesis, and mineralisation occurs after 10-14 days (Karp *et al.*, 1992; Natu *et al.*, 2014). This strain usually consists of tension or stretching force, however distraction devices that apply tension and compression forces have been trialled and shown to have some success in regenerating cartilage as well as bone (Schuelke *et al.*, 2018). After the distraction phase, a consolidation period of 8 to 12 weeks allows for healing of the site before the distractor is removed (Natu *et al.*, 2014).

1.4.1.1 *Mechanotransduction*

Cells may be subjected to different types of mechanical strain, which are broadly categorised into tension/tensile, compression or shear stress (Chen, 2008) (*Figure 7*). These forces may be the result of outside influences as with orthodontic tooth movement, or by internal processes such as the forces exerted on the periodontium during tooth eruption. Internal causes of mechanical strain include cytoskeleton changes, the movement of blood through the vasculature, muscle contraction or tissue growth, all of which may be potent signals (Henderson and Carter, 2002; Ingber, 2006; Shwartz, Blitz and Zelzer, 2013). Mechanotransduction, the conversion of mechanical stimulus to a chemical response, is thought to cause direct changes to gene expression, protein conformation, molecule recruitment and effectors such as ion channels (Orr *et al.*, 2006; Jaalouk and Lammerding, 2009; Lecuit, 2010). Mechanotransduction has been shown to propagate signals much faster than diffusion or translocation-based signalling, and mechanical forces have even been shown to displace organelles such as mitochondria up to 20 μ M (Wang *et al.*, 2001; Na *et al.*, 2008). In this way, mechanical strain can have widespread effects on cellular processes, however in many cases the downstream effects are unknown. Mechanosensors include the cytoskeleton, cilia, cell-cell adhesion complexes and focal adhesions which connect the cell to the ECM (Jaalouk and Lammerding, 2009). Systems such as these are particularly important, as force that deforms a random place on the cell membrane will only have local effects, but force applied to integrins can be propagated right into the cell (Wang *et al.*, 2001).

There is a theory called the tensegrity model which states that cells have an inbuilt tension in their cytoskeleton that allows them to withstand mechanical forces (D E Ingber, 1997; D. E. Ingber, 1997). This tension is produced by contraction of myosin motor proteins within microfilaments in the cytoskeleton, which is increased on repeated exposure to strain (Xu, Tseng and Wirtz, 2000; Ingber, Wang and Stamenović, 2014). This tension or pre-stress is said to reduce free movement and prime the cytoskeleton for an immediate response to any external forces (Ingber, 2008). In this way, the configuration of the cytoskeleton is important to the cells' reaction to strain; pre-stress of the cytoskeleton allows for a more efficient reaction to strain, while the cytoskeleton is also key to mechanotransduction (McBeath *et al.*, 2004; Ingber, 2008). Additionally, changes in cell morphology begin with changes to the cytoskeleton, and this is also seen in stem cells as they differentiate (Yourek, Hussain and Mao, 2007; Treiser *et al.*, 2010).

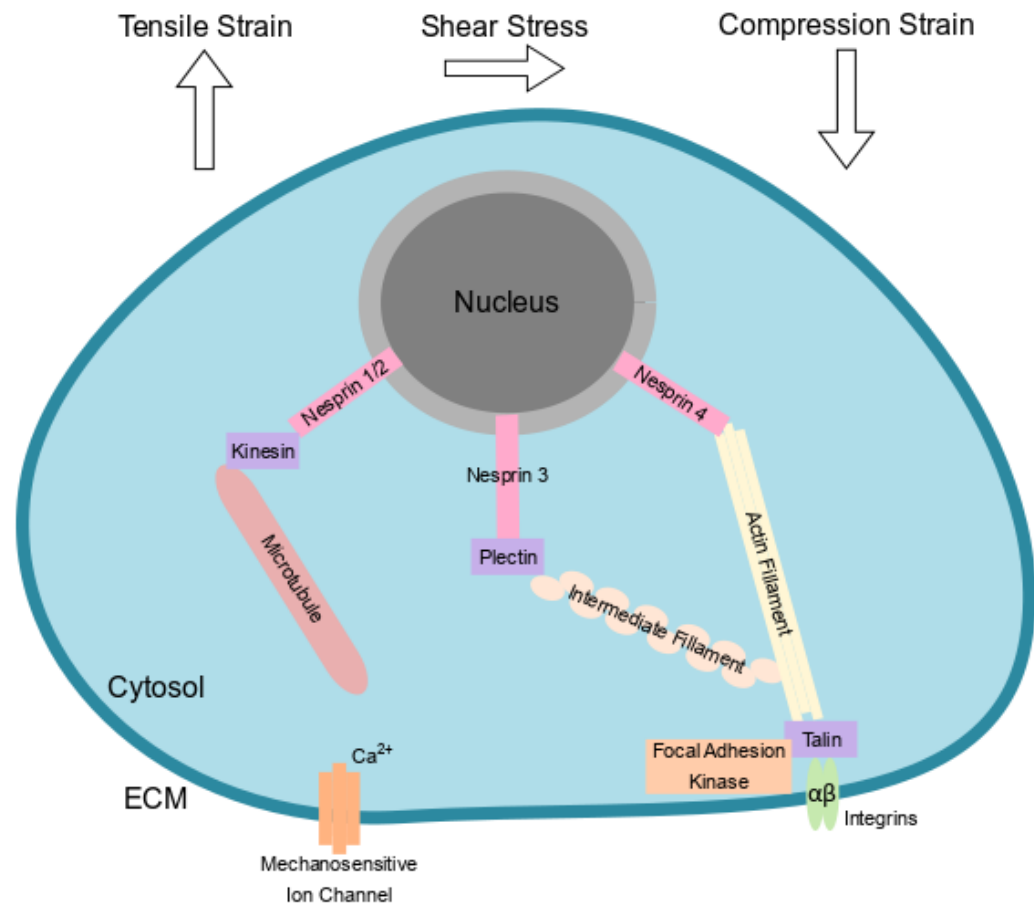


Figure 7: **Mechanotransduction**; Mechanical strain, including tensile, compressive or shear strain, can activate mechanosensitive ion channels, or the force can be propagated into the cell via focal adhesion complexes or through the movement of the cytoskeleton (adapted from Guilak *et al.*, 2009, Martino *et al.*, 2018). ECM = extracellular matrix.

There are many known biological effects of mechanical strain, with more being uncovered as the field develops. Dysfunction of mechanotransduction is implicated in many diseases, including cancer metastasis and muscular dystrophy (Jeanes, Gottardi and Yap, 2008; Jaalouk and Lammerding, 2009). The most commonly used example is that of mechanosensitive hair cells in the inner ear. These stereocilia are precisely aligned and connected together at their tips by tip links. Sound wave vibrations move the cilia, causing mechanical strain at the tip links which results in the opening of ion channels and downstream signalling (Meyer *et al.*, 2005; Muhamed, Chowdhury and Maruthamuthu, 2017). Noise induced hearing loss can occur when exposure to long periods of loud sound causes the hair cells to become damaged and die (Watanabe *et al.*, 2005; Jaalouk and Lammerding, 2009).

Additionally, mechanical forces are involved in many aspects of development, including that of the blood vessels, heart, lung, kidney and bone (Serluca, Drummond and Fishman, 2002; Gutierrez, Suzara and Dobbs, 2003; Mammoto *et al.*, 2009; Mammoto and Ingber, 2010).

One example is in the development of functional, contracting muscle which allows for the onset of embryonic movement. The importance of embryonic movement to development is shown in fetal akineia deformation sequence, a syndrome characterised by limb and craniofacial deformities and abnormal growth caused by movement restrictions in utero (Shwartz, Blitz and Zelzer, 2013). In fact, muscle contractions directly regulate the formation of bone ridges as sites of attachment for tendons to bone during development (Blitz *et al.*, 2009; Berendsen and Olsen, 2015), and muscular dysgenesis mice which lack muscle contraction were found to have reduced chondrocyte proliferation and subsequently smaller skeletal growth plates (Blitz *et al.*, 2009).

Mechanical loading has been investigated in relation to chondrocyte and osteoblast differentiation, both essential to bone development. *In vitro*, primary chondrocytes exposed to periodic matrix deformation which altered their mechanical environment had increased expression of collagen-X, a marker of terminal differentiation of these cells (Wu and Chen, 2000). In several animal studies, periodic strain on the mandible was found to increase the production of Indian hedgehog (Ihh), an important signal in chondrocyte and osteoblast differentiation (Ng TC, Chiu KW, Rabie AB *et al.*, 2006). Additionally, osteoblasts express a number of mechanosensitive ion channels including Piezo1/2 and Transient Receptor Potential (TRP) channels (Katsianou *et al.*, 2018). In particular Polycystin-1, a member of the TRPP family, has been demonstrated to instigate osteogenic differentiation of PDL-derived pre-osteoblasts by upregulating RUNX2 expression in response to tensile strain (Dalagiorgou *et al.*, 2013).

Mechanical loading also influences the size, shape and mass of bone; during development force exerted by developing muscle was found to influence bone length (Sharir *et al.*, 2011), but this is also seen postnatally; for instance, in the example described above of tennis players having larger bones in their racket arms and bed-bound patients losing bone mass due to the lack of

strain from movement or gravity (Haapasalo *et al.*, 2000; Shwartz, Blitz and Zelzer, 2013). One paper utilising a microgravity model demonstrated that osteoblasts have much lower expression of Piezo1, a mechanosensitive ion channel, in response to decreased mechanical. In this instance Piezo1 was found to have roles in MSC differentiation to the osteoblast lineage and Piezo1 knockout mice had defects in osteogenesis, demonstrating the significance of mechanical strain to bone remodelling (Sun *et al.*, 2019). Additionally, osteoporosis patients were found to have decreased levels of Piezo1, a mechanosensitive ion channel which upregulates RUNX2 expression in osteoblasts in response to shear strain (Zhou *et al.*, 2020).

Strain-related bone remodelling is altered with age, with younger individuals having a stronger and more efficient response to changes in mechanical loading than older individuals. This is thought to be related to a reduction in MSC abundance and plasticity with age (Pearson and Lieberman, 2004; Pekovic and Hutchison, 2008; Berendsen and Olsen, 2015). Changes in strain cause MSCs to reorganise their actin cytoskeleton and alter their nuclear pores, which has the capacity to directly influence activation and differentiation (Pekovic and Hutchison, 2008; Swift *et al.*, 2013; Berendsen and Olsen, 2015). The actin cytoskeleton has been shown to stimulate MSC differentiation to osteoblasts by propagating mechanical signals directly into the nucleus (Sen *et al.*, 2015, 2017). Additionally, different mechanical strain profiles have been shown to have different effects on differentiation (Engler *et al.*, 2006; Kurazumi *et al.*, 2011). One paper demonstrated that different mechanical environments had opposite effects on stem cell differentiation, as culturing MSCs on soft gels was neurogenic, gels of medium stiffness were myogenic and culturing on stiff gels or glass was osteogenic (Engler *et al.*, 2006). Reorganisation of the cytoskeleton was found to be key to this change, which may be due to substrate stiffness mimicking the different tissues of the body, for instance brain tissue has less rigidity than bone. Attempts to elucidate the effects of mechanical stress on MSCs have established that fluid shear stress causes MSCs to differentiate to osteoblasts via Transient Receptor Potential Melastatin 7 (TRPM7), a mechanosensitive ion channel that upregulates Osterix expression (Y. S. Liu *et al.*, 2015). This is physiologically relevant with the movement of interstitial fluid inside the canaliculi,

channels inside the bone (Wittkowske *et al.*, 2016). The shear stress produced by the movement of the fluid is thought to be sensed by the dendritic processes of osteocytes, via its actin cytoskeleton (Klein-Nulend, Bacabac and Bakker, 2012; Cowin and Cardoso, 2015). These cells are mechanosensors and are known to regulate bone resorption by interacting with osteoblasts, however the exact mechanisms underlying how mechanotransduction in osteocytes may cause MSC differentiation to osteoblasts are unclear.

Compression force has been established to have a chondrogenic effect on MSCs, perhaps mimicking the tightly packed environment of MSC condensations during development (Luo and Seedhom, 2007). MSCs exposed to periodic tensile strain seem to start expressing early osteogenic markers, including alkaline phosphatase and bone morphogenic protein 2 (BMP2) (Sumanasinghe, Bernacki and Lobo, 2006). However, little is known about the effects of constant tensile strain on MSC differentiation, which is relevant to the periodontium during orthodontic tooth movement.

1.4.1.2 *Stretching Models*

Several strain models are used in the literature to mimic the effects of mechanical strain under different clinical scenarios (Kamble *et al.*, 2016; Muhamed, Chowdhury and Maruthamuthu, 2017). *In vivo* tooth movement has been carried out in rodent, canine, porcine and rabbit models, although more so in rat and dog models than other species (Meikle, 2005; Persson, 2005; Ibrahim *et al.*, 2017). Rat models are useful in terms of rodents' prevalence in *in vivo* research as a whole, with many cellular processes being well-established in this model. Additionally, husbandry is relatively inexpensive and the ability to use transgenic models allows for greater flexibility in experiment design. However, tooth movement experiments often cause an initial reduction in bone volume in rats which is not seen in canine models (Ibrahim *et al.*, 2017). Canine models have also been used in periodontal research for many years, however recently they appear to be being phased out due to ethical reasons (Bayne *et al.*, 2015; Sneddon, Halsey and Bury, 2017). Care must be taken in choosing the correct method for translational

research and understanding its limitations, for instance rodent incisors are constantly occluded due to gnawing behaviour therefore they are constantly growing, unlike human incisors (Warshawsky *et al.*, 1981).

A classic rat tooth movement experiment attaches the first molar to an orthodontic spring which is anchored to the incisor to allow for movement of the molar towards the incisor tip (Nakano *et al.*, 2014; Hikida *et al.*, 2016). While these achieve effective tooth movement, the growth of the incisor means that the device needs to be re-adjusted, typically every week. This method can also be achieved by surgically implanting a device into the alveolar bone to attach the orthodontic spring to. These skeletal anchorage devices do not require re-adjustment of the device therefore are better for long-term studies, however this method requires more invasive surgery than others (Kaipatur *et al.*, 2015). These methods are generally used to apply constant tensile strain, similar to that used by current orthodontic methods.

Step-wise bite jumping appliances may be used which move the mandible intermittently (Ng TC, Chiu KW, Rabie AB *et al.*, 2006; Oksayan, Sokucu and Ucuncu, 2014). Devices to apply compressive loads have also been used to examine periodontal compression in relation to jaw movement or orthodontic tooth movement (Magara *et al.*, 2012). Aside from tooth movement models, other *in vivo* models of mechanical strain involve spinal cord compression in rats and the effects of forced ventilation on mice (Abrams *et al.*, 2009; Xue *et al.*, 2013). With many of these *in vivo* models, measuring the amount of strain is a challenge; some papers use strain gauges or track magnets with MRIs, while others compare microCT images of before and after strain (Huang *et al.*, 2019).

For *in vitro* models, microfluidic devices are well-established for use in investigating shear stress (Qi, Hoelzle and Rowat, 2012), however compression strain is more difficult to apply and maintain *in vitro* (Anderson and Johnstone, 2017). Some methods involve compressing cells via capillary action or by placing agarose sheets and coverslips or weights onto monolayer cultures, although it is difficult to control the precise amount of compression the cells are receiving (King,

Veltman and Insall, 2011). Compression systems are commercially available however the level and duration of strain is more limited than with the majority of tensile strain models (Alihemmati *et al.*, 2017). Early experiments produced tensile strain *in vitro* using micropipettes, forceps or magnets (Sun *et al.*, 2004; Sniadecki *et al.*, 2008; Kamble *et al.*, 2016). While these were effective, it was difficult to quantify the amount of strain applied, to ensure the strain was given to the correct axis (for instance uniaxial or biaxial strain), or to do long-term or high throughput experiments. Current *in vitro* models often rely on flexible culture plates composed of silicone or polydimethylsiloxane (PDMS) membranes. These allow for the use of normal cell culture techniques for the most part, however these materials are hydrophobic and therefore require coating to allow cell attachment. Commonly used coating solutions include collagen, fibronectin or laminin coating, which are fairly simple and inexpensive (Halldorsson *et al.*, 2015). Sometimes hydrogels, collagen gels or sponges are used to mimic the ECM and provide a 3D environment for cells (Wu and Chen, 2000; Kanayama *et al.*, 2008; Tondon and Kaunas, 2014). Alternatively, alginate or gelatine scaffolds or hydrogels are used to mimic the *in vivo* situation (Altman *et al.*, 2002; Awad *et al.*, 2004; Guilak *et al.*, 2009). However, depending on the cell stretching mechanism used, these gels or scaffolds may deform differently in some areas to others, meaning not all cells are exposed to the same level or direction of strain at the same time. More precise methods of applying tensile strain are achieved *in vitro* through computer-controlled mechanical motors or pneumatic actuators acting on flexible PDMS membranes (Neidlinger-Wilke *et al.*, 1994; Ahmed *et al.*, 2010; Huh *et al.*, 2010; Moraes *et al.*, 2010; Simmons *et al.*, 2011; Huang and Nguyen, 2013). Alternatively, microelectromechanical systems (MEMS) and electromagnetic devices use actuators controlled by an electric charge, which again can be controlled on a computer for more precise application of strain (Kamotani *et al.*, 2008; Harshad *et al.*, 2016; Poulin *et al.*, 2016). One such device produced by Professor Herbert Shea's lab was trialled as an *in vitro* cell stretching model for this thesis. Additionally, a commercial system produced by Strex was used which used PDMS-based well plates (Tondon and Kaunas, 2014;

Koseki *et al.*, 2019; Yamada *et al.*, 2019). The comparison and optimisation of these stretching devices is discussed in section 3.2.2.

1.4.2 Periodontitis

Inflammation is known to stimulate osteoclast differentiation and activation, as is evidenced in some inflammatory disorders that exhibit excessive bone loss. One such disease that is of particular interest to the dental field is periodontitis. Periodontitis describes a chronic inflammatory disease of the oral cavity stimulated in response to bacteria forming a plaque biofilm over the tooth surface which extends below the gingival barrier (*Figure 8*). Cytokines and growth factors, such as TNF α , IL1, IL6, IL17, and TGF β activate T-cells and dendritic cells and cause them to produce RANKL, the key factor involved in osteoclast differentiation (Cochran, 2008; Hienz, Paliwal and Ivanovski, 2015). Additionally, inflammation causes osteoblasts to express monocyte chemoattractant protein 1 (MCP1) to recruit circulating osteoclast precursors to the bone surface which then differentiate into active osteoclasts (Graves, Jiang and Valente, 1999; Chen *et al.*, 2018). This increase in osteoclast activity is not balanced by osteogenesis, resulting in alveolar bone loss, the destruction of the periodontium and subsequent tooth loss (Wiebe *et al.*, 1996; Hienz, Paliwal and Ivanovski, 2015). Inflammatory cues have previously been established to alter the activation or differentiation status of stem cells and immune regulation is inbuilt into many facets of macrophage polarisation, activation and differentiation (Pietras, 2017; Yang, Yu and Zhou, 2017; Cafiero *et al.*, 2018). Therefore, there are many stages where osteoclast differentiation may be affected by a dysregulated immune system.

There are several species of bacteria associated with periodontal disease, however *Porphyromonas gingivalis* (*P.gingivalis*) is the most commonly studied as an increase in the prevalence of this species in the oral cavity unbalances the microbiome of patients with periodontitis. Local inflammation ultimately leads to an increase in the number of active osteoclasts which is not balanced by osteoblasts, and results in net alveolar bone loss (Cochran, 2008; Hienz, Paliwal and Ivanovski, 2015).

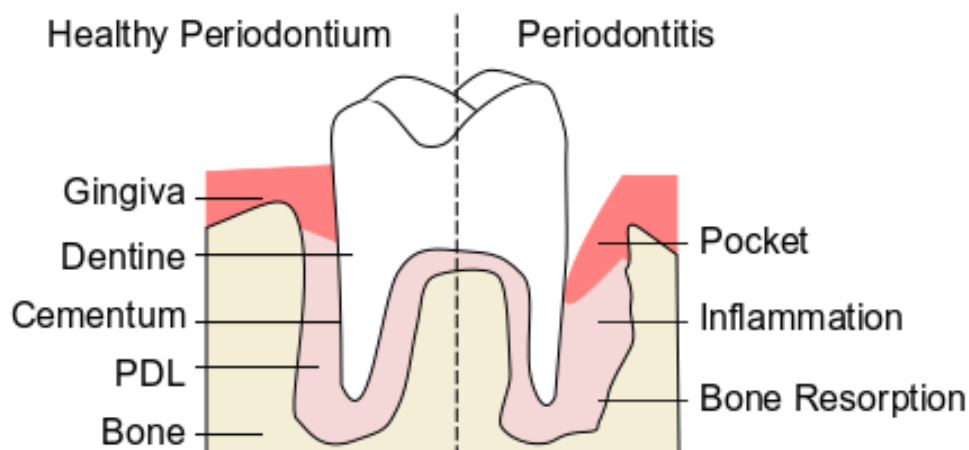


Figure 8: **Periodontitis**; In advanced periodontitis, excess inflammation results in alveolar bone loss and destruction of the gingiva leading to deep periodontal pockets (adapted from Fan & Cook, 2004). PDL = periodontal ligament.

Periodontitis can also activate monocytes that circulate to other parts of the body, and there is some evidence for *P.gingivalis* itself travelling through the bloodstream and causing inflammation at other sites (Hayashi *et al.*, 2010). Links have been made between periodontal disease and stroke (Sfyroeras *et al.*, 2012; Chi *et al.*, 2019), rheumatoid arthritis (Detert *et al.*, 2010), diabetes (Lakschevitz *et al.*, 2011), cardiovascular disease (Belstrøm *et al.*, 2012; Nguyen *et al.*, 2015) and pre-term births in pregnant women (Katz *et al.*, 2009; Faas *et al.*, 2014). Between 2005 and 2015 there was an increase of 25.4% in the cases of periodontal disease recorded worldwide, therefore considering the prevalence of this health condition it is even more important to understand the mechanisms behind the disease (GBD 2015 Disease and Injury Incidence and Prevalence Collaborators, 2016).

While the elevated presence of *P.gingivalis* is commonly associated with periodontal disease, it is not considered to be solely responsible for causing the disease and its associated health detriments, but rather that factors within the host play a large role (Page *et al.*, 1997; Al-Qutub *et al.*, 2006). It is thought to be the host's innate immune system reacting to the presence of the pathogen which is ultimately responsible for alveolar bone loss, and may explain how some patients with good oral health have periodontitis while others with poor dental health practices never develop the disease (Al-Qutub *et al.*, 2006). However, the exact mechanisms involved remain unknown.

1.4.2.1 Lipopolysaccharide (LPS)

In periodontitis, cells in the periodontal pocket are constantly exposed to bacterial stimuli, specifically that of lipopolysaccharide (LPS), a molecule found in the cell walls of Gram-negative bacteria. It was originally referred to as endotoxin as it was thought to be a toxin released into the environment by bacteria after destruction of their cell wall, compared to exotoxin which were readily released into the environment (Rietschel and Cavaillon, 2003). The current understanding is that LPS is released from the cell wall on the destruction of the bacterium and actively secreted via outer membrane vesicles (Beveridge, 1999).

Generally, LPS consists of a polysaccharide O-antigen, an outer and inner polysaccharide core, and lipid A (*Figure 9*). The structure and function of LPS as well as its downstream signalling potential in mammalian cells has mostly been characterised using *Escherichia coli* (*E.coli*) LPS, however many of the key structures are conserved across other Gram negative species (Raetz and Whitfield, 2002).

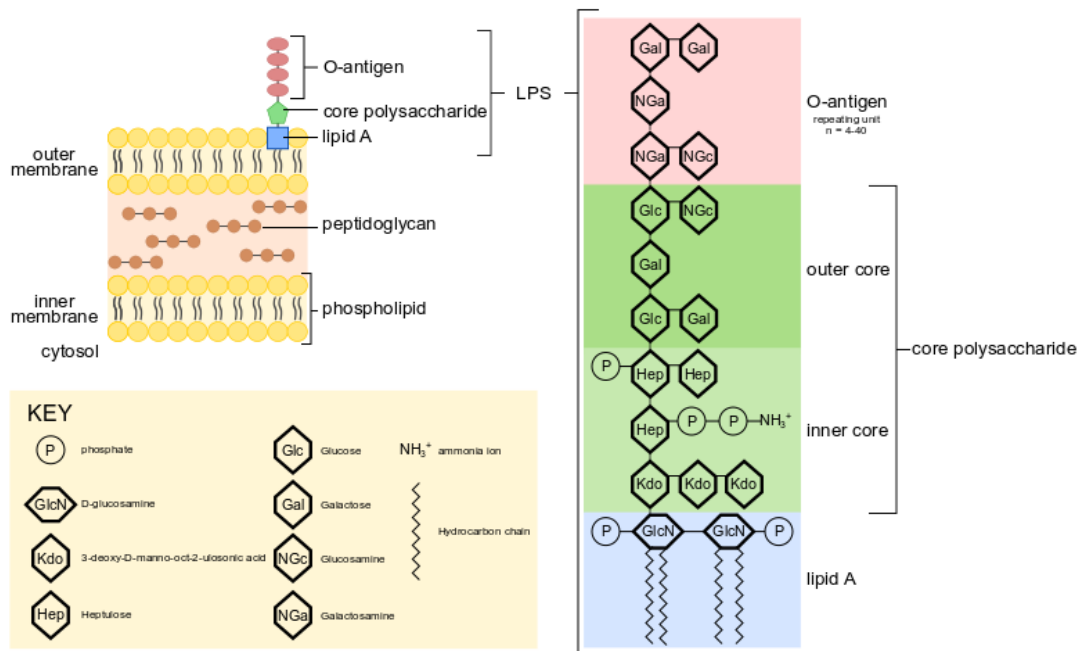


Figure 9: LPS chemical structure and location; LPS is located in the outer membrane of Gram-negative bacteria and consists of lipid A, core polysaccharide and O-antigen. The lipid A and inner polysaccharide core are highly conserved however the outer core and O-antigen differ between bacterial serotypes. The O-antigen has between 4 and 40 replicates of the same structural unit, although only one is demonstrated here. (adapted from Bagheri, Keller & Dathe, 2017, Beutler & Rietschel, 2003). LPS = lipopolysaccharide.

Lipid A is a hydrophobic phospholipid found in the outer membrane of Gram-negative bacteria, and was found to be the endotoxic component of LPS capable of stimulating the inflammatory response (Beutler and Rietschel, 2003). On destruction of the bacterium, lipid A molecules are released from where they are anchored in the bacterial membrane, and may cause harmful downstream effects on the host, including septic shock. The two phosphate groups and two acyloxyacyl groups that comprise the basic structure of lipid A are conserved across the majority of Gram-negative bacteria (Raetz and Whitfield, 2002).

Lipid A is attached to the rest of the LPS molecule by a polysaccharide core. This core is divided into an inner, which is bound to lipid A, and an outer, which attaches to the O-antigen. The inner core is structured as a chain of 3-deoxy-D-manno-oct-2-ulosonic acid (Kdo) residues which is conserved across the majority of Gram-negative bacteria (Rietschel *et al.*, 1994). The structure of the outer core is more varied across different species (Raetz and Whitfield, 2002).

The O-antigen is a polysaccharide chain extending from the outer core to the cell surface of the bacterium. It has roles in attempting to prevent activation of the host's complement system, a cascade of proteins that ultimately leads to the destruction of the pathogen (Joiner *et al.*, 1983; Whitfield, Amor and Köplin, 1997; Raetz and Whitfield, 2002). Across different species the O-antigen has perhaps the most structural diversity compared to other parts of LPS, with changes in the length and orientation of the chain, as well as acetylation or glycosylation modifications. Additionally, some species, such as *Salmonella minnesota*, contain rough LPS which does not contain an O-antigen at all (Triantafilou, Triantafilou and Fernandez, 2000).

Differences in LPS structure are seen between bacterial species and serotypes, altering which receptors are activated on the host and therefore the downstream signalling activated. Two species of note for this work are *E.coli* and *P.gingivalis*. *E.coli* is a prevalent, pathogenic strain of Gram negative bacteria which is associated with many human diseases, including sepsis, pneumonia, meningitis and urinary tract infections (Eisenstein and Jones, 1988; Marrie *et al.*, 1998; Conceição *et al.*, 2012). It is well characterised in terms of its LPS structure, signalling and downstream effects on its host, therefore it is useful to study both as a positive control and to investigate the molecular mechanisms of inflammation and its effect on other processes in the host cell. *E.coli* LPS causes activation of the TLR4 receptor present on many human cells including macrophages, and the downstream signalling described earlier in this section.

P.gingivalis LPS has a similar structure to that of *E.coli* LPS, however it differs in the number of lipid A molecules, their position and phosphorylation (Kumada *et al.*, 1995; Darveau *et al.*, 2004; Reife *et al.*, 2006). Currently there is some debate over which host receptors are activated by *P.gingivalis* LPS, which mainly centres around toll-like receptors (TLRs) 2 and 4. The general consensus has been that both TLR2 and TLR4 are activated (Bainbridge, Coats and Darveau, 2002; Darveau *et al.*, 2004; Nativel *et al.*, 2017), however some papers argue that *P.gingivalis* LPS acts exclusively through TLR4 and that studies citing activation of TLR2 have issues with LPS purity (Nativel *et al.*, 2017). It is important to note that these observations were specific to mice,

and that human studies may demonstrate activation of TLR2. In addition, *P.gingivalis* LPS activates an immune response in C3H/HeJ mice which do not have TLR4 activity (Kirikae *et al.*, 1999; Hirschfeld *et al.*, 2001). Therefore, for the purpose of this work both TLR2 and TLR4 were considered when *P.gingivalis* LPS was used.

1.4.2.1.1 Signalling & Inflammation

Recognition of LPS by macrophages is known to cause inflammation as the host attempts to tackle the pathogen (*Figure 10*). This involves the upregulation of cytokines and recruitment and activation of phagocytes and antigen-presenting cells (Beutler and Rietschel, 2003). The downstream effects of LPS signalling are mediated by its receptors, including TLRs and CD14. In addition to LPS, CD14 and TLRs 2 and 4 can also be stimulated by other PAMPs or endogenous molecules, such as hyaluronan (HA) (Termeer *et al.*, 2002).

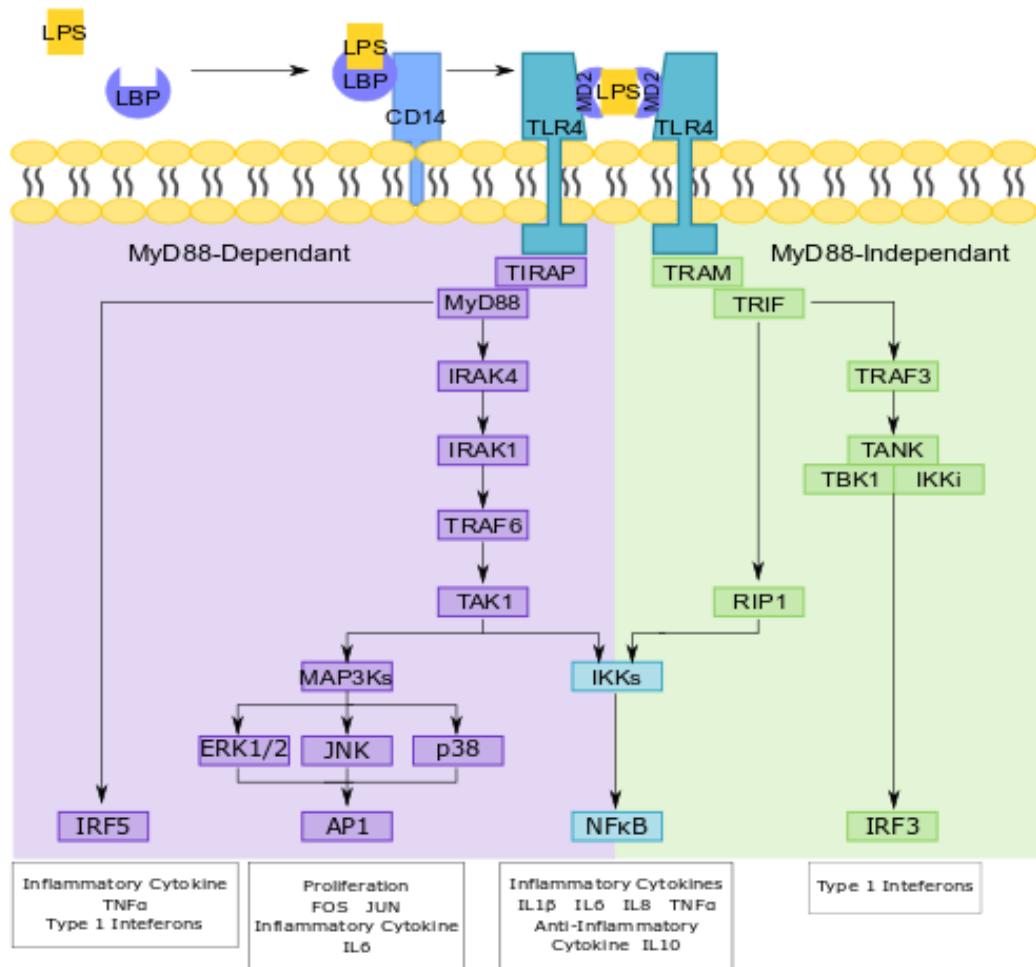


Figure 10: **LPS signalling**; LBP binds LPS and presents it to CD14, which facilitates its binding to TLR4 and MD2. Downstream of TLR4 signalling, AP-1 and NF-κB are activated and cytokines are produced that may act on the cell to further activate or attempt to modulate inflammation. MyD88-dependant signalling also results in IRF5 upregulation, while MyD88-independant signalling causes IRF3 production (adapted from Lu, Yeh & Ohashi, 2008).

LPS binding protein (LBP) binds LPS in plasma and transports it to cells of myeloid lineage, where it may interact with cell surface receptors such as CD14 and TLR4 (Tobias, Soldau and Ulevitch, 1986; Wright *et al.*, 1990; Ryu *et al.*, 2017). CD14 binds LPS and regulates downstream signalling by chaperoning it to TLR4 (da Silva Correia *et al.*, 2001). TLR4 was discovered as an LPS receptor when C3H/HeJ mice were found to have a spontaneous point mutation in the *Lps* locus, a homologue of the human *TLR4* gene, which eliminated any response to LPS exposure (Heppner and Weiss, 1965; Watson and Riblet, 1974, 1975). TLR4 forms a complex with MD2 and once activated will dimerize and stimulate a signalling cascade via its intracellular toll-interleukin 1 (TIR) domains. Several proteins contain a TIR binding domain which confers downstream

signalling by TLR4, including myeloid differentiation primary response gene 88 (MyD88), TIR domain-containing adaptor protein (TIRAP), TIR domain-containing adaptor inducing IFN β (TRIF), TRIF-related adaptor molecule (TRAM), and sterile α and HEAT-armadillo motifs-containing protein (SARM). There are thought to be two main signalling cascades connected to LPS activation of TLR4; MyD88-dependant signalling utilises MyD88 and TIRAP and induces the expression of inflammatory cytokines, while MyD88-independent signalling involves TRIF and TRAM proteins and induces interferon (IFN) production for immune regulation (Akira and Takeda, 2004). MyD88-independent signalling also causes LPS-induced endocytosis of TLR4, which is CD14-dependant (Z. Jiang *et al.*, 2005; Kagan *et al.*, 2008; Zanoni *et al.*, 2011).

Both pathways result in the activation and nuclear translocation of the nuclear factor kappa light-chain enhancer of activated B cells (NF- κ B) and activator protein 1 (AP-1); transcription factors with roles in cytokine upregulation (Lu, Yeh and Ohashi, 2008). Downstream of LPS-dependant TLR4 signalling, macrophages produce IL1, IL6, IL8, IL12, and TNF α (Akira and Kishimoto, 1992; Tichomirowa *et al.*, 2005). Each of these cytokines may then bind to receptors on macrophages themselves. These autocrine loops stimulate and regulate the inflammatory response, including the production of prostaglandin E2, IFN- β , TGF β , IL10 and macrophage inhibitory protein (MIP-1 α) (Xaus *et al.*, 2000; Arango Duque and Descoteaux, 2014).

P.gingivalis is also said to cause inflammation by activating the complement system, as its gingipain, a protease secreted by the bacteria, cleaves C5 to form C5a which activates C5aR to trigger inflammation and TLR2-dependant cross-talk with leukocytes (Hajishengallis, Darveau and Curtis, 2012). On activation, TLR2 forms heterodimers with TLR1 for downstream activation of the MyD88-dependant pathway, or TLR6 for MyD88-independent signalling, resulting in NF- κ B and AP-1 activation and downstream cytokine production (Oliveira-Nascimento, Massari and Wetzler, 2012). Dimerization with TLR1 is associated with Gram negative bacteria, while dimers with TLR6 occurs due to recognition of Gram positive bacteria (Farhat *et al.*, 2008). In addition

to certain forms of LPS, TLR2 is also activated by lipoproteins and peptidoglycan (Lien *et al.*, 1999).

Chronic exposure to LPS can cause tolerance whereby the host's innate immune response is diminished, either as a survival mechanism or the result of a dysregulated immune system (Raetz *et al.*, 1991). Periodontitis is an example of how changes in inflammation may alter osteoclast activation and result in disease, therefore it stands to reason that LPS tolerance, which drastically modulates the immune response, may have roles in disease either by contributing to or protecting against it. Therefore, this thesis attempted to investigate whether LPS tolerance plays a role in disease progression by studying its effect on osteoclast differentiation.

1.4.2.1.2 LPS Tolerance

LPS tolerance describes when cells that have been exposed to repeated LPS treatment exhibit a diminished inflammatory response compared to cells exposed to LPS only once. It is also related to concentration, with repeated low level LPS exposure allowing the organism to withstand subsequent exposure to lethal levels of LPS (Heremans *et al.*, 1990; Wilson *et al.*, 1997; Rocksén *et al.*, 2004; Maitra *et al.*, 2012). Tolerance has been described both *in vivo* and *in vitro*, and with exposure to native LPS and non-toxic or synthetic forms of LPS such as MPLA (Qureshi *et al.*, 1998; Stark *et al.*, 2016; Vergadi, Vaporidi and Tsatsanis, 2018). It results from the persistent activation of TLRs causing the innate immune system to be reprogrammed (Biswas and Lopez-Collazo, 2009; Vergadi, Vaporidi and Tsatsanis, 2018). A cell that has been tolerized to LPS has lower expression of inflammatory cytokines TNF α , IL1 and IL6, and upregulation of anti-inflammatory cytokines such as IL10, on further exposure to LPS (Medvedev, Kopydlowski and Vogel, 2000).

There have been several LPS tolerance mechanisms proposed where TLR4 is altered in some way to prevent downstream signalling (*Figure 11*). Some papers suggest a decrease in the expression of TLR4 or modifications to the receptor (Medvedev *et al.*, 2007), however several studies have demonstrated that there is not a decrease in TLR4 expression in cells tolerized to LPS (Medvedev

and Vogel, 2003; Medvedev *et al.*, 2007). Post-translational modifications of proteins involved in TLR4 signalling are altered in tolerized cells; this includes impaired phosphorylation of TLR4 and its downstream signalling partners TIRAP, MyD88 and IL-1R-associated kinase (IRAK)-Myd88 complexes (Medvedev *et al.*, 2007), and the ubiquitination of IRAK1, TNF receptor-associated factor (TRAF) -3 and -6, which leads to their degradation and inhibition of signalling through these mediators (Boone *et al.*, 2004; Xiong *et al.*, 2011; Li *et al.*, 2016). Cells tolerized to LPS also have increased expression of negative regulators of TLR4 signalling, including Toll-interacting protein (Tollip), SH-2 containing inositol 5' polyphosphatase 1 (SHIP-1), suppressor of cytokine signalling 1 (SOCS-1), and tumour necrosis factor alpha-induced protein 3 (A20) (Piao *et al.*, 2009; Xiong and Medvedev, 2011). In fact, one paper demonstrated that LPS tolerance is not achievable if SHIP-1 is inhibited or knocked out (Sly *et al.*, 2004). Additionally, the activation of microRNAs that target IRAK1 and TRAF6 in tolerised cells prevents downstream Myd88-dependant signalling (Nahid *et al.*, 2009; Curtale, Rubino and Locati, 2019). There may also be an epigenetic cause, with one paper demonstrating TLR-induced chromatin modifications that cause inflammatory genes to be silenced and anti-inflammatory genes to be primed for activation (Foster, Hargreaves and Medzhitov, 2007). All of these factors ultimately lead to inhibition of TLR signalling, decreased expression of the NF- κ B transcription factor, and a subsequent reduction in inflammatory cytokine expression (Böhrrer *et al.*, 1997; Fan and Cook, 2004).

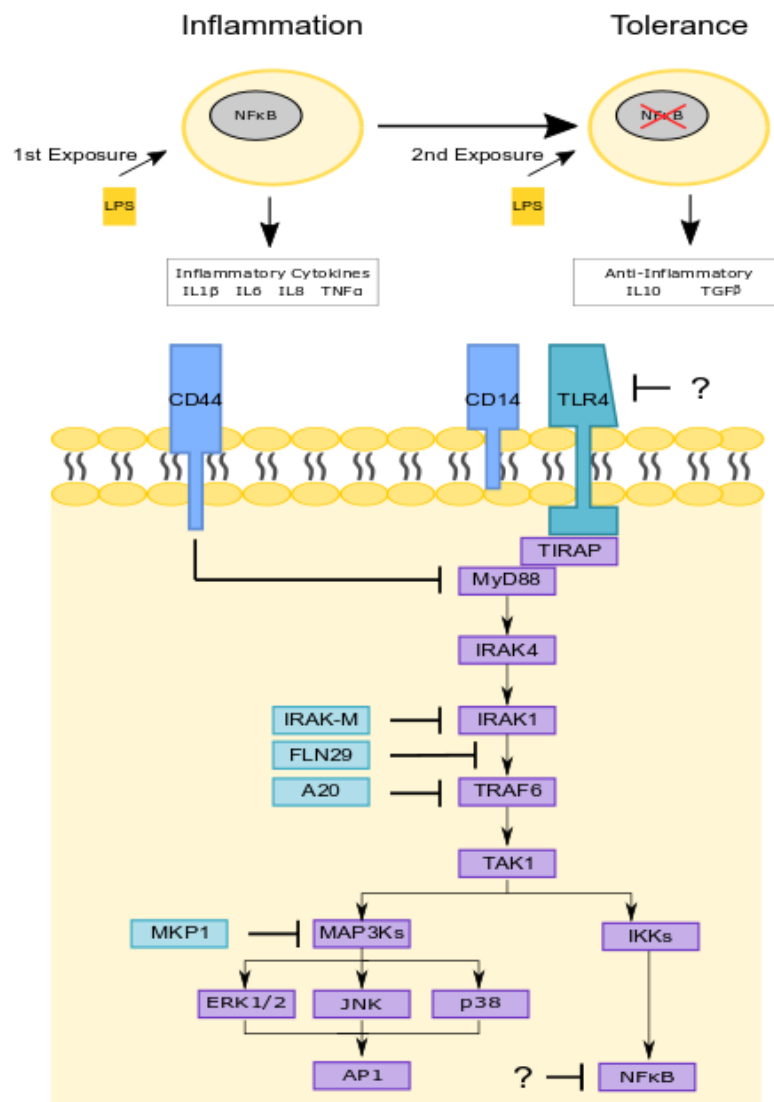


Figure 11: **The molecular mechanisms behind LPS tolerance**; repeated exposure to LPS results in a reduction in inflammatory cytokine expression and an increase in anti-inflammatory proteins. There are several known inhibitors of various parts of MyD88-dependant TLR signalling that are implicated in LPS tolerance, however the exact mechanisms remain unknown (adapted from Biswas & Lopez-Collazo, 2009, Lopez-Collazo & Fresno, 2013).

LPS tolerance may be a sign of a dysregulated immune system, however it was originally thought to be a survival mechanism and there is still evidence for this in the literature. While inflammation is a survival mechanism, it can have detrimental effects on the organism if it is not well controlled. For instance, excess NF-κB and TNFα are thought to be responsible for the potentially toxic effects of inflammation seen in conditions such as sepsis, as they maintain high cytokine production which leads to tissue damage (Wentowski, Mewada and Nielsen, 2019). Sepsis describes an acute intravascular infection, resulting in a large and prolonged

overproduction of inflammatory cytokines and subsequent organ failure (van der Bruggen *et al.*, 1999; Wentowski, Mewada and Nielsen, 2019). LPS tolerance has been observed in septic patients or models of sepsis; in one example, neutrophils that were isolated from the blood of a septic patient did not exhibit an increase in inflammatory cytokine production when exposed to a subsequent LPS challenge *ex vivo*, unlike control cells from a healthy patient (McCall *et al.*, 1993). Similarly, cells tolerized to low levels of LPS have been found to survive a subsequent lethal dose of LPS, or have an attenuated inflammatory response to treatment with a higher concentration of LPS which could cause inflammatory tissue damage (Heremans *et al.*, 1990; Wilson *et al.*, 1997; Rocksén *et al.*, 2004; Maitra *et al.*, 2012).

However, patients that survive sepsis have an altered immune response which makes them vulnerable to further infections (Munoz *et al.*, 1991), similar to what is seen in cystic fibrosis patients who became immunocompromised following tolerance to LPS (del Fresno *et al.*, 2008, 2009). This is sometimes called compensatory anti-inflammatory syndrome, and demonstrates that LPS tolerance may also cause health concerns (Bone, Grodzin and Balk, 1997; Adib-Conquy and Cavaillon, 2009).

LPS tolerance has been well established to occur in monocytes and macrophages, however it has also been demonstrate in neutrophils and epithelial, endothelial and dendritic cells in the literature (Ogawa *et al.*, 2003; Fekete *et al.*, 2012; Günther *et al.*, 2017; Vergadi, Vaporidi and Tsatsanis, 2018). Since osteoclasts come from the monocyte lineage, we considered two hypotheses regarding LPS tolerance for this thesis: Firstly, that tolerised monocytes or macrophages altered osteoclast differentiation in periodontitis, and secondly that the osteoclast precursors themselves were tolerised to LPS which affected their differentiation to functional osteoclasts.

In addition to investigating the effect of LPS tolerance on osteoclast differentiation, Hyaluronan (HA) signalling was considered as a potential mechanism for several reasons. Not only is HA synthesis upregulated in chronic inflammation, but HA has roles in modulating stem cell

activation and differentiation (Vigetti *et al.*, 2010; Cyphert, Trempus and Garantziotis, 2015). Most significantly to this work, signalling via high molecular weight (HMW) HA has been shown to inhibit osteoclast differentiation and has been investigated regarding periodontal wound healing (Luo and Seedhom, 2007; Fujioka-Kobayashi *et al.*, 2017).

1.4.2.2 Hyaluronan

HA is a glycosaminoglycan consisting of alternating D-glucuronic acid and N-acetyl D-glucosamine disaccharide molecules bound by β 1,3 and β 1,4 glycosidic bonds (Figure 12). It is a prominent component of the ECM, providing structure, elasticity and shock-absorbance to the tissue, and hydration to the surrounding cells due to its hydrophilic properties (Day and Prestwich, 2002; Vigetti, Karousou, *et al.*, 2014). HA has also been identified to have signalling properties, with roles in inflammation, cell migration, division, activation and differentiation (Cyphert, Trempus and Garantziotis, 2015).

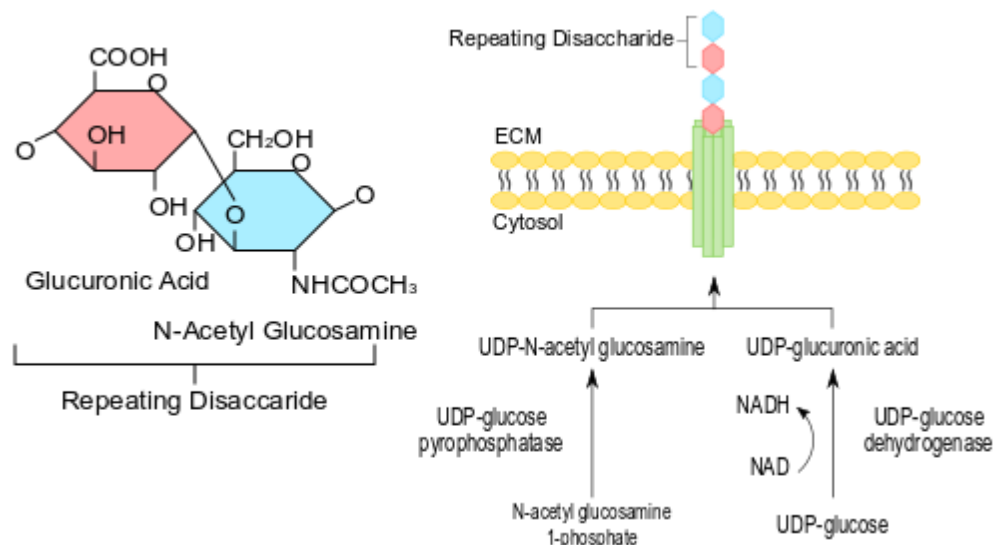


Figure 12: **Hyaluronan structure and synthesis**; A: HA is composed of repeating units of glucuronic acid and N-acetyl glucosamine; B: HAS enzymes produce HA into the extracellular space (adapted from Wheeler-James, Farrar & Pitsillides, 2010, Tammi *et al.*, 2011). HA = hyaluronan, ECM = extracellular matrix, UDP = urine diphosphate, NAD = nicotinamide adenine dinucleotide, NADH = nicotinamide adenine dinucleotide + hydrogen.

The substrates required for HA synthesis are formed from the conversion of N-acetyl glucosamine 1-phosphate to urine diphosphate (UDP) N-acetyl glucosamine (UDP-GlcNAc) and the production of UDP-glucuronic acid (UDP-GlcUA) by the removal of a hydrogen from UDP-glucose. The removal of UDP from these substrates produces a disaccharide chain of alternating

GLcUA and GlcNAc molecules, forming HA (Wheeler-Jones, Farrar and Pitsillides, 2010; Moretto *et al.*, 2015; Kuipers *et al.*, 2016) (Figure 12).

Glycosaminoglycans often have many modifications including acetylation and sulfation, however HA does not undergo any of these modifications and is not branched, meaning it is a simple molecule that differs only in the number of disaccharide chains it possesses (Vigetti, Karousou, *et al.*, 2014). HA molecules can be as large as 10^4 kDa, and any HA molecule of approximately 800 kDa or more is designated as high molecular weight (HMW) (Toole, 2001; Li *et al.*, 2007). The definition of low molecular weight (LMW) HA can vary from paper to paper, however it often includes molecules below 25 disaccharides, or approximately 10 kDa (West *et al.*, 1985; Weigel and Baggenstoss, 2017). These distinctions are significant, as HMW and LMW HA often have opposite signalling effects. Additionally, the molecular weight may also impact HA's role in the ECM. Many papers demonstrate that as HA size decreases, the molecule undergoes a conformational change from a coil to a rod (Mendichi, Šoltés and Giacometti Schieron, 2003; La Gatta *et al.*, 2010). This has implications in its role as a structural molecule, as the large, coiled molecules are more flexible than smaller, rod-like HA (La Gatta *et al.*, 2010).

Unlike other glycosaminoglycans, HA is not synthesised in the Golgi apparatus but instead is produced into the extracellular space by hyaluronan synthases (HAS) in the plasma membrane (Laurent and Fraser, 1992). There are three types of these enzymes in mammals; HAS1 and HAS2 are associated with HMW HA, whilst HAS3 produces LMW HA (Tammi *et al.*, 2011). Additionally, LMW HA is also formed when HMW HA molecules are degraded by hyaluronidases, free radicals, or lysosomes if HA is internalised by the cell (Greenwald and Moy, 1980; Šoltés *et al.*, 2006; Girish and Kemparaju, 2007).

In adult tissue, expression of HAS enzymes is stimulated by TGF β , IL-1 β , TNF α , FGF2, EGF or PDGF, which can be expressed locally or by circulating cells such as monocytes (Jacobson *et al.*, 2000; Oguchi and Ishiguro, 2004; Tammi *et al.*, 2011). HAS2 is the most ubiquitous HAS enzyme present in adult mammalian cells, and synthesis of HA via this enzyme is stimulated by

inflammatory cytokines and NF- κ B signalling (Vigetti *et al.*, 2010). It has been suggested that HA synthesis by HAS2 requires ubiquitination of K190, a lysine residue in the intracellular domain HAS, and dimerization of HAS2, either as a homodimer or a heterodimer with HAS3 (Karousou *et al.*, 2010; Tammi *et al.*, 2011). HAS1 requires a higher concentration of UDP-GlcUA and UDP-GlcNAc for HA synthesis than the other enzymes, therefore is more active in hyperglycaemia when the proportions of these disaccharides are high (Rilla *et al.*, 2013). HAS3 is highly expressed in inflammatory conditions, upregulating production of LMW HA (Saari, 1991; McKee *et al.*, 1996) (Kultti *et al.*, 2006; Tammi *et al.*, 2011).

Once translated, HAS enzymes are transported from the ER to the Golgi then to the plasma membrane, which is a glucose-dependant process (Müllegger *et al.*, 2003; Tammi *et al.*, 2011). HAS enzymes have been observed intracellularly as a reserve, however they are usually not active until they reach the plasma membrane and can produce HA into the extracellular environment (Rilla *et al.*, 2005; Törrönen *et al.*, 2014). However, HA may be produced intracellularly in times of hyperglycaemia, inflammation or ER stress (Hascall *et al.*, 2004, 2014; A. Wang *et al.*, 2011). This was of particular interest for this thesis as glucose availability and cellular stress are well-established modulators of the autophagy pathway (see section 1.5 for details).

1.4.2.2.1 Signalling

HA signalling has been established in many cell types and with roles in angiogenesis, inflammation, cell migration, activation and differentiation (Litwiniuk *et al.*, 2016) (*Figure 13*). The main receptor of HA is CD44, a membrane-bound receptor with an intracellular region and extracellular binding domain, which is present on almost all cell types (Aruffo *et al.*, 1990; Bajorath *et al.*, 1998). There are 10 isoforms of CD44 due to alternative splicing of the extracellular portion of the protein, resulting in different HA binding properties; these isoforms are present in different cell types, which may explain the range of downstream effects exhibited by different cells (Lesley *et al.*, 1997). In addition to stimulating downstream intracellular

signalling, CD44 binding also mediates the binding of HA in the ECM to other molecules, including the hyaladherins aggrecan, versican, and CD38 (Lesley *et al.*, 1997; Day and Prestwich, 2002). HA in the ECM may also bind CD44 receptors on leukocytes leading to accumulation of these cells and local inflammation (Termeer, Sleeman and Simon, 2003). On HA binding to CD44, the receptors' intracellular domain is cleaved and is translocated to the nucleus. There it interacts with CBP-p300 to activate transcription of CD44, a positive feedback loop that results in cell adhesion and migration (Ponta, Sherman and Herrlich, 2003; Nagano and Saya, 2004; Misra *et al.*, 2015). HA binding of CD44 also stimulates activation of Nanog signalling, which is associated with stem cell activation and survival (Chanmee *et al.*, 2015). Some papers have found fragments of the HA molecule itself are internalised by CD44, where the intracellular HA is then degraded in lysosomes (Harada and Takahashi, 2007). In inflammatory conditions however these HA fragments are not internalised and are instead left in the ECM, able to interact with receptors and confer downstream signalling which could lead to chronic inflammation (Vigetti *et al.*, 2010).

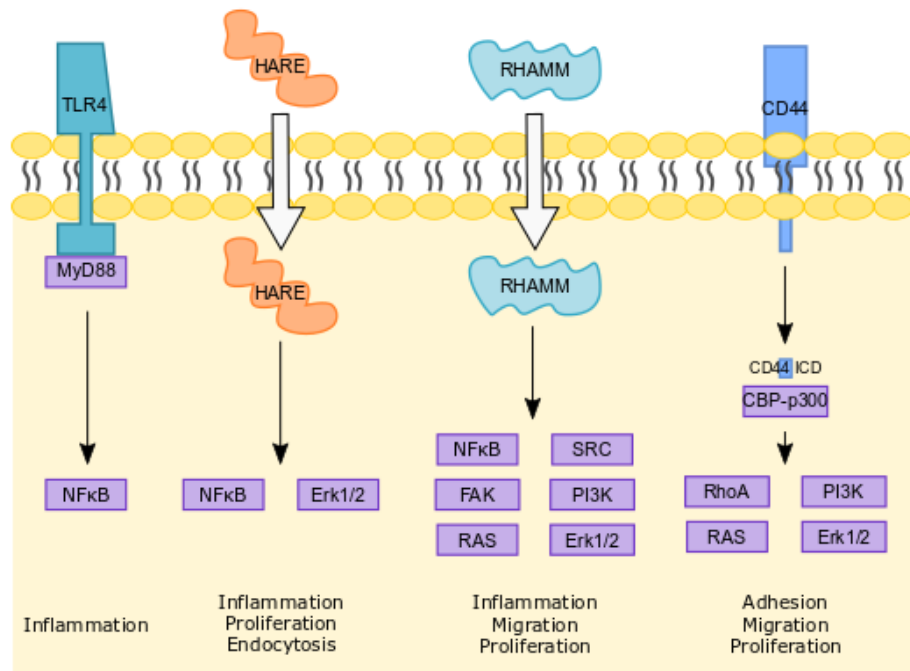


Figure 13: **Hyaluronan signalling**; the four key receptors of HA (TLR4, HARE, RHAMM and CD44) result in inflammation, proliferation, migration or cell adhesion (adapted from Litwiniuk *et al.*, 2016). TLR4 = toll-like receptor 4, HARE = hyaluronan receptor for endocytosis, RHAMM = receptor for hyaluronan-mediated motility, CD44 = cluster of differentiation 44.

HA may also bind to receptor for hyaluronan-mediated motility (RHAMM) extracellularly which increases intracellular RHAMM expression and activates downstream ERK, Ras, PI3k and NF-κB signalling to stimulate inflammation, proliferation, angiogenesis and rearrangement of the cytoskeleton (Cheung, Cruz and Turley, 1999; Jordan *et al.*, 2015). RHAMM is also associated with the retention of stem cell pluripotency during development (Choudhary *et al.*, 2007). Other receptors for HA include hyaluronan receptor for endocytosis (HARE) which causes clearance of HA, and lymphatic vessel endothelial HA receptor (LYVE-1) which is expressed on endothelial cells and instigates cell migration during wound healing (Banerji *et al.*, 1999; Zhou *et al.*, 2000; Stern, Asari and Sugahara, 2006).

The most important aspect of HA signalling is its size. While the exact mechanisms involved in the signalling of HMW and LMW HA have yet to be fully elucidated, the downstream effects are numerous; in general, HMW HA is anti-inflammatory while LMW HA is thought to be inflammatory and potentially pathogenic (Powell and Horton, 2005; Cyphert, Trempus and Garantziotis, 2015). One reason for this is that HMW HA promotes polarisation of macrophages

to the M2 phenotype, which is more associated with wound healing, while LMW HA stimulates the formation of M1 inflammatory macrophages (Rayahin *et al.*, 2015). LMW HA is also associated with proliferation, differentiation, angiogenesis and tumour progression, while the opposite is true of HMW HA (West *et al.*, 1985; Deed *et al.*, 1997; Toole *et al.*, 2005; Toole, Ghatak and Misra, 2008; Zhao *et al.*, 2016). The importance of HA molecular weight has been demonstrated via CD44 signalling (Itano, 2008), however it has also been seen in the activation of TLR2 and 4 receptors on macrophages (Termeer *et al.*, 2002; D. Jiang *et al.*, 2005). HA-induced TLR2/4 signalling is MyD88-dependant, and results in the activation of NF- κ B for downstream inflammatory cytokine release, including that of TNF α and IL1 β (Z. Jiang *et al.*, 2005). It has been reported that LMW HA, not HMW HA, can bind to TLR4, and that HMW HA causes upregulation of the TLR negative regulator IL-1R-associated kinase-M (IRAK-M), therefore LMW HA is associated with pro-inflammatory signals (McKee *et al.*, 1996; Fresno *et al.*, 2005). LMW HA also activates dendritic cells through TLR4 signalling and has been shown to upregulate cytokine expression to similar levels as LPS treatment (Gerber and Mosser, 2001; Termeer *et al.*, 2002). Interestingly, macrophages stimulated with LPS have increased expression of HAS1 and inhibition of hyaluronidases 1 and 2, suggesting a role for HA in the innate immune response (Chang *et al.*, 2014). This theory is supported by the fact that LPS treatment causes CD44 expression to be upregulated on monocytes, which would increase the effect of HA signalling (Gee *et al.*, 2002).

Several studies have suggested that not all HA is active for signalling, with only HA ranging from 1.2-400kDa able to activate macrophages (McKee *et al.*, 1996). However, these papers have been hit with criticism for not ensuring samples were endotoxin free, and they often used sonication to produce different sized HA fragments, which may not be representative of the molecule size, shape or confirmation of native HA (Dong *et al.*, 2016). Other papers have linked the size of the receptors' HA binding domain to the length of the HA molecule recognised, for instance HA molecules of 10 disaccharides in length are thought to be the smallest HA molecule that can bind to CD44 (Lesley *et al.*, 2000; Day and Prestwich, 2002). This may explain why HA

molecule size is one of the most important aspects of HA signalling. Another theory as to why HA size confers different downstream signalling effects is that HMW HA binds and clusters receptors in a way that LMW HA does not, however the exact mechanisms have not been proven (D. Jiang *et al.*, 2005; Vigetti, Karousou, *et al.*, 2014).

1.4.2.2.2 Hyaluronan: Relevance to Periodontitis

One hallmark of periodontitis is the breakdown of the extracellular matrix (ECM) composing the periodontium. The relationship between cells and their ECM is highly important to their differentiation, as evidenced in the effects of the mechanical environment on MSC differentiation discussed earlier. HA is a significant component of the ECM in the periodontium therefore the breakdown of the ECM in periodontitis would increase the amount of LMW HA in the periodontium. This idea has been demonstrated in other diseases of chronic inflammation, where the inflammation was linked to an upregulation of HA synthesis and fragmentation of HA into the LMW form (Vigetti *et al.*, 2010). This is significant as the presence of HMW HA was shown to inhibit osteoclast differentiation by binding to TLR4 on BMCs and instigating their differentiation to macrophages (Chang *et al.*, 2007; Rayahin *et al.*, 2015), however there is little information in the literature on the effect LMW HA might have on osteoclast differentiation specifically. HA not only has links to osteoclast differentiation but also their activity, as HA has been shown to bind CD44 receptors on differentiated osteoclasts which decreases their resorptive activity (Chang *et al.*, 2007) therefore HA may be a significant component to consider when looking at periodontitis.

HA has already been implemented as a therapy for Rheumatoid arthritis, another inflammatory disease which results in the degradation of the synovial fluid surrounding joints of which HA is a main component. In this case, HA is not only used as a treatment against disease but serum concentrations of HA have been developed as a diagnostic tool (Dougados *et al.*, 1993; Singh, Kumar and Sharma, 2014). Currently, HA-based products have been effective in the treatment of gingivitis due to its structural role in the ECM (Goa and Benfield, 1994; Jentsch *et al.*, 2003)

but little is known of its roles in periodontitis and its suitability as a possible treatment or biomarker of disease.

Considering these factors, the hypothesis at the beginning of this work was that periodontitis results in LPS tolerance which affects osteoclast differentiation via a change in HA signalling.

1.5 Autophagy

There are three types of autophagy in mammals, those being chaperone-mediated, microautophagy and macroautophagy. Macroautophagy, hereafter referred to simply as autophagy, is the most widely studied and has been implicated in changes in osteogenesis and osteoclastogenesis, cell fate determination, and diseases of the immune system among others (Yang and Klionsky, 2010).

Autophagy is an intracellular degradation system which is induced in times of cellular stress but may also be a form of cell death (Hale *et al.*, 2013; Ryter, Mizumura and Choi, 2014). It was first discovered when membrane-bound vesicles were identified containing degraded mitochondria or endoplasmic reticulum (Ashford and Porter, 1962; de Duve and Wattiaux, 1966). Originally it was theorised to be simply a degradation system for damaged or misfolded proteins, but since then the theory has expanded to include energy and nutrient production at times of cellular stress (Yang and Klionsky, 2010). Autophagy is induced by nutrient deficiency, hypoxia, heat stress, accumulation of reactive oxygen species (ROS) and oxidative stress, and ER stress due to the accumulation of misfolded proteins.

1.5.1 The Autophagy Pathway

In normal conditions, mammalian target of rapamycin (mTOR) negatively regulates autophagy by forming a complex with Unc-51 like autophagy activating kinase (ULK1), autophagy-related gene 13 (ATG13) and FAK family kinase-interacting protein of 200kDa (FIP200) (Hale *et al.*, 2013). Initiation of autophagy involves the nucleation and formation of a double-membrane structure called the phagophore (*Figure 14*).

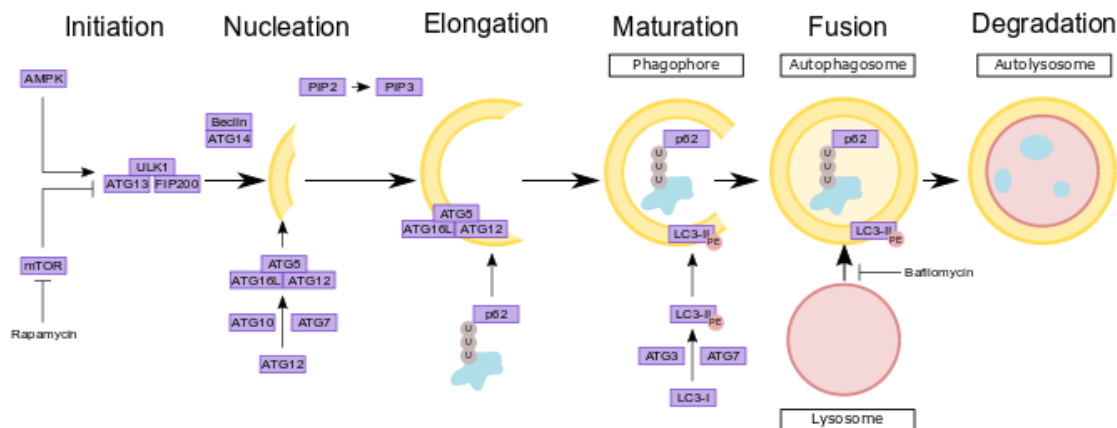


Figure 14: **The autophagy pathway**; Once autophagy is initiated, the phagophore membrane is produced and elongated, and the substances to be broken down are encapsulated within the phagophore. The autophagosome matures and fuses with a lysosome to form an autolysosome. As the substances within are degraded by acid lysosome enzymes, so is the autolysosome itself. Drugs can interfere with this pathway, as rapamycin inhibits mTOR to induce autophagy, while bafilomycin inhibits autophagosome lysosome fusion (adapted from Hansen, Rubinsztein & Walker, 2018).

In the case of nutrient deficiency, AMP-activated protein kinase (AMPK) is activated and inhibits mTOR, resulting in the dephosphorylation and release of ULK1 from the mTOR complex. ULK1 then phosphorylates ATG13 and FIP200 which induces nucleation, a process involving the conversion of PIP2 to PIP3 by PI3K. The phagophore membrane is then elongated to encapsulate the cargo for degradation and becomes a mature autophagosome (Hale *et al.*, 2013). The specific cargo to be degraded, be that protein or organelle, is tagged with ubiquitin, which is identified and delivered to the phagophore by p62 (Shin, 1998; Myeku and Figueiredo-Pereira, 2011). Elongation requires the autophagy-related-12 (ATG12), -5 (ATG5) and -16 light 1 (ATG16L1) complex, and microtubule-associated proteins 1A/1B light chain 3B (LC3). First ATG12 is activated by autophagy-related 7 (ATG7) and becomes conjugated to ATG5 via autophagy-related 10 (ATG10). ATG16L1 forms a complex with ATG12-ATG5 and this complex accumulates on the autophagosomal membrane as it forms (Hale *et al.*, 2013). Meanwhile, autophagy-related 4B (ATG4B) cleaves 22 residues from the C-terminal of LC3 to form LC3-I. LC3-I is then conjugated with phosphatidylethanolamine (PE) by ATG7 and autophagy-related 3 (ATG3), to form LC3-II which is incorporated into the autophagosomal membrane (Saitoh *et al.*, 2008). Once the autophagosome is formed, ATG12-ATG5-ATG16L1 are removed and the autophagosome uses

dynein motors to move along microtubules towards lysosomes (Mehrpour *et al.*, 2010; Cheng *et al.*, 2015). The autophagosome then fuses with a lysosome to form an autolysosome, and the cargo begins to be degraded by lysosomal proteases. The acidic environment of the autolysosome also works to degrade the membrane and thus degrade the autolysosome itself (Hale *et al.*, 2013).

Both the nucleation and maturation of autophagosomes require Beclin, therefore binding of Beclin by Rubicon or UV irradiation resistance-associated gene (UVRAG) allows for autophagy regulation (Matsunaga *et al.*, 2009; Mehrpour *et al.*, 2010). Other regulatory mechanisms involve the negative regulation of autophagy initiation by mTOR, and the inhibition of autophagosome fusion with lysosomes by RAS-related protein Rab 7 (RAB7), soluble N-ethylmaleimide-sensitive factor activating protein receptor (SNARE) proteins and homotypic fusion and protein sorting (HOPS) complexes (Ganley *et al.*, 2011; Moreau, Renna and Rubinsztein, 2013; Jiang *et al.*, 2014).

Autophagy results in the destruction of proteins and cellular debris which provides energy and peptides that are recycled by the cell. Stem cells reside in a state of quiescence until activated, when they require energy for cell division and an upregulation of proteins required for differentiation. Since autophagy provides both energy and building blocks for the production of new proteins and molecules, it can regulate stem cell activation (Valenti, Dalle Carbonare and Mottes, 2016). The exact mechanisms and effects of autophagy on stem cell pluripotency and differentiation are context dependant, for instance MSCs have been suggested to have a high basal level of autophagy which is then reduced as they differentiate to osteoblasts (Oliver *et al.*, 2012); likewise, autophagy levels are high in HSCs, which seems to be crucial for their stemness retention (Liu *et al.*, 2010; Mortensen *et al.*, 2011). However neural and cardiac stem cells have low basal levels of autophagy which is increased as they differentiate (Vázquez *et al.*, 2012; Zhang *et al.*, 2012). One theory as to the role of autophagy in stem cell maintenance or differentiation, is that in removing unwanted proteins it prevents these proteins from impairing

the identity of the stem cell, either in keeping itself pluripotent or in the initial stages of differentiation (Vessoni, Muotri and Okamoto, 2012; Pan *et al.*, 2013). Other papers have suggested that by autophagy removing misfolded proteins or damaged organelles it allows the stem cell to avoid becoming senescent, thus retaining it in a quiescent state (Pan *et al.*, 2013).

Along with nutrient or peptide deficiency, autophagy can be stimulated *in vitro* using rapamycin, a drug which targets mTOR, the negative regulator of autophagy (Ravikumar *et al.*, 2004). Inhibition of autophagy is possible by using bafilomycin which inhibits fusion of the autophagosome to the autolysosome (Tanida *et al.*, 2005). 3-methyladenine (3MA) is a PI3K inhibitor which has also been used as an inhibitor of autophagy, however the literature seems to suggest that 3MA may act to activate or inhibit autophagy under different circumstances (Mizushima, Yoshimori and Levine, 2010; Wu *et al.*, 2010).

1.5.2 Autophagy & Bone Remodelling

Autophagy has been demonstrated in many cell and tissue types, including that of bone (Shapiro *et al.*, 2014). Autophagy contributes to the action of osteoblasts, by increasing osteoid mineralisation (Nollet *et al.*, 2014) and blocking Beclin or ATG5 in bone marrow cells (BMCs) was found to impair osteogenic differentiation and instead cause differentiation of adipocytes (Qi *et al.*, 2017). Additionally, Vitamin D3 which is required for osteogenesis was found to elevate calcium levels in the cytosol to activate autophagy (Høyer-Hansen, Nordbrandt and Jäättelä, 2010).

Like autophagy, bone resorption by osteoclasts requires lysosomal activity. Furthermore, osteoclast secretory function is thought to be regulated by autophagy as LC3, ATG5 and ATG7 are required for the localisation of lysosomes to the bone surface (DeSelm *et al.*, 2011; Chung *et al.*, 2012). This is evidenced in mouse models, for example osteoclast-specific ATG5 knockouts displayed impaired bone resorption resulting in excessive bone growth (Gelman and Elazar, 2011). Osteoclast differentiation is enhanced by the induction of autophagy, as evidenced in the treatment of osteoclast progenitor cell line with rapamycin (Shui, Riggs and Khosla, 2002; Boyle,

Simonet and Lacey, 2003). Additionally, mutations of *p62* were found in 25% of patients with familial Paget's disease, a pathology characterised by hyper-active osteoclasts and bone loss (Hocking *et al.*, 2004) (Helfrich, 2005; Shaker, 2009). The effect of autophagy on osteoclastogenesis is currently being researched as a potential target for the treatment of osteoporosis (Lin *et al.*, 2016).

In aged bones there is increased ROS production and a decrease in the production of sex steroids such as oestrogen, resulting in upregulated autophagy (Wang *et al.*, 2019). This has many downstream effects, including reducing the proliferative and differentiation capabilities of both osteoclast and osteoblast precursors in the bone marrow (K. Wang *et al.*, 2011; Yin *et al.*, 2019). In addition, increased autophagy results in decreased osteoclast maturation and activation, meaning less bone resorption, whilst osteoblasts undergo apoptosis (Wang *et al.*, 2019). This means that in the aged phenotype, both bone formation and resorption are reduced, contributing to more fragile bones and reduced regenerative capacity if injury occurs (Almeida, 2012). However, while autophagy in the aged phenotype seems to have a destructive effect on bones, the apoptosis of osteoblasts may not be a result of autophagy itself, as autophagy can be used to prevent apoptosis and prolong cell survival (G. Liu *et al.*, 2015). There is also the link between autophagy and stem cell maintenance, which may be implicated in the role of autophagy in aged bones (Pan *et al.*, 2013).

1.5.2.1 Autophagy & Mechanical Strain

Autophagy is initiated in response to cellular stress, and it has been theorised that different types, levels or intervals of mechanical strain can contribute to cell stress (Hirt and Liton, 2017). The first paper to demonstrate strain-related autophagy induction showed compressive strain inducing autophagosome formation increased by 20-fold compared to basal levels (King, Veltman and Insall, 2011). Compression strain has also been linked to autophagy induction in models of increased intracranial pressure, and activating autophagy with rapamycin was found to have a protective effect on cartilage explants exposed to mechanical strain *in vitro* by reducing

cell death (Tanabe *et al.*, 2011; Caramés *et al.*, 2012). One recent paper using an *in vitro* compressive strain model found that PDL cells had increased autophagy levels when compressed. They also suggested autophagy to be a negative regulator of compression-induced osteoclastogenesis, as mice given rapamycin treatment whilst undergoing tooth movement had decreased osteoclast differentiation and higher alveolar bone density than controls (Chen, Mo and Hua, 2019). While this paper focussed on the effects of compression on autophagy levels in the periodontium, there are few to no papers in the literature looking at autophagy levels in relation to the tensile strain of orthodontic tooth movement.

One example of shear stress being linked to autophagy is in atherosclerosis, a chronic heart disease where arterial plaques cause an increase in shear stress to the vasculature. Vascular cells were found to have increased levels of autophagy in the atherosclerotic condition, with p62 and LC3 expressed in atherosclerosis plaques (Guo *et al.*, 2017).

Tension strain has been demonstrated to initiate apoptosis and autophagy-related cell death in various tissues and cell types (Kearney, Prendergast and Campbell, 2008; Caramés *et al.*, 2012). Autophagy induction has been demonstrated to be protective in chondrocytes undergoing intermittent tensile strain (Xu *et al.*, 2014), and in the case of biaxial tensile strain of the trabecular tissue of the eye (Porter, Jeyabalan and Liton, 2014). Additionally, exposure of mouse BMCs to 5% intermittent tensile strain caused osteogenic differentiation (Zhou *et al.*, 2018). However, the effects of constant tensile strain on autophagy and how this relates to osteoblast differentiation is as yet unknown.

1.5.2.2 *Autophagy & Chronic Inflammation*

There is strong evidence for a link between autophagy and the immune system in the literature. One key paper that demonstrated this found that *Streptococcus pyogenes* was sequestered into autophagosomes and degraded as part of the innate immune response (Nakagawa *et al.*, 2004). In this context autophagy avoids apoptosis of infected cells and instead eliminates the specific pathogen within the cell.

Inflammatory cytokines such as IL1 β and TNF α have been demonstrated in the literature to induce autophagy, while autophagy is inhibited by IL10, an anti-inflammatory cytokine (Harris, 2011). On the other hand, autophagy has been shown to affect inflammation, as damage-associated molecular patterns (DAMPs) released from cells undergoing autophagy are known to stimulate the immune response (Zhang *et al.*, 2013).

There are currently no papers directly linking autophagy levels to LPS tolerance, however an *in vitro* model of LPS tolerance in THP1 cells, a pre-monocyte cell line, showed an increase in LC3 puncta staining suggesting upregulated autophagy (Widdrington *et al.*, 2018). In terms of periodontitis specifically, there have been several papers demonstrating that autophagy levels are higher in the PDL of patients with periodontitis compared to those without the disease, which was thought to be a protective mechanism against apoptosis (Bullon *et al.*, 2012; Jiang, Li and Zhu, 2020). Another paper showed that the presence of butyrate, a key component of dental plaque, induced autophagy in gingival epithelial cells which led to autophagic cell death (Tsuda *et al.*, 2010), therefore the effects of autophagy on cell death even within the periodontium seems to depend on the specific cell type.

As discussed in section 1.5.2, autophagy has often been shown in the literature to stimulate osteoclastogenesis. However, one recent paper found that inhibiting autophagy in PDL cells reduced osteoclastogenesis via the upregulation of A20, an anti-inflammatory protein which inhibits NF- κ B signalling (Yan *et al.*, 2020). Autophagy is known to be a highly context-dependant process however, the findings of this paper are inconsistent with the role of autophagy in the context of periodontitis seen in the literature thus far; periodontitis patients have upregulated autophagy levels in the periodontium, yet increased alveolar bone loss is a hallmark of the disease. This demonstrates that the effect of autophagy on osteoclastogenesis in the context of periodontitis requires further research in order to elucidate the mechanisms at play.

1.6 Aims

This thesis aimed to research the role of the autophagy pathway in two scenarios of abnormal bone remodelling: orthodontic tooth movement and periodontitis.

Autophagy is an intracellular degradation system used to recycle misfolded proteins and make available energy or nutrients at times of cellular stress. There is much evidence in the literature that autophagy can be activated by both mechanical stretching and inflammation, however the mechanisms involved are highly context dependant. Autophagy may also be important for bone remodelling in the oral cavity. Two scenarios where bone remodelling is key to the physiological outcome are orthodontic tooth movement and inflammatory-induced periodontal disease. This thesis aims to investigate the hypothesis that autophagy is involved in bone remodelling during orthodontic tooth movement and periodontal disease.

Tooth Movement

It is well established in the literature that mechanical strain can activate the autophagy pathway, however, it is still unclear whether mechanical strain-induced autophagy is protective or destructive and how constant mechanical strain, as with orthodontic tooth movement, may alter the autophagy pathway. It was theorised that perhaps cells exposed to tensile strain undergo an altered state of autophagic flux which could contribute to MSC activation or differentiation to osteoblasts.

Ultimately, understanding the molecular mechanisms underpinning orthodontic tooth movement will help find new therapeutic targets to improve patient outcomes, and at present these exact mechanisms are unknown.

Periodontitis

Periodontitis is a chronic inflammatory disease caused by the presence of Gram-negative bacteria, including *P. Gingivalis*, leading to local inflammation in the periodontium, but it is also clear that disease susceptibility and progression are affected by host factors.

This study considered the notion that the chronic inflammation occurring in periodontitis may result in LPS tolerance. LPS tolerance has been investigated in connection to many inflammatory conditions, but its role in periodontitis has yet to be fully explored. Understanding that LPS tolerance has been linked to chronic inflammation in other disease models and the known effects of chronic inflammation on osteoclast function, this study aimed to investigate whether LPS tolerance could affect osteoclastogenesis directly.

The proposed mechanism linking periodontitis and osteoclastogenesis was HA signalling. HA was selected as a research target in this condition as not only is HA synthesis upregulated in chronic inflammation, but also HA signalling affects bone resorption by inhibiting osteoclast differentiation. Considering these factors, the hypothesis at the beginning of this work was that periodontitis results in LPS tolerance which affects osteoclast differentiation via altered autophagic flux and a change in HA signalling.

Summary of Aims

Therefore, the overall aims of this thesis were to investigate the mechanism of autophagy in:

1. Orthodontic tooth movement
2. Inflammation induced periodontitis

The first aim was undertaken by:

- a. Optimising an *in vitro* cell stretching system for use as a model for orthodontic tooth movement.
- b. Determining the expression of osteogenic and autophagic proteins in rat periodontiums during orthodontic tooth movement.
- c. Determining osteogenic and autophagic gene and protein expression of osteoblast-precursors in response to constant tensile stretching force *in vitro*.
- d. Modulating autophagy in these models to determine its role on strain-induced osteogenesis.

The second aim was undertaken by:

- a. Optimising an *in vitro* protocol for LPS tolerance for use as an experimental model of chronic inflammation in periodontitis, and to determine whether cells could be tolerised to *P.gingivalis* LPS, as determined by their expression of inflammatory and anti-inflammatory cytokines.
- b. Determining the expression of autophagy genes and proteins in cells tolerised to LPS, and how this may affect the differentiation of osteoclast precursors under inflammatory conditions.
- c. Establishing if LPS tolerance affects HA synthesis and whether HA signalling alters osteoclast differentiation *in vitro*.

2 Chapter 2: Materials & Methods

2.1 Cell Culture

2.1.1 Maintenance

All cells were incubated at 37°C with 5% CO₂, and media was changed every 2-3 days unless stated otherwise. Adherent cells were passaged by washing in Hank's balanced salt solution (HBSS; 14175-053, Gibco), then incubating in TrypLE (12563-029, Gibco) at 37°C until the cells had detached from the plate surface. The TrypLE was neutralised by adding an equal volume of culture media containing foetal bovine serum (FBS), and the solution was centrifuged at 1000rcf for 5 minutes. The resulting supernatant was discarded, and the pellet re-suspended in culture media and re-plated. Non-adherent cells were passaged by centrifugation of the media, re-suspending the pellet in fresh culture media and re-plating.

Cells were frozen by collecting and centrifuging the cells at 1000rcf for 5 minutes, then re-suspending the pellet in a 10:1 solution of FBS (F7524, Sigma) and dimethyl sulfoxide (DMSO; D2650, Sigma). The solution was transferred to cryovials at a density of 1×10^6 cells per vial. These were incubated overnight at -80°C, before transferring to liquid nitrogen for storage. Cells were thawed by incubation in pre-warmed culture media.

Human bone marrow cells (hBMCs) were received from Professor Stefan Scheming of Lund University. Cells were thawed and cultured in Dulbecco modified Eagle's medium/F12 (DMEM-F12; 31331-028, Gibco) with 20% FBS (F7524, Sigma) and 1% penicillin-streptomycin-antimycotic (Pen-Strep; 15240-062, Gibco), overnight at a density of 1.25×10^5 cells per ml. After which the non-adherent cells, containing a population of CD14-positive monocytic cells, were removed and used for osteoclastogenesis experiments, while the adherent cells, containing of population of mesenchymal stem cell-like cells, were retained for osteogenesis work. hBMCs were maintained by culturing cells in DMEM-F12 with 20% FBS, 1% Pen-Strep, and 1% MEM Vitamin Solution (M6895, Sigma). THP1 cells were cultured in Roswell Park Memorial Institute 1640

medium (RPMI; 11520586, Gibco) with 10% FBS, 1% Pen-Strep, and 2mM L-glutamine (G7513, Sigma).

2.1.2 Osteogenesis Induction

Adherent hBMCs were incubated in culture media with the addition of established osteogenesis induction reagents 100nM Dexamethasone (D4902, Sigma), 200mM β -glycerol phosphate disodium salt pentahydrate (50020, Biochemika), and 50 μ M ascorbic acid (A4403, Sigma) (Langenbach and Handschel, 2013). Cells were incubated at 37°C and 5% CO₂, and media was changed every 2 days.

2.1.3 Viral Infection

The KI67 fluorescence ubiquitin cell cycle indicator (FUCCI) viral reporter system was provided by Professor Alexander Zambon of the University of California (San Diego). hBMCs were infected with the virus by incubating cells in DMEM-F12 with 20% FBS, 10 μ g/ml polybrene (TR-1003, Sigma) and the lentivirus (at MOI: 1) for 24 hours. After which time the media was changed for fresh culture media (DMEM-F12 with 20% FBS, 1% Pen-Strep, 1% MEM Vitamin Solution) containing 10 μ g/ml Blasticidin and 25 μ g/ml Neomycin for antibiotic selection of the infected cells.

2.1.4 Cell Stretching

The first cell stretching device tested was provided by Professor Herbert Shea of École Polytechnique Fédérale de Lausanne (EPFL). This system uses carbon electrodes printed onto a polydimethylsiloxane (PDMS) membrane to form an electrical circuit between the stretching device and a powerpack. When current is applied to the device the membrane is stretched. The membranes were sterilised by incubating in 70% ethanol for 20mins then washing briefly in sterile distilled water.

The Strex manual cell stretching system (STB-10-10, Strex Inc.) consisted of a metal scaffold into which a PDMS block containing four wells (STB-CH-4W, Strex Inc.) could be inserted. The scaffold

was attached to a screw which was turned to cause the block to be stretched. Each full turn of the screw equated to 2.5% of stretch, with a maximum of 20% uniaxial stretching force. The PDMS blocks were autoclaved to sterilise them before use. Adherent hBMCs were seeded at 6.25×10^4 cells for 4-well blocks, and 2.5×10^5 cells for 1-well blocks, and incubated at 37°C and 5% CO₂. Cells were exposed to 10-20% uniaxial strain 24 hours later.

PDMS is a hydrophobic compound, therefore both cell stretching devices were collagen-coated prior to cell seeding. The collagen coating solution was specified by Strex and consisted of a 1:1 solution of 1mM hydrochloric acid (HCl; H1758, Sigma) and 3mg/ml rat-tail collagen I (A10483-01; Gibco). The membrane was covered in collagen coating solution and incubated at 37°C for 6 hours. Membranes were washed with HBSS (14175-053, Gibco), before the cells were seeded in culture media.

2.1.5 Cell Sorting

Magnetic-Activated Cell Sorting (MACS) was used to isolate CD14-positive cells from non-adherent hBMCs for osteoclastogenesis induction experiments. The manufacturer's instructions were followed; briefly, media containing the non-adherent hBMCs was collected and spun down at 600rcf for 5 minutes. Cells were counted and re-suspended in 80µl culture media, to which 20µl of CD14 MicroBeads (130-050-201, Miltenyi Biotec) was added. Cells were incubated at 4°C for 1 hour, before washing with 1ml culture media and centrifugation at 600rcf for 5 minutes. The pellet was re-suspended in 500µl culture media. A MS MACS column (130-042-201, Miltenyi Biotec) was added to a MACS stand and rinsed with 500µl culture media. The cell suspension was added to the column and washed with 500µl culture media three times. The resulting solution was collected, containing the unlabelled cell fraction. The column was then removed from the MACS stand and 1ml culture media was added. A plunger was pushed firmly over the top of the column, and the resulting solution containing the CD14-labelled fraction was collected. Both the labelled and unlabelled fractions were centrifuged at 600rcf for 5 minutes, re-suspended in culture media, counted and seeded in plates for culture.

Cell counts for the CD14-labelled and unlabelled fractions were input into PRISM 5 software (Graph Pad) and analysed by determining the percentage of each fraction from the total cell number. A Student's t-test was carried out and statistical significance was set at * $p < 0.05$, ** $p < 0.01$, and *** $p < 0.001$.

2.1.6 Osteoclastogenesis Induction

CD14-positive hBMCs were isolated using MACS, as described above, and cultured in culture media overnight. Cells were seeded a density of 5×10^5 cells/ml and treated with 25ng/ml macrophage colony-stimulating factor (M-CSF; 216-MC-005, R&D) for 5 days, then with 25ng/ml M-CSF and 100ng/ml receptor activator of nuclear factor kappa-B ligand (RANKL; Hu Recombinant RANKL, R&D) for a further 5 days. Cells were incubated at 37°C and 5% CO₂, and media was changed every 2 days throughout.

2.1.7 LPS Tolerance

THP1 cells were treated with 10ng/ml phorbol 12-myristate 13-acetate (PMA; P8139, Sigma) for 24 hours, washed three times with HBSS then seeded at 1.25×10^4 /ml and incubated in fresh culture media for 24 hours.

After this point, cells were treated differently according to three different conditions: control (no exposure to LPS), single exposure (1x) or multiple exposure (2x) to LPS.

Control cells were maintained in only culture media throughout the experiment.

'1x' cells were incubated in culture media only during the first treatment, and treated with 1µg/ml LPS at the second treatment only.

'2x' cells were treated with 1µg/ml of either *Escherichia coli* LPS (*E.coli* LPS; tlr1-pek1ps, Invivogen) or *Porphyromonas gingivalis* LPS (*P.gingivalis* LPS; LPS-PG Ultrapure, tlr1-ppglps, Invivogen) for 4 hours, then cells were washed twice with HBSS and cultured in fresh culture media for 24 hours. Cells were then treated with 1µg/ml LPS for the second time. After 4 hours, cells were

either collected for analysis or washed twice with HBSS and placed in fresh culture media.

Further collections took place at 24 hours and 72 hours post-second LPS treatment.

All cells were incubated at 37°C and 5% CO₂, and media was changed every 2 days.

2.2 RNA Analysis

2.2.1 RNA Extraction & Quantification

RNA was extracted from cells based on the acid guanidinium thiocyanate-phenol-chloroform method (Chomczynski and Sacchi, 1987). Briefly, cells were washed with HBSS before incubation in Tri-reagent (93289, Sigma) for 5 minutes at room temperature. Chloroform (C2432, Sigma) was added at a 5:1 ratio (lysate:chloroform). Samples were mixed by vortexing, and centrifuged at 13000rpm for 15 minutes at 4°C. This allowed the formation of three layers: a pink layer on the bottom containing protein, a white interphase layer containing DNA, and a clear supernatant containing the RNA. The supernatant was collected and an equal volume of isopropanol (34965, Sigma) was added. At this stage 1µl GlycoBlue (AM9515, Ambion Applied Biosystems) was added to each sample, so that the pellet could be identified later. The samples were mixed by vortexing and incubated overnight at -20°C, after which they were centrifuged at 13,300rpm for 45 minutes at 4°C. The supernatant was discarded and replaced with 1ml 70% ethanol (20821.321, VWR Chemicals) made up with 0.1% diethyl pyrocarbonate (DEPC; D5758, Sigma) treated water. Samples were centrifuged at 9000rpm for 10 minutes at 4°C, and the resulting pellet was re-suspended in an appropriate volume of DEPC-treated water. RNA samples were stored at -80°C.

The concentration and purity of the RNA was determined by quantifying the samples using a NanoDrop 2000 UV-Vis Spectrophotometer (Thermo Fisher Scientific). The sample concentrations were normalised against that of the DEPC-treated water alone. Purity was determined by examination of the 260/280 and 260/230 ratios; 260/280 indicates the presence of protein or other contaminants that absorb UV at 280nm or below, while 260/230 specifies contaminants that absorb UV at 230nm or below. A 260/280 of 1.8-2.1 and a 260/230 ratio greater than 1.5 was accepted as adequate purity for further analysis.

2.2.2 Reverse Transcription

RNA samples were converted to cDNA by reverse transcription polymerase chain reaction (RT-PCR), using a High Capacity cDNA Reverse Transcription kit (4368814, Applied Biosystems), in accordance with the manufacturer's instructions. A Veriti™ Thermal Cycler 96 well (Applied Biosystems) machine was used to subject the samples to a RT-PCR program consisting of 25°C for 10 minutes, 37°C for 120 minutes, 28°C for 5 minutes, then 4°C for storage. cDNA samples were diluted in DEPC-treated water at a ratio of 1:9, and stored at -20°C.

2.2.3 Q-PCR

Quantitative polymerase chain reaction (Q-PCR) was used to analyse the relative expression of the gene of interest.

2.2.3.1 Primer Design

Primers were designed using the coding sequence for each gene, which was taken from NCBI gene (<http://www.ncbi.nlm.nih.gov/gene/>), and the Primer 3 website (http://biotools.umassmed.edu/bioapps/primer3_www.cgi). The resulting primers were validated using the UCSC Genome Institute website (<http://genome.ucsc.edu/cgi-bin/hgPcr?command=start>). Primers were designed to cross exons, in order to reduce the risk of DNA contamination being amplified, and were designed against the 5' end of the cDNA to ensure RNA degradation would not result in the removal of the primer's binding site.

2.2.3.2 Primers Used

Details for the primers used are recorded in Table 1:

Gene	Forward Primer	Reverse Primer
36β4	GCAATGTTGCCAGTGTCTGT	GCCTTGACCTTTTCAGCAAG
ATG3	TTTGGCTATGATGAGCAACG	AAGTTCTCCCCCTCCTTCTG
ATG5	CAGATGGACAGTTGCACACA	CTGTTGGCTGTGGGATGATA
DMP1	GACTGCCAAGACGGCTATTA	CTCTTTGGCTGTGTTCTGGT
GAPDH	ATCACTGCCACCCAGAAGAC	CAGTGAGCTTCCCGTTTCAG
HAS1	GAGGCCTGGTACAACCAGAA	TGTACAGCCACTCACGGAAG
HAS2	TCCCGGTGAGACAGATGAGT	ACAGATGAGGCTGGGTCAAG
HAS3	GTCATGTACACGGCCTTCAA	CTGCTCAGGAAGGAAATCCA

IL10	CTGCCTAACATGCTTCGAGA	GGTCTTGTTCTCAGCTTGG
IL1 β	GGAGAATGACCTGAGCACCT	GGAGGTGGAGAGCTTTTCAGT
IL6	AGTCCTGATCCAGTTCCTGC	AAGCTGCGCAGAATGAGATG
IL8	TCCAAACCTTTCCACCCCAA	CCAGTTTTCTTGGGGTCCA
LC3	CGTCCTGGACAAGACCAAGT	TCCTCGTCTTTCTCTGCTC
Osteopontin	ACTGATTTCCACGGACCT	CCATTCAACTCCTCGCTTTC
p62	TGGACCCATCTGTCTTCAAA	ATGGACAGCATCTGGGAGAG
RUNX2	AAATGCTGGAGTGATGTGGT	TATGAAGCCTGGCGATTTAG
TNF α	GTCAACCTCTCTCTGCCAT	CCAAAGTAGACCTGCCAGA

Table 2: Primers used for Q-PCR.

2.2.3.3 Program

Primer stocks were produced by diluting the forward and reverse primer in sterile DEPC-treated water, to a ratio of 1:1:18. Primers and cDNA samples were prepared using the LightCycler 480 SYBR Green I Master (04887352001, Roche), according to the manufacturer's instructions. Briefly, this consisted of preparing master-mixes of SYBR Green, sterile water and primer stock (2:2:1) or SYBR Green, sterile water and cDNA sample (3:1:1). Samples were tested in triplicate, in order to determine the reliability of results by calculation of the standard deviation from Ct values.

A LightCycler 480 Instrument II 384-well block real-time PCR machine (Roche) was used, and samples were subjected to 45 cycles of the following program: 95°C for 5 minutes, 60°C for 20 seconds, 72°C for 10 seconds, 95°C for 5 seconds, 65°C for 1 minute, 97°C until the temperature was reached, before dropping to 95°C.

2.2.3.4 Data Analysis & Statistics

Data was exported into Excel for comparative Ct analysis. Experimental data was analysed using PRISM 5 software. A two-way ANOVA with Bonferoni correction was performed, and statistical significance was set at * $p < 0.05$, ** $p < 0.01$, and *** $p < 0.001$.

Melting curves were analysed to determine the reliability of results; a peak seen before the true melting curve could indicate issues with the primer design causing primer dimers to form, while a peak seen after the melting curve could indicate non-specific binding of the primer and sample. Samples with peaks outside the expected melting curve range were rejected.

2.3 Protein Analysis

2.3.1 Protein Extraction & Quantification

Protein lysis buffer was prepared using Halt Protease and Phosphatase Inhibitor Cocktail (78442, Thermo Fisher Scientific) and Pierce RIPA Buffer (89901, Thermo Fisher Scientific) in a 1:100 ratio. Adherent cells were washed with HBSS and covered with protein lysis buffer. A sterile cell scraper was used to detach the cells from the plate surface, and the cell suspension was collected and incubated on ice for 30 minutes with frequent agitation. The samples were centrifuged at 10,000rpm for 10 minutes at 4°C, and the supernatant was collected. Protein samples were stored at -20°C.

Quantification of the protein was carried out using a Bicinchoninic acid assay kit (BCA; 23227, Thermo Fisher Scientific), following the manufacturer's instructions. Briefly, samples were diluted 1:10 in phosphate buffered saline (PBS; P4417, Sigma), and pipetted alongside BCA standards in a 96well plate. The BCA reagents were made up in a 1:50 ratio of reagent A:B, and 200µl added to each well. The plate was incubated at 37°C for 20 minutes, before the absorbance of each sample was measured using a Tecan spectrophotometer (Genios). Data was analysed in Excel.

2.3.2 Western Blotting

Protein samples were extracted using the above protocol, then western blots were carried out using the NuPage® electrophoresis system (Invitrogen) and iBind™ Western System (Invitrogen), according to the manufacturer's instructions. Briefly, samples were prepared with NuPage® LD Sample buffer (NP0007, Invitrogen), NuPage® Reducing Agent (NP0009, Invitrogen), DEPC-treated water, and an equal concentration of protein per sample. Samples were heated at 95°C for 5 minutes then placed on ice. Running buffer was prepared with distilled water, using the buffer most suited to the protein of interest: 3-(N-morpholino)propanesulfonic acid (MOPS buffer; NP0001, Invitrogen) for the majority of proteins of 14kDa and above, and 2-(N-morpholino)ethanesulphonic acid (MES buffer; NP0002, Invitrogen) for better separation of

small proteins between 2.5 and 60 kDa. The NuPage® XCell SureLock™ Mini-Cell Electrophoresis System (electrophoresis apparatus; EI0001, Invitrogen) was assembled with a pre-cast 4-12% Bis-Tris gradient gel (NP0336BOX, Invitrogen), and filled with running buffer. The samples were loaded into each well, alongside PageRuler protein ladder (26616, Thermo Fisher Scientific) and Magic Mark XP protein standard (LC5602, Invitrogen), and the gel was exposed to 200V for 45-50 minutes, using a Powerease 300W power-pack (Invitrogen).

Blotting pads were pre-soaked in transfer buffer for 30 minutes at 4°C. A Polyvinylidene fluoride (PVDF) filter paper sandwich contained PVDF membranes which were activated in 100% methanol (494437-2L, Sigma) then placed in distilled water. The membranes contained either 0.22µM (LC2002, Invitrogen) or 0.45µM (LC2005, Invitrogen) pores, depending on the size of the protein of interest. Transfer buffer (NP0006-1, Invitrogen) was prepared with methanol and distilled water. Depending on the size of the protein of interest, the proportion of methanol could either be decreased from 10% to 5% for large proteins, or increased up to 20% for small proteins. After the electrophoresis was completed, the gel was released from the cassette and the NuPage® XCell II Blot Module (transfer apparatus; E19051, Invitrogen) was assembled with the following: two blotting pads, one filter paper, the gel, the transfer membrane, one filter paper and two more blotting pads. The inner chamber of the transfer apparatus was filled with transfer buffer, and the outer chamber with distilled water. The power-pack was connected and run at 36V for 1 hour 45 minutes.

A ponceau stain was carried out on the membrane to ensure the transfer had been successful: the membrane was immersed in Ponceau S solution (P7170-1L, Sigma) for 3 minutes at room temperature, then washed twice for 5 minutes with 5% acetic acid (ARK2183, SAFC) in distilled water. Red bands on the membrane indicated the presence of protein. The membrane was then washed for 5 minutes with distilled water, three times for a total of 15 minutes.

The iBind™ Western System was used for blocking and antibody incubation. iBind™ buffer (SLF1020, Invitrogen) was prepared as per the manufacturer's instructions, and used to dilute

the primary and secondary antibodies to the desired concentration. The membrane was incubated in iBind™ buffer for 5 minutes at room temperature. An iBind™ card (SLF1010, Invitrogen) was placed inside the iBind™ apparatus (SLF1000, Invitrogen) and the surface was saturated in iBind™ buffer. The membrane was placed protein-side down onto the iBind™ card and the lid of the apparatus was closed. The primary and secondary antibody solutions and iBind™ buffer were placed in the specified slots of the apparatus, and the membrane was incubated until the apparatus slots were dry; approximately 2 hours 45 minutes at room temperature, or overnight at 4°C.

The membrane was washed briefly in distilled water, before a second wash for 5 minutes at room temperature. ECL buffer was prepared using a 1:1 ratio of peroxide solution and ECL Enhancer Solution from the Western Sure premium chemiluminescent substrate kit (926-95000, LiCOR). This buffer was incubated on the surface of the membrane for 5 minutes at room temperature, then the membrane was imaged using a C-Digit 3600 scanner (LiCOR). Western blot membranes were washed in distilled water and stored in clingfilm at -20°C after use.

If they were to be probed for another antibody, they were stripped using Restore Plus Western Blot Stripping buffer (46430, Thermo Fisher Scientific) for 5 to 10 minutes at room temperature, before washing with distilled water three times. The antibody incubation steps were then repeated as described using the iBind™ system, above.

Details for the antibodies used are recorded in Table 2:

Antibody	Supplier	Catalogue Number	Lot Number
anti-rabbit RUNX2 (M70)	Santa Cruz	SC-10758	G2815
anti-mouse GAPDH (96C5)	Santa Cruz	SC-32233	K1216
Rabbit HRP	Cell Signalling	7074P2	26
Mouse HRP	Cell Signalling	7076P2	5

Table 3: Antibodies used for Western Blotting

2.3.3 Flow Cytometry

Cells were analysed for their expression of MSC markers using a Human Mesenchymal Stem Cell Marker Antibody Panel kit (SC017, R&D Systems). The kit contained several primary antibodies,

including antibodies of interest Stro-1, CD19, CD44, CD45, CD90, CD105, CD106, CD146 and CD166. Mouse IgG1 (MAB002, R&D Systems), and IgG2a (MAB003, R&D Systems) and IgM (14-4752, eBioscience, Affymetrix) were used as controls. Alexa 488 donkey anti-mouse IgG (A21202, Life Technologies) was used as the secondary antibody.

Cells were detached from the plate surface using TrypLE, and the resulting cell suspension was neutralised with culture media and centrifuged at 1000rcf for 5 minutes. The pellet was re-suspended in 1ml flow staining buffer (FC001, R&D Systems) and the cells were counted using the Countess II FL (Life Technologies). The cell suspension was made up to ensure a density of 2×10^6 cells per ml. Samples were incubated in primary antibody at 1:10 dilution for 30 minutes at room temperature, before washing with flow staining buffer and centrifugation at 1000rcf for 5 minutes. The pellet was re-suspended in 100 μ l flow staining buffer and incubated with secondary antibody at 1:20 dilution for 30 minutes at room temperature. Samples were then washed with flow staining buffer and centrifuged at 1000rcf for 5 minutes. The pellet was re-suspended in 200 μ l flow staining buffer and the samples run through a BD Accuri C6 flow cytometer (BD Biosciences), with BD CSampler software.

Results were analysed using FlowJo (BD Biosciences) where the following gating strategy was implemented: first the forward and side scatter dot plot was used to gate the hBMCs and isolate the cell data from that of cell debris or other particles. A histogram was used to compare the FITC fluorescence of the gated population from each sample against that of the appropriate isotype control. The percentage of cells positive for each marker was quantified by setting a bar gate at 1% for the isotype control, and recording the percentage within this bar gate from each sample. The median fluorescence intensity was calculated within the FlowJo software based on the gated population from each sample.

The percentage of positive cells within the gate and the median fluorescence intensity were input into PRISM 5 software and analysed using a two-way ANOVA with the statistical significance set at * $p < 0.05$, ** $p < 0.01$, and *** $p < 0.001$.

2.3.4 Enzyme-Linked Immunosorbent Assay (ELISA)

Cell culture media was collected as supernatant from cells and stored at -20°C. ELISAs were carried out on supernatant samples to analyse the concentration of TNF α produced and secreted by the cells.

Purified mouse anti-human TNF (TNF α capture antibody; 551220, BD Biosciences) was diluted to 1 μ g/ml in PBS, and 50 μ l was added to each well of a 96well microtiter plate. The plate was covered with a film lid and incubated overnight at 4°C. Wells were washed three times with ELISA wash buffer, containing 0.05% Tween 20 (P1379, Sigma) in PBS. Blocking buffer was prepared with 2% bovine serum albumin (BSA; A2153, Sigma) in PBS, and 100 μ l was added to each well. The plate was incubated at room temperature for 4 hours, then washed three times with ELISA wash buffer. Standards were prepared in culture media using serial dilutions of recombinant human TNF α protein (210-TA-005, R&D) in order to produce a standard curve at the following concentrations: 0ng, 0.06ng, 0.18ng, 0.55ng, 1.66ng, and 5ng. 50 μ l of standard and supernatant samples were added to the plate and incubated overnight at 4°C. Wells were washed three times in ELISA wash buffer. Biotin mouse anti-human TNF (TNF α detection antibody; 554511, BD Biosciences) was diluted to 0.5 μ g/ml in blocking buffer, and 50 μ l was added to each well. The plate was incubated for 4 hours at room temperature, before washing three times in ELISA wash buffer. Streptavidin horseradish peroxidase (890803, R&D) was prepared at a ratio of 1:250 in blocking buffer, and 50 μ l was added to each well. The plate was incubated at room temperature for 1 hour, then washed three times in ELISA wash buffer. 3,3',5,5'-Tetramethylbenzidine (TMB) peroxidase solution was prepared with a 1:1 ratio of TMB Peroxidase Solution (50-76-01, Invitrogen) and Peroxidase Substrate Solution B (50-65-00, Invitrogen), and 100 μ l was added to each well. The plate was incubated at room temperature for approximately 12 minutes, until the colour had developed. Stop solution (SS01, Invitrogen) was added to each well to stop the reaction, and the absorbance was measured at 405nm using a FLUOstar Omega spectrophotometer (BMG Labtech).

Absorbance data was exported to Excel and used to calculate the concentration of TNF α in the sample based on the standard curve. PRISM 5 software was used to carry out a Student's t-test, and statistical significance was set at * $p < 0.05$, ** $p < 0.01$, and *** $p < 0.001$.

2.3.5 Cell Fixation

Adherent cells cultured in normal cell culture plates were fixed by washing in HBSS and incubating in 4% paraformaldehyde (PFA; 158127-500G, Sigma) in PBS, for 20 minutes at room temperature. Cells were then washed three times in PBS, before covering in fresh PBS. The plates were covered in parafilm to prevent the sample drying out, and were stored at 4°C.

2.3.5.1 Fixation of Cells from Stretching Experiments

Cells cultured on PDMS sheets were gently washed with HBSS and fixed by incubation in 4% PFA in PBS for 20 minutes at room temperature. PDMS sheets were then washed three times in PBS before placing into a well plate containing fresh PBS and stored at 4°C.

Cells cultured on Strex well blocks were fixed by washing the wells gently with HBSS and incubating in 4% PFA in PBS, for 20 minutes at room temperature. Wells were then washed three times in PBS very gently, before covering in fresh PBS. A scalpel was used to cut the membrane out of the surrounding well and into several square pieces, depending on the number of antibody combinations that would be used. The sections of membrane were placed into well plates and submerged in fresh PBS. The plates were covered in parafilm to prevent the samples from drying out, and were stored at 4°C.

2.3.5.2 Fixation of Non-Adherent THP1 Cells

Non-adherent THP1 cells were collected into eppendorf tubes and centrifuged at 1000rcf for 5 minutes. The supernatant was removed, and the pellet was re-suspended in HBSS to wash the cells. The cells were spun down again and the pellet re-suspended in 4% paraformaldehyde (PFA; 158127-500G, Sigma) in PBS, for 20 minutes at room temperature. Cells were washed by continued spinning down and re-suspension of the pellet with PBS.

2.3.6 Immunofluorescence

2.3.6.1 *Immunofluorescence Staining: Monolayer Cell Culture in Well Plates*

Fixed cells were washed in PBS either with or without 0.1% triton (PBS-T; Triton-X100, Sigma). Triton was used if the protein of interest was expected to be located inside the cell so that the antibody would be able to penetrate the cell membrane, however for proteins expected to be found in the plasma membrane, triton would compromise the integrity of the membrane and therefore the protein of interest, consequently PBS alone was used. Wells were incubated for 1 hour at room temperature in blocking buffer, made up of either PBS or PBS-T with 5% donkey serum (D9663, Sigma), 0.25% bovine serum albumin (BSA; A2153, Sigma), and 0.25% cold water fish gelatine (G7765, Sigma). Samples were then covered in blocking buffer containing the desired concentration of primary antibody and incubated overnight at 4°C. Slides were washed three times in PBS or PBS-T before being covered in blocking buffer containing secondary antibody at the desired concentration. After 2 hours of incubation at room temperature and in the dark, nuclei were counterstained with 2µg/ml 4', 6-diamidino-2-phenylindole (DAPI; D9542, Sigma) in PBS or PBS-T, for 10 minutes at room temperature and in the dark. Wells were washed twice in PBS or PBS-T and mounted using DAKO Fluorescent Mounting Media (S3023, DAKO). Samples were incubated in the dark at room temperature for 2 hours, to allow the mounting media to polymerise, then were stored at 4°C.

2.3.6.2 *Immunofluorescence Staining: Cells from Stretching Experiments*

Fixed PDMS membranes containing adherent cells from stretching experiments were washed with PBS or PBS-T, depending on the location of the protein of interest, prior to incubation in blocking buffer for 1 hour at room temperature. Samples were then submerged in blocking buffer containing the desired concentration of primary antibody and incubated overnight at 4°C. Membranes were washed three times in PBS or PBS-T before being submerged in blocking buffer containing secondary antibody at the desired concentration. After 2 hours of incubation at room temperature and in the dark, nuclei were counterstained with 2µg/ml DAPI in PBS or PBS-T, for

10 minutes at room temperature and in the dark. Samples were washed twice in PBS or PBS-T and mounted onto modified polysine slides (J2800AMNZ, Thermo Fisher). Strips of PET plastic were made from OCT moulds (4133, Sakura Finetek) and adhered onto the surface of the slide using clear nail polish to create a well-like structure. The membrane was placed cell-side up inside the well-like structure and mounted using DAKO Fluorescent Mounting Media and a 24mm (10573462, Thermo Fisher) or 50mm (12373128, Thermo Fisher) coverslip, depending on the membrane size. Slides were incubated in the dark at room temperature for 6 hours, to allow the mounting media to polymerise, then were stored at 4°C.

2.3.6.3 Immunofluorescence Staining: Non-adherent THP1 Cells

Fixed cells were re-suspended in blocking buffer, made up of PBS with 5% donkey serum (D9663, Sigma), 0.25% bovine serum albumin (BSA; A2153, Sigma), and 0.25% cold water fish gelatine (G7765, Sigma) and incubated for 1 hour at room temperature. Samples were then spun down at 1000rcf for 5 minutes and the pellet resuspended in blocking buffer containing the desired concentration of primary antibody and incubated overnight at 4°C. Cells were washed three times in PBS using the spinning down method, as before, before being re-suspended in blocking buffer containing secondary antibody at the desired concentration. After 2 hours of incubation at room temperature and in the dark, nuclei were counterstained with 2µg/ml 4', 6-diamidino-2-phenylindole (DAPI; D9542, Sigma) in PBS, for 10 minutes at room temperature and in the dark. Cells were washed twice in PBS using the re-suspension method, as before. After washing, cells were spun down and re-suspended in 50µl DAKO Fluorescent Mounting Media (S3023, DAKO) and the liquid was placed in a drop on the middle of a slide. The coverslip was carefully placed onto the droplet, spreading it out beneath the coverslip. Samples were incubated in the dark at room temperature for 2 hours, to allow the mounting media to polymerise, then were stored at 4°C.

2.3.6.4 Antibodies Used

Details for the antibodies used for immunofluorescence of fixed cells are recorded in Table 3:

Antibody	Supplier	Catalogue Number	Lot Number
Alexa 488 donkey anti-goat	Life Technologies	A11055	1182671
Alexa 488 donkey anti-mouse	Life Technologies	A21202	1820538
Alexa 488 donkey anti-rabbit	Life Technologies	A21206	1387792
Alexa 488 donkey anti-rat	Life Technologies	A21208	1789917
Alexa 568 donkey anti-goat	Life Technologies	A11057	1235787
Alexa 568 donkey anti-mouse	Life Technologies	A10037	1303018
Alexa 568 donkey anti-rabbit	Life Technologies	A10042	1964370
Alexa 647 donkey anti-rabbit	Life Technologies	A31573	1903516
DMP1	R&D	AF4386	0
DMP1 (LFMb-31)	Santa Cruz	SC-73633	C0308
HAS3 (3C9)	Novus	NBP2-37494	140326
LAMP1 (D2D11)	Cell Signalling	9091	2
LC3A/B (D3U4C)	Cell Signalling	127415	3
MAP LC3 a/b	Santa Cruz	SC-16756	B0615
Osteopontin	Larry Fisher	LF-166	1
RUNX2 (M70)	Santa Cruz	SC-10758	G2815
Tubulin (YOL1/34)	Abcam	Ab6161	GR229236-2

Table 4: Antibodies used for Immunofluorescence of fixed cells

2.3.6.5 Imaging & Quantification

Immunofluorescence images were taken using a DMI6000 confocal microscope with a TCS SP8 attachment (Leica), and LAS AF software. The same image acquisition settings were used to obtain images within the same experiment in order for the relative fluorescence to be compared between experiment groups. Images were processed using Photoshop CC (Adobe).

Quantification of RUNX2-positive cells was carried out using Photoshop and Image-J (Fiji). RUNX2-positive cells were classified as cells with RUNX2 staining co-expressed with DAPI-stained nuclei, as RUNX2 is a transcription factor that is active in the nucleus. The number of RUNX2-positive cells were determined by marking a dot over the nucleus in a separate layer in Photoshop. This layer was then exported and opened in Image-J where it was made a binary image and the analyse particles function was used to count the number of dots denoting RUNX2-positive cells. The result for each image was recorded in an Excel spreadsheet then PRISM 5 software was used to carry out either a Student's t-test or ANOVA with Bonferoni correction, depending on the requirements of the data. Statistical significance was set at * $p < 0.05$, ** $p < 0.01$, and *** $p < 0.001$.

The fluorescent intensity of RUNX2-positive nuclei was determined in Photoshop; the nucleus of each RUNX2-positive cell was drawn round using the lasso tool, and the histogram function was used to record the mean fluorescent pixels within the drawn area in the red channel. The result for each RUNX2-positive cell was recorded in an Excel spreadsheet then statistical analysis was carried out in PRISM-5, as above. Additionally, three RUNX2-negative cells were recorded per image and used as a negative control to compare against the results obtained from the RUNX2-positive cells.

Imaris image analysis software (Bitplane) was used to produce 3D images from Z-Stacks and for quantification of LC3 puncta and cytoskeleton breakage. LC3 puncta, representing autophagosomes, were quantified using the spots function and the acceptable vesicle size was set to a range of 300nm to 1 μ M in order to reduce the risk of background staining being quantified as a LC3-positive vesicle. The number of spots for each image was produced within the statistics section of the Imaris software and were exported to Excel before inputting into PRISM-5 for statistical analysis.

Cytoskeletal breakage was determined by creating a surface representative of the α -tubulin or phalloidin staining in Imaris software. The surface had background subtraction set at 1 μ M and a voxel filter applied, to reduce background staining being included in the analysis. The area and volume of the surface as well as the number of disconnected components were produced within the statistics section of the Imaris software, and were exported to an Excel spreadsheet.

Statistical analysis was carried out in PRISM 5 software using either a Student's t-test or ANOVA with Bonferoni correction, depending on the requirements of the data. Statistical significance was set at * $p < 0.05$, ** $p < 0.01$, and *** $p < 0.001$.

2.3.7 Tartrate-Resistant Acid Phosphatase (TRAP) Staining

TRAP staining was carried out to determine the presence of osteoclasts. Adherent cells were fixed as described previously, and an acid phosphatase staining kit (387A-1KY, Sigma) was used for TRAP staining. This was performed according to the manufacturer's instructions, although

the volumes of solutions required were reduced for staining cells rather than tissue sections. Briefly, the staining solution was prepared using diazotized fast garnet GBC solution, naphthol AS-BI phosphate, acetate, tartrate, and distilled water. The solution was pre-warmed to 37°C, then 200µl added to each well of a 96 well plate. Cells were incubated in the staining solution for 1 hour at 37°C, before washing with distilled water. Wells were mounted in with ImmunoHistoMount™ (I1161, Sigma) and imaged using a MC170 HD camera (Leica) attached to a DMIL LED microscope (Leica), and using LAS AF Lite software (Leica).

Quantification of TRAP-positive multinucleated cells was carried out using Photoshop and Image-J. For each TRAP-positive cell with 3 or more nuclei a dot was marked in a separate layer in Photoshop. This layer was then exported and made a binary image in Image-J before the analyse particles function was used to count the number of dots denoting TRAP-positive and multinucleated cells. The same method was used to quantify the total cell number, the results for each image were recorded in an Excel spreadsheet and the percentage of osteoclasts in each image were calculated. PRISM 5 software was used to carry out either a Student's t-test or ANOVA with Bonferoni correction, depending on the requirements of the data. Statistical significance was set at * $p < 0.05$, ** $p < 0.01$, and *** $p < 0.001$.

2.4 *In vivo* Sample Processing & Analysis

2.4.1 Rat Tooth Movement Samples

A tooth movement experiment was carried out in a rat model by Professor Kai Yang of Capital Medical University, Beijing. Five female Sprague Dawley® rats were used per time point, which were 6 weeks old at the start of the experiment. The first molar was anchored to the upper incisor via an orthodontic spring, allowing the molar to be moved towards the distal part of the maxilla. The experiment was carried out over 21 days, with the device being re-fitted every 7 days, as the continuous growth of the incisor affected the angle of strain. Animals were sacrificed at 10 time points during that period: 0hr, 1hr, 3hr, 6hr, 12hr, 24hr, 72hr, 7day, 14day and 21day-post the initial onset of strain. The maxillae were dissected out and fixed with 4% PFA for 48

hours, before washing with PBS and decalcification with 18% ethylenediaminetetraacetic acid in PBS (EDTA) for 1 month. Samples were paraffin embedded and sectioned at 5 μ M, in the sagittal plane. Slides containing formalin fixed paraffin embedded (FFPE) samples were obtained from Professor Kai Yang and transported to Plymouth University for haematoxylin and eosin (H&E) and immunofluorescence (IF) analysis.

2.4.2 H&E Staining

H&E staining was carried out to analyse tissue structure. Solutions of 95% and 70% ethanol (20821.321, VWR) were prepared in distilled water, and Eosin Y (318906-500ml, Sigma) was diluted 1:4 in 80% ethanol.

Slides were heated at 55°C for 20 minutes to melt the wax, then were submerged twice in xylene (534056, Sigma) for 5 minutes at room temperature. Samples were then submerged twice in 100% ethanol for 5 minutes, then once in 95% ethanol (in distilled water) for 2 minutes and in 75% ethanol (in distilled water) for 2 minutes, before washing briefly in distilled water. The tissue was covered in Harris haematoxylin solution (HH516-500ml, Sigma) and incubated at room temperature for 8 minutes, before washing under running tap water for 5 minutes. Slides were then submerged in 1% acid alcohol (56694-100ML-F, Fluka) for 30 seconds, and washed under running tap water again for 5 minutes. The slides were then dipped 10 times into 95% ethanol, before the tissue was covered in eosin solution for 8 minutes. Slides submerged twice in 100% ethanol for 5 minutes, then placed into xylene twice for 5 minutes. Samples were mounted with Eukitt mounting media (03989-100ML, Fluka) and 55mm coverslips, and stored at room temperature. Images were taken using a MC170 HD camera (Leica) attached to a DMIL LED microscope, and LAS AF Lite software.

2.4.3 Immunofluorescence

2.4.3.1 *Immunofluorescence Staining: FFPE Samples*

FFPE samples were deparaffinised by heating to 55°C for 20 minutes. The slides were then submerged twice in xylene for 5 minutes, twice in 100% ethanol for 1 minute, then once in 95%

ethanol (in distilled water) and in 75% ethanol (in distilled water) for 1 minute. Samples were then washed in distilled water, before being submerged in citrate buffer and microwaved on full power (approximately 900watts) for 1 minute, before immediately being immersed in cold tap water. Samples were washed once more in cold tap water, then once in either PBS or PBS-T, depending on the location of the protein of interest. Slides were incubated for 1 hour at room temperature in blocking buffer, made up of either PBS or PBS-T with 5% donkey serum, 0.25% BSA, and 0.25% cold water fish gelatine. The sections were then covered in blocking buffer containing the desired concentration of primary antibody and incubated overnight at 4°C. Slides were washed three times in PBS or PBS-T before being covered in blocking buffer containing secondary antibody at the desired concentration. After 2 hours of incubation at room temperature and in the dark, nuclei were counterstained with 2µg/ml DAPI in PBS or PBS-T, for 10 minutes at room temperature and in the dark. Slides were washed twice in PBS or PBS-T and mounted using DAKO Fluorescent Mounting Media and 55mm coverslips. Slides were incubated in the dark at room temperature for 2 hours, to allow the mounting media to polymerise, then were stored at 4°C.

2.4.3.2 Antibodies Used

Details for the antibodies used for immunofluorescence of FFPE tissue are recorded in Table 4:

Antibody	Supplier	Catalogue Number	Lot Number
Alexa 488 donkey anti-goat	Life Technologies	A11055	1182671
Alexa 488 donkey anti-mouse	Life Technologies	A21202	1820538
Alexa 568 donkey anti-rabbit	Life Technologies	A10042	1826664
DMP1	R&D	AF4386	0
MAP LC3 a/b	Santa Cruz	SC-16756	B0615
Osteopontin	Larry Fisher	LF-166	1
RUNX2 (M70)	Santa Cruz	SC-10758	G2815

Table 5: Antibodies used for immunofluorescence of FFPE tissue

2.4.3.3 Imaging & Quantification

Immunofluorescence images were taken using a DMI6000 confocal microscope with a TCS SP8 attachment, and LAS AF software. The same image acquisition settings were used to obtain

images within the same experiment in order for the relative fluorescence to be compared between experiment groups. Images were processed using Photoshop.

The mask function in Imaris software was used to split images of rat maxilla into three regions containing the bone-PDL, PDL and PDL-dentine. For each region the quantification of LC3 puncta was carried out using Imaris and the number of fluorescent intensities of RUNX2-positive cells were determined using Photoshop and Image-J. Statistical analysis was carried out using PRISM 5 software, as was described for fixed cells (section 2.3.6.5).

3 Chapter 3: The role of Autophagy in the Periodontium during Experimental Orthodontic Tooth Movement

3.1 Introduction

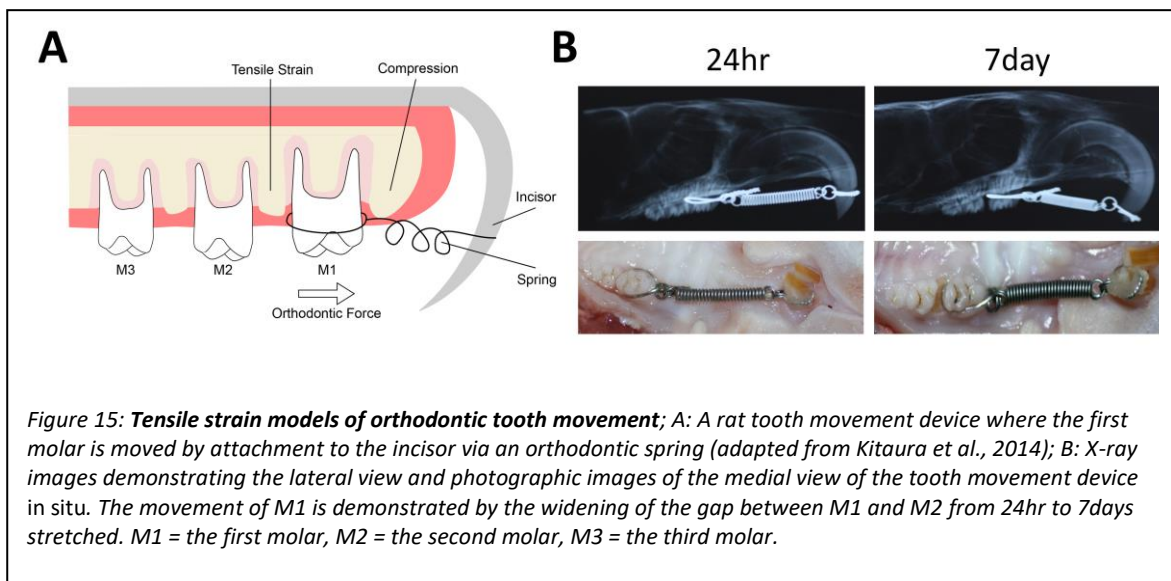
Tooth movement exposes cells of the periodontium to different mechanical stresses, including compression and tensile strain. These forces have different effects on stem cell differentiation for bone remodelling including that of osteoblasts for osteogenesis (Engler *et al.*, 2006; Dalagiorgou *et al.*, 2013; Zhou *et al.*, 2020). However, the exact mechanisms involved in this process are unknown. Additionally, while it is well established in the literature that mechanical strain can activate the autophagy pathway, it is still unclear whether mechanical strain-induced autophagy is protective or destructive and how constant mechanical strain, as with orthodontic tooth movement, may alter the autophagy pathway. It was theorised that perhaps cells exposed to tensile strain underwent an altered state of autophagic flux which could contribute to MSC activation or differentiation to osteoblasts. However, papers linking osteogenesis and autophagy have mostly been in *in vitro* studies rather than *in vivo*, and there are few papers exploring autophagy levels in the PDL during tooth movement.

This chapter investigates the effect of constant tensile strain on MSC differentiation into osteoblasts and attempts to establish the autophagic status of cells exposed to this mechanical strain, both *in vivo* and *in vitro*. The *in vivo* model system provided rat periodontium samples which were analysed for their expression of osteogenesis and autophagy markers at different stages of tooth movement. An *in vitro* cell stretching system was then trialled and optimised for use as an *in vitro* tooth movement model. hBMCs, containing osteoblast progenitors, were then analysed for their expression of osteogenesis and autophagy markers on exposure to constant tensile strain. The *in vitro* model was also used to further investigate the interplay between autophagy, osteogenesis and mechanical strain by experimental modification of the autophagy pathway.

3.2 Results

3.2.1 Tooth Movement *In Vivo*

In order to investigate the effect of mechanical strain on osteogenesis, a tooth movement experiment was carried out in female Sprague Dawley® rats by Professor Kai Yang of Capital Medical University in Beijing. This well-established model simulates tooth movement from orthodontic procedures, as the rat's first molar is anchored to the upper incisor by an orthodontic spring and is moved towards the distal end of the incisor (*Figure 15*).



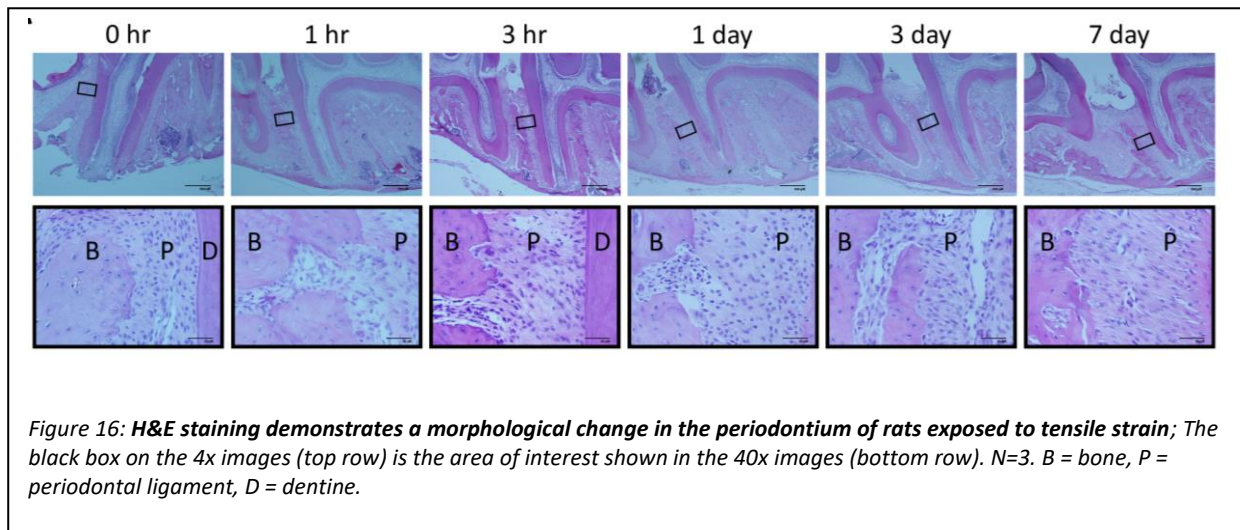
Rodent incisors continuously grow in order to compensate for gnawing behaviours. This meant that the angle of strain was slightly altered at different points during the experiment as the growing incisor moved the device in relation to the plane of the teeth. To compensate for this, the device was re-fitted every 7 days during the 21 day stretching period. Additionally, the nature of many orthodontic devices is such that there is a greater force exerted at the crown compared to the root. Therefore, the exact stretching conditions the periodontium was placed under was not constant during the experiment, thus the accuracy of this model when compared to the clinical situation, where the same level and angle of strain is used throughout, is debateable. However, it should be noted that in using this as a model of orthodontic tooth movement in human orthodontic tooth movement using braces, there are slight alterations in the strain patterns throughout treatment, which is mirrored by the above model.

Rats were 6 weeks old at the beginning of the experiment; at this age the rats have reached sexual maturity and their teeth are fully developed and erupted, thus are classified as adults (Denes *et al.*, 2018). Postnatally, each day for a rat relates to approximately 34.8 days of development for a human, when the differences in developmental stages and lifespan are considered (Sengupta, 2013). In considering the translational capacity of the work, the 21 day stretching period accounts for just over 2 human years, and with the average orthodontic treatment period for humans being between 2-3 years, the rat experiment may be comparable to the duration of human orthodontic tooth movement (Fink and Smith, 1992; Mavreas and Athanasiou, 2008).

Animals were sacrificed at 0hr, 1hr, 3hr, 6hr, 12hr, 24hr, 72hr, 7day, 14day and 21day-post the initial onset of strain with 5 animals in each group, and sagittal sections of the FFPE maxillae were obtained for analysis. It is well-established in the literature that in the scenario of tooth movement, one side of the periodontium will be exposed to tensile stretching force while the other is compressed. The stretched side undergoes osteogenesis, while the compressed side has increased bone resorption, and in this way the alveolar bone is remodelled, and the tooth is moved (Krishnan and Davidovitch, 2009). Therefore, the regions of interest of the periodontium included the alveolar bone, periodontal ligament and dentine between the first and second molars which had undergone constant tensile strain as the first molar was moved.

3.2.1.1 Morphology

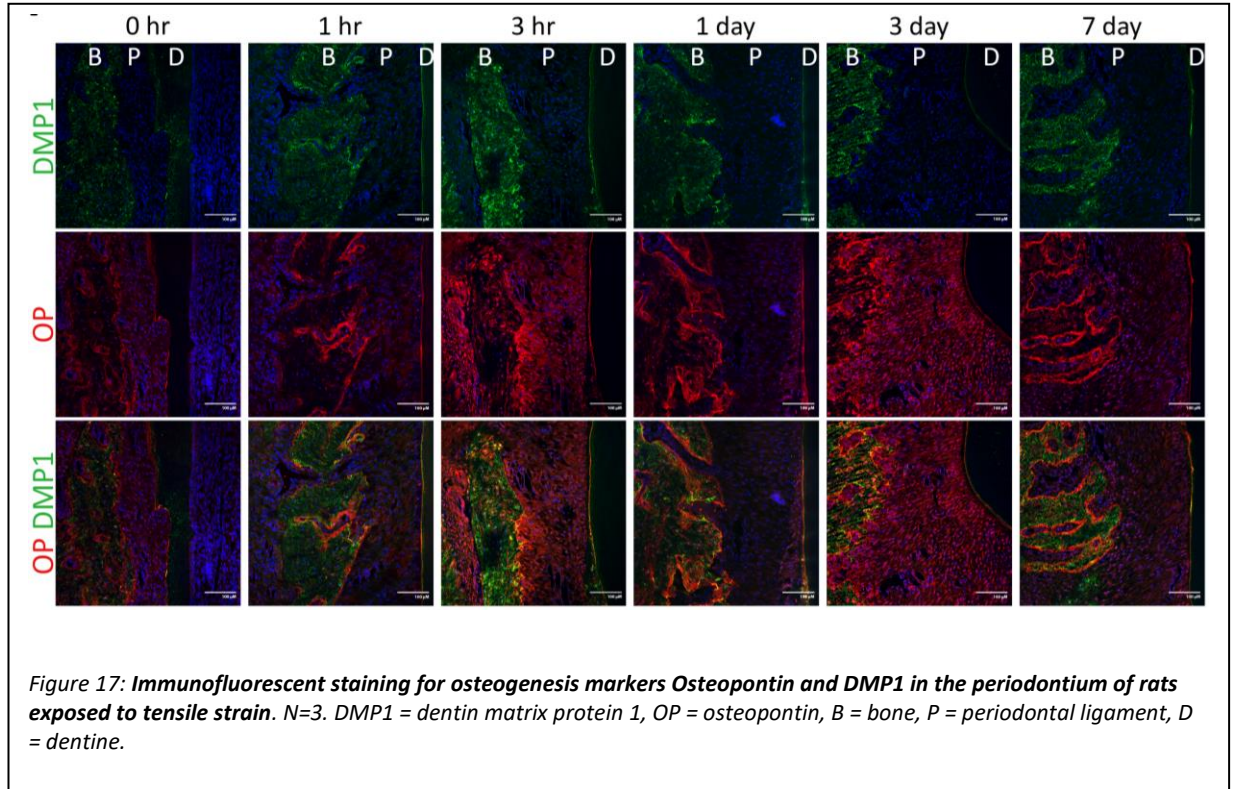
H&E staining was used to analyse morphological changes in the periodontium when exposed to constant tensile strain for between 1 hour and 7 days (*Figure 16*). Haematoxylin stains nucleic acids while eosin is a non-specific protein stain, therefore H&E staining can be used to identify basic cell shape, size and location within the tissue (Fischer *et al.*, 2008).



H&E staining demonstrated a morphological change in the periodontium of rats exposed to tensile strain. Indents in the bone were observed along the bone-PDL border on the side that had been stretched from 1 hour to 3 days. These indents seemed to have cells accumulated in them, which was especially obvious at 3 hours and 1 day. The indents ranged from slight, to holes that spanned the width of the bone, seen at 3 hours, or going down into the length of the bone, with the most pronounced indent being observed at 3 days stretched. By 7 days stretched the bone had less indents observed along the stretched side. There were also changes in the PDL, as it appears wider from 1 day to 7 days stretched, compared to the previous time points. The organisation of the PDL at 7 days stretched seemed more uniform than that of previous time points, with longer fibres between the nuclei than that seen at 0 hours.

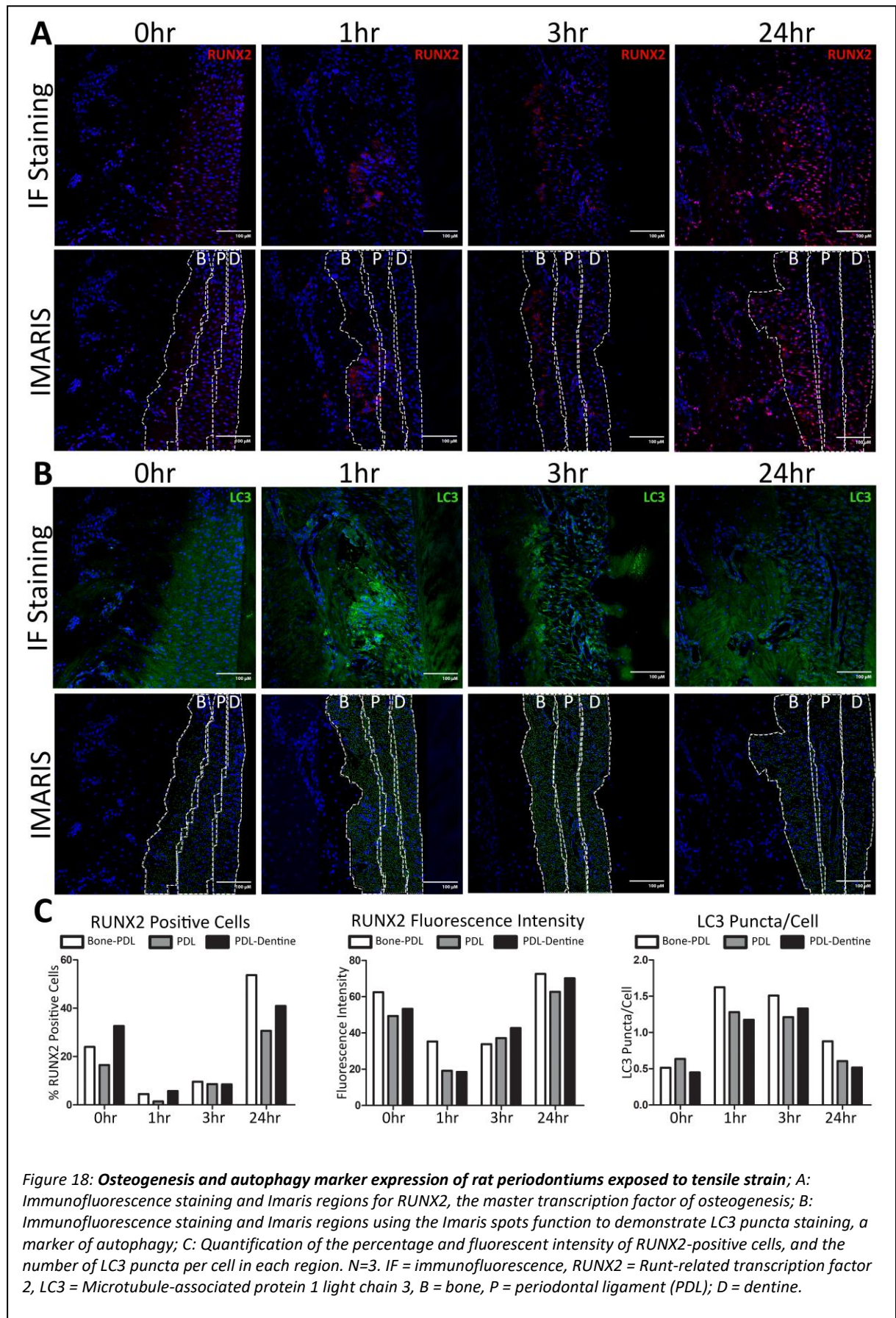
3.2.1.2 Osteogenic Marker Expression

Immunofluorescence was carried out for osteogenesis marker Osteopontin and DMP1, a protein involved in dentine and bone mineralisation (Figure 17).



There was an upregulation in DMP1 in the bone from 0 hour to 7 days stretched, with the highest expression being observed at 3 hours. The osteopontin staining increased steadily along the bone-PDL border over time as the tissue was stretched. In the PDL itself osteopontin expression was more varied, with little expression being observed at 0 and 1 hour, an upregulation in the PDL at 3 hours, a reduction at 1 day then another increase at 3 days before a reduction in expression at 7 days stretched. At 3 hours stretched osteopontin staining was higher on the side of the PDL that was being compressed by the tooth movement compared to the side that was being stretched. The cementum along the PDL-dentine border also seemed to show osteopontin staining from 1 hour to 7 days stretched, with no staining observed in this area at 0 hour. DMP1 staining was also observed along the cementum at 1 hour, 3 hours, 1 day and 7 days stretched, with no staining observed at 0 hour or 3 days.

Additionally, RUNX2 staining was carried out to analyse the expression of the master transcription factor of osteogenesis (*Figure 18*). The images were divided into regions of the periodontium using Imaris image analysis software and RUNX2 staining was quantified with two parameters: firstly, the number of RUNX2-positive cells, that being cells where RUNX2 staining was found co-localised with the nucleus, and secondly the fluorescence intensity of RUNX2 staining.



Compared to the 0 hour control, there was a decrease in the number of RUNX2-positive cells at 1 hour and 3 hours but an increase at 24 hours after the onset of strain. The greatest percentage of RUNX2-positive cells were identified in the bone-PDL region of the periodontium at 24 hours stretched. The relative expression of RUNX2 was compared by analysing the fluorescent intensity of RUNX2 staining in the RUNX2-positive cells. RUNX2 fluorescent intensity was decreased at 1 hour and 3 hours compared to 0 hour, but was increased at 24 hours stretched. The bone-PDL region was had a higher relative fluorescent intensity of RUNX2 than the PDL or PDL-dentine regions (*Figure 18C*).

3.2.1.3 Autophagy Marker Expression

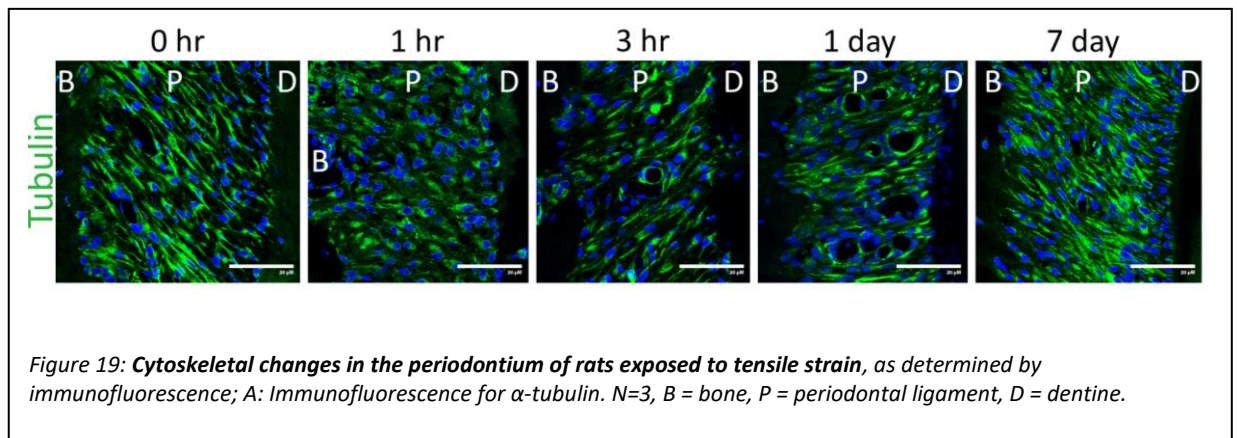
Autophagy levels were analysed in the rat tooth movement samples using immunofluorescence and quantification of LC3 puncta staining (*Figure 18*). Puncta staining of LC3 is widely accepted to be indicative of autophagy activation as it represents the conversion of LC3-I, present in the cytosol, to LC3-II, bound to the autophagosome membrane (Mizushima, Yoshimori and Levine, 2010). The LC3 puncta present in different areas of the periodontium were quantified using the spots function in Imaris, an image analysis software.

LC3 staining was increased at 1 hour and 3 hours stretched compared to 0 hour, but was then decreased at 24 hours. Imaris image analysis software was used to divide the images into three distinct regions, those being the bone-PDL, PDL and PDL-dentine, in order to better analyse the effects of stretching force on the periodontium (*Figure 18B*). The Imaris spots function was used to quantify LC3 puncta staining in each region which was normalised to the number of cells in the region to provide the number of LC3 puncta per cell. This quantification supported the observation that there was an increase in LC3 puncta at 1 hour and 3 hours compared to 0 hour. The highest number of LC3 puncta were observed in the bone-PDL region at 1 hour and 3 hours stretched. The number of LC3 puncta per cell was then decreased at 24 hours back to basal levels in the PDL and PDL-dentine regions, however in the bone-PDL region LC3 puncta was decreased

compared to the 1 hour and 3 hour samples, but was still higher than was observed at 0 hour (Figure 18C).

3.2.1.4 Cytoskeleton Expression

The cytoskeleton is a key cellular structure for mechanotransduction, therefore the rat tooth movement samples were analysed for tubulin staining, a cytoskeleton marker. The following immunofluorescence staining was carried out by Charlotte Illsley at Plymouth University and these samples were then provided for analysis.



Tubulin expression was decreased in the PDL after 1 hour of stretching compared to the 0 hour control, after which there was an increase in tubulin staining observed from 3 hours to 7 days (Figure 19). The staining pattern observed at 7 days looked to indicate cells with long, thin morphology which could suggest the fibroblasts present in the PDL were staining positive for tubulin. There were also hole structures seen in the PDL with the absence of α -tubulin staining at 3 hours and 1 day after the onset of strain.

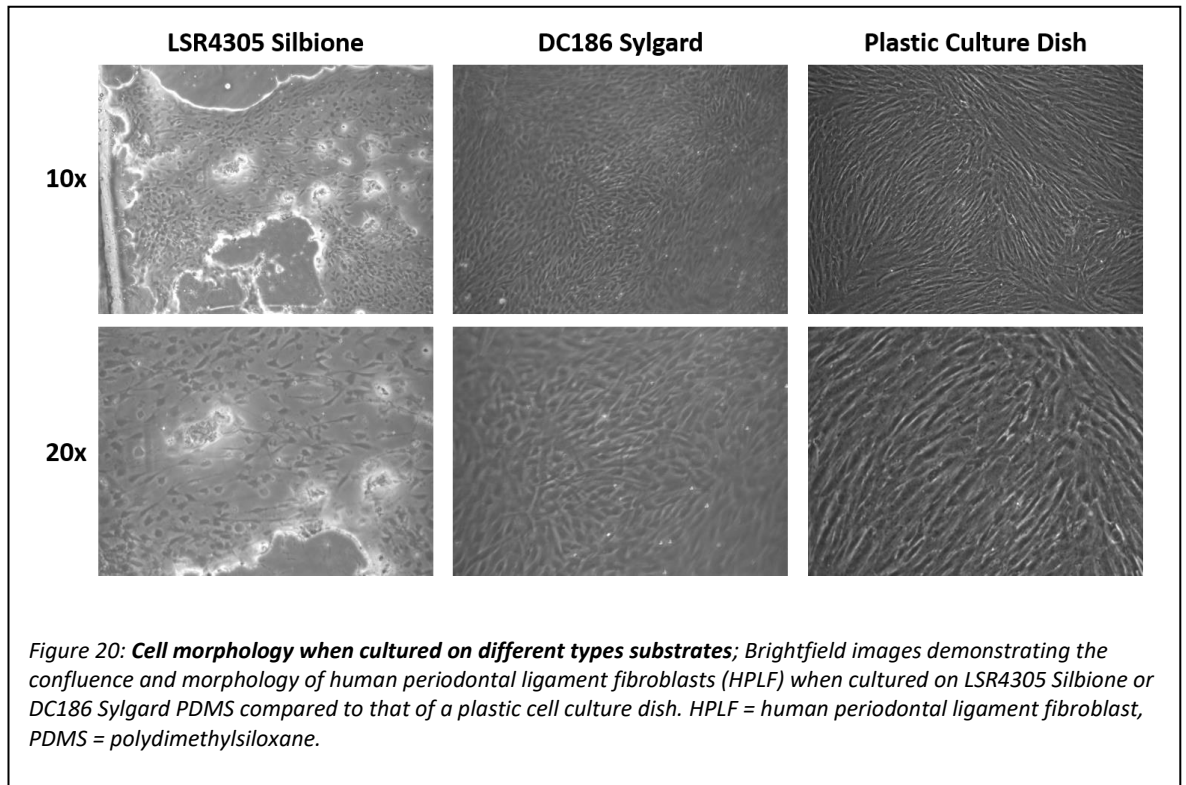
3.2.2 Optimising an *In Vitro* Cell Stretching Model

An *in vitro* cell stretching model was required in order to analyse the effects of constant tensile strain on stem cell activation and differentiation to osteoblasts. Initially, a collaboration was set up with Professor Herbert Shea of École Polytechnique Fédérale de Lausanne (EPFL), who was developing a cell stretching device for biological research.

3.2.2.1 *Optimising the Culture Conditions*

Initial experiments were aimed at optimising the culture conditions required to grow cells on polydimethylsiloxane (PDMS) and to determine which type of PDMS would be the best choice for producing the cell stretching devices. EPFL provided two types of PDMS in sheet form: LSR4305 Silbione and DC186 Sylgard. The sheets were produced by making up the PDMS solution, pouring it onto an A4 acrylic sheet and allowing it to set then covering it in a thin plastic to prevent damage or dust sticking to the PDMS during transit to Plymouth University.

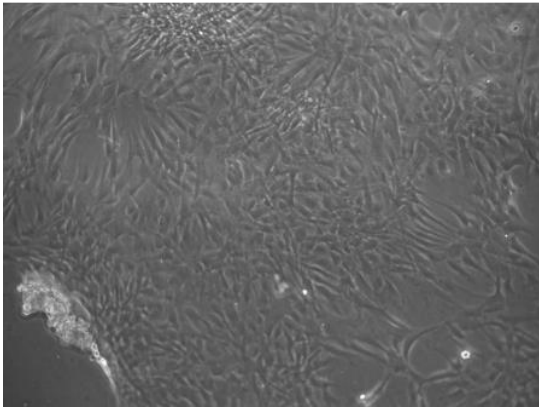
A 1cm by 1cm square was cut out of each sheet and the thin plastic covering removed before the PDMS square was sterilised in 100% ethanol for 20mins at room temperature. The squares were then washed briefly in sterile distilled water, placed into wells of a 12well cell culture plate and coated by covering in a sterile collagen coating solution and incubating at 37°C for 2hrs. The coating solution was aspirated and the sheets washed gently with HBSS in order to remove any excess solution, before cells were seeded. Primary human periodontal ligament fibroblast (HPLF) cells were used to optimise the initial culture solutions, as not only were they accessible and easy to maintain in culture, but they were relevant to the PDL during orthodontic tooth movement and therefore were considered for potential future experiments.



Some detachment of the cells and collagen coating was observed on the LSR4305 Silbione PDMS which was not observed on the DC186 Sylgard PDMS (*Figure 20*). Additionally, cells cultured on the normal culture dish had a long, fibroblastic morphology which was comparable to cells cultured on the DC186 Sylgard PDMS, whereas the LSR4305 Silbione PDMS contained cells which were shorter and had a rounder cell body. Therefore, it was determined that the DC186 Sylgard PDMS was the best choice for use in future experiments.

EPFL provided a tester device consisting of the DC186 Sylgard PDMS assembled within the structure of the device but not including the electrode contact points required for the device to be stretched (*Figure 21*). This device was sterilised, washed and collagen coated using the previously established protocol. HPLF cells were seeded onto the device at a density of 5×10^4 cells and incubated overnight at 37°C and 5% CO_2 .

Tester Device



Plastic Culture Dish

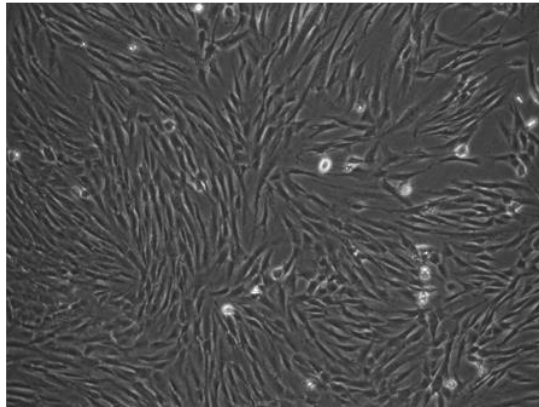
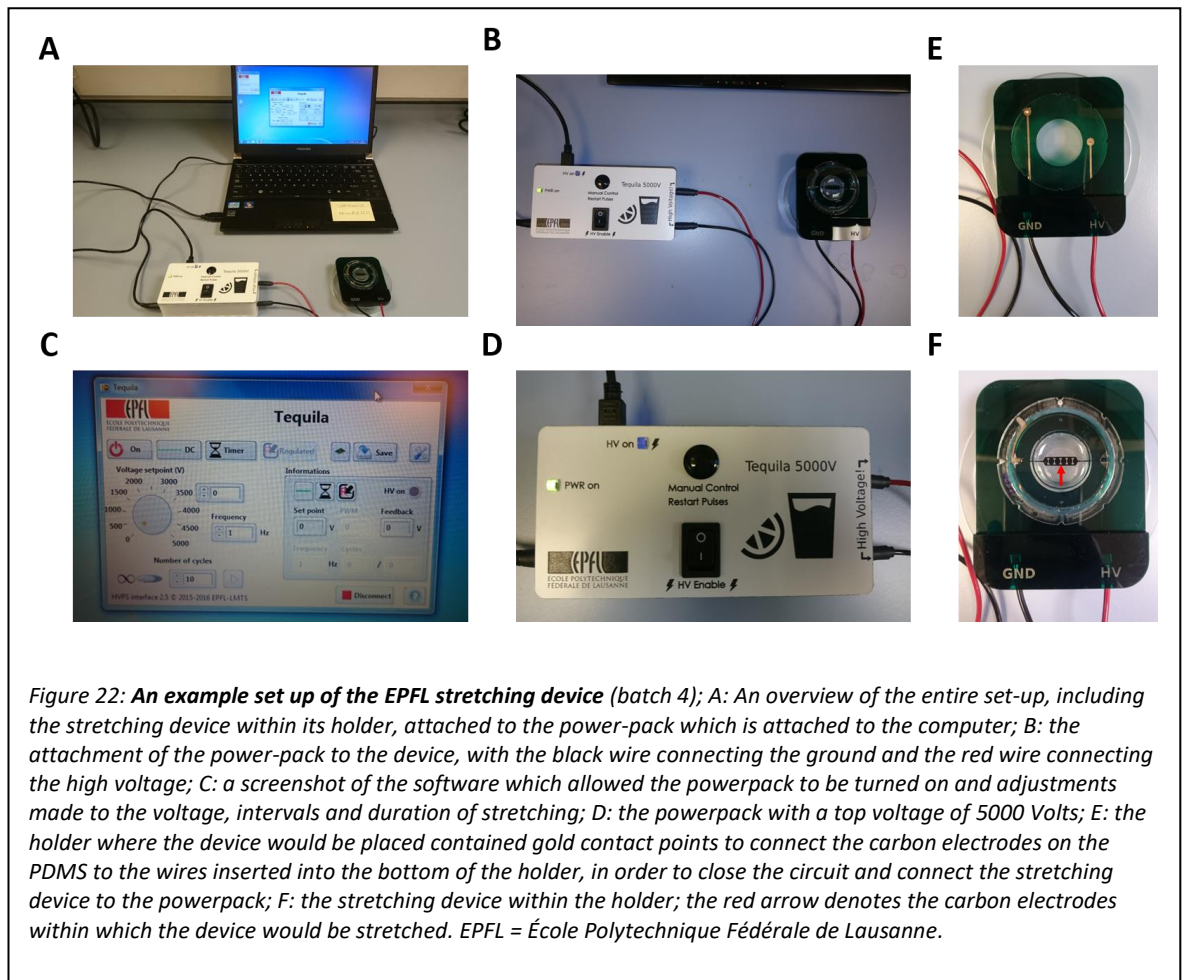


Figure 21: Cell morphology on EPFL cell stretching devices; Brightfield images demonstrating the confluence and morphology of HPLF cells cultured on the EPFL tester device compared to that of a plastic cell culture dish. HPLF = human periodontal ligament fibroblast.

After 24 hours cells were observed to have attached to the device with the expected morphology. These cells were cultured on the device for a further 5 days and were found to grow well and reach near full confluency. There did seem to be some detachment of the collagen coating, and thus also the cells, in some areas of the membrane however the majority had good cell confluency. This indicated that the culture conditions previously established by PDMS sheet cultures would be sufficient for use on the actual stretching devices.

3.2.2.2 EPFL Cell Stretching Device

EPFL provided several batches of stretching devices using the DC186 Sylgard PDMS. The design of the stretching device was being optimised throughout the collaboration as this was an ongoing project for Professor Shea's group, however there were some basic components to the device that were consistent in all of the batches. An example set-up of the EPFL stretching device is depicted in *Figure 22*.



The device consisted of a PDMS membrane stretched taut between rings of PET plastic, and printed with carbon electrodes on the PDMS surface. Once assembled, the carbon electrodes came into contact with metal electrodes on wires which connected the device to a power-pack. The power-pack was connected to a computer containing specialised software that could control the voltage used and duration the device would be stretched (Poulin *et al.*, 2016). It is important to note that the only area of the membrane that would undergo stretching was the space between the carbon electrodes (see the red arrow depicted in *Figure 22F*).

Initial experiments were carried out by culturing HPLF cells on these devices in order to establish how the device worked and the methods that would be suitable for analysing any molecular and cellular changes resulting from cell stretching. Several other cell types were also tested on the device, including the human bone marrow cells (hBMCs) which contain several cell types including mesenchymal osteoblast progenitors and were therefore clinically relevant to

osteogenesis during orthodontic tooth movement. An overview of these experiments and their outcomes is shown in *Table 6*.

EPFL Device	Cells (Passage)	Stretching	Outcome	Key Takeaways
Batch 1	HPLF (P8)	✓	Cell attachment observed and cells were able to be stretched using the device.	Cell culture was successful and the stretching device could connect to the software and powerpack and stretch the cells.
	HPLF (P10)	✓	Cells attached and stretched. Bubbles observed in the media during stretching, thought to be from the edge of the membrane where the carbon electrodes meet the gold electrode contacts.	Any liquid present on the sides or underside of the membrane should be avoided to prevent the device short-circuiting.
	HPLF (P11)	✓	The device was fully assembled prior to collagen coating or cell seeding to prevent liquid being present on both sides of the membrane. Cells attached and stretched with consistent stretching movements and no sparks observed.	The culture conditions were sufficient for HPLF attachment and stretching.
	hBMC (P8)	✗	Good cell attachment but the dish was knocked in incubator and the membrane was dry	Culture conditions were sufficient for hBMC attachment.
Batch 2	Ki67 FUCCI hBMC (P14)	✗	Low cell attachment and morphology was not as expected for fibroblasts	Thought that Ki67 FUCCI-infected hBMCs may not withstand culturing in this way. Decided to attempt the FUCCI reporter again once the system was set up and to revert back to using hBMCs to determine if it was a cell issue or another problem.
	hBMC (P13)	✗	PDMS membrane split overnight	EPFL informed us that the batch 2 devices were made of PDMS that was out of date. The devices were discarded.
Batch 3	hBMC (P8)	✗	No cell attachment was observed	Devices had been produced using a different oil in the oil-backing layer that seemed to be seeping through onto the surface of the device. Washing was unsuccessful, the devices were discarded.
Batch 4	hBMC (P5)	✗	Good cell attachment. Software issue meant the device could not connect to the powerpack therefore the device could not be stretched. Phalloidin staining of fixed cells could be visualised using the confocal microscope.	hBMCs cultured on the EPFL stretching device could be fixed and stained for immunofluorescence analysis. Re-installed the drivers and tested that the software could once again connect the powerpack to the device and stretch the device using a batch 3 device.

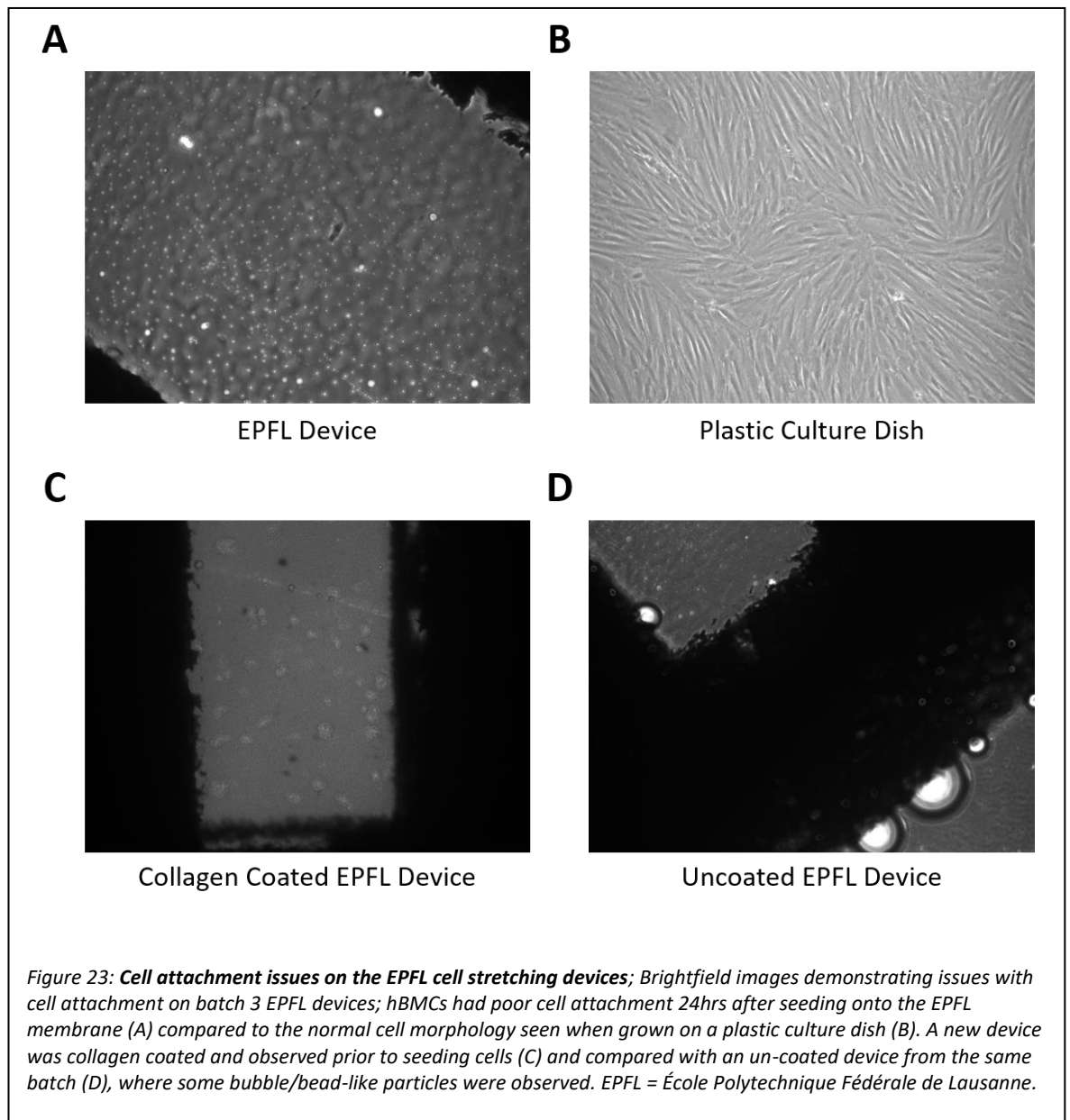
	hBMC (P5)	✓	Good cell attachment. CMDII could be visualised using the confocal microscope. Cells were stretched and imaged using the time lapse feature of the Leica software.	hBMCs could be visualised for live cell imaging using the Leica confocal microscope.
	Ki67 FUCCI hBMC (P8)	✓	Good cell attachment. Visualised cells using the confocal microscope and imaged during strain.	Some technical issues with keeping the device stationary and in focus, as even small strain caused the device to shift slightly. hBMCs infected with the Ki67 FUCCI virus were less proliferative.
Batch 5	Ki67 FUCCI hBMC (P10)	X	Good cell attachment seen a few hours after cell seeding, however 24hrs after seeding a white film was observed across the membrane that obscured the view of the cells.	The while film was determined to be an interaction between the media and oil from the oil backing layer, which was once again seeping through onto the top of the membrane. The devices were discarded.
	Ki67 FUCCI hBMC (P11)	X		

Table 6: An overview of the work carried out with the EPFL stretching devices and the key lessons learnt from these experiments. HPLF = human periodontal ligament fibroblasts, hBMC = human bone marrow cells, Ki67 FUCCI hBMC = human bone marrow cells infected with the Ki67 fluorescence ubiquitin cell cycle indicator (FUCCI) viral reporter, PDMS = polydimethylsiloxane, Ki67 FUCCI CLE = cervical loop epithelial cells infected with the Ki67 fluorescence ubiquitin cell cycle indicator (FUCCI) viral reporter.

The first batch of devices had some success in culturing HPLF cells, with good confluency and cell morphology similar to the cells when cultured on normal plastic dishes. In the initial test of the stretching function of the device, the device was assembled and stretched while dry in order to ensure all the components functioned properly, and the membrane was clearly seen to be moving when looked at down the microscope. However, when the device was stretched with cells and media present the movement of the device was much more subtle and some bubbles and even sparks were observed on one side of the device, near where the electrodes connected. The cells remained attached to the device throughout the test and were still attached with normal morphology after culturing 24 hours in the incubator after the test, therefore this did not seem to affect cell viability but there were questions as to whether this issue would affect gene expression or alter the electrical circuit and efficiency of the stretching device. It was decided that for future experiments the devices should be fully assembled, including the wires attached, prior to collagen coating and cell seeding in order to prevent any liquid being present on the sides or underside of the device which might cause it to short circuit. Some larger cell culture dishes were obtained for this purpose, so that the device could be fully assembled but still kept in as sterile conditions as possible.

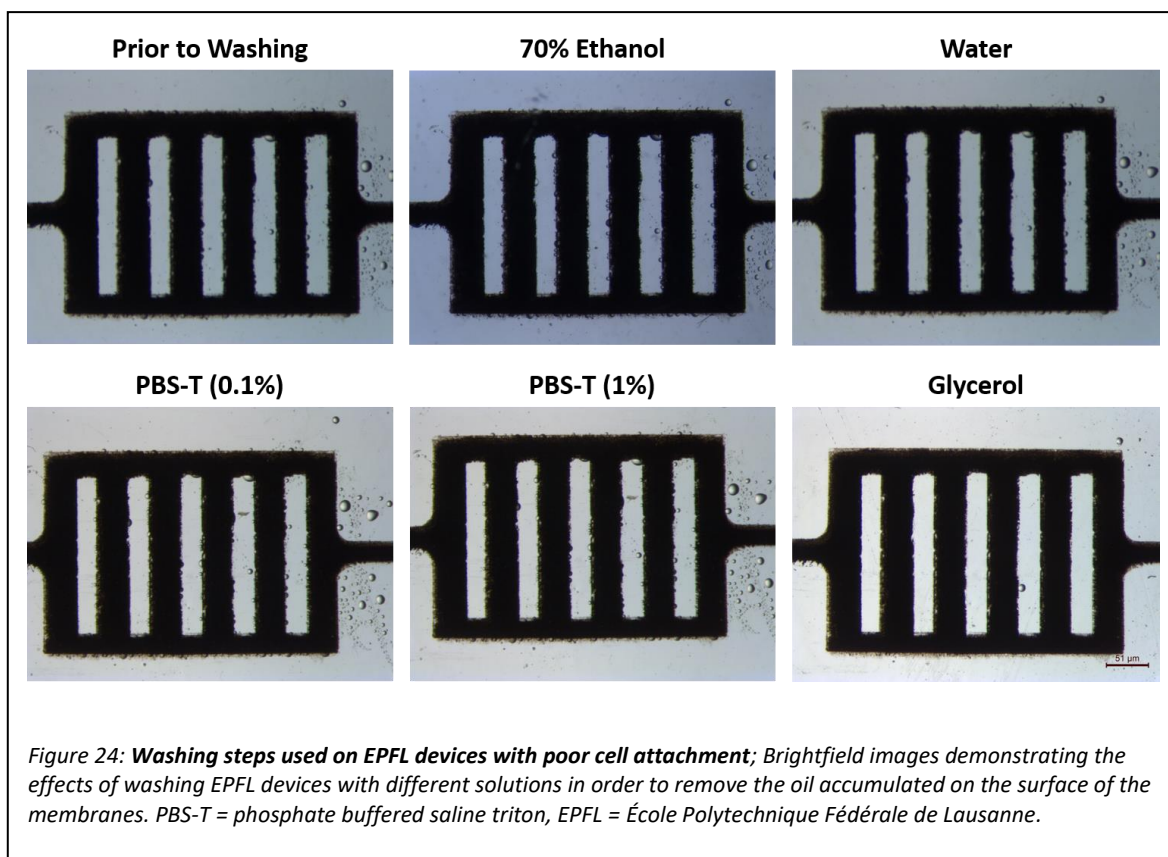
The second batch of devices were produced by myself on a visit to EPFL where I was trained in the production of the cell stretching devices. These devices differed in design to the first batch of devices that we received, as they contained silver contacts requiring conductive gel for easier attachment to the powerpack, a thicker plastic casing that ensured the PDMS ring was not required, and a higher number of carbon electrodes across the surface of the membrane for a larger surface area the cells could be stretched in. They also included an oil backing layer covered in thin cover-glass on the underside of the membrane which aimed at improving the visualisation of cells by microscopy. On my arrival to EPFL it was discovered that the only PDMS they had in stock was out of date however despite this we proceeded with making the devices. Several of the devices produced had the membrane split at some point during production, resulting in a batch of 30 devices remaining by the end of the process which were transported to Plymouth University for stretching experiments. However, they had a high failure rate during experiments including the membrane splitting and cells not attaching despite the same protocols being used as previous tests. Our collaborators determined that the PDMS being out of date may have resulted in more imperfections being present in the membrane which distorted the strain the membrane was under simply from being held taut in the device. This batch of devices was therefore discarded.

The third batch of devices also had issues with cell attachment (*Figure 23A*), with few hBMCs observed attached to the device 24hrs after seeding. From looking at the device down the microscope, some bubbles or round particles were observed which had not been seen in previous batches. Other devices from the same batch seemed to have beads of liquid on the membrane surface which was also observed for devices that had not been collagen-coated and should therefore have been dry (*Figure 23C-D*).



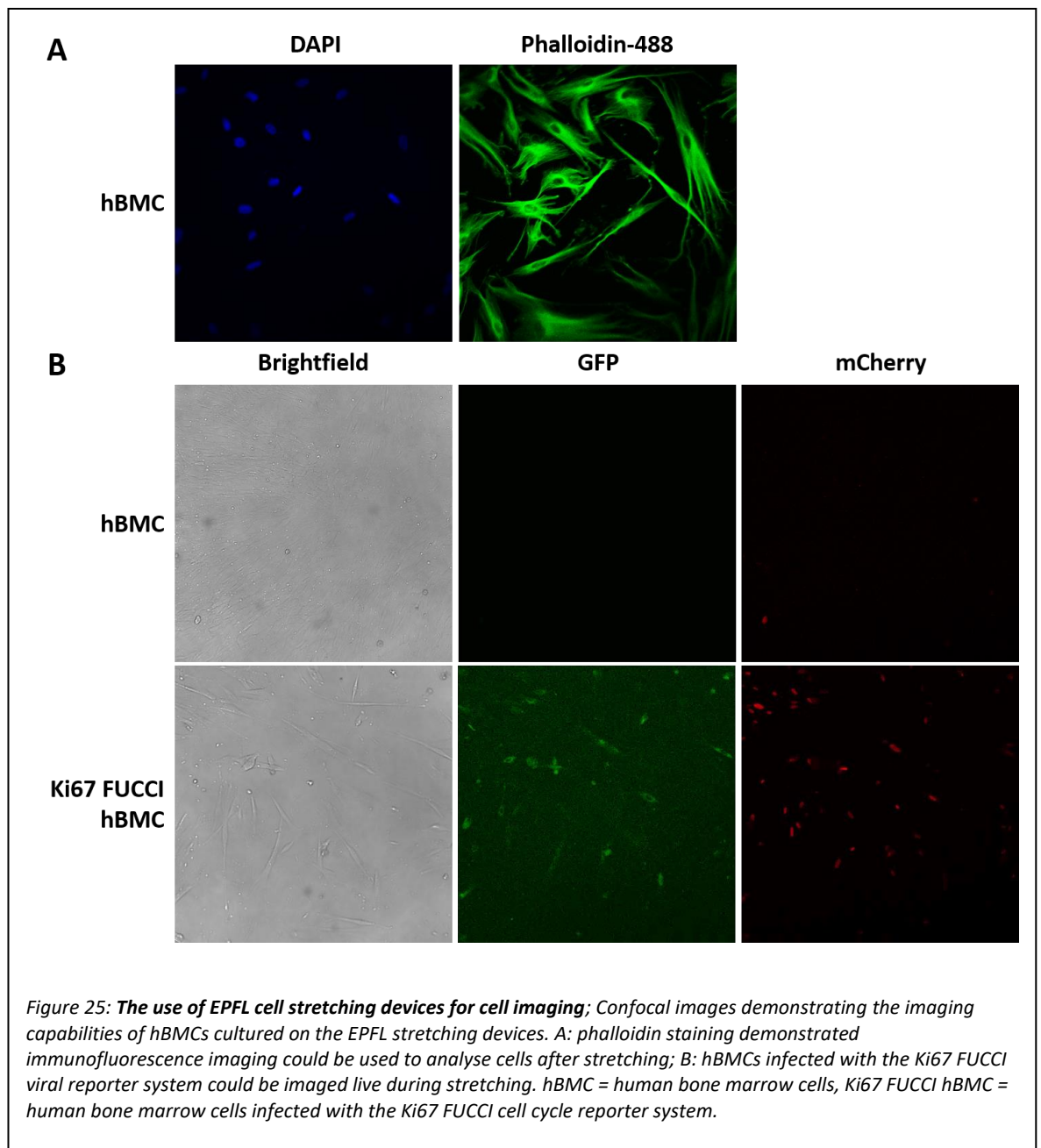
These beads would be present even after sterilising and washing the membranes and could be seen to absorb into a tissue but would then appear again a short time later. Our collaborators informed us that they had been experimenting with different oils for the oil backing layer in

order to refine their protocol, and had sent us a batch of devices which contained safflower oil rather than the Cargille microscopy immersion oil which was used in previous batches. They determined that the oil may be seeping through the membrane causing the beaded liquid that was observed. This would also have affected attempts to collagen coat and seed cells onto the device, resulting in the high failure rate of this batch of devices. To attempt not to waste the devices, several solutions were tested for washing including ethanol, methanol, detergent and glycerol due to its nature of being a polyatomic alcohol (Figure 24).



The glycerol wash seemed to have the greatest effect in decreasing the number of oil droplets observed on the membrane, however none of the solutions tested were able to completely remove the oil and even if the membranes were sterilised and collagen coated immediately after washing, cells were not successfully seeded on these membranes. It was decided that this batch of devices could not be used either.

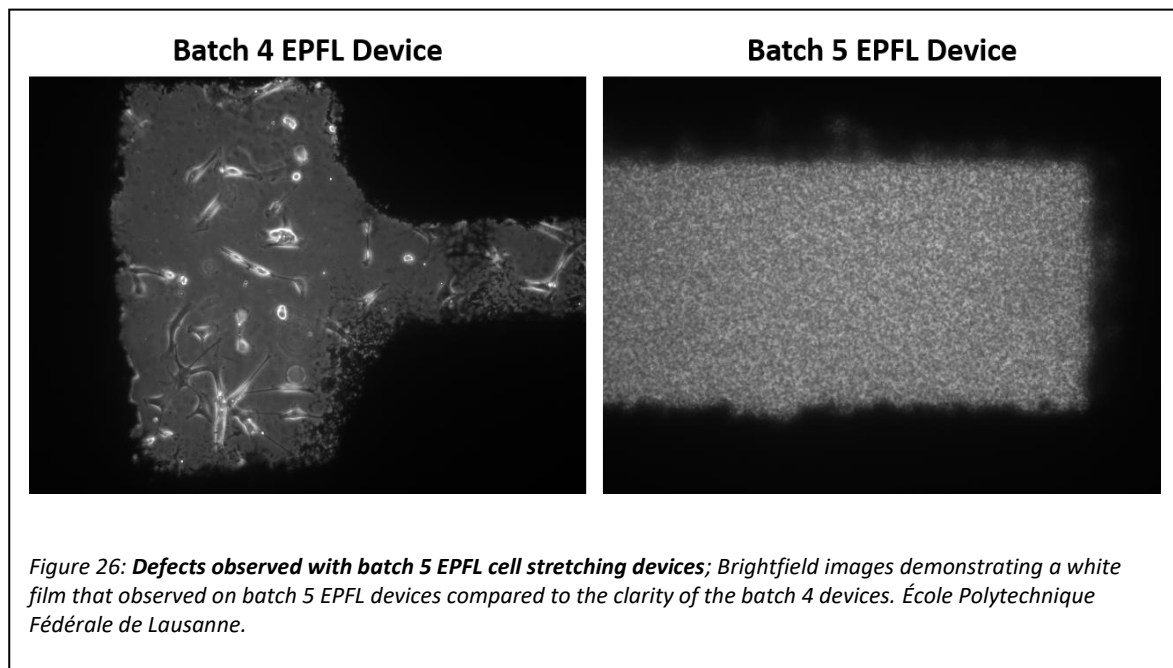
The fourth batch of devices did not have as many technical issues and were used to determine whether cells could be imaged on the stretching devices. Firstly, phalloidin was used to stain the actin cytoskeleton of hBMCs cultured on the EPFL stretching device (*Figure 25A*).



The cells could be observed using a Leica confocal microscope, however phalloidin could not be used to image the cells during the stretching process, only after fixation of the cells. Therefore, a viral reporter system was trialled for live cell imaging. hBMCs infected with the Ki67 fluorescence ubiquitin cell cycle indicator (FUCCI) viral reporter were cultured on the EPFL stretching device (*Figure 25B*). This reporter system utilises fluorescent-tagged proteins that are involved in different stages of the cell cycle and then rapidly degraded, allowing the

determination of a cell's cell cycle stage by the presence of red, green or yellow fluorescence (Zambon, 2010; Henderson, Lim and Zambon, 2014). The infected cells did not seem to proliferate as fast as normal hBMCs cultured on the EPFL devices and more debris was observed in the media suggesting there was some cell death in wells containing infected hBMCs. However, green and red fluorescence was observed in Ki67 FUCCI hBMCs, indicating that the EPFL stretching devices could be used for live cell imaging using this reporter system.

The fifth batch of devices received were again seeded with hBMCs that had been infected with the Ki67 FUCCI viral reporter system in order to observe any cell cycle progression occurring during stretching. Good cell attachment was observed initially after seeding however after 24 hours a white, opaque film had formed over the membrane (*Figure 26*). This obscured the view of the cells both using brightfield and fluorescence, therefore these devices could not be used to track cell cycle changes during stretching.



Several devices were tested and it was suspected that the film was likely to be an interaction between the media and oil from the oil backing layer which was slowly seeping through the membrane, therefore unfortunately these devices were also discarded.

Ultimately it was decided that the EPFL devices could not be used at that time to carry out the planned experiments, due to an issue in the consistency and volume of devices that would be

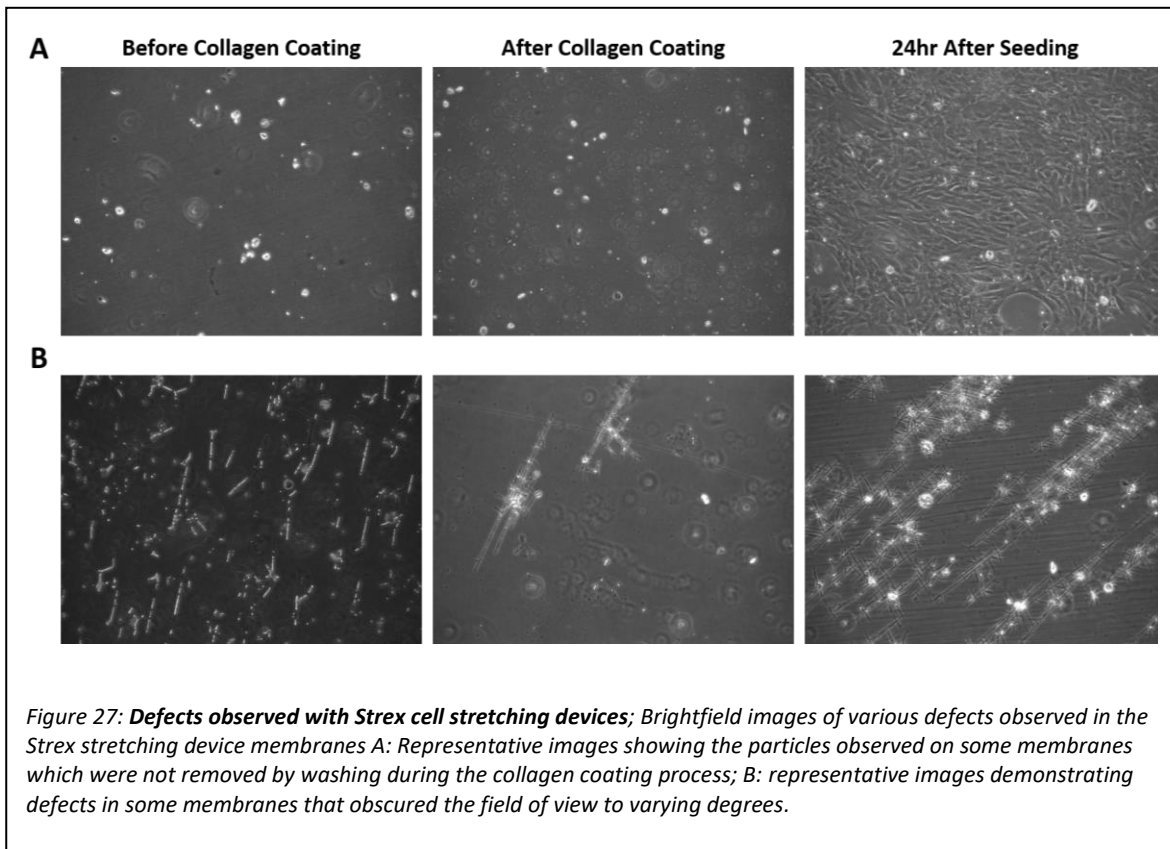
required. Therefore, stretching devices were sourced from Strex. The company provided stretching devices that were cruder in design than the EPFL system but were more reproducible and able to be obtained in a higher volume.

3.2.2.3 *Strex Cell Stretching Device*

The Strex manual cell stretching system consisted of a metal scaffold into which a PDMS block containing four wells could be inserted. The scaffold was attached to a screw which was turned to stretch the wells. Each full turn of the screw equated to 2.5% of stretch, with a maximum of 20% uniaxial stretching force.

The collagen coating solution specified by the manufacturer consisted of a 1:1 solution of 1mM hydrochloric acid (HCl) and 3mg/ml rat-tail collagen I. The membrane was covered in collagen coating solution and incubated at 37°C for 6 hours. Membranes were washed with HBSS, before the cells were seeded in culture media. Adherent hBMCs were seeded at 6.25×10^4 cells/cm², as recommended by the supplier, and incubated at 37°C and 5% CO₂. Cells could then be exposed to constant uniaxial strain 24 hours later.

In general, the Strex system was more reliable than the EPFL system and was able to be used to produce enough results for the later experimental work, however there were a few technical difficulties encountered that could not be avoided. Firstly, the blocks varied from batch to batch in their uniformity. Despite using the recommended technique for setting up the device, some of the blocks failed during stretching and detached themselves from the stretching apparatus. In another instance, one batch had a series of filamentous lines across the membrane when looked at down the microscope, and another had visible particles present prior to washing or collagen coating (*Figure 27*).



While these defects did not seem to affect the stability of the membranes, with no devices failing during stretching, they did pose difficulties when using the membranes for immunofluorescence as these defects auto-fluoresced and marred the field of view. The biggest problem encountered with the Strex cell stretching system however was cell detachment, as the cells were attached to the collagen coating rather than the membrane itself. Care was taken during washing steps to try to avoid dislodging the collagen from the membrane, however despite this some samples were still compromised in this way. It was observed that there were greater variances in the success of collagen coating and cell attachment in experiments that required several well blocks to be coated (*Figure 28*).

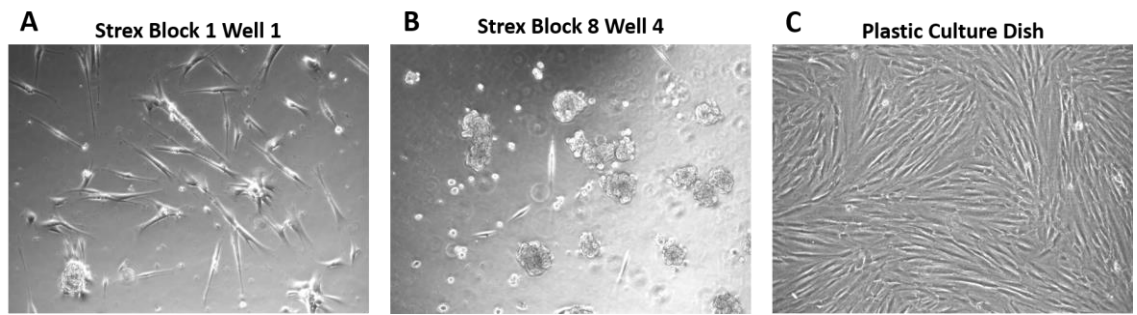


Figure 28: Cell attachment on Strex cell stretching devices; Representative brightfield images demonstrating the variation in the success of cell attachment within the same experiment. A&B: Images show wells in the Strex cell stretching block which were coated and seeded with hBMCs at the same time with the same components, the only difference being A depicts the first and B the last well to be collagen coated; C: the expected cell morphology and attachment in a plastic cell culture dish for comparison.

This was improved by coating the membranes in smaller batches, as although efforts were made to mix the solution, the viscosity of the collagen meant that it did not form a totally homogenous mixture. Vortexing was not recommended as it would introduce air bubbles, therefore collagen coating solutions were made up immediately before use and only for one block at a time. One factor that was found to be very important in the success of cell attachment over time was confluency. Once the cells began to reach around 80% confluency they were at risk of detaching from the membrane surface. The hBMCs grew well and could withstand seeding at lower cell densities, reducing the risk of cell detachment.

In terms of sample collection, the Strex devices did not require any additional optimisation for RNA or protein collection, with the protocols used being very similar to that of normal culture dishes. However, the normal fixation and immunofluorescence protocol had to be adapted for the Strex system. Fixing and staining the cells *in situ* in the wells was attempted, however the flexible nature of the block meant that it was difficult to get the membrane to lay flat. This meant that it was difficult to focus several cells in the same field of view and obtain good images. Placing the block onto a petri dish or glass slide for imaging helped to flatten the membrane somewhat, however this then raised the block above the stage and gave an extra layer for the laser to penetrate meaning cells could not be visualised at higher magnifications. Additionally, using this method meant a higher volume of antibody was required which was not cost effective.

Instead, a method was developed that consisted of excising the membrane, staining in a well plate then mounting on a slide, which provided better imaging results. As the underside of the membranes had not been collagen-coated they were still hydrophobic and were at risk of floating and exposing the cells to the air during incubations, therefore membranes were placed cell-side down in the well plate for staining. This meant that the cells would always been submerged in liquid throughout the staining protocol but meant that even more care had to be taken during the solution replacement, washes or movement of the membrane to avoid the cells from touching the bottom or sides of the plate.

These methods were developed in order to use the Stex cell stretching device as an *in vitro* model for investigating the effect of constant tensile stretching on osteogenesis.

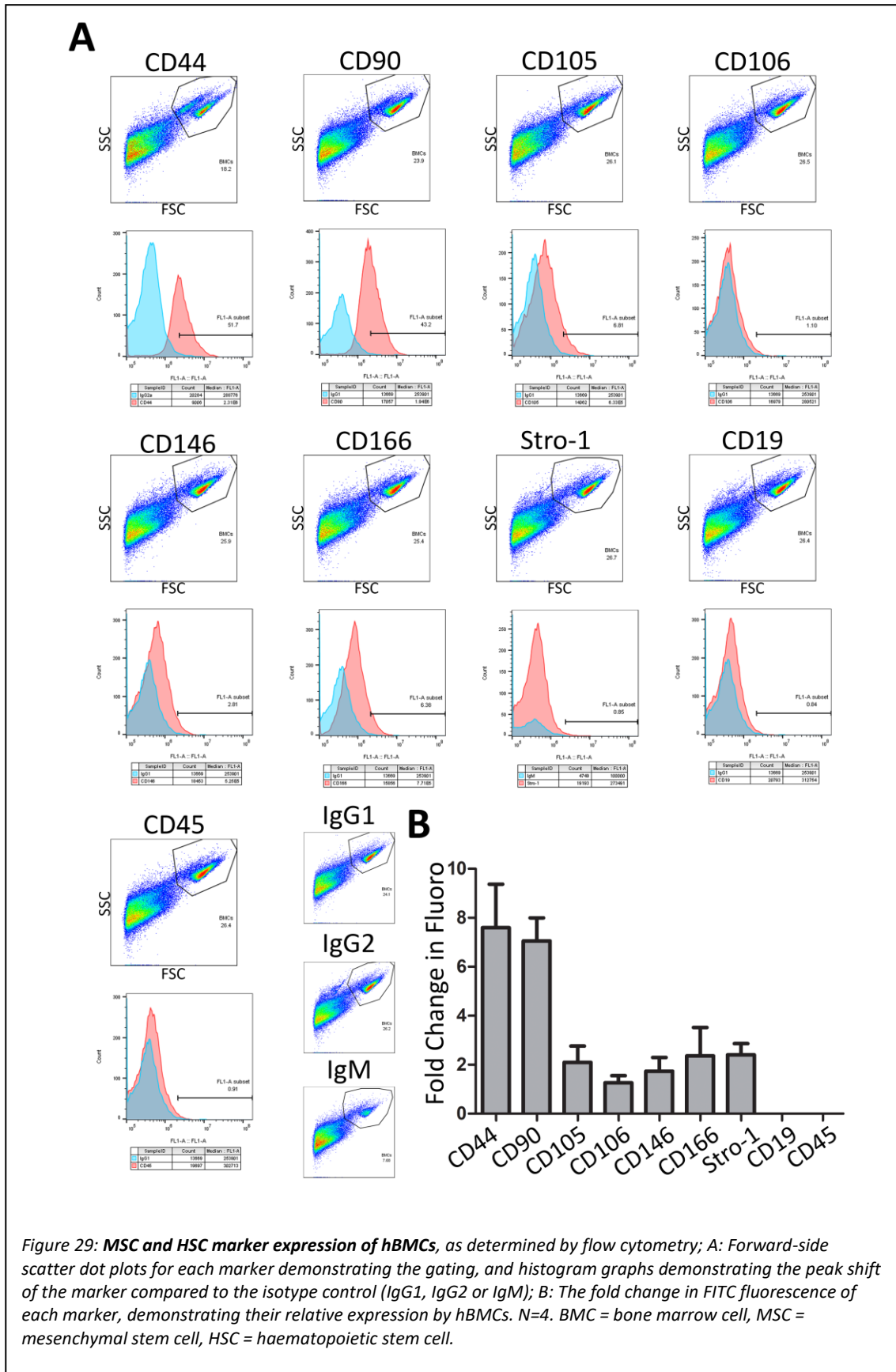
3.2.3 Human Bone Marrow Cell Characterisation

Primary human bone marrow cells (hBMCs) were used as a source of MSC-like and osteoblast progenitor cells. When first placed in culture, hBMCs were small, round, non-adherent cells. Over time in culture some cells adhered and these adherent cells were isolated for this work. After around two passages the hBMCs had a longer and more fibroblastic morphology. The cells were characterised for their marker expression and capacity to differentiate to osteoblast-like cells, to ensure their suitability for use as a model of the osteoblast-precursors that would be affected by tensile strain in the periodontium.

3.2.3.1.1 MSC Marker Expression

hBMCs were analysed for their expression of a panel of human MSC markers using flow cytometry (*Figure 29*). A commercial kit provided a panel of antibodies including Stro-1, CD44, CD90, CD105, CD106, CD146 and CD166. The kit also contained two HSC markers, CD19 and CD45, which were used as negative MSC markers. For each marker tested, the first graph demonstrates the forward and side scatter, with the gate used to isolate the hBMCs from cell debris or other particles, and the heat signature showing the relative number of cells present within that gate. The second graph shows the histogram peak shift in FITC fluorescence for each

sample compared to the relevant isotype control. The percentage of positive cells is quantified by setting the bar gate at 1% for the isotype control.



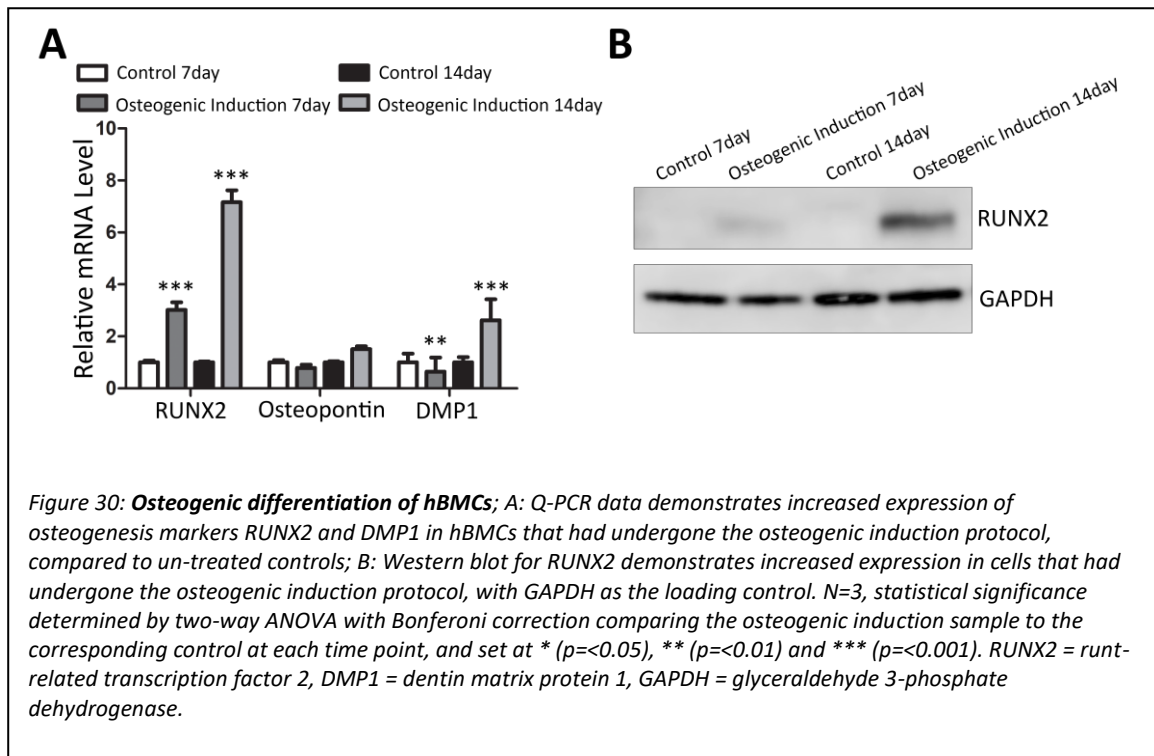
The hBMCs contained a population of cells that were positive for all the MSC markers, to varying degrees. There was a larger proportion of cells that were positive for CD44 and CD90, which was significant compared to the isotype control ($p < 0.001$). A smaller proportion of cells were positive for CD105, CD146, CD166 and Stro-1, and hBMCs contained a very small proportion of CD106 positive cells although these were not found to be significantly different when compared to the isotype control. The HSC markers, CD19 and CD45, were negative for the hBMCs with no significant difference between sample and isotype control, suggesting that the adherent hBMCs tested did not contain HSCs.

Different passages of hBMCs, ranging from P3 to P12, were tested for their expression of these markers. All the passages contained a comparable proportion, around 60%, of CD90 positive cells, however there was a higher proportion of CD45 in the lower passage cells (P3 and P5) compared to the higher passage cells (P12).

These results suggest that the hBMCs contain a population of cells that are MSC-like, in that they express cell surface markers associated with MSCs.

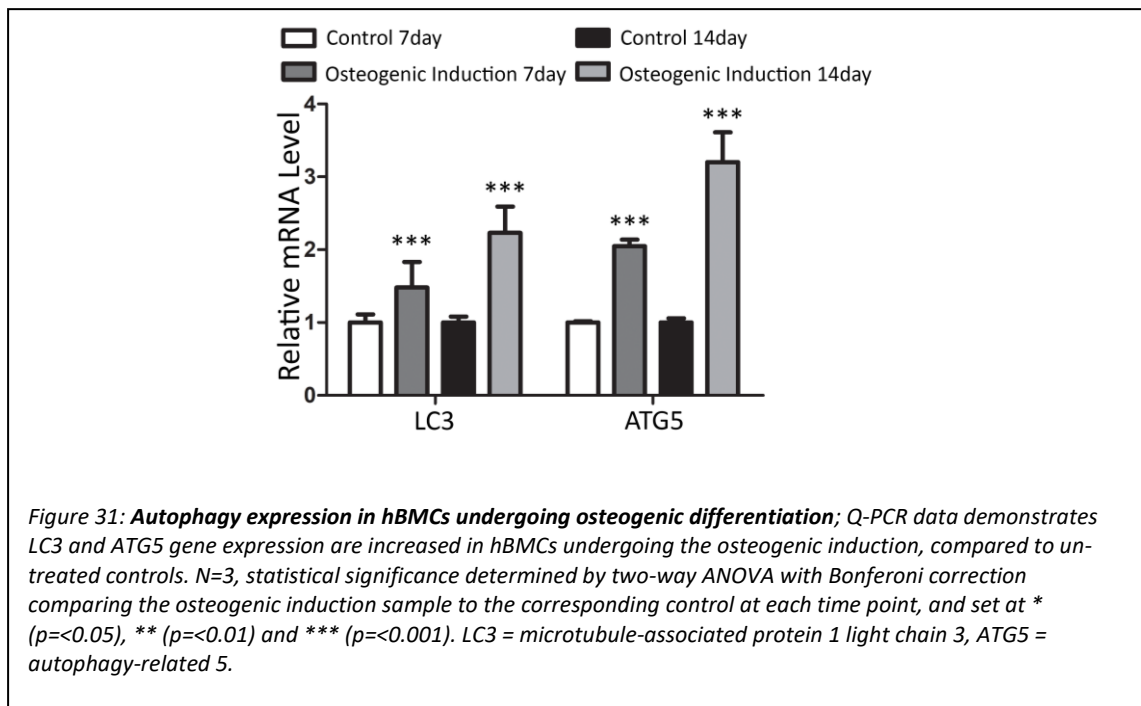
3.2.3.1.2 Osteogenic Differentiation

The plasticity and differentiation potential of hBMCs was tested by treating them with a well-established osteogenic induction medium (*Figure 30*). Cells were incubated in culture media containing dexamethasone, β -glycerol phosphate and ascorbic acid, for 7 or 14 days. Dexamethasone enhances hBMCs' responsiveness to RUNX2 and BMP2 which promote osteogenic differentiation (Yuasa *et al.*, 2015). Ascorbic acid is required for collagen production and therefore for the production of osteoid, while β -glycerol phosphate promotes mineralisation (Langenbach and Handschel, 2013).



Treated hBMCs had significantly increased expression of *RUNX2*, a key gene for initiating osteogenesis, compared to controls ($p < 0.001$). Additionally, *RUNX2* expression had almost doubled from 7 days to 14 days in treated cells. Treated samples had decreased *DMP1* expression at 7 days compared to controls ($p < 0.01$) but expression was increased in treated samples at 14 days ($p < 0.001$). There was no change in *osteopontin* gene expression between the control and treated cells at either time point (Figure 30A). Western blotting showed that at the protein level *RUNX2* was expressed at 7 and 14 days in the treated samples, while no bands were observed in the control samples at either timepoint. A darker band observed in the 14 days treated sample lane indicates that the amount of *RUNX2* protein was increased from 7 days to 14 days in the treated samples (Figure 30B). This suggests that hBMCs have the capacity to differentiate to osteoblast-like cells, therefore are suitable for use in determining the effect of constant tensile strain on differentiation.

These hBMCs that had undergone the osteogenesis induction protocol were also analysed for their expression of autophagy-related genes, to determine the cells' basal levels of autophagy during osteogenesis (Figure 31).



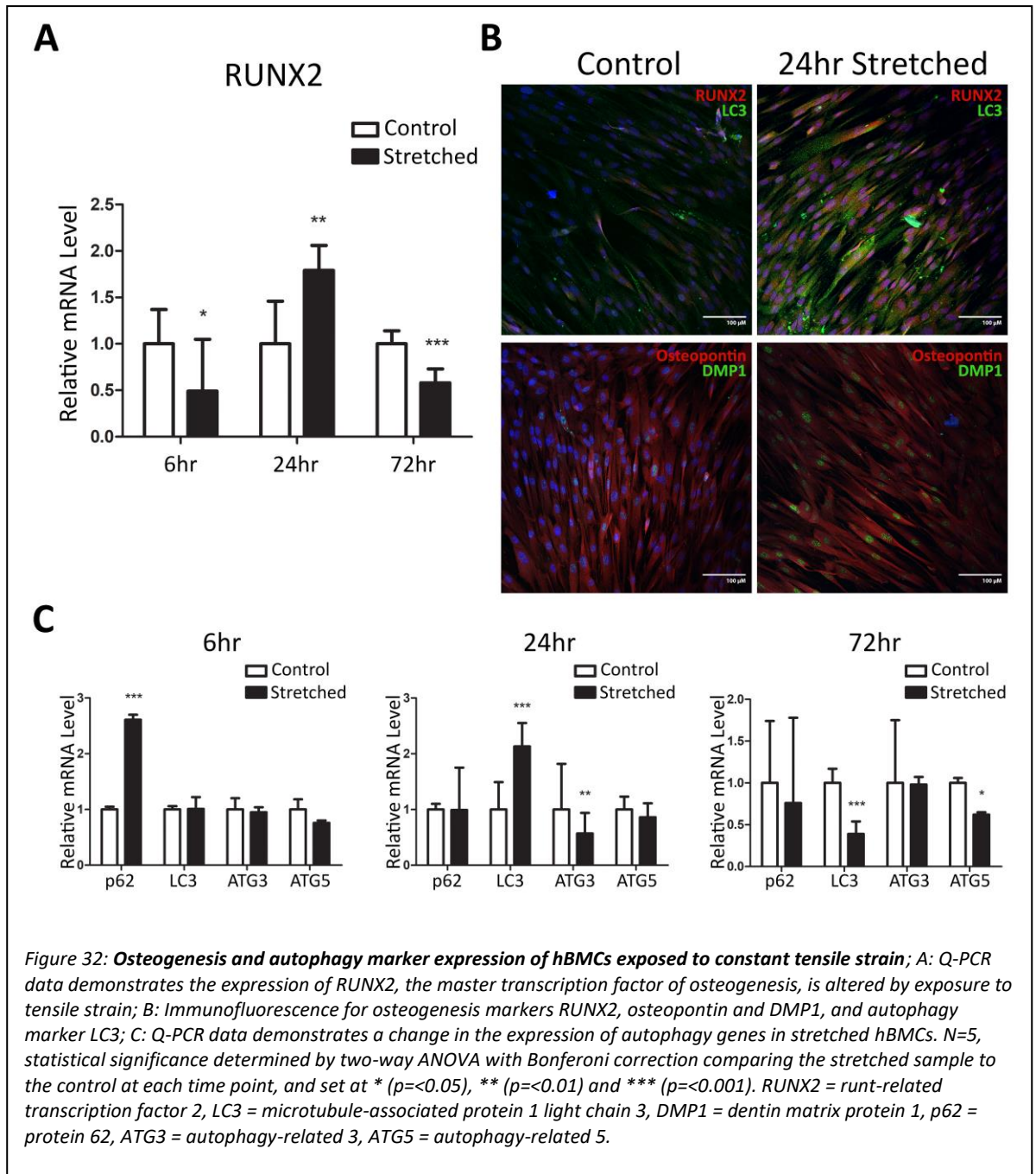
Treated hBMCs had increased expression of autophagy markers LC3 and ATG5 compared to the corresponding control at both 7 and 14 days ($p < 0.001$).

3.2.4 Tooth Movement *In Vitro*

Once it was established that the hBMCs contained a population of cells that were MSC-like and could differentiate to osteoblast-like cells, these cells were used to determine the effects of constant tensile strain on osteogenic differentiation using the Strex manual cell stretching device. Due to the constraints of the cell stretching system, specifically that of cell detachment when full confluency was reached, only experiments up to 72 hours of strain were viable. Experiments were carried out using the cells' standard maintenance culture media without the addition of the small molecules used in the osteogenic induction protocol (used for experiments shown in Figures 30 & 31), so that any changes in osteogenic marker expression were attributable to the stretching alone.

3.2.4.1 Stretching hBMCs

hBMCs were exposed to 20% constant uniaxial strain for 6, 24 or 72 hours, before RNA was collected and cells fixed for immunofluorescence (Figure 32).

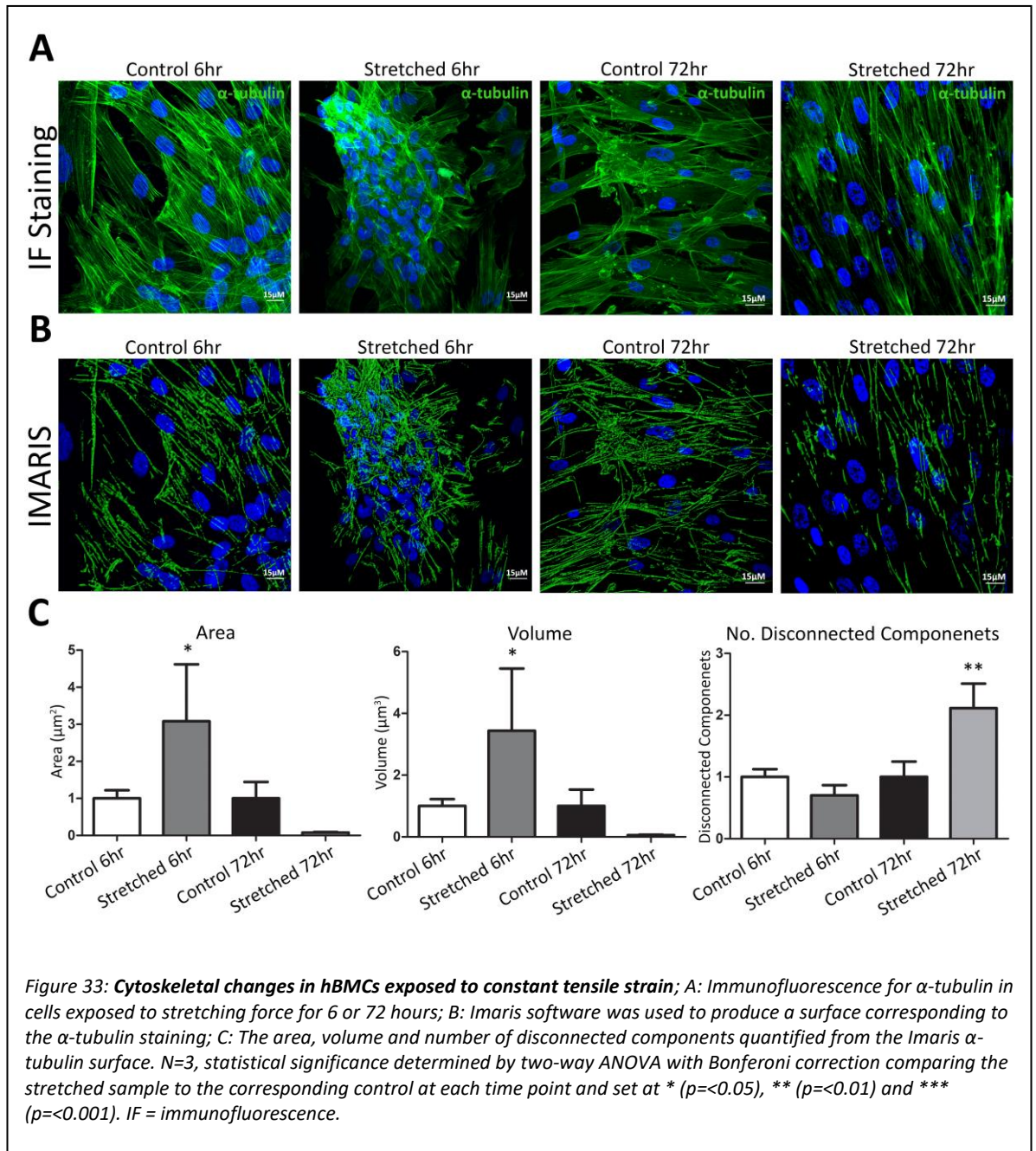


RUNX2 gene expression was initially downregulated at 6 hours in stretched samples ($p < 0.05$) but was increased at 24 hours compared to controls ($p < 0.01$). At 72 hours stretched RUNX2 expression was decreased again ($p < 0.001$; Figure 32A). Immunofluorescence revealed that at 24 hours RUNX2 staining was increased and was nuclear localised, while staining was much lower in control cells. Osteopontin and DMP1 staining was increased, and DMP1 was found to

be nuclear localised in stretched cells compared to controls (*Figure 32B*). Stretched cells were also analysed for their expression of several autophagy-related genes, including *p62*, *LC3*, *ATG3* and *ATG5*. At 6 hours stretched cells had upregulated expression of *p62* ($p < 0.001$), while there was little change in *LC3*, *ATG3* or *ATG5* expression compared to control cells. *LC3* expression was significantly increased in stretched cells compared to controls at 24 hours ($p < 0.001$), while *ATG3* expression was decreased ($p < 0.01$). At 72 hours stretched *LC3* and *ATG5* expression were downregulated in stretched samples compared to controls ($p < 0.001$ and $p < 0.05$, respectively). There was no change observed in *p62* or *ATG3* expression at this time point (*Figure 32C*). The level of autophagy occurring in stretched cells was determined by the presence of LC3 puncta staining, quantified using IMARIS software. At 24 hours, stretched cells had an increase in the number of LC3 puncta staining observed compared to control cells (*Figure 32B*).

3.2.4.2 Strain and Cytoskeleton Breakage In Vitro

hBMCs were exposed to 20% constant uniaxial strain for 6 or 72 hours, before immunofluorescence for α -tubulin. Z-stacks were input into Imaris software and a surface was created for the α -tubulin staining. The Imaris software provided statistics for the area, volume and the number of disconnected components for that surface, allowing for quantification of cytoskeleton breakage (*Figure 33*).



While cells are positioned randomly in the control conditions, hBMCs stretched for 72 hours alter their alignment in line with the direction of strain (Figure 33A). The surfaces created using Imaris demonstrate the α -tubulin filaments analysed, which are comparable to the staining observed (Figure 33B). Quantification of these α -tubulin filaments showed an increase in area and volume at 6 hours ($p<0.05$), which was decreased at 72 hours stretched compared to controls ($p=ns$). There was little change in the number of disconnected components at 6 hours stretched, however this was increased at 72 hours stretched compared to controls ($p<0.01$; Figure 33C).

3.2.5 Autophagy Modulation using an *In Vitro* Stretching Model

In order to investigate the role of autophagy in strain-induced osteogenesis two drugs that modulate autophagy were used. Rapamycin is a well-established activator of the autophagy pathway, while bafilomycin inhibits autophagy. The previously established *in vitro* cell stretching model was used, with cells being treated with either rapamycin or bafilomycin 24 hours prior to exposure to constant tensile strain. Due to the constraints of the cell stretching system, specifically that of cell detachment when full confluency was reached, only experiments up to 72 hours of strain were viable.

3.2.5.1 *Autophagy Induction and Strain In Vitro*

hBMCs were treated with rapamycin, an inducer of autophagy, prior to exposure to 20% constant tensile strain for 6, 24 or 72 hours (*Figure 34*).

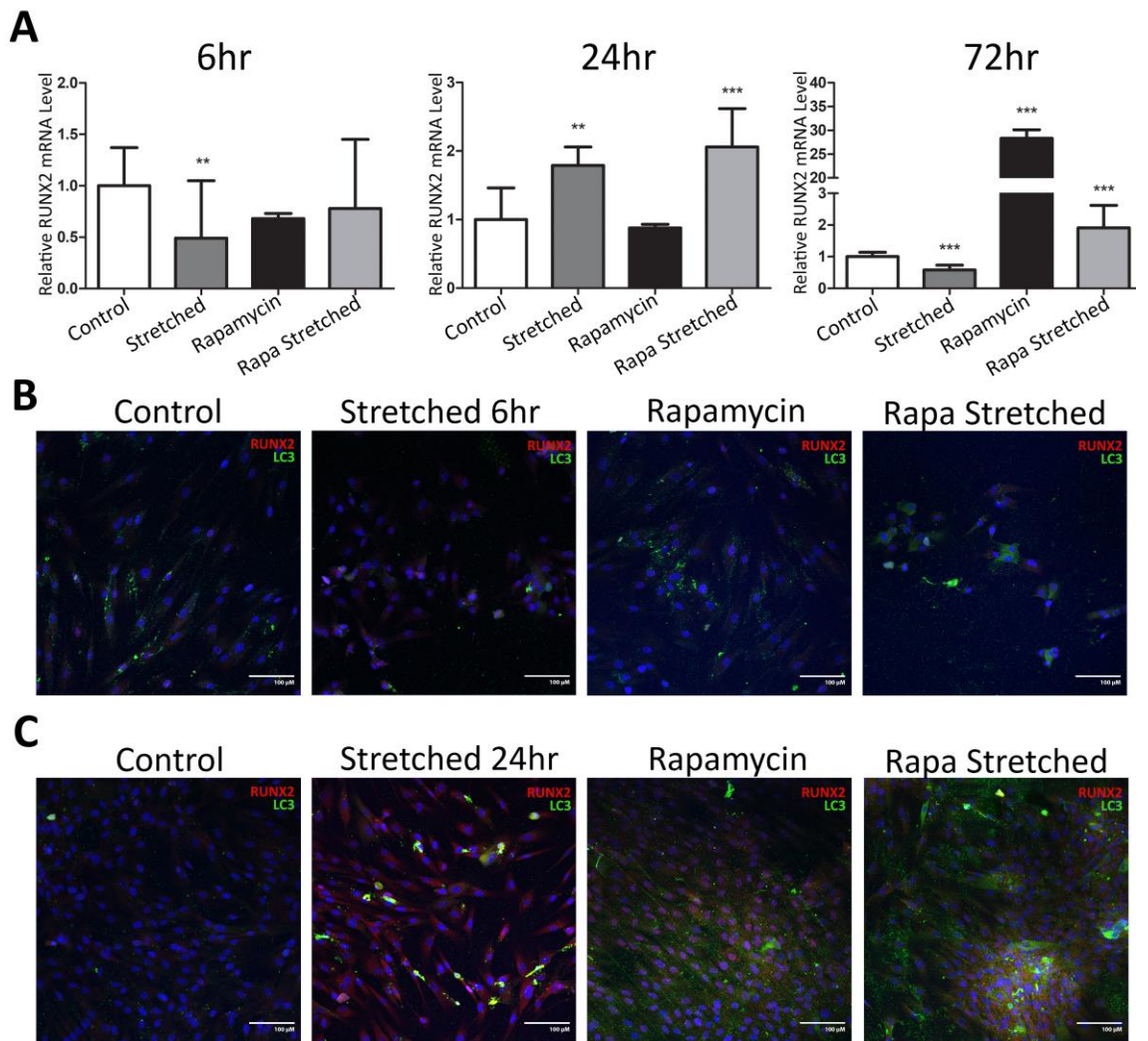


Figure 34: Autophagy activation enhances osteogenic differentiation in response to tensile strain in vitro; A: *RUNX2* gene expression in hBMCs treated with autophagy-inducer rapamycin prior to exposure to tensile strain; B: *RUNX2* and LC3 expression in cells exposed to stretching force for 6 hours, as shown by immunofluorescence; C: *RUNX2* and LC3 expression in cells exposed to stretching force for 24 hours, as shown by immunofluorescence. N=4, statistical significance determined by two-way ANOVA with Bonferoni correction comparing each sample to the corresponding control at each time point, and set at * ($p < 0.05$), ** ($p < 0.01$) and *** ($p < 0.001$). *RUNX2* = runt-related transcription factor 2, LC3 = microtubule-associated protein 1 light chain 3, Rapa = rapamycin.

There was no significant change in *RUNX2* gene expression in cells exposed to rapamycin alone or rapamycin and stretching force at 6 hours compared to controls. At 24 hours the cells that were treated with rapamycin and stretched had significantly increased *RUNX2* expression ($p < 0.001$), which was higher than that of stretched cells that had not been exposed to rapamycin treatment. Compared to controls, *RUNX2* expression was greatly increased in cells that had been treated with rapamycin at 72 hours ($p < 0.001$). Cells that were treated with rapamycin and exposed to stretching force also had increased *RUNX2* expression compared to controls at 72 hours ($p < 0.001$), however this was less than that of cells that had been treated

with rapamycin alone (*Figure 34A*). RUNX2 protein expression was unchanged across all conditions at 6 hours, however at 24 hours it was increased in cells that were stretched, exposed to rapamycin, or exposed to both rapamycin and stretching force, compared to controls. The highest level of nuclear RUNX2 was observed in cells treated with rapamycin alone. LC3-II puncta staining were observed in control cells at 6 hours, but were reduced in cells that were stretched for 6 hours. There was a slight increase in LC3 puncta in cells treated with rapamycin and rapamycin and stretching force, compared to controls at 6 hours. There was relatively little LC3 puncta staining observed in control cells at 24 hours, but this was increased in stretched cells. Cells treated with rapamycin had increased LC3 puncta staining at 24 hours, however the most LC3 puncta were observed in cells treated with rapamycin and stretching force for 24 hours (*Figure 34B*).

3.2.5.2 *Autophagy Inhibition and Strain In Vitro*

hBMCs were treated with bafilomycin to inhibit autophagy prior to exposure to 20% constant tensile strain (*Figure 35*).

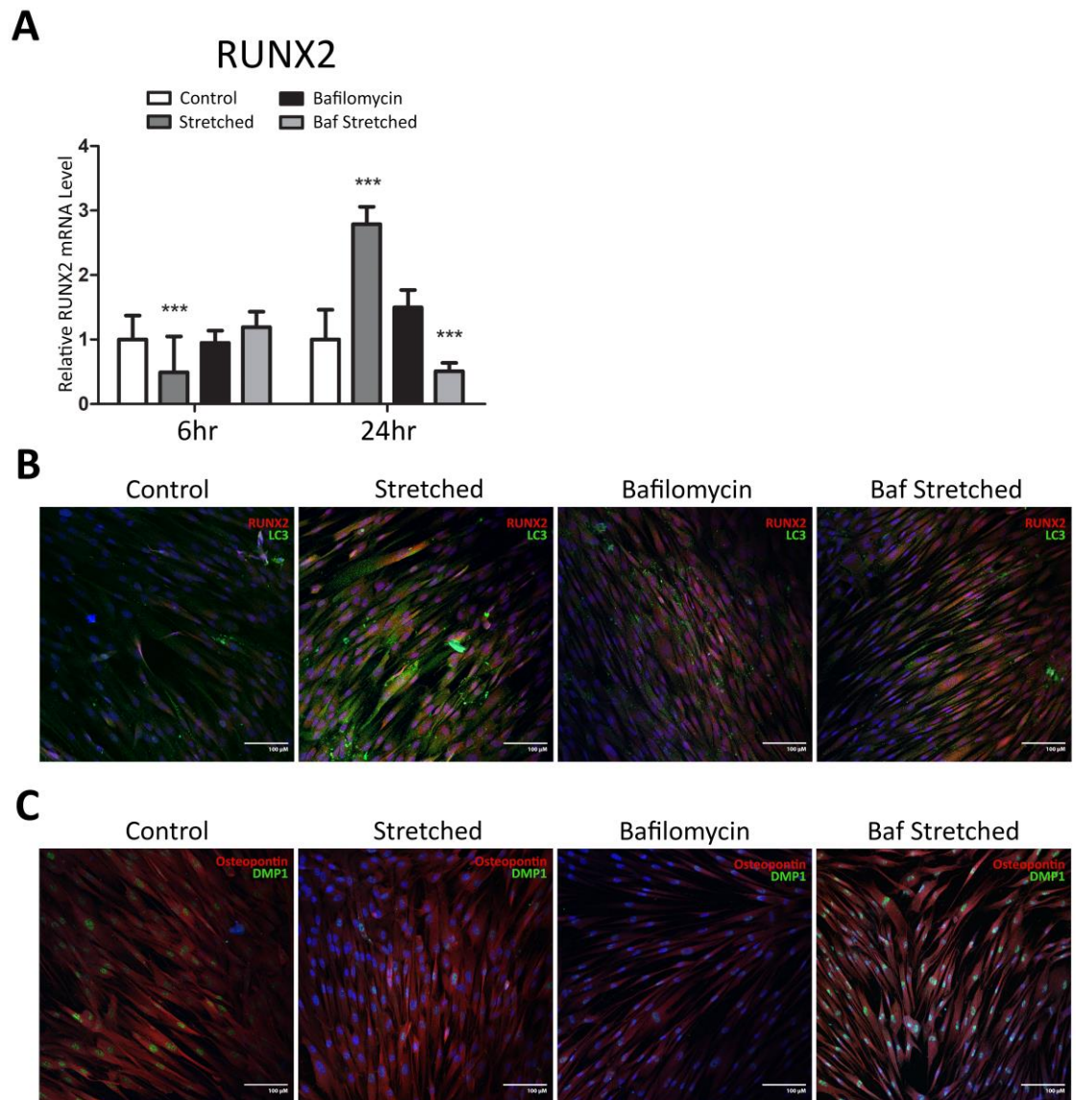


Figure 35: Autophagy inhibition impedes osteogenic differentiation in response to tensile strain in vitro; A: *RUNX2* gene expression in hBMCs treated with bafilomycin, an inhibitor of autophagy, prior to exposure to tensile strain; B: *RUNX2* and LC3 expression in cells exposed to stretching force for 24 hours, as shown by immunofluorescence; C: Osteopontin and DMP1 expression in cells exposed to stretching force for 24 hours, as shown by immunofluorescence. $N=4$, statistical significance determined by two-way ANOVA with Bonferroni correction comparing each sample to the corresponding control at each time point, and set at * ($p<0.05$), ** ($p<0.01$) and *** ($p<0.001$). *RUNX2* = runt-related transcription factor 2, LC3 = microtubule-associated protein 1 light chain 3, DMP1 = dentin matrix protein 1, Baf = bafilomycin.

At 6 hours, there was a reduction in *RUNX2* expression in stretched cells ($p<0.001$), but no significant change was observed in cells treated with bafilomycin or bafilomycin and strain. At 24 hours the cells exposed to bafilomycin and 20% tensile strain had a reduction in *RUNX2* expression compared to controls ($p<0.001$), while cells that were only stretched had increased *RUNX2* levels ($p<0.001$; Figure 35A). Immunofluorescence of 24 hour samples demonstrated an increase in nuclear-localised *RUNX2* and LC3 puncta staining in cells exposed to stretching

force. Cells exposed to bafilomycin had RUNX2 staining however this seemed to be mostly cytosolic rather than localised to the nucleus. Cells exposed to bafilomycin and 20% tensile strain had some nuclear RUNX2 staining but mostly the staining was cytosolic. In both the cells treated with bafilomycin and those treated with bafilomycin and stretching force there was a reduction in LC3 puncta staining compared to controls (*Figure 35B*). Osteopontin staining was high in controls and reduced in cells exposed to bafilomycin at 24 hours. Cells exposed to stretching or bafilomycin and stretching had comparable osteopontin staining to controls. DMP1 staining was observed in controls and seemed to be nuclear-localised, which was comparable to the staining seen in cells treated with bafilomycin and 20% tensile strain. Some DMP1 staining was observed in the nuclei of cells exposed to stretching force alone, however this was much less than in controls. Little to no DMP1 staining was observed in cells treated with bafilomycin (*Figure 35C*).

4 Chapter 4: The Association of Autophagy with Osteoclastogenesis

4.1 Introduction

Periodontitis is an important health issue both in terms of its prevalence and its contribution to alveolar bone loss. This chronic inflammatory disease is caused by the presence of excess *P.gingivalis* bacteria causing local inflammation in the periodontium, but it is also clear that disease susceptibility and progression are affected by host factors. LPS tolerance has been investigated in connection with many inflammatory conditions, and has been found to alleviate or exacerbate disease, but its role in the chronic inflammation seen with periodontitis has yet to be fully explored. Therefore, it was decided to investigate whether LPS tolerance could affect osteoclastogenesis, with the idea that tolerance may be achieved through the chronic inflammation observed in periodontitis.

There were two key considerations made in terms of the cells affected; are the osteoclast precursors themselves that are affected by tolerance to LPS, altering their differentiation? Or is it the interaction of tolerised cells such as monocytes with osteoclast precursors which affects their differentiation? In addition, it was decided to investigate both *E.coli* and *P.gingivalis* LPS for tolerance, as while *P.gingivalis* was the strain implicated in periodontitis, *E.coli* is well-established to cause LPS tolerance in the literature and is relevant to many diseases of chronic inflammation.

The mechanism considered in linking osteoclastogenesis and periodontitis was HA signalling, as not only is HA synthesis upregulated in chronic inflammation, but HA affects bone resorption by inhibiting osteoclast differentiation. Activation of osteoclast differentiation processes has also been suggested as a downstream effect of autophagy in the literature, however there has been little exploration of this in relation to periodontal disease. Additionally, there were a small number of publications indicating that autophagy targets HASs to prevent downstream HA

signalling. Different molecular weights of HA have been linked to inflammation and LPS tolerance, as well as to the activation or inhibition of osteoclast differentiation, therefore we aimed to investigate the links between autophagy, HA and osteoclastogenesis.

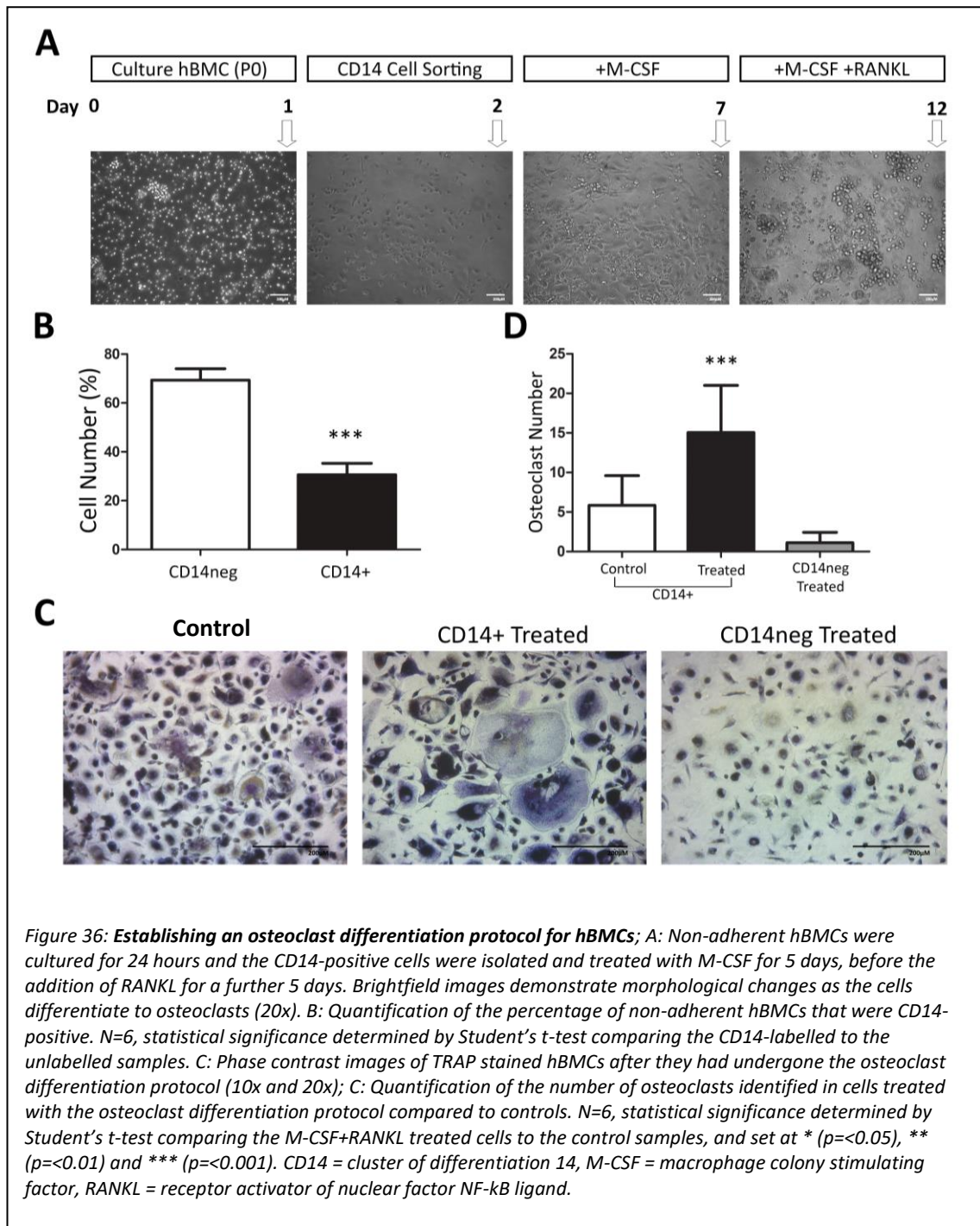
4.2 Results

4.2.1 Characterising hBMCs as cells capable of Osteoclast Differentiation

hBMCs were exposed to an osteoclast differentiation protocol to determine whether they had the capacity to differentiate to osteoclast-like cells (*Figure 36*).

The first protocol trialled was to culture hBMCs overnight, collect the non-adherent cells and seed them into cell culture plates, with 25ng/ml macrophage colony-stimulating factor (M-CSF) and 100ng/ml receptor activator of nuclear factor kappa-B ligand (RANKL) added to the culture media. The cells were cultured for 14 days, changing the media every 2-3 days before the cells were then fixed and stained with TRAP, which denotes the presence of osteoclasts. The cells did not attach to the plate surface however the morphology was mostly small, round cells and there were very few cells if any that were TRAP-positive and multi-nucleated which could be confidently classified as osteoclasts.

The protocol was optimised based on suggestions from the literature, to increase the density of CD14-positive cells and to stagger the addition of receptor activator of nuclear factor kappa-B ligand (RANKL) as this was involved in late-stage osteoclast differentiation. hBMCs were cultured overnight, the non-adherent cells were collected and underwent magnetic-activated cell sorting (MACS) for CD14, to isolate the CD14-positive cells (*Figure 36A*). CD14-positive cells accounted for 29% of non-adherent hBMCs on average, which was statistically significant according to a Student's t-test ($p < 0.001$; *Figure 36B*). These cells were seeded at a high density (5×10^5 /ml) and treated with 25ng/ml macrophage colony-stimulating factor (M-CSF) for 5 days to stimulate differentiation to monocytes, followed by the addition of 100ng/ml RANKL for 5 days to stimulate osteoclast precursor cell fusion and differentiation to osteoclasts (*Figure 36A*).



This protocol yielded a high proportion of osteoclast-like cells compared to controls cells that were CD14-labelled but not treated with M-CSF and RANKL, as demonstrated by the significantly increased number of TRAP-positive cells with three or more nuclei ($p < 0.001$; Figure 36C-D).

4.2.2 Determining the effects of LPS on Osteoclast Differentiation

In order to represent the chronic inflammation of periodontitis, the effect of LPS tolerance on osteoclast differentiation was investigated. There were broadly two avenues that could have been pursued: firstly, that LPS tolerance affected osteoclast precursors themselves, and

secondly in LPS tolerance affecting other cells that would then cross-talk with osteoclast precursors. In the context of periodontal disease, either scenario could have been relevant as *P.gingivalis* has been shown to activate monocytes which then circulate in the bloodstream to cause chronic inflammation systemically (Hayashi *et al.*, 2010).

The first step was to determine the effects of LPS treatment on osteoclast differentiation hBMCs. hBMCs underwent the osteoclast differentiation protocol established in Figure 36 with the addition of LPS to the media at the same time M-CSF was added. Therefore, hBMCs were cultured overnight, the non-adherent cells were sorted for CD14 using MACS. The CD14-positive cells were seeded in culture media containing 25ng/ml M-CSF and 1µg/ml LPS for 5 days, and 25ng/ml M-CSF, 1µg/ml LPS and 100ng/ml RANKL for a further 5 days. Cells were fixed and TRAP stained to determine the effects of LPS on the differentiation of hBMCs to osteoclast-like cells (Figure 37).

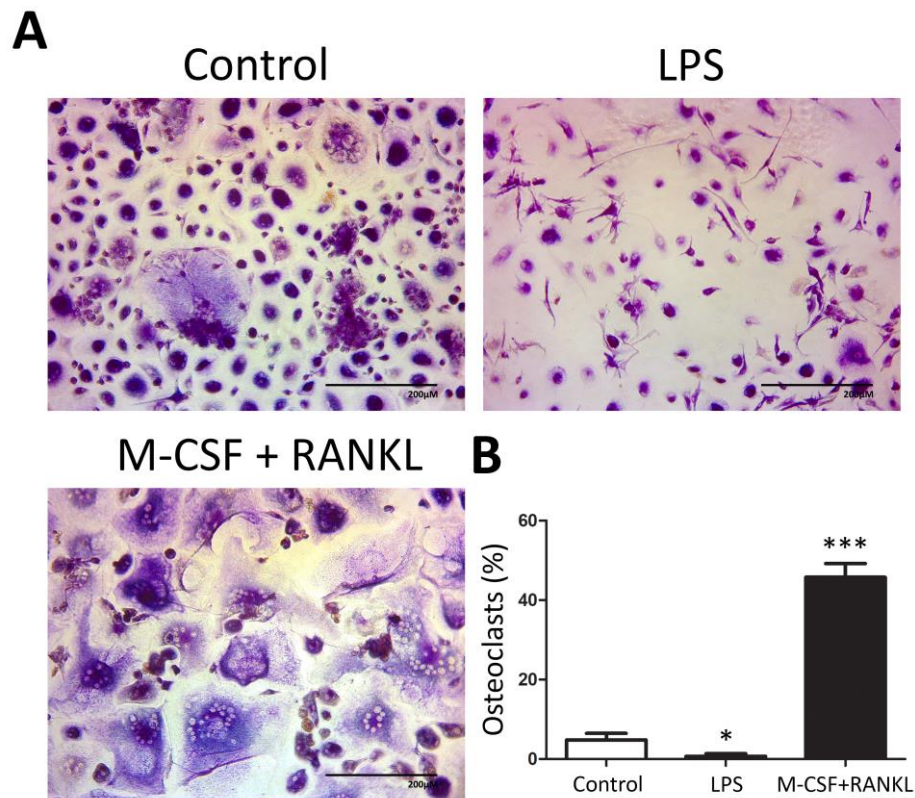


Figure 37: The effect of LPS on osteoclast differentiation of hBMCs; A: Phase contrast images of TRAP-stained hBMCs cultured M-CSF and RANKL with or without *E.coli* LPS, or culture media alone (the Control); B: Quantification of TRAP-stained and multinucleated osteoclasts in each sample. N=4, statistical significance determined by Student's t-test comparing each sample to the control, and set at * ($p < 0.05$), ** ($p < 0.01$) and *** ($p < 0.001$). LPS = lipopolysaccharide, M-CSF = macrophage colony stimulating factor, RANKL = receptor activator of nuclear factor NF- κ B ligand.

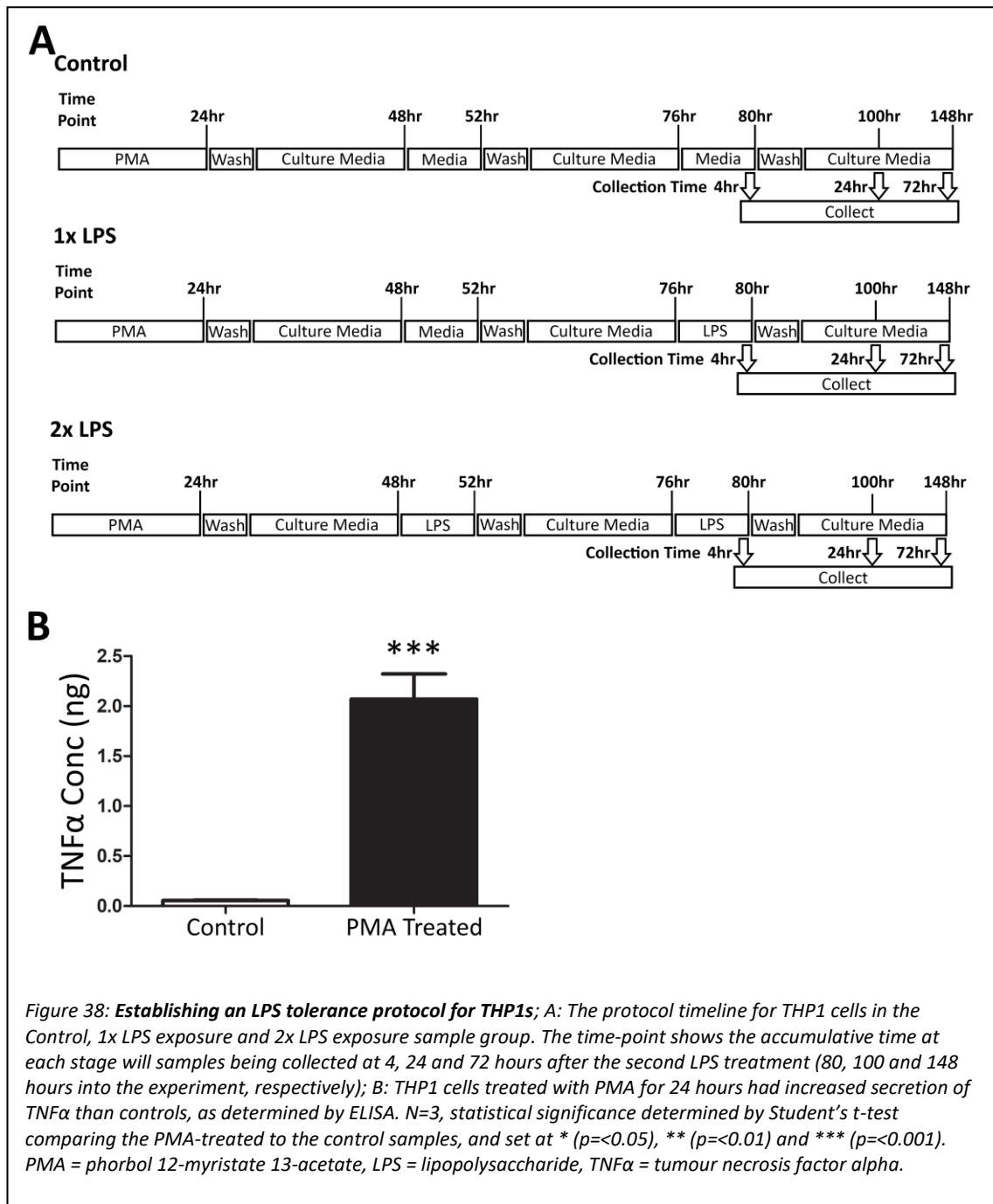
hBMCs treated with LPS had decreased numbers of osteoclast-like cells compared to cells treated with M-CSF and RANKL, which was statistically significant according to a Student's t-test ($p < 0.001$; Figure 37B). Additionally, cells treated with LPS had lower osteoclast-like cells observed than control samples consisting of cells that were CD14-positive but not treated with M-CSF, RANKL or LPS. This suggests that hBMCs treated with LPS had a reduced capability to differentiate to osteoclast-like cells. Based on these results it was decided that the direct interaction between hBMCs and LPS was not an accurate model of periodontitis since bone loss, and thus osteoclasts, is a hallmark of the disease. Therefore, the hypothesis where LPS tolerance affects the cells surrounding osteoclast precursors was explored.

4.2.3 LPS Tolerance

THP1 cells, a pre-monocyte cell line, were used to represent the peripheral monocytes that would likely come into contact with LPS and circulate to cause systemic inflammation. These cells have also been established in the literature to exhibit LPS tolerance which gave a starting point for establishing the LPS tolerance protocol.

Due to the role of *P.gingivalis* in periodontitis, the LPS of this bacteria was used in this experimental model. *E.coli* LPS was also used as a positive control and during the optimisation of the protocols, due to its known clinical relevance in other inflammatory conditions such as sepsis, and its common use in LPS tolerance work published in the literature. While *P.gingivalis* is the bacterial strain most implicated with periodontitis, its presence alone is not sufficient to cause disease as it has also been found in the periodontal flora of patients without the disease (Grossi *et al.*, 1994; Alpagot *et al.*, 1996; Griffen *et al.*, 1998). The discrepancy in severity of periodontal disease seen in different patients is thought to be caused by an underlying mechanism within the host which either protects against or enhances disease, and which was of interest for this thesis.

THP1 cells were exposed to a LPS tolerance protocol (*Figure 38A*) which began with cells being treated with 10ng/ml phorbol 12-myristate 13-acetate (PMA) for 24 hours in order to stimulate differentiation of cells to inflammatory macrophages and prime the cells for inflammatory cues.



THP1s that had been pre-treated with PMA had increased TNFα protein expression compared to controls, which was statistically significant according to a Student's t-test ($p < 0.001$; Figure 38B), indicating a stimulation of inflammation pathways. After PMA treatment, cells were exposed to either 1μg/ml *E.coli* or *P.gingivalis* LPS which is the concentration widely used for these compounds and in tolerance work (Ye *et al.*, 2008; Belfield *et al.*, 2017). Cells were washed and cultured in culture media for 24 hours before the first treatment with 1μg/ml LPS. After 4 hours, cells were washed and cultured in culture media for 24 hours before the second LPS treatment for 4 hours. Cells were either collected 4 hours post-second LPS treatment or washed

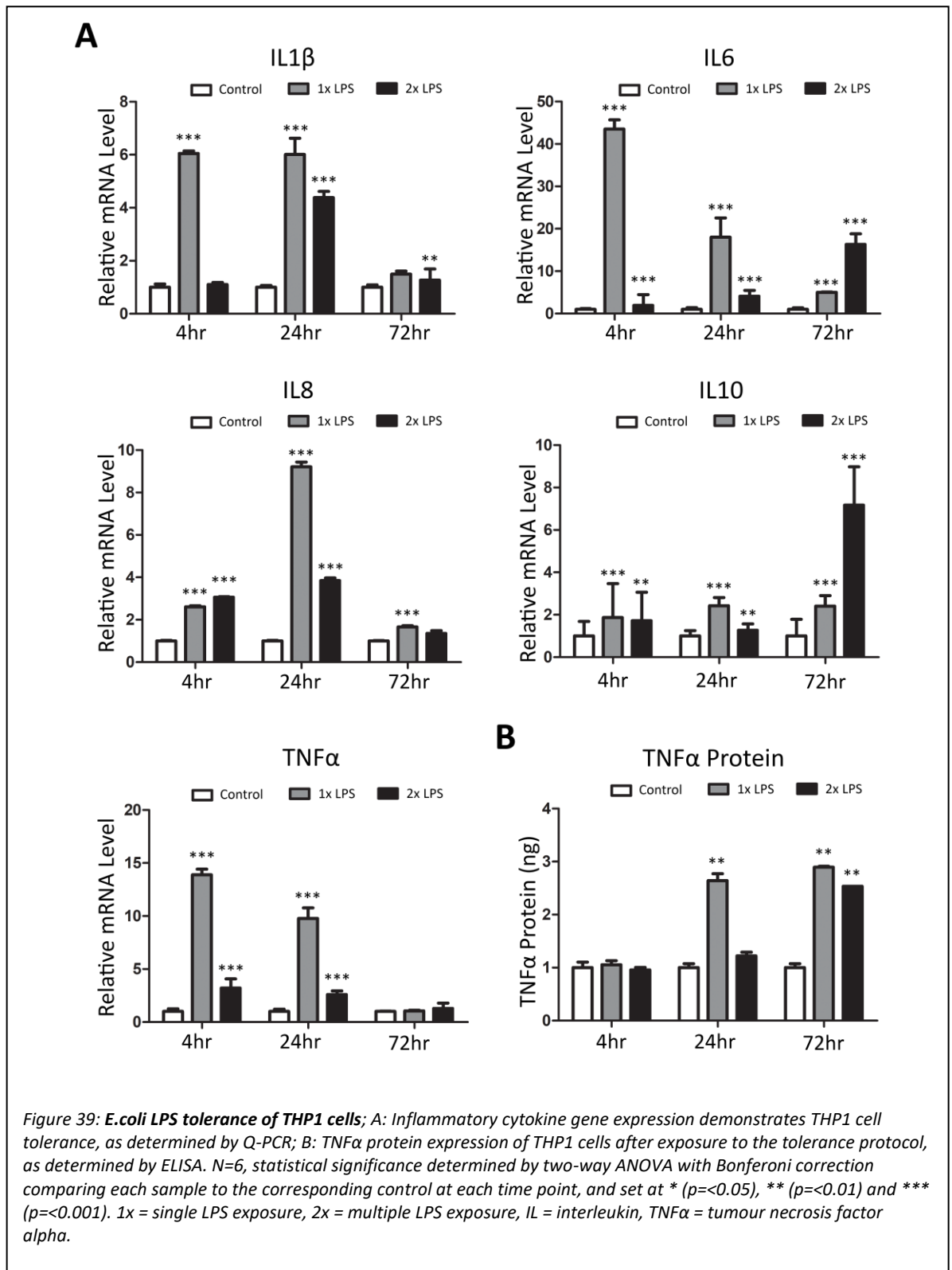
and placed in culture media until collections at 24 hours and 72 hours (*Figure 38A*). Tolerance refers to a downregulation in the inflammatory response in cells with repeated LPS exposure compared to cells which had only been exposed to LPS once.

4.2.3.1 *E.coli* LPS

E.coli LPS is well characterised in the literature and therefore was used for the LPS tolerance protocol in order to optimise the model and determine the potential mechanisms taking place in THP1s treated with multiple exposures to LPS (2x) compared to single exposure (1x) or control cells.

4.2.3.1.1 *E.coli* LPS Tolerance of Inflammatory Pre-Monocytes

THP1 cells that had undergone the tolerance protocol with *E.coli* LPS were analysed for their expression of inflammatory and anti-inflammatory cytokines (*Figure 39*).



1x cells were found to have an upregulation of inflammatory cytokine gene expression compared to unstimulated controls. This included increased *IL1 β* , *IL6* and *IL8* expression at 4, 24 and 72 hours post-second LPS treatment ($p < 0.001$). TNF α mRNA was upregulated at 4 and 24 hours ($p < 0.001$), and TNF α protein expression was increased at 24 and 72 hours in 1x cells

compared to controls (*Figure 39B*). Anti-inflammatory cytokine IL10 had slightly increased gene expression at 4, 24 and 72 hours ($p < 0.001$). 2x cells had increased TNF α mRNA compared to controls, but vastly less expression than was seen by 1x cells at 4 and 24 hours, with little change at 72 hours. TNF α protein expression was increased in 2x cells compared to control cells at 72 hours, but was decreased compared to 1x cells at 24 and 72 hours. 2x cells' expression of *IL1 β* and *IL6* was comparable to controls at 4 hours ($p = ns$), but *IL8* expression was increased at 4 hours ($p < 0.001$). While transcription of these inflammatory cytokines was higher than controls at 24 hours, it was lower than that of 1x cells. At 72 hours, *IL1 β* and *IL6* expression were increased in 2x cells compared to controls ($p < 0.01$ and $p < 0.001$, respectively), while *IL8* expression was comparable to controls ($p = ns$). There was little difference observed between control and 2x cells in *IL10* expression at 4 and 24 hours, however it was significantly upregulated at 72 hours in 2x cells ($p < 0.001$; *Figure 39A*). These results indicated that THP1 cells could show tolerance to *E.coli* LPS at 24 hours after the second LPS treatment, based on RNA and protein expression.

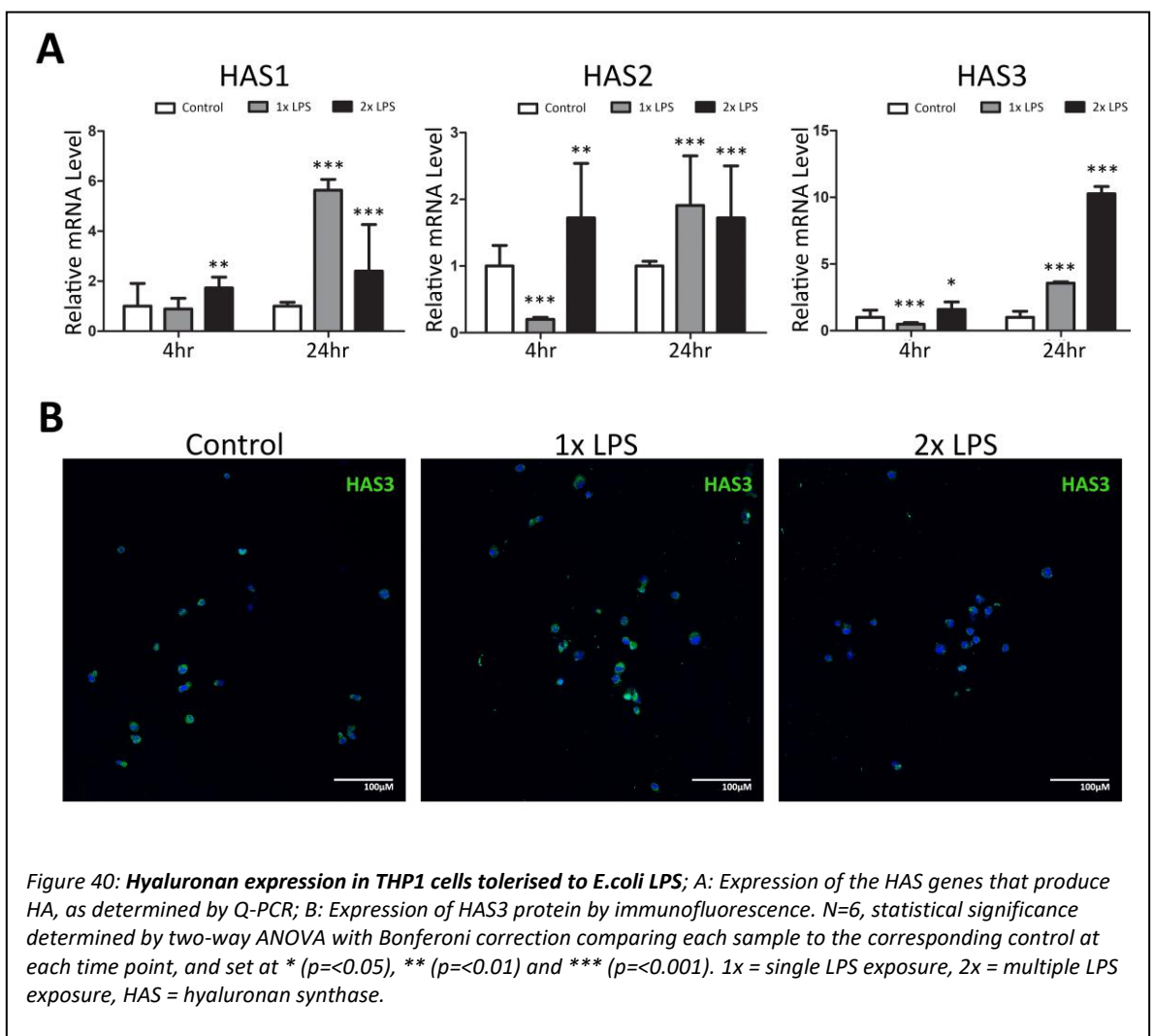
4.2.3.1.2 Investigating *E.coli* LPS Tolerance and the expression of Hyaluronan Synthases

HA is a molecule found in the ECM which has roles in structural support and shock absorbance however it may also act as a signal (Day and Prestwich, 2002; Cyphert, Trempus and Garantziotis, 2015). HA signalling was considered as the mechanism regulating osteoclast production in this model, as it is established in the literature that HA modulates osteoclast differentiation and activation (Xu *et al.*, 2007; Rayahin *et al.*, 2015). Additionally, one paper linked immune tolerance to intracellular deposition of HA in a model of autoimmune type 1 diabetes. Blocking HA synthesis was found to inhibit tolerance and subsequent progression of the autoimmune disease in this model (Nagy *et al.*, 2015). This suggests a link between HA and tolerance which, despite being in a different disease area, was believed to be worth exploring.

Signalling functions generally depend on the molecular weight of the HA produced: high molecular weight (HMW) is thought of as immunosuppressive, while low molecular weight

(LMW) is associated with inflammation and thought of as more pathogenic (Powell and Horton, 2005; Cyphert, Trempus and Garantziotis, 2015). There are three enzymes involved in the production of HA, which are located in the plasma membrane and produce HA into the ECM (Rilla *et al.*, 2005; Törrönen *et al.*, 2014). HAS 1 and 2 produce HMW HA, while HAS3 produces LMW HA (Tammi *et al.*, 2011).

Therefore, to determine whether LPS tolerance was linked to hyaluronan signalling, THP1 cells that had undergone the LPS tolerance protocol were analysed for mRNA and protein expression of the hyaluronan synthase (HAS) enzymes (Figure 40).



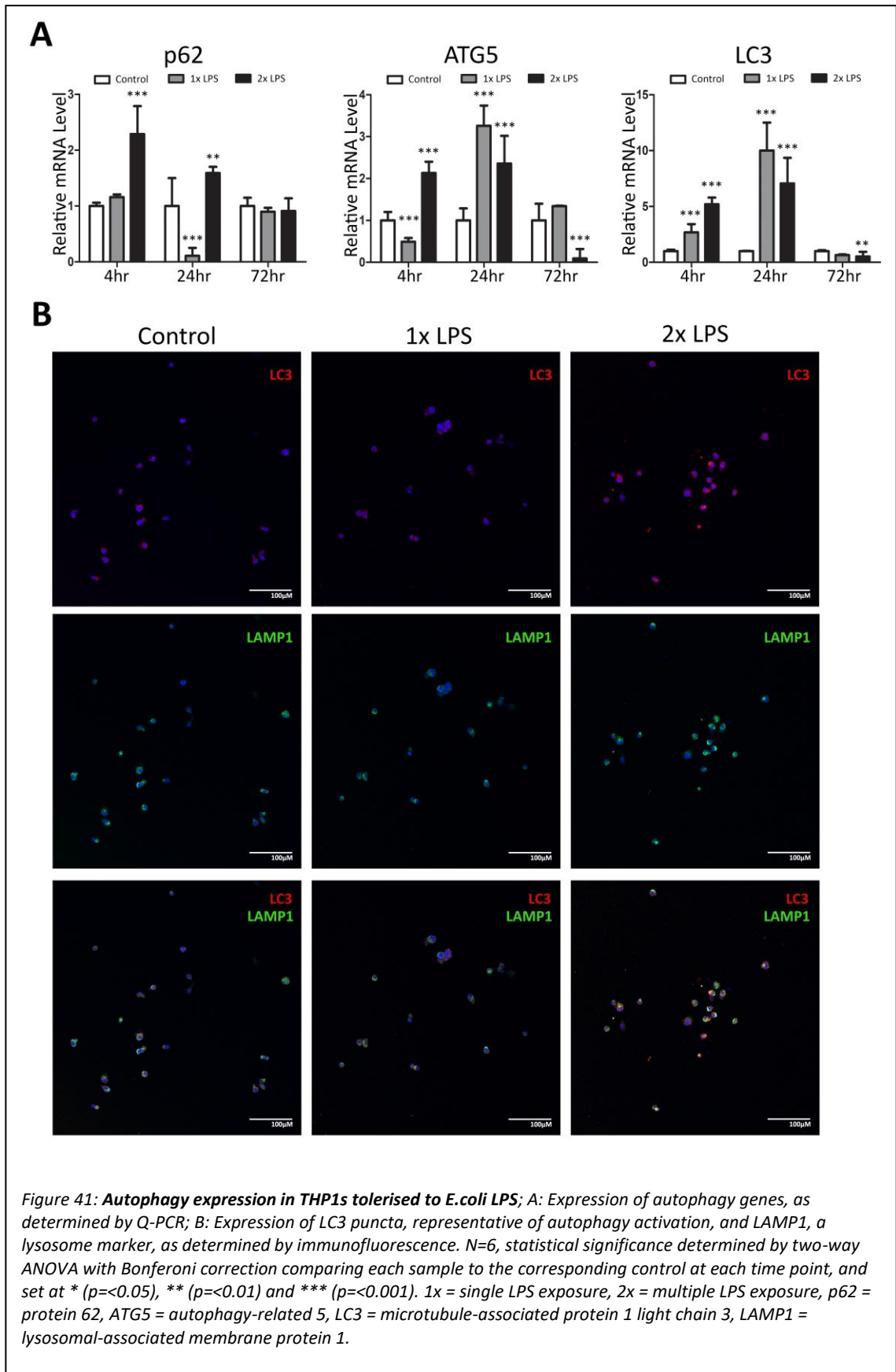
HAS1 expression was increased in 2x cells at 4 hours and 24 hours compared to controls ($p < 0.01$ and $p < 0.001$, respectively), while 1x cells had upregulated HAS1 at 24 hours only ($p < 0.001$). HAS2 expression was significantly decreased in 1x cells at 4 hours ($p < 0.001$), but slightly

upregulated for 2x cells at 4 hours and 24 hours, and 1x cells at 24 hours. 2x THP1s had increased expression of *HAS3* mRNA at 4 and 24 hours-post second LPS treatment ($p < 0.05$ and $p < 0.001$, respectively). 1x cells had downregulated expression of *HAS3* at 4 hours and upregulated expression at 24 hours ($p < 0.001$), but not as high as was seen for 2x cells (*Figure 40A*). However, at protein level it was observed that 2x cells had reduced immunofluorescence staining of *HAS3* at 4 hours and 24 hours. *HAS3* staining was present in control cells and seemed to be increased in 1x cells (*Figure 40B*).

The discrepancy between *HAS3* mRNA and protein expression in 2x THP1s could be explained by post-transcriptional modifications resulting in ubiquitination of the protein. However, the speed in which the reduction of *HAS3* staining is observed (within 4 hours) could indicate another cause. Autophagy was considered as a potential mechanism of rapid removal of *HAS3* protein, as it has been found to be utilised and have roles in many processes.

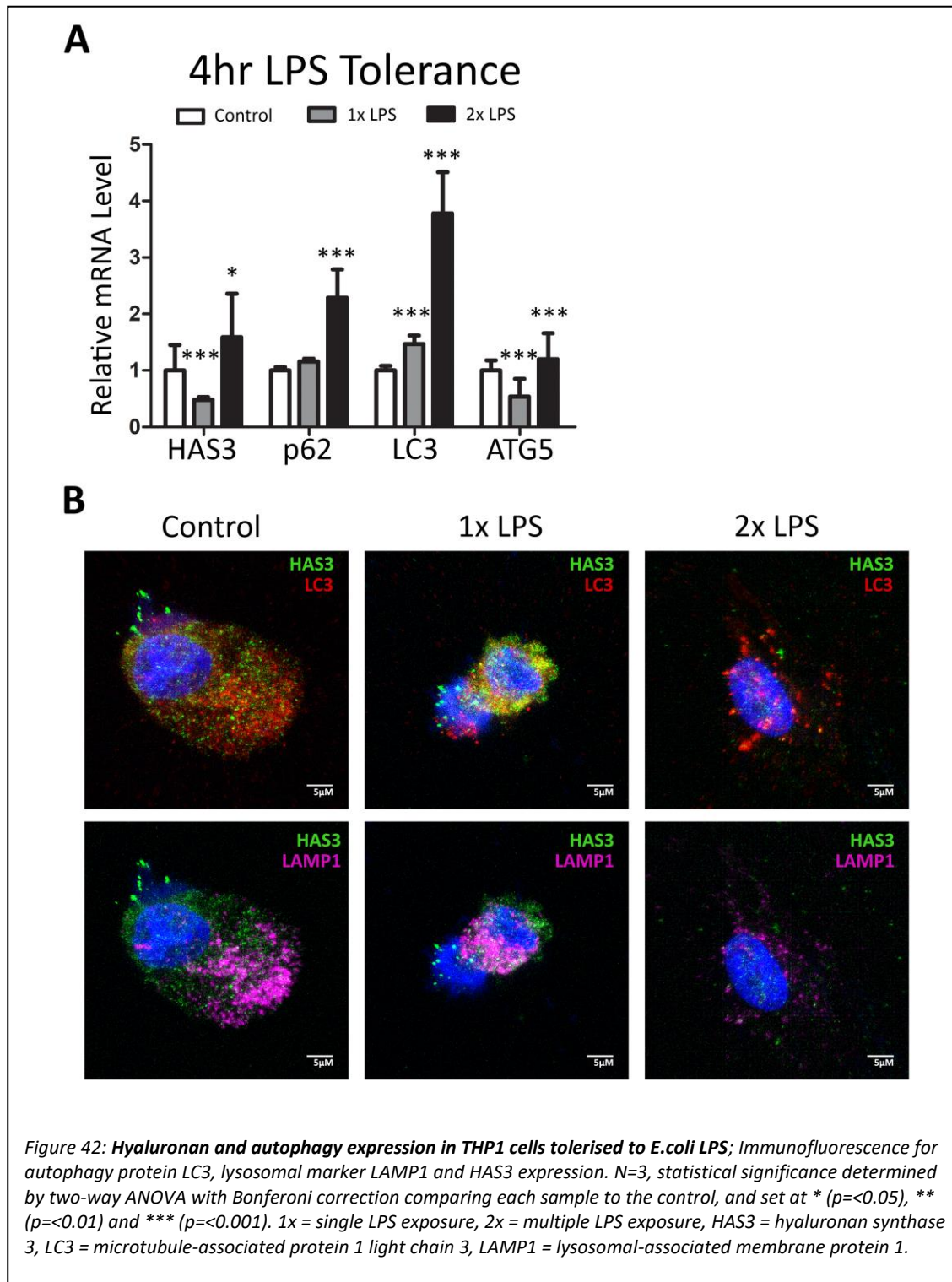
4.2.3.1.3 Investigating *E. coli* LPS Tolerance and the expression of Autophagy

Autophagy is a process by which proteins are rapidly captured in vesicles called autophagosomes. These vesicles fuse with lysosomes to form autolysosomes, and the proteins are degraded. Autophagy has been demonstrated to rapidly tag, capture and degrade proteins, and has been found to regulate many molecular processes. THP1 cells that had undergone the LPS tolerance protocol were analysed for their expression of key autophagy genes, including *p62*, *ATG5* and *LC3* (*Figure 41*).



1x cells had downregulated *p62* gene expression at 24 hours post-second LPS treatment. *p62* was upregulated at 4 and 24 hours in 2x cells. *ATG5* and *LC3* were upregulated in 2x cells at 4

and 24 hours, compared to controls. 1x cells had upregulated *ATG5* and *LC3* expression at 24 hours, which was higher than that of 2x cells. *ATG5* and *LC3* were downregulated in 2x cells at 72 hours, but all other conditions had little to no change in autophagy markers at 72 hours (Figure 41A).



As evaluated by immunofluorescence staining, there was little change in LC3 or lysosomal-associated membrane protein 1 (LAMP1), a lysosome protein, expression levels between control and 1x cells at 24 hour post-second LPS treatment (*Figure 42B*). However, staining for LC3 and LAMP1 were increased in 2x THP1s compared to 1x or control cells, and patterns of expression seemed to indicate co-localisation of these markers in 2x cells, which was investigated at higher magnification (*Figure 42*).

The presence of LC3 puncta staining is widely accepted to be indicative of autophagosome formation due to the conversion of LC3-I to LC3-II. At high magnification, 2x cells were found to have more puncta LC3 staining, while in 1x and control cells the LC3 staining was more dispersed across the cell. LAMP1 protein expression was analysed to determine whether active autophagy, with the formation of autolysosomes, was taking place. LAMP1 was found to be upregulated and co-localised with LC3 staining in 2x THP1s. LAMP1 staining was also observed in control and 1x cells and was localised to one side of the cell, while in 2x cells this staining was seen in puncta across the cell (*Figure 42B*).

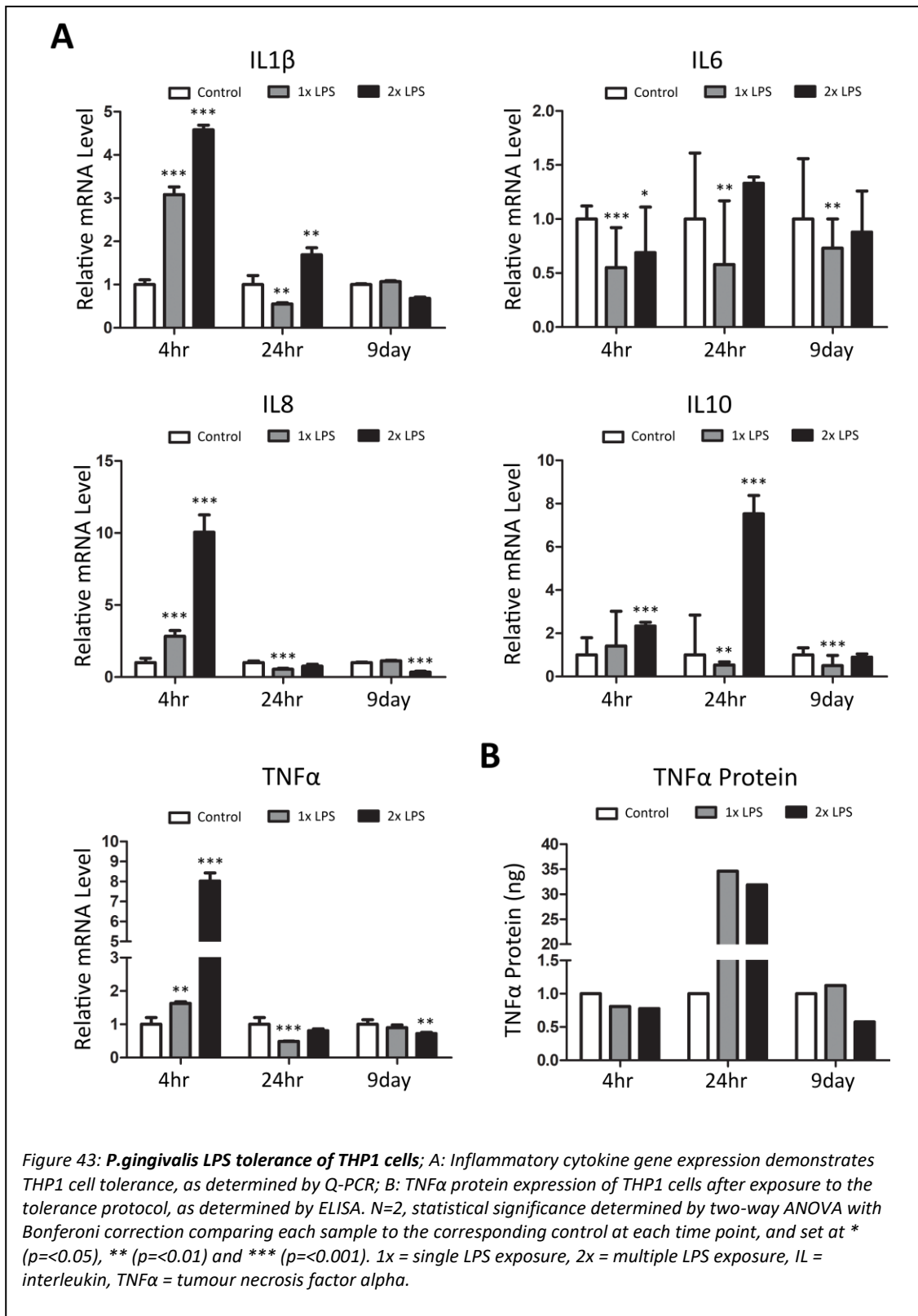
4.2.3.2 *P.gingivalis* LPS

P.gingivalis LPS is the form of LPS most associated with periodontal disease, therefore it is clinically relevant to study the mechanisms associated with tolerance against *P.gingivalis* LPS. The LPS tolerance protocol established with *E.coli* LPS (*Figure 38*) was carried out using *P.gingivalis* LPS with the expression of cytokines being analysed at 4 hours, 24 hours and 9 days after the second exposure. The later time-point of 9 days post-exposure was included due to discrepancies in the literature on the time-point required to obtain a tolerance phenotype using *P.gingivalis* LPS.

4.2.3.2.1 *P.gingivalis* LPS Tolerance of Inflammatory Pre-Monocytes

Cells that had undergone the tolerance protocol with *P.gingivalis* LPS were analysed for their expression of inflammatory and anti-inflammatory cytokines (*Figure 43*). When repeating this experiment there were issues in the reliability of the data with several markers producing no Ct

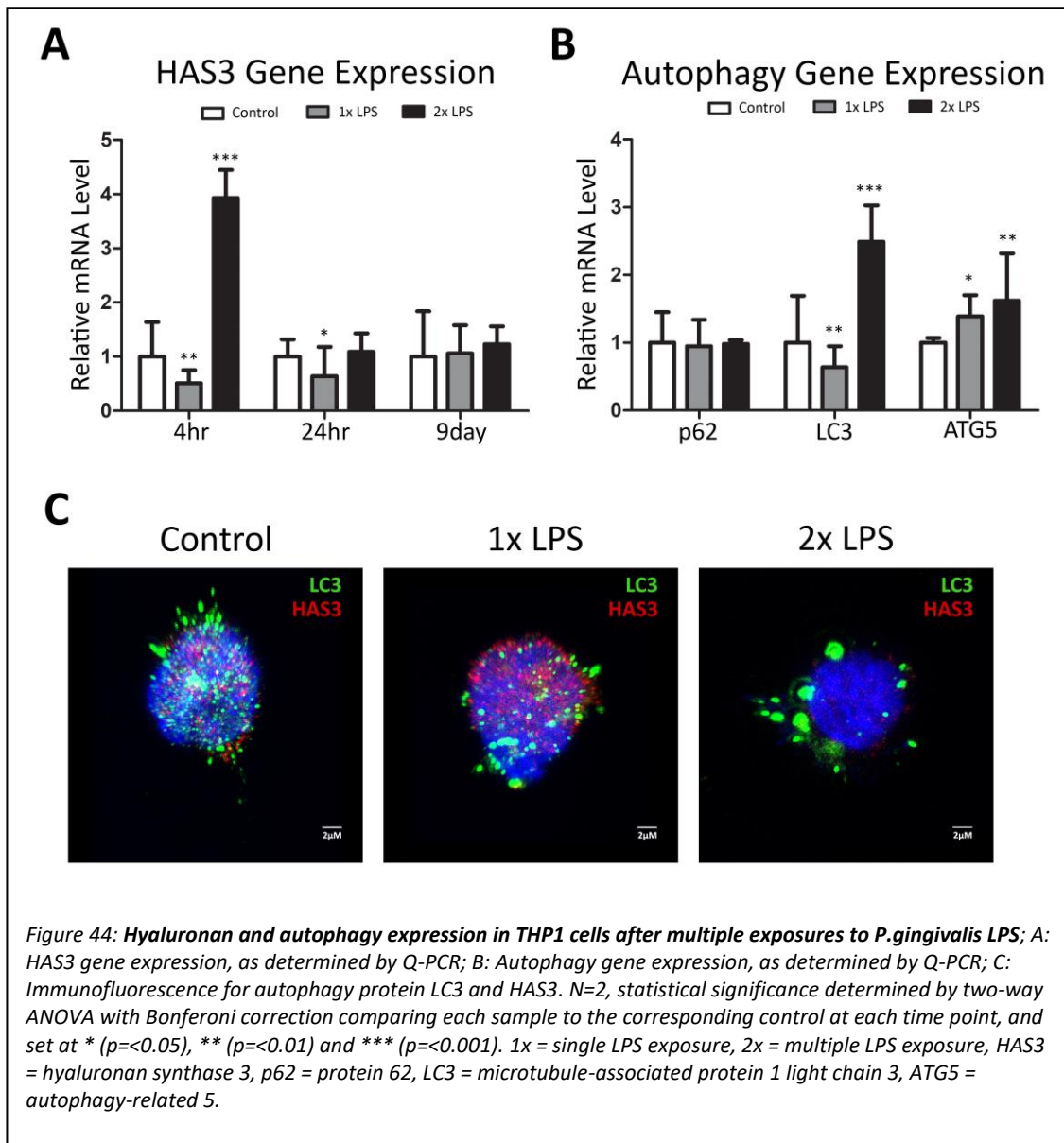
value during Q-PCR analysis. While this could indicate that the expression of these markers was low, these results were not able to be replicated across different experiments therefore the results shown are the culmination of only two datasets (n=2).



Compared to controls, 1x cells had upregulated expression of inflammatory cytokines *IL1β*, *IL8* and *TNFα* at 4 hours (Figure 43). However, at 24 hours and 9 days-post second LPS treatment there was no change observed in inflammatory cytokines gene expression in 2x THP1 cells compared to 1x or control cells. 1x cells were also found to have little change in anti-inflammatory *IL10* expression. There was no significant difference observed in *IL6* gene expression at any time point between the three conditions. 2x THP1 cells were found to have increased expression of *IL1β*, *IL8* and *TNFα* genes compared to control and 1x cells at 4 hours. This was maintained for *IL1β* at 24 hours, but no change was observed between 2x and control cells for *IL8* or *TNFα* at this time point. 2x cells were observed to have decreased expression of *IL1β*, *IL8* and *TNFα* at 9 days compared to 1x and control cells, and anti-inflammatory *IL10* was upregulated at 4 and 24 hours in 2x cells (Figure 43A). *TNFα* protein was greatly increased in 1x cells at 24 hours, and slightly increased at 9 days, compared to controls. 2x cells had increased *TNFα* protein at 24 hours compared to controls, however this was less than that for 1x cells. At 9 days, 2x cells had decreased production of *TNFα* compared to both 1x and control cells (Figure 43B). These results suggest that tolerance could occur in THP1s at 9 days post second *P.gingivalis* LPS treatment, however the variability in the results obtained across different datasets reduces the reliability of these results.

4.2.3.2.2 Investigating *P.gingivalis* LPS Tolerance and the expression of Hyaluronan Synthases

To determine whether LPS tolerance affected hyaluronan signalling, THP1 cells that had undergone the LPS tolerance protocol were analysed for the expression of HAS enzymes (Figure 44A,C).



HAS3 gene expression was upregulated in 2x THP1 cells at 4 hours post-second *P.gingivalis* LPS treatment. 2x cells had no change in HAS3 gene expression at 24 hours or at 9 days, when tolerance was indicated. There was little to no change observed for 1x cells compared to controls (Figure 44A). Immunofluorescence staining demonstrated an increase in HAS3 protein in 1x THP1 cells at 4 hours post-second LPS treatment, while 2x cells had a marked decrease in HAS3 protein (Figure 44C).

4.2.3.2.3 Investigating *P.gingivalis* LPS Tolerance and the expression of Autophagy

The expression of autophagy-related genes was analysed to investigate a link between LPS tolerance and autophagy (Figure 44B-C). At 4 hours post-second LPS treatment, there was an upregulation in LC3 gene expression in 2x THP1 cells. There was little to no change in p62 or

ATG5 expression in 2x cells. 1x cells were observed to exhibit a downregulation in *LC3* gene expression compared to controls, and no change in *p62* or *ATG5* expression (*Figure 44B*). High magnification staining demonstrated an increase in number and size of LC3 puncta present in 2x THP1s than were present in control or 1x cells at 4 hours (*Figure 44C*).

4.2.4 Determining the effects of Hyaluronan on the Differentiation of Osteoclast Precursors

To determine the effect of HA on osteoclast differentiation, hBMCs were treated with high (HMW) or low molecular weight (LMW) HA protein alongside the osteoclast differentiation protocol. As it wasn't known what stage of differentiation the HA may affect, adding the HA at 'early' (alongside M-CSF; *Figure 45A*) or at 'late' differentiation (alongside RANKL; *Figure 45B*) was also tested. TRAP staining was carried out and osteoclasts were counted as TRAP-positive cells with three or more nuclei.

For the purpose of this work, LMW HA was defined as 14-40 kDa, while HMW HA was more than 950 kDa, fitting with the general guidelines seen in the literature (Toole, 2001; Weigel and Baggenstoss, 2017).

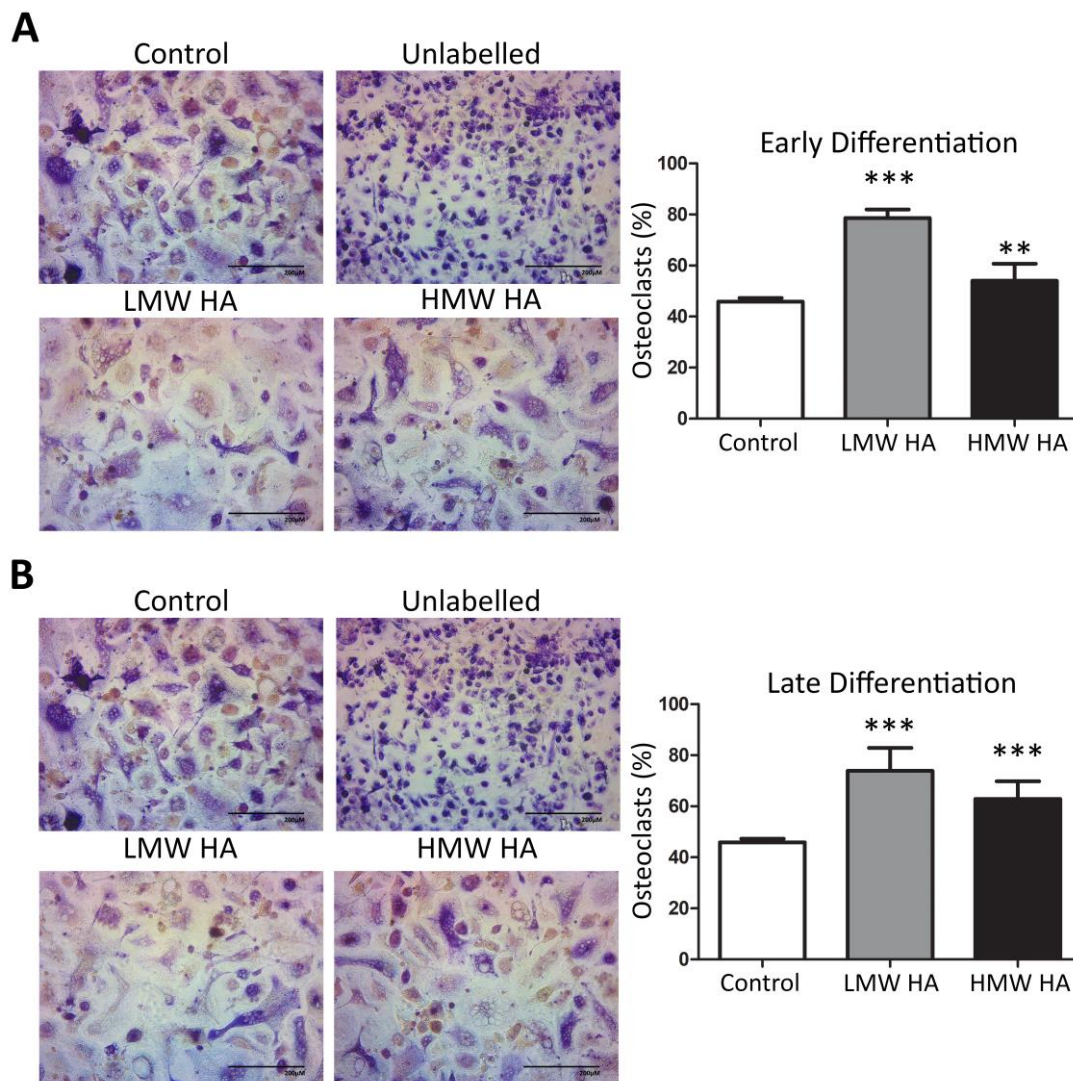


Figure 45: The effect of hyaluronan on osteoclast differentiation; A: Phase contrast images of TRAP stained hBMCs treated with HA at the early osteoclast differentiation stage, and quantification of osteoclast percentage in each sample; B: Phase contrast images of TRAP stained hBMCs treated with HA at the late osteoclast differentiation stage, and quantification of osteoclast percentage in each sample. N=4, statistical significance determined by two-way ANOVA with Bonferoni correction comparing each sample to the corresponding control at each time point, and set at * ($p < 0.05$), ** ($p < 0.01$) and *** ($p < 0.001$). LMW HA = low molecular weight hyaluronan, HMW HA = high molecular weight hyaluronan.

hBMCs treated with HMW or LMW HA had increased numbers of osteoclasts compared to controls, however the cells treated with LMW HA had the highest number of osteoclasts. Additionally, the osteoclasts in the wells treated with LMW HA were larger on average than the osteoclasts from the control or HMW HA conditions. The cells treated with LMW HA from the 'early' stage had the highest number of osteoclasts (Figure 45B). From these results it was determined that there was a difference in osteoclast production when cells are exposed to HA treatment, specifically LMW HA, and that, while this change could be seen whether the cells

were treated at the early or late stages, treatment at the early differentiation stage had the greatest effect on osteoclast formation.

4.2.5 Determining the effects of LPS and Hyaluronan treatment on the Differentiation of Osteoclast Precursors

The hypothesis was that there was a difference in HA secretion between THP1s exposed to LPS once (1x) or multiple times (2x) which contributed to the difference in osteoclast production and bone loss seen with some patients with periodontitis. The question now was which specific cell populations were directly affected. Was it the osteoclast precursors themselves, or cells of the inflammatory monocyte/macrophage lineage communicating with osteoclast precursors at the bone surface to alter their differentiation?

The osteoclast differentiation protocol on the hBMCs (osteoclast precursors) was carried out with the addition of *E.coli* LPS and/or HA treatment, to determine whether osteoclast differentiation was affected by LPS and HA (*Figure 46*).

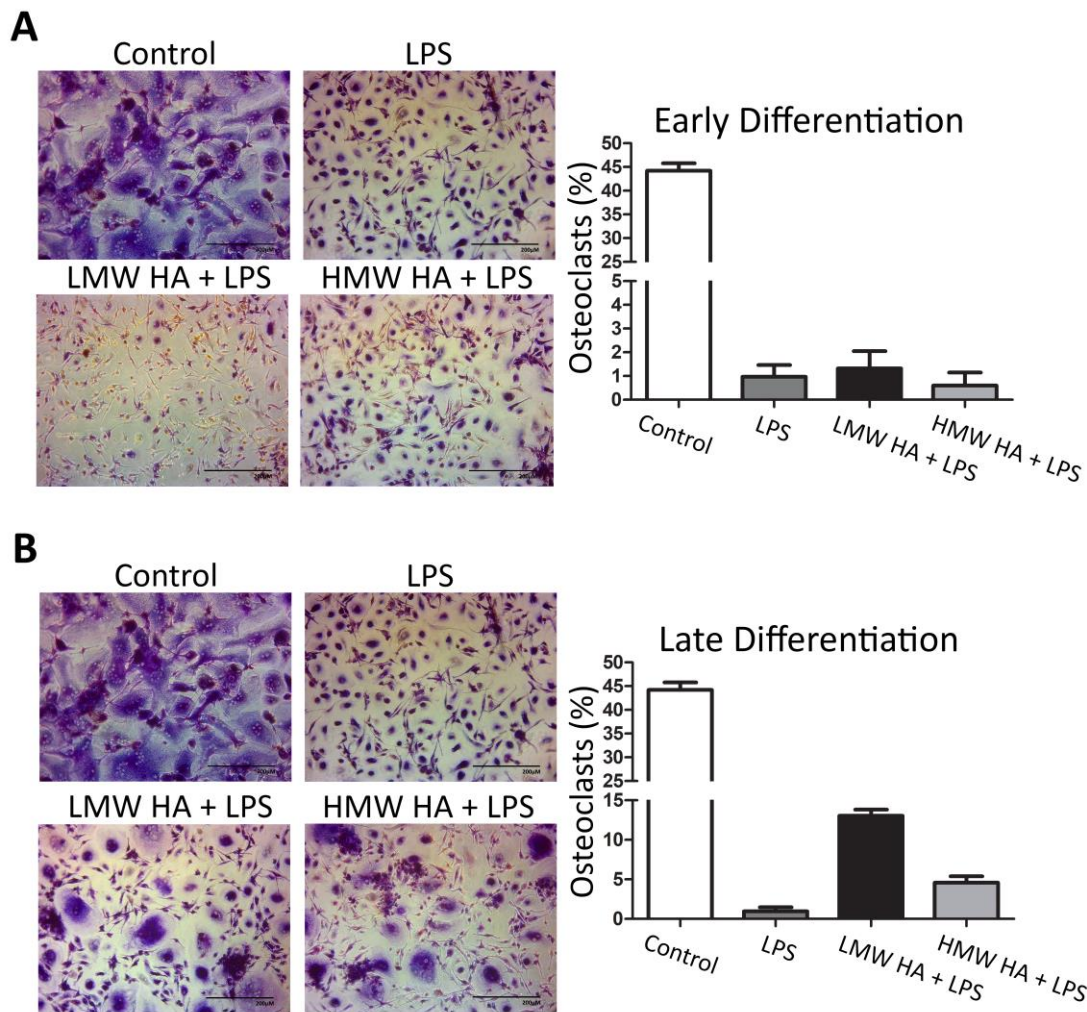


Figure 46: The effect of hyaluronan and LPS on osteoclast differentiation; A: Phase contrast images of TRAP stained hBMCs treated with LPS alongside the osteoclast differentiation protocol, and quantification of osteoclast percentage; B: Phase contrast images of TRAP stained hBMCs treated with HA and LPS at the early osteoclast differentiation stage, and quantification of osteoclast percentage in each sample; C: Phase contrast images of TRAP stained hBMCs treated with HA and LPS at the late osteoclast differentiation stage, and quantification of osteoclast percentage in each sample. N=4, statistical significance determined by two-way ANOVA with Bonferoni correction comparing each sample to the corresponding control at each time point, and set at * ($p < 0.05$), ** ($p < 0.01$) and *** ($p < 0.001$). LPS = lipopolysaccharide, LMW HA = low molecular weight hyaluronan, HMW HA = high molecular weight hyaluronan.

In the control condition, hBMCs treated with the osteoclast differentiation protocol, there was a high number of osteoclasts identified, numbering 42.9% on average. By contrast, there were very few osteoclasts identified when hBMCs were treated with LPS alongside the osteoclast differentiation protocol. Similarly, in conditions where cells were treated with HA alongside LPS, there were significantly fewer osteoclasts identified than in the control condition. When HA was given at the early differentiation stage, there was little difference between the LPS alone, LMW HA with LPS or HMW HA with LPS conditions in terms of the number of osteoclasts identified

(*Figure 46A*). Of the combination treatments, LMW HA with LPS at the late differentiation stage had the highest number of osteoclasts identified, however this was still significantly lower than in the control condition (*Figure 46B*). Therefore, it was determined that it was not the osteoclast precursors themselves which were directly affected by repeated LPS exposure and tolerance which altered HA secretion and downstream osteoclast production, in the manner that was identified earlier.

4.2.6 Co-culturing Inflammatory Monocytes and Osteoclast Precursors

This thesis tested the hypothesis that it was cells of the inflammatory monocyte/macrophage lineage which were affected by LPS tolerance, which in turn modulated their communication with osteoclast precursors in a potential cross-talk mechanism (*Figure 47*). THP1 cells were exposed to the *E.coli* LPS tolerance protocol, and hBMCs were prepared for the osteoclast differentiation protocol, as before (see sections 5.3.1 and 5.3.3). THP1 cells at 24 hours post the second LPS treatment were then co-cultured with hBMCs at the early differentiation stage (when M-CSF was first added; *Figure 47A*). Osteoclasts were identified as TRAP-positive cells with three or more nuclei (*Figure 47B*) and were quantified (*Figure 47C*).

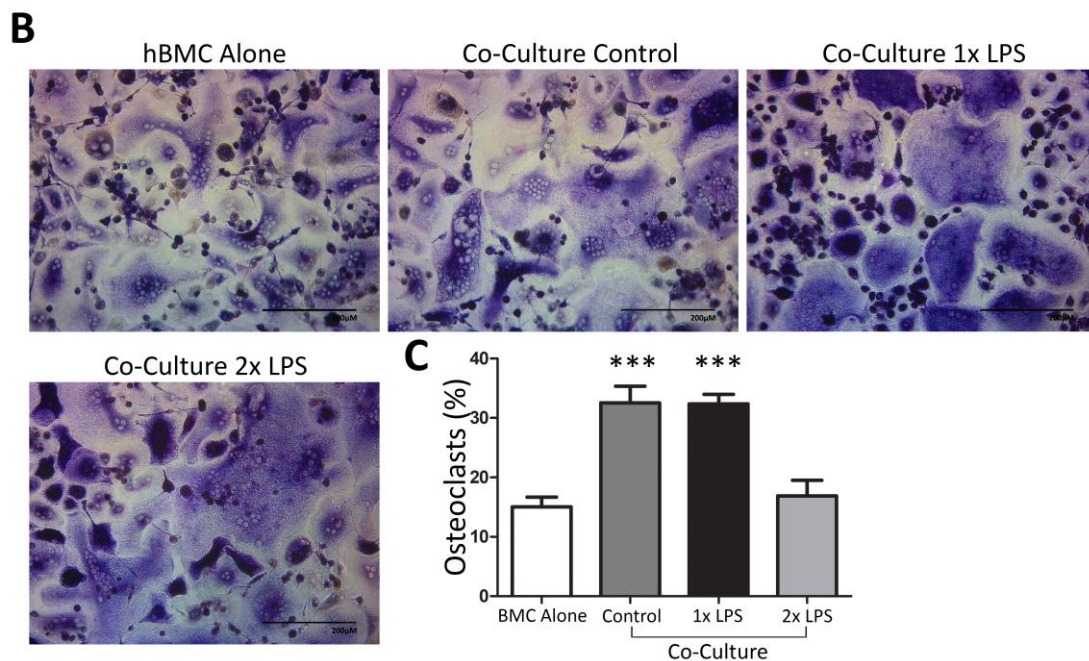
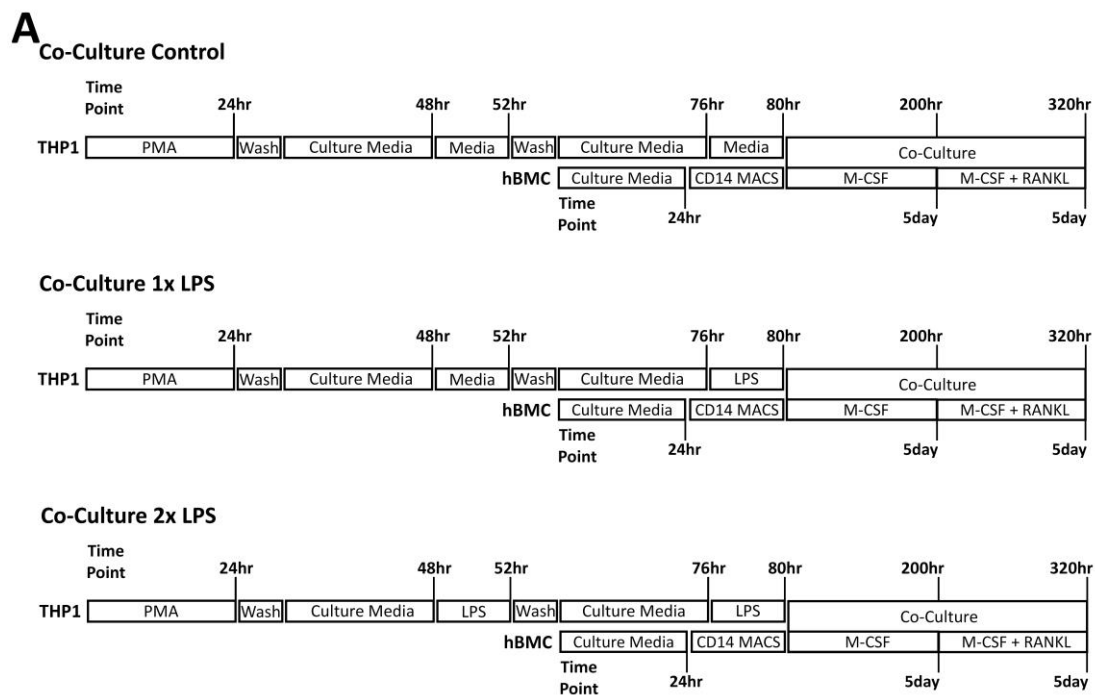


Figure 47: Co-culturing osteoclast precursors with THP1 cells tolerised to *E.coli* LPS; A: Schematic demonstrating the experiment procedure whereby THP1 cells undergo the previously established tolerance protocol using *E.coli* LPS prior to co-culture with hBMCs undergoing osteoclast differentiation; B: Phase contrast images of TRAP stained hBMCs co-cultured with tolerised THP1 cells at early osteoclast differentiation; C: Quantification of osteoclast percentage in each sample. N=4, statistical significance determined by two-way ANOVA with Bonferoni correction comparing each sample to the BMC Alone control, and set at * ($p < 0.05$), ** ($p < 0.01$) and *** ($p < 0.001$). 1x = single LPS exposure, 2x = multiple LPS exposure, PMA = phorbol 12-myristate 13-acetate, LPS = lipopolysaccharide, CD14 = cluster of differentiation 14, M-CSF = macrophage colony stimulating factor, RANKL = receptor activator of nuclear factor NF- κ B ligand, BMC = bone marrow cell.

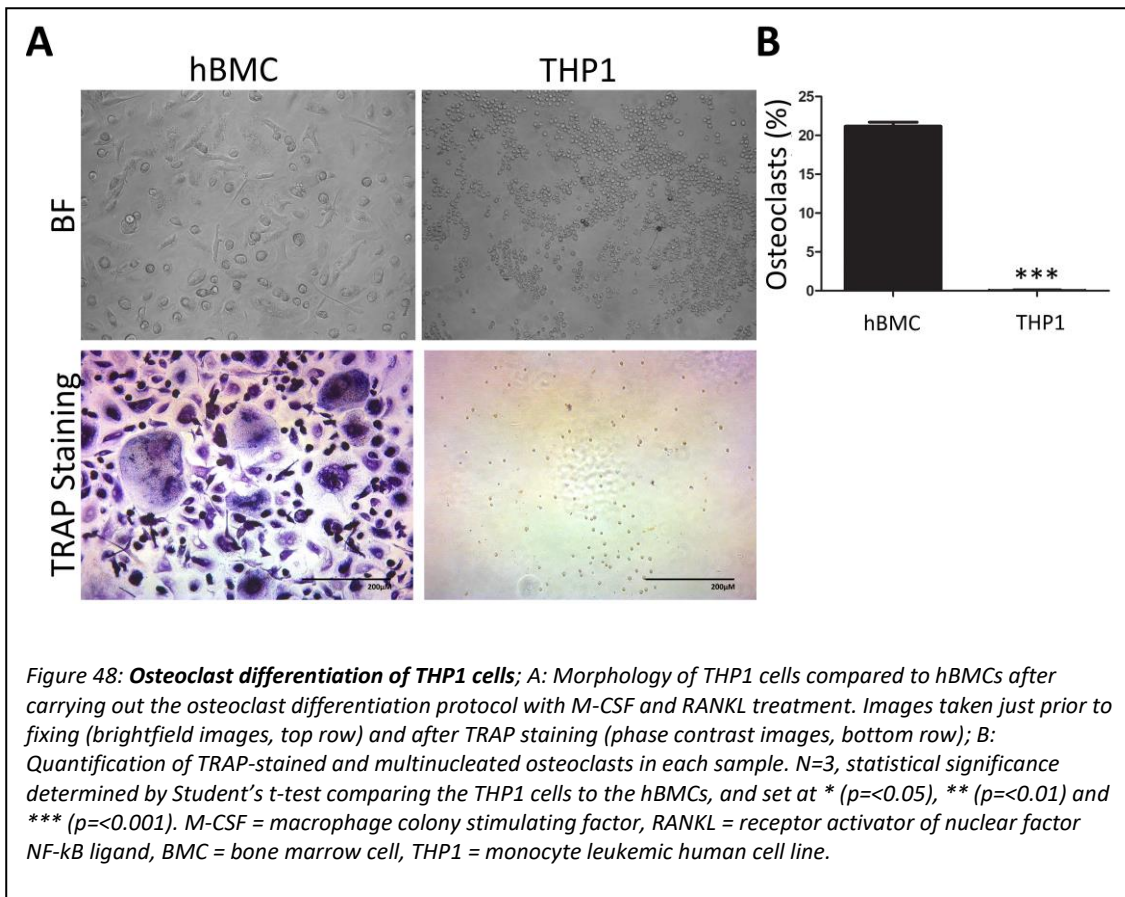
In the BMC control, hBMCs underwent the osteoclast differentiation protocol without co-culture with THP1 cells, and osteoclasts were identified. The conditions where hBMCs were co-cultured

with control THP1 cells or 1x THP1 cells had an increased number of osteoclasts identified compared to the BMC control condition. In the condition where hBMCs were co-cultured with 2x THP1 cells, there was a slight increase in osteoclast number compared to the BMC control, however this was significantly less than was identified in the conditions with 1x or control THP1 cells (*Figure 47C*). These results indicate that the addition of THP1 cells affects hBMC differentiation to osteoclasts, however this effect is negated when the THP1 cells had undergone *E.coli* LPS tolerance. Perhaps this is indicative of the effects of LPS tolerance on osteoclast differentiation and subsequent bone loss in periodontal disease.

4.2.7 Determining the capability of THP1s to Differentiate to Osteoclasts in this Model

Since THP1 cells are pre-monocytes there is the potential for them to differentiate to osteoclasts under certain conditions. In order to ensure that the change in osteoclast number observed in the co-culture of hBMC and THP1 cells was representative of the hBMCs alone, the THP1 cells were treated to the osteoclast differentiation protocol.

THP1 cells underwent the previously established osteoclast differentiation protocol and hBMCs were used as a positive control. Cells were cultured overnight and the non-adherent cells were sorted for CD14 using MACS. The CD14-positive cells were seeded in culture media containing 25ng/ml M-CSF for 5 days, then 25ng/ml M-CSF and 100ng/ml RANKL for a further 5 days. Cells were fixed and TRAP stained to determine the capability of THP1 cells to differentiate to osteoclast-like cells (*Figure 48*).



There were no cells present in the THP1 samples that could be identified as osteoclasts based on their characterisation as TRAP-positive and multinucleated cells. This was a significant decrease compared to the hBMC control, as determined by a Student's t-test. Despite the same number of cells being seeded into each well there was a marked decrease in the overall number of cells observed in the THP1 wells at the end of the experiment compared to the hBMC wells, as the majority of THP1 cells did not attach to the plate surface. This can be seen in the brightfield images taken just prior to fixation, where there is a higher number of cells visible in the THP1 sample compared to after TRAP staining (*Figure 48A*). Additionally, the cells that had attached in the THP1 wells had a small, round morphology that did not align with the expected morphology of osteoclast cells (*Figure 48A*). These results indicated that in this model THP1 cells could not differentiate to osteoclast-like cells, therefore the change in osteoclast number seen with the co-culture of hBMC and THP1 cells (*Figure 47*) could not be explained simply by THP1 cell differentiation.

5 Chapter 5: Discussion & Conclusions

5.1 Discussion

This thesis aimed to research the role of the autophagy pathway in two scenarios of exogenously induced bone remodelling: orthodontic tooth movement and periodontitis.

When considering the first scenario, the effects of constant tensile strain on the differentiation of osteoblast precursors and the levels of autophagy in these cells were investigated in two models of orthodontic tooth movement. The *in vivo* work demonstrated an initial increase in autophagy that was associated with a decrease in *RUNX2* expression in rat periodontiums exposed to constant tensile strain. However, at 24 hours stretched, autophagy levels were reduced and *RUNX2* expression was increased, indicating osteogenic differentiation. Using an *in vitro* cell stretching model, osteoblast precursors were found to have both increased osteogenic marker expression and cytoskeleton breakage when exposed to constant tensile strain for 24 hours. In modulating the autophagy pathway alongside mechanical strain exposure, this demonstrates that inhibiting autophagy reduced *RUNX2* expression, meanwhile inducing the autophagy pathway increased *RUNX2* expression. This could indicate that upregulation of the autophagy pathway enhances strain-induced osteogenesis differentiation, perhaps by acting as a protective mechanism against the stretching force.

In the second scenario being investigated, the effects of repeated LPS exposure to pre-monocytes' inflammatory response and autophagy levels were investigated, to determine how these may affect osteoclast differentiation in the context of periodontal disease. Pre-monocytes that had been exposed to LPS only once had an increased inflammatory response, low autophagy levels and increased expression of *HAS3*, an enzyme that produces LMW HA into the ECM where it can come into contact with other cells including osteoclast precursors.

This thesis also found LMW HA caused an increase in the number of osteoclasts differentiated from osteoclast precursor cells, as determined by TRAP staining. In a clinical scenario an increase

in osteoclast number is related to bone resorption, which may not be balanced by osteogenesis and therefore results in net bone loss.

Interestingly, pre-monocytes that had undergone repeated exposure to LPS had a reduced inflammatory response, comparable to literature examples of LPS tolerance. These 'tolerised' cells (labelled as '2x') also exhibited an increase in HAS3 mRNA however HAS3 protein was significantly reduced. This could be due to HAS3 being degraded by the autophagy pathway, as autophagy was upregulated in these cells and immunofluorescence staining demonstrated co-localisation of autophagy and lysosome proteins with HAS3. This work puts forward the hypothesis that autophagy-related HAS3 degradation leads to a reduction in the amount of LMW HA produced, meaning osteoclast precursors potentially do not get that extra signal to differentiate, hence fewer osteoclasts. LPS tolerance has been related to chronic inflammation in the literature, in this work tolerization may mimic the altered response to chronic inflammation seen in periodontitis. Thus, these results could begin to explain how some people do not experience alveolar bone loss, even with poor dental hygiene practices or signs of early disease (Al-Qutub *et al.*, 2006).

Further research would be required to validate these hypotheses and investigate the molecular mechanisms involved, some examples of which will be discussed in the following section: an in-depth discussion of the data presented in this thesis compared against the current understanding in the literature.

5.2 The role of Autophagy in the Periodontium during Experimental Orthodontic Tooth Movement

5.2.1 Tooth Movement *In Vivo*

5.2.1.1 Morphology

H&E staining of rat periodontiums from an *in vivo* tooth movement model indicated that the greatest morphological changes occurred at the bone-PDL boundary as observed at 3 hours and 1 and 3 days, compared to the 0 hour control (*Figure 16*). This corroborates one paper which investigated the idea that strain has a greater effect in regions where dissimilar tissues are attached, for instance the bone-PDL boundary (Grandfield *et al.*, 2015). This paper also describes the formation of finger-like protrusions of bone as indicative of new bone being formed which could be what is being observed with the indents of bone identified with cells accumulating within these regions from 1 hour to 3 days stretched. These results are comparable with H&E staining of stretched periodontiums from other papers (Wada *et al.*, 2017). The accumulations of cells could be that of inflammatory cells, similar to that of the first stages of wound healing, as the force required for tooth movement can be damaging to the tissue (Wise and King, 2008). Alternatively, these cells could be an influx of bone marrow cells such as MSCs or their progenitors, including osteoblasts for new bone formation (Su *et al.*, 2018). Other papers show cement lines or microcracks in bone that has been exposed to tensile stretching force, which represents areas of local remodelling and osteogenesis (Robling, Castillo and Turner, 2006; Herber *et al.*, 2012). This was not identified in the H&E images of these samples, perhaps due to the time points being too early for osteogenesis to be completed, as bone formation can take several weeks to complete (Burr *et al.*, 1989).

The boundary between the cementum and PDL is less defined in the later timepoints compared to the 0 hour sample. Changes in cementum thickness and overall structure are known to impact the success of PDL attachment (van den Bos *et al.*, 2005; Foster, 2012). The changes in cementum structure observed at 7 days could be related to the remodelling of the PDL caused

by tooth movement. The PDL undergoes dynamic changes as it is stretched in this model. In the 0 hour control, the PDL is densely packed with little space between the fibres and both horizontal and oblique fibres are observed, while at 1 hour stretched the PDL is more sparse. This has been observed in other tooth movement models, perhaps due to the initial onset of stretching forcing the fibres apart (Grandfield *et al.*, 2015). From 3 hours to 7 days stretching, new fibres are formed to re-populate the PDL space, and by 7 days the PDL has a clear fibrous structure.

5.2.1.2 Osteogenic Marker Expression

Immunofluorescence for three key osteogenic markers was carried out in order to analyse the effects of strain on osteogenesis. These included RUNX2, the master transcription factor of osteogenesis, osteopontin, a marker of early osteoblast differentiation, and DMP1 which is expressed by differentiated osteoblasts for the mineralisation of osteoid (Narayanan *et al.*, 2003; Rutkovskiy, Stensl kken and Vaage, 2016).

Osteopontin had increased expression in the bone-PDL boundary as the time stretched elapsed, whereas DMP1 was upregulated in the bone from 0 hour to 7 day stretched however the brightest fluorescence was observed at 3 hours (*Figure 17*).

One paper showing osteopontin of the same region on the periodontium as seen in this work demonstrated that cement lines stain positive for osteopontin (Herber *et al.*, 2012). This staining looks similar to the regions of the bone-PDL boundary that stained highly positive for osteopontin in this work, and may represent areas of bone remodelling after exposure to mechanical strain as established in the literature (Nanci, 1999; Robling, Castillo and Turner, 2006; Herber *et al.*, 2012). In the PDL exposed to tensile strain osteopontin expression was varied with little expression at the earlier time points, an increase at 3 hours followed by a reduction at 1 day, an increase again at 3 days and a decrease at 7 days stretched. One paper found constant compression strain caused osteopontin to be upregulated in the PDL (Wongkhantee, Yongchaitrakul and Pavasant, 2007), while others have suggested that

osteopontin gene expression is highly affected by mechanical strain in osteoblasts (Toma *et al.*, 1997), therefore this could be what is being observed in the 3 hour and 3 day samples. Since the PDL also contains stem cells that are able to differentiate into osteoblasts it could be that the osteopontin expression at 3 hours and 3 days represents osteogenic differentiation in this region (Tomokiyo, Wada and Maeda, 2019; Trubiani *et al.*, 2019). It would have been interesting to investigate the contribution of MSCs from the bone marrow and PDL to alveolar bone remodelling, as it is still unknown whether one or both stem cell niches are utilised during tooth movement. Additionally, at 3 days stretched there was increased osteopontin expression in the compressed region of the periodontium, which mirrors the expression of osteopontin in osteoclasts seen in the literature (Herber *et al.*, 2012).

Osteopontin and DMP1 were also observed in the cementum adjacent to the dentine from 1 hour to 7 days stretched. Both DMP1 and osteopontin are established to be expressed in the cementum and are important for PDL integrity (Ye *et al.*, 2008; Foster, 2012), therefore these results may represent remodelling of the periodontium as a whole. DMP1 is expressed in many cell types, but it is known to be highly expressed in osteocytes, which are embedded in the bone (Toyosawa *et al.*, 2004), where the majority of DMP1 staining was observed throughout the stretching process. There was little to no DMP1 expression in the PDL at any time point, which is expected based on the literature (Ye *et al.*, 2008). Overall, the osteopontin and DMP1 staining observed in the rat periodontium samples seemed to match the literature, validating these samples and this experiment as a good model to look at osteogenesis in relation to tooth movement.

RUNX2 was observed by immunofluorescence to be decreased at 1 and 3 hours but by 24 hours of stretching the RUNX2 staining was increased and nuclear localised, which is crucial to its function as a transcription factor (*Figure 18*). RUNX2 positive cells, classified as cells with RUNX2 staining co-localised with the nucleus, were quantified and the relative fluorescence intensity of RUNX2 positive cells was determined in Photoshop by drawing around the nucleus of each cell

and noting the number of pixels in the red channel within the nucleus. A similar methodology was employed in one paper to determine RUNX2 fluorescent intensity in images of mice periodontiums after orthodontic tooth movement (Vidoni *et al.*, 2019). That paper found increased RUNX2 in the PDL exposed to tensile strain at 3days; while this was later than the time-points used in this work, this observation was comparable to results seen at 24 hours. The quantification of RUNX2 demonstrated an initial decrease in the percentage of RUNX2-positive cells and relative fluorescence intensity, however by 24 hours of stretching there was an increase in both the RUNX2-positive cell percentage and fluorescence intensity of these samples (*Figure 18C*). One paper using a similar orthodontic tooth movement device demonstrated increased RUNX2 expressed in the alveolar bone and tissues surrounding the tooth exposed to tensile strain which is comparable to the results presented in this thesis (Zhang, Liu and Wang, 2020). Another paper demonstrated RUNX2 nuclear localisation in cells of the bone-PDL and PDL-dentine boundaries at 7days stretched compared to controls (Aonuma *et al.*, 2020). Interestingly, the regions specified in that paper are the same regions that had the greatest morphological change seen by the H&E staining presented earlier (see *Figure 16*). While that paper did not show any H&E staining or results from earlier time-points that could be directly compared to the data presented here, these data sets may help corroborate the current theory that stretching force has a greater effect on regions where dissimilar tissues join (Grandfield *et al.*, 2015). Overall, these results suggested there is an initial delay to osteogenesis after the periodontium is exposed to tensile strain, followed by an increase in RUNX2-positive cells at the bone-PDL boundary at 24 hours.

5.2.1.3 *Autophagy and Osteogenesis*

The interplay between osteogenesis and autophagy has been explored in the literature, with the activation of autophagy being associated with increased osteoid mineralisation (Nollet *et al.*, 2014) and inhibiting autophagy in bone marrow cells influenced their differentiation to adipocytes rather than the osteogenic lineage (Qi *et al.*, 2017). Therefore, the effects of the

constant tensile strain of tooth movement on autophagy and how this relates to osteoblast differentiation was of interest.

Immunofluorescence for LC3 was carried out as a method of determining autophagic flux which is well established in the literature (*Figure 18*). Imaris software was used to divide the images into regions of interest in the periodontium, with LC3 puncta staining being quantified using the spots function. LC3 puncta were increased at 1 hour and 3 hours stretched but decreased at 24 hours stretched, indicating an increase in autophagy levels at the earlier time points of the experiment. The region with the highest levels of LC3 puncta seen were the bone-PDL regions, which was also the region with the highest RUNX2 expression, albeit at different time points. More concrete evidence of autophagy levels in these samples could be achieved by staining for additional markers, such as p62 or ATG5, however LC3 not only demonstrates the presence of the protein by the intensity of fluorescent staining but also the presence of autophagosomes by the quantification of puncta, hence why it is the gold standard for determining autophagy levels. For this reason, LC3 is an appropriate choice for immunofluorescence staining and quantification in demonstrating the expression of autophagy as a whole.

In comparing the staining patterns of RUNX2 and LC3 expression, there is a clear juxtaposition in the activation of autophagy and the onset of osteogenic differentiation in this model. Initially, stretching caused autophagy to be upregulated and RUNX2 expression to be downregulated, however by 24 hours of tensile strain the reverse is observed. While these patterns of expression are observed in all the regions exposed to tensile strain in the periodontium, the region with the largest change in expression was the bone-PDL region, probably due to an influx of bone marrow cells to the region, including those of immune cells and osteoblast precursors. It is unknown whether autophagy and osteogenesis are directly linked or regulating each other, however it could be that autophagy is initially activated as a protective mechanism in this model, as this is also seen in other scenarios of cell stress (Hirt and Liton, 2017); Autophagy has been shown to prolong the life of cells and prevent apoptosis, and has previously been established to be

activated by mechanical strain (Tanabe *et al.*, 2011; Hirt and Liton, 2017). The hypothesis after these experiments was therefore that constant tensile strain of the periodontium initially activates autophagy as a protective mechanism, and once autophagy levels are decreased back to basal levels osteogenesis is activated for remodelling of the alveolar bone.

5.2.1.4 Cytoskeleton Expression

An investigation into the mechanosensory mechanisms involved was attempted by analysing the rat tooth movement samples for their expression of tubulin, a cytoskeleton marker. α -tubulin is a component of microtubules in the cytoskeleton, and microtubules have been demonstrated in the literature to be key to cell polarity and tissue reorganisation in response to strain (Morioka *et al.*, 2011; Hamant *et al.*, 2019).

There was decreased α -tubulin staining in the PDL at 1 hour stretched compared to the 0 hour control, however from 3 hours to 7days α -tubulin staining was increased back to basal levels (*Figure 19*). This contradicts the results of one paper which demonstrated an increase tubulin expression after exposure to cyclic tensile strain (Morioka *et al.*, 2011), however this was in smooth muscle cells and therefore this effect may be context dependant. There are few examples in the literature of α -tubulin staining in rat periodontiums in response to mechanical strain therefore it is difficult to ascertain whether the results seen in this thesis were expected. However, one paper where periodontal ligament cells were treated with colchicine, to block microtubule formation, demonstrated that microtubules play a significant role in tooth eruption (Beertsen *et al.*, 1984), therefore there is literature precedent for the role of microtubules in periodontium remodelling.

If time and resources would have allowed it would have been interesting to process these images in Imaris in order to quantify the α -tubulin staining pattern, as was carried out on the *in vitro* samples (*Figure 33*). However, whilst not definitive these results demonstrate a change in tubulin staining which could reflect altered cytoskeleton dynamics in response to the stretching force of tooth movement.

5.2.2 Optimising an *In Vitro* Cell Stretching Model

An *in vitro* model of tensile strain was developed to mimic that of the periodontium during tooth movement. Initially, two *in vitro* cell stretching devices were considered for use as a model of the tensile strain involved in orthodontic tooth movement, one commercial system by Strex and one device provided by EPFL.

In comparing the features of the two cell stretching systems it was clear that the EPFL system was more accurate as it took the human element of applying the stretching force out of the equation. The ability to change the stretch patterns was also appealing in order to investigate changes in constant strain compared to intermittent strain with different intervals or durations. However, constant tensile strain was more relevant for the purpose of researching orthodontic tooth movement.

The systems varied in the air-liquid interface the cells were exposed to; the EPFL system did not have well walls, meaning that a maximum of 1ml culture media could be carefully placed on top of the 2.5cm diameter membrane and surface tension meant that it formed a dome of media which was slightly higher in the middle than at the edges. The Strex system was constructed in a structure closer to that of a cell culture well plate, with high well walls, therefore 1ml culture media was used for each 1cm² well, which was evenly spread across the well of the Strex system. This meant that the cells seeded on the Strex membranes were exposed to an air-liquid interface that was closer to that of a normal cell culture plate than the EPFL system. Despite this, there seemed to be little difference between the systems in the hBMCs ability to attach and grow, instead the biggest variance in these factors seemed to be due to the success of the collagen coating. This was optimised by testing different collagen coating protocols and reducing the number of samples coated in each batch for more consistent cell attachment.

The EPFL system had also been designed with microscopy work in mind, with the underside of the PDMS membrane having a layer of microscopy oil and glass coverslip built in, therefore would have been useful for immunofluorescence work. However, the fact that only a portion of

the cells would be stretched on the membrane was an issue; while this would work for microscopy-based analysis as you could use the un-stretched cells from the same membrane as an internal control, it would have been a hindrance in trying to analyse changes in RNA, or protein by Western Blotting, as the sample would contain some cells that had not been stretched. It was considered that attempting to only collagen-coat the area of the membrane which would be stretched to avoid this issue, however this idea turned out to not be realistic from a technical perspective, and would also result in a low yield of RNA or protein being collected due to the low cell number. Additionally, as a prototype the EPFL devices were constantly being updated and improved. This meant there were large variations between batches which made it difficult to apply to research where consistency is important to ensure reliable results. The Strex system was therefore taken forward for the *in vitro* cell stretching experiments detailed in the rest of this thesis.

In using the devices several optimisation steps were taken which did improve the useability of the devices over time including altering the collagen coating protocol and establishing a method for immunostaining and mounting the membranes to improve sample quality for imaging. Despite this it is clear that both devices still provided challenges which impacted the scope of this work, therefore the optimisation detailed in this thesis, although not perfect, does have value in providing a starting off point for future research using cell stretching devices such as these.

5.2.3 Human Bone Marrow Cell Characterisation

In order to investigate the effects of constant tensile strain on osteogenesis *in vitro*, a pool of cells that were able to differentiate into osteoblasts were required. In the context of tooth movement, it is thought that MSCs and osteoblast progenitors from the bone marrow are stimulated to migrate and differentiate into osteoblasts in order for osteogenesis to occur (Su *et al.*, 2018), therefore hBMCs were a relevant choice of cells for this work.

Adherent hBMCs had a long, fibroblastic morphology and grew well in DMEM-F12 media. A higher proportion of FBS (20% rather than the 10% used for other cell types) which contains various growth factors, was used to encourage the maintenance of the stem cells contained within this pool of cells (Horwitz *et al.*, 1999; Lee and Lee, 2011; Kwon *et al.*, 2016). Likewise, a multivitamin solution containing folate, calcium and vitamins A and B was used, as folic acid maintains pluripotency (Kasulanati and Venkatesan, 2018), nicotinamide promotes stem cell survival *in vitro* (Peled *et al.*, 2012; Meng *et al.*, 2018), and calcium and its derivatives have been shown to prime MSCs for differentiation to osteoblasts (Müller *et al.*, 2007; Viti *et al.*, 2016; Millan *et al.*, 2018).

It is widely established in the literature that MSCs are characterised by their expression of certain markers and their negative expression of other markers including those of HSCs or more differentiated cells. In addition, the ability of cells to differentiate into the osteogenic, adipogenic or chondrogenic lineages helps to establish the presence of MSCs in a cell pool.

5.2.3.1 MSC Marker Expression of hBMCs

Flow cytometry demonstrated that hBMCs contained a population of cells that were positive for MSC markers CD44, CD90, CD105, CD106, CD146, CD166 and Stro-1, while the HSC markers CD19 and CD45 were negative (*Figure 29*). Lower passage hBMCs (P3-5) contained a relatively higher proportion of cells that were positive for CD44 and CD105 than higher passage cells (P12). MSCs do not proliferate as rapidly as other cell types, therefore it may be that over time in culture MSCs make up a smaller proportion of the cells present, or that the time in culture causes them to begin to differentiate resulting in an overall reduction in the proportion of cells that are positive for the MSC markers. Overall, these results indicated that hBMCs do contain a population of cells that are MSC-like based on their marker expression therefore they are relevant to the study of osteogenesis.

5.2.3.2 Osteogenic Differentiation

hBMCs were treated with osteogenic induction media to determine whether hBMCs could differentiate into osteoblasts, and overall treated cells had increased expression of osteogenic markers than controls (*Figure 30*). A well-established osteogenesis protocol was used and cells were collected 7 or 14 days after the on-set of treatment as these time-points had been established in papers using this protocol on osteoblast-precursors (Langenbach and Handschel, 2013).

In the literature, RUNX2 expression is one of the first signs of MSC differentiation to osteoblasts, therefore the increase in RUNX2 gene and protein expression seen from 7 to 14 days would be expected in cells that had started to differentiate into osteoblasts. *DMP1* gene expression was decreased in 7 day treated samples but was increased in treated samples at 14 days compared to controls. There was also a slight increase in *osteopontin* expression after 14 days of treatment, however this was not significant. While these are key markers of osteogenesis, increased expression of additional osteoblast markers as well as the decreased expression of adipogenic or chondrogenic markers would have provided more concrete evidence of osteogenic differentiation. Additionally, the cells treated with the osteogenic induction media were not determined to be functional osteoblasts capable of mineralisation using Alizarin Red staining. Therefore, these results cannot determine that the hBMCs can differentiate into osteoblasts, only that they can be induced to express markers consistent with differentiating osteoblast-like cells.

Overall, the characterisation of hBMCs indicated that these cells have the expected marker expression and capacity to differentiate into osteoblast-like cells that made them a suitable choice for analysing the effects of tensile strain on osteogenesis.

5.2.3.3 Autophagy Levels in Differentiating hBMCs

In order to establish the baseline autophagy levels in hBMCs undergoing osteogenic differentiation, hBMCs that were treated with the osteogenic differentiation medium were

analysed for their expression of genes related to autophagy (Figure 31). Both LC3 and ATG5 gene expression were increased at 7 days and further increased at 14 days in treated samples compared to controls. In the autophagy pathway, ATG5 slightly precedes LC3 as it is involved in the phagophore membrane while LC3 aids the formation of the outer autophagosome membrane (Hale *et al.*, 2013). The increase in ATG5 in treated samples therefore indicates an upregulation or activation of the autophagy pathway. The LC3 primer used was specific to total LC3 protein, rather than LC3-II, the form of the protein associated with autophagosomes. However, when autophagy is activated there is an increase in the production of LC3 protein for the formation of autophagosomes (Mizushima, Yoshimori and Levine, 2010), so the increase in LC3 seen in treated cells could also be indicative of autophagy activation.

Some papers have previously shown MSCs to have high basal levels of autophagy which are reduced when they differentiate into osteoblasts (Oliver *et al.*, 2012). The results shown in this thesis do not fit this pattern, as the expression of key autophagy genes were increased in cells undergoing induced osteogenic induction. However, the cells used for these experiments are not a pure population of MSCs, and the literature demonstrates that autophagy levels are highly context dependant (Dower *et al.*, 2018). Additionally, there are numerous examples in the literature demonstrating the activation of autophagy is associated with differentiation of MSCs to the osteogenic lineage, as previously mentioned in this thesis. Therefore, these results determined that hBMCs had increased autophagy levels during osteogenic differentiation, which corroborates literature examples of osteogenic differentiation. In this context, hBMCs comprise a good model of osteoblast progenitors for the study of mechanical strain *in vitro*.

5.2.4 Cell Stretching as an *In Vitro* Model of Tooth Movement

5.2.4.1 Stretching hBMCs

hBMCs that were exposed to 20% constant uniaxial tensile strain for 24 hours had both increases in RUNX2 gene and protein expression and LC3 puncta staining compared to controls, indicating the activation of osteogenesis and autophagy (Figure 32).

RUNX2 gene expression was increased at 24 hours stretched but was decreased at 6 and 72 hours compared to controls (*Figure 32A*). Immunofluorescence showed *RUNX2* staining to be both increased and nuclear localised at 24 hours stretched compared to controls. As a transcription factor, the fact that it was nuclear localised is indicative of its activation and of osteogenic differentiation. Osteogenic markers downstream of *RUNX2*, osteopontin and *DMP1*, were also analysed using immunofluorescence and while there was little change in osteopontin expression, *DMP1* staining was increased in stretched cells compared to controls (*Figure 32B*). *DMP1* also seemed to be nuclear localised; previous papers have demonstrated that *DMP1* contains a nuclear localisation signal (NLS), and is present in the nucleus of pre-osteoblasts (Narayanan *et al.*, 2003; Siyam *et al.*, 2012). While the exact mechanisms are unknown, it is thought that *DMP1* may have a regulatory role in osteogenesis (Lin *et al.*, 2014). Overall, these results indicate that osteogenic differentiation may have been activated in hBMCs that have been exposed to tensile stretching force for 24 hours.

The Q-PCR results also demonstrated an increase in *p62* expression in stretched samples compared to controls at 6 hours. *p62* is involved early in the autophagy pathway for the tagging of proteins for capture in autophagosomes, and therefore an increase in this protein indicates upregulated autophagy. At 24 hours stretched there was a decrease in *ATG3* and an increase in *LC3* expression, which could be indicative of autophagosome formation. At 72 hours stretched there was a decrease in *LC3* and *ATG5* expression compared to controls but little change in *p62* and *ATG3*, perhaps indicating that autophagy had stabilised back to basal levels (*Figure 32C*). Immunofluorescence revealed *LC3* puncta staining, demonstrating autophagosome formation, was increased in stretched samples at 24 hours compared to controls. Together these results indicate an upregulation of autophagy from 6 hours after the onset of strain until 72 hours.

In the osteogenic induction experiments cells were exposed to osteogenic induction media for 7 or 14 day time points, however, for stretching experiments these time points were not suitable for several reasons: Firstly, mechanotransduction has been shown to propagate signals up to 40

times faster than diffusion or translocation-based signalling, therefore the effects of stretching on differentiation would be expected to be seen much earlier than that used by the osteogenic induction media (Na *et al.*, 2008). Secondly, culturing cells on the Strex system was very delicate as once cells began to reach confluency they were at risk of detaching from the membrane surface. This coupled with the fact that the hBMCs grew very well meant that cells would reach confluency rapidly, therefore studies of more than 72 hours were unlikely to be successful.

In comparing the osteogenic and autophagy marker expression of both the *in vitro* and *in vivo* models, the data from the rat model demonstrated an initial increase in autophagy that was associated with a decrease in RUNX2 expression (*Figure 18*). The *in vitro* results could be seen to corroborate the *in vivo* data as autophagy markers were first upregulated at 6 hours, before the osteogenic markers were upregulated at 24 hours. However, 24 hours was found to be a key time-point for both RUNX2 and LC3 expression *in vitro*, rather than the opposing expression patterns observed *in vivo*. This could be an argument that the *in vitro* model is not a perfect representation of the *in vivo* situation, however this is often the case for setting up any model. Overall, including the fact that the hBMCs had increased expression of autophagy-related genes when undergoing osteogenic differentiation (*Figure 31*), these results suggest an activation of the autophagy pathway as an initial reaction to constant tensile strain, perhaps as a protective mechanism. This has been seen in other systems, for instance autophagy is upregulated to protect against apoptosis in patients with periodontal disease (An *et al.*, 2016). Therefore, chemically modulating the autophagy pathway prior to mechanical strain *in vitro* was tested to investigate whether this would affect osteogenic differentiation of hBMCs.

5.2.4.2 Autophagy Modulation and Strain

Inducing or inhibiting the autophagy pathway clearly had different effects on osteogenic marker expression in the *in vitro* cell stretching model. hBMCs that had autophagy induced by rapamycin treatment had an increase in *RUNX2* gene expression after 24 hours strain, while inhibiting autophagy with bafilomycin treatment prior to strain caused the opposite trend.

However, immunofluorescence revealed that at the protein level both bafilomycin and rapamycin treatment increased RUNX2 expression compared to controls. However, cells treated with rapamycin had nuclear-localised RUNX2 expression which was higher than that seen in cells exposed to stretching alone (*Figure 34C*). These results could indicate that autophagy enhances the activation of strain-related osteogenic differentiation in hBMCs.

5.2.4.2.1 Autophagy Induction Stretching hBMCs

hBMCs treated with rapamycin prior to exposure to 20% tensile strain had little change in *RUNX2* gene expression at 6 hours, however at 24 hours and 72 hours these cells had increased *RUNX2* expression, which was higher than the levels seen in controls and hBMCs that were stretched but not treated with rapamycin (*Figure 34*). As seen in previous experiments, cells that were stretched only had decreased expression of *RUNX2* at 6 hours, an increase at 24 hours and a decrease compared to controls at 72 hours (*Figure 34A*). Interestingly, hBMCs treated with rapamycin alone had the highest expression of *RUNX2* at 72 hours, corroborating accounts from the literature which state the autophagy pathway is linked to cell differentiation, and osteogenic differentiation in particular.

Immunofluorescence images demonstrate little RUNX2 protein expression in any condition at 6 hours stretched, but a slight increase in LC3 staining in cells treated with rapamycin, compared to controls (*Figure 34B*). This was expected as rapamycin stimulates the autophagy pathway resulting in an increase in autophagosome formation and the associated LC3-II which is observed by punctate staining with immunofluorescence (Ravikumar *et al.*, 2004). At 24 hours the stretched samples had increased expression of LC3 compared to controls, however puncta LC3 staining was seen more in the rapamycin and rapamycin stretched conditions, as the drug increases autophagosome formation (*Figure 34C*). At 24 hours, stretched hBMCs had an increase in cytoplasmic RUNX2 staining but not nuclear, which is required for its function as a transcription factor. However, cells treated with rapamycin had increased nuclear RUNX2 indicating that these cells have received a signal to differentiate.

5.2.4.2.2 Autophagy Inhibition

hBMCs treated with bafilomycin to inhibit autophagy prior to 24 hours exposure to tensile strain had decreased *RUNX2* gene expression compared to controls (*Figure 35A*). This would suggest that bafilomycin treatment inhibited osteogenic differentiation of hBMCs. Immunofluorescence of 24 hour samples demonstrate that *RUNX2* protein expression was very low in control cells and increased in cells exposed to stretching force and those treated with bafilomycin and stretched. *RUNX2* staining seemed to be co-localised with DAPI staining in stretched cells, indicating nuclear localisation of this transcription factor. However, in cells treated with bafilomycin or bafilomycin and stretched, *RUNX2* staining may be nuclear localised but is also seen in the cytoplasm (*Figure 35B*). These results may suggest that *RUNX2* is expressed but may not be being transported into the nucleus efficiently.

Osteopontin, another marker of osteogenesis, was decreased in cells exposed to bafilomycin but in cells treated with bafilomycin and stretching force osteopontin expression was increased as seen with immunofluorescence staining. DMP1 seemed to be expressed in the nucleus of control cells as its expression co-localised with DAPI staining, however in cells exposed to stretching force or bafilomycin DMP1 staining was decreased. Cells that were treated with bafilomycin prior to exposure to stretching force did exhibit nuclear DMP1 staining, similar to controls. These results could indicate that the combination of bafilomycin and stretching treatments bring osteogenic markers back to basal levels, as osteopontin and DMP1 staining was similar to that of control cells (*Figure 35C*).

At 24 hours there was an increase LC3 puncta staining in cells treated with either bafilomycin alone or in combination with stretching force, compared to controls (*Figure 35B*). This is expected from the literature, as while bafilomycin is an autophagy inhibitor, it acts by preventing autophagosome fusion to lysosomes. Since this prevents degradation of the autophagosomes that are present, it causes an increase in LC3-II in cells treated with bafilomycin as autophagosomes accumulate in the cell (Tanida *et al.*, 2005).

5.2.4.2.3 *The Significance of Autophagy Modulation*

The literature states that inhibiting or inducing the autophagy pathway is rarely a clear-cut process, partly due to the context-dependant nature of this pathway (Dower *et al.*, 2018). The autophagy pathway has numerous roles in different tissues, and therefore medically altering this pathway may have wide-ranging implications and side effects (Levine, Packer and Codogno, 2015). Inhibition of autophagy has received some interest in medicine in recent years, especially in the cancer field (Marinković *et al.*, 2018). Chloroquine is the only FDA-approved autophagy inhibitor drug that is currently available. It is a malaria medication which inhibits the autophagy pathway by preventing lysosome fusion with the autophagosome, however it often has severe side effects including seizures and deafness (Solitro and Mackeigan, 2016; Mauthe *et al.*, 2018). Additionally, inhibiting autophagy has been linked with several diseases including Alzheimer's disease, Parkinson's disease and cancer (Galluzzi *et al.*, 2017). There are several FDA-approved drugs that have been found to activate autophagy, including the mTOR inhibitors temsirolimus and rapamycin, which are used to treat some cancers or cardiac diseases, respectively (Galluzzi *et al.*, 2017). Other drugs may indirectly activate autophagy by starvation, ER-stress or a rise in intracellular calcium levels (Marinković *et al.*, 2018). Long-term treatment with drugs that activate autophagy may do more harm than good, and it is unclear whether any therapeutic effects can be sustained with only a short treatment period (Levine, Packer and Codogno, 2015). Ultimately, the implications of modulating the autophagy pathway are still unknown and further research is required before a viable osteogenesis enhancer treatment that uses this approach could be proposed for use in humans.

5.2.4.3 *Strain and Cytoskeleton Breakage*

Mechanical strain has been shown to cause direct changes to gene expression via the cytoskeleton, and cytoskeletal tension is thought to be key to the cells' responsiveness to mechanical strain (Ingber, 2008; Jaalouk and Lammerding, 2009). One study found that mechanical cues from the microenvironment influence cytoskeletal organisation, including that of F-actin and α -tubulin, in embryonic stem cells (Gerecht *et al.*, 2007). Therefore, hBMCs

exposed to constant tensile strain were stained for α -tubulin in order to determine the effects of stretching on the cytoskeleton in this model (*Figure 33*).

α -tubulin staining demonstrated that stretched hBMCs seemed to align in the direction of strain while control cells were still randomly aligned at 72 hours (*Figure 33*). This corroborates many examples in the literature where cells have altered their polarity and alignment in monolayer culture when exposed to mechanical strain, including MSCs (Liu *et al.*, 2014; Rens and Merks, 2017), myocytes, (Collinsworth *et al.*, 2000; van der Schaft *et al.*, 2011) and fibroblasts (Eastwood *et al.*, 1998; Chaubaroux *et al.*, 2015; Wada *et al.*, 2017).

Imaris image analysis software was used to provide quantitative data from the cytoskeletal immunofluorescence images and to standardise sample analysis. A surface was created from the Z-stacks of α -tubulin staining, which can be compared to the true staining in *Figure 33A-B*. The volume, area and number of disconnected components were measured for the α -tubulin staining of each image, and results were normalised to the number of cells in each field of view. This normalisation method is suitable to ensure that the differences seen were not attributable to a difference in cell number, however in order to consider these results outside of the dataset and compare them to the literature, a better validation of this analysis method should be made. One example could be to analyse hBMCs treated with a tubulin inhibitor such as colchicine (Lu *et al.*, 2012) in order to determine that cytoskeletal breakage or remodelling is adequately depicted using this methodology.

At 6 hours stretched there was an increase in the area and volume of α -tubulin in the stretched samples compared to controls which was decreased at 72 hours (*Figure 33C*). These results seem to contradict the results of another paper which showed that mechanical strain decreases tubulin expression, despite an increase in the number of other elements of the cytoskeleton including actin filaments and focal adhesions (Meazzini *et al.*, 1998). However, that paper used osteoblasts that were extracted from chickens, which may be expected to react differently to human bone marrow cells that were differentiated *in vitro*. Additionally, adjustments to the

cytoskeleton are important to the morphological changes seen in MSC differentiation (Yourek, Hussain and Mao, 2007; Treiser *et al.*, 2010), therefore cytoskeleton changes could be explained by the hBMCs differentiating. However, no clear morphological change in stretched hBMCs was observed that would corroborate this theory. Alongside the fact that there was an increase in the number of disconnected components measured in the stretched samples at 72 hours, these cytoskeletal changes could be indicative of microtubule breakage (*Figure 33*). Other papers have also demonstrated cytoskeleton breakage on exposure to mechanical strain; actin filaments break when exposed to between 30-100% strain, depending on which other cytoskeleton elements they are crosslinked with (Gardel *et al.*, 2008), and a neural model showed microtubule breakage at strains as low as 16% (Wu and Adnan, 2018). It is important to remember that hBMCs exposed to 72 hours of tensile strain also had decreased expression of *RUNX2* and autophagy genes *LC3* and *ATG5*; if resources had allowed, an exploration of whether the cytoskeleton breakage was linked to the reduction in osteogenesis and autophagy gene expression would have been carried out.

Immunofluorescence of the rat tooth movement samples demonstrated a decrease in tubulin staining in the PDL at 1 hour after the onset of strain, which was then increased from 3 hours to 7 days back to basal levels, compared to the 0 hour control (*Figure 19*). The *in vitro* stretching model demonstrated a decrease in tubulin staining in the 72 hour stretched sample compared to the 72 hour control, or either of the 6 hour samples (*Figure 33A*). Therefore, while the time-points that these changes occur to do not corroborate between the *in vitro* and *in vivo* data, there is a general staining pattern of a decrease in tubulin staining after the cells are exposed to tensile strain. There are many reasons why the time-points that these staining patterns are seen do not align, not least of which because the cells *in vivo* are in a specific niche environment that cannot be recapitulated in an *in vitro* system. While the *in vivo* results do not themselves prove that cytoskeletal breakage is occurring in the PDL on exposure to tensile strain, it corroborates the staining pattern seen in the *in vitro* data.

Strain-induced breakage of the cytoskeleton network, both within microtubules and between its connections to focal adhesions and integrins, has been linked to remodelling of the cytoskeleton for increased efficiency of mechanotransduction (Martino *et al.*, 2018). However, the reorganisation of the cytoskeleton is also a key event in apoptosis (Kulms *et al.*, 2002; Povea-Cabello *et al.*, 2017). Stabilisation of the cytoskeleton was found to protect against apoptosis when cells were exposed to stressors such as ischemia or mechanical strain (Gefen and Weihs, 2016). Therefore, this could be an avenue to explore in investigating whether cytoskeleton breakage in this system limits osteogenic differentiation of hBMCs. Additionally, it would have been interesting to see if altering autophagy levels in these cells prior to exposure to mechanical force could protect against cytoskeleton breakage, as autophagy activation is protective in many other cell stress scenarios (Heymann, 2006; An *et al.*, 2016). The hypothesis resulting from this thesis is therefore that strain modulates autophagy in PDL cells which may have a protective function on cytoskeleton breakage. Strain-induced autophagy also contributes to osteogenic differentiation of hBMCs by upregulating expression of the RUNX2 transcription factor.

5.2.5 Future Work

The results presented here require further investigation in order to establish the exact mechanisms involved, some examples of which have been previously discussed in this chapter.

Analysis of these samples using further markers of osteogenesis, such as Osterix, BMPs and DLx5 would give further proof of osteogenic differentiation, as would Alizarin Red staining to determine the presence of functional osteoblasts capable of mineralising osteoid.

It would have been interesting to investigate the effects of autophagy modulation over a longer time-point than 72 hours, however the constraints of the *in vitro* cell stretching system meant that experiments over this time-point were not productive due to cell detachment. Therefore, investigating autophagy modulation in the rat tooth movement model would be an important alternative future experiment. One option for this would be injecting rapamycin directly into the periodontal ligament prior to fitting the orthodontic device and moving the tooth. Not only

would this allow for longer time-points for analysis but it could also corroborate the *in vitro* results *in vivo*. This experiment is currently underway by the collaborators of this work under Professor Kai Yang.

Another point to be further examined would be an investigation into the initial downregulation of RUNX2 observed in samples exposed to mechanical strain. This was seen in the rat tooth movement samples, and with the *in vitro* stretching experiments using hBMCs (Figures 18 & 32). This decrease in RUNX2 expression was accompanied by an upregulation in genes and proteins involved in the autophagy pathway, however whether RUNX2 was degraded by autophagy is unknown. Autophagosomes could be isolated and a western blot carried out for RUNX2 in order to prove that RUNX2 was captured in the autophagosome (Chen *et al.*, 2014; Takahashi *et al.*, 2017). An issue with using this method in our model is that a high cell number would be required to isolate enough autophagosomes for analysis, and our *in vitro* cell stretching model does not produce enough samples. The literature also suggests that tracking autophagic flux, that being the degradation of autophagosomes, is a better measure of the levels of autophagy active in a cell (Mizushima, Yoshimori and Levine, 2010; Mauthe *et al.*, 2018). Therefore, an alternative experiment would be to carry out immunofluorescence showing co-localisation of RUNX2 with proteins involved in the autophagosome and autolysosome, for example LC3 and LAMP1. This experiment could also be carried out using both the *in vivo* and *in vitro* models used in this chapter.

Relating the *in vitro* findings to the *in vivo* scenario are crucial in providing translational research. While human samples would be preferred, the chances of obtaining human periodontal samples during tooth movement are very slim, and animal models are well-established in the literature, such as the rat experiment discussed earlier in this chapter. Repeating the rat tooth movement experiment with the addition of a drug treatment to induce autophagy would determine whether inhibiting autophagy could increase the speed or efficiency of osteogenesis during tooth movement. Drugs that activate autophagy include temsirolimus, resveratrol and

spermidine (Park *et al.*, 2016; Kania *et al.*, 2017; Madeo *et al.*, 2019), however rapamycin, the drug used in this work, has also been established for use *in vivo* (Galluzzi *et al.*, 2017). Micro-CT scanning of the periodontium throughout the period of tooth movement would provide real-time results on alveolar bone remodelling, including that of the movement of the tooth, the formation of new bone and the thickness of the new bone formed. Samples could then be obtained for H&E staining in order to analyse differences in overall morphology of the tissue, and immunofluorescence imaging for markers of osteogenesis, autophagy and tissue health, such as the production of ROS or periostin, a marker of PDL health (Rios *et al.*, 2008; Schieber and Chandel, 2014; Du and Li, 2017). Additionally, immunofluorescence staining of these samples for cytoskeleton markers such as α -tubulin and processing these images in Imaris could provide information on the role of autophagy in this scenario and to determine whether cytoskeleton breakage is occurring during strain-related bone remodelling.

Finally, a key thing to remember is that enhancing osteogenesis in this system may not translate to a treatment that enhances tooth movement alone, as both the formation and resorption of bone is required for bone remodelling. As mentioned previously, compression is known to stimulate osteoclastogenesis however how this may be linked to autophagy or affect cytoskeleton breakage is unknown. *In vitro* analysis would be challenging due to the drawbacks in compression strain devices available, however this could be achieved *in vivo* by analysing the compressed side of the periodontium in tooth movement samples.

5.3 The Association of Autophagy with Osteoclastogenesis in the Context of Periodontitis

5.3.1 Characterising hBMCs as cells capable of Osteoclast Differentiation

Primary hBMCs were used for the osteoclast differentiation as they contained several different cell types including osteoclast precursor cells. These cells were physiologically relevant to the study of LPS tolerance and osteoclast differentiation in relation to human periodontal disease. As described above, the cells were first cultured overnight in standard media, in which time some of the cells would adhere to the bottom of the plate while others would remain free-floating.

Optimisation of the osteoclast differentiation protocol involved varying several factors, including the density of osteoclast precursors. Many papers suggested seeding osteoclast precursors at a high density however since osteoclast precursors only make up a portion of hBMCs, the precursors were isolated using MACS prior to seeding. CD14 is a marker of HSCs and their progenitors, therefore CD14-conjugated beads were used with MACS to isolate these cells from those of other lineages (Sørensen *et al.*, 2007; Hackett, Flaminio and Fortier, 2011; Quan *et al.*, 2018).

CD14-positive cells accounted for an average of 29% of non-adherent hBMCs (*Figure 36B*). In searching the literature, it is unclear the proportion of CD14-positive cells that would be expected to be present in the bone marrow. The majority of papers discuss the fractions of CD14-positive cells in peripheral blood, perhaps partly due to the relative ease of obtaining blood samples compared to bone marrow (Schlegel *et al.*, 2000; Sørensen *et al.*, 2007; Cafiero *et al.*, 2018). Additionally, removal of cells from their natural environment and the processing they underwent, although minimal, will have altered the cell proportions slightly from cells *in vivo*. One paper found 17.6% of bone marrow cells were CD14-positive, however this was within a CD45-positive cell fraction so may not be representative of whole aspirates (Mandl *et al.*, 2014).

Another paper found 15% of equine bone marrow cells were positive for CD14, however it is unclear how this may relate to human bone marrow (Hackett, Flaminio and Fortier, 2011).

Immediately after isolation, CD14-positive cells were seeded at a density of 5×10^5 /ml (Tevlin *et al.*, 2014; Motiur Rahman *et al.*, 2015) and treated with M-CSF. Another key factor that was considered in optimising the osteoclast differentiation protocol was the concentrations of the key stimulating proteins, M-CSF and RANKL, and the timing that these proteins are administered. M-CSF is involved in the initial differentiation of osteoclast precursors, while RANKL is involved in late stage osteoclast differentiation, therefore it was more efficient to treat cells with M-CSF alone for 5 days, followed by the addition of RANKL for 5 days (Wani *et al.*, 1999). Accepted concentrations ranged from 12-50ng/ml for M-CSF and 10-120ng/ml for RANKL, however some papers suggested a higher concentration of RANKL than M-CSF for a higher yield of osteoclasts, therefore 25ng/ml M-CSF and 100ng/ml RANKL were used (Wani *et al.*, 1999; Cody *et al.*, 2011; Marino *et al.*, 2014; Motiur Rahman *et al.*, 2015).

Using this protocol, hBMC morphology changed from small, non-adherent cells when first plated, to adherent cells after CD14 MACS and the start of M-CSF treatment. After 5 days of M-CSF treatment, there were a few distinct morphologies; some slightly longer cells were observed alongside aggregates of mid-sized round cells, and small, round cells. After a further 5 days of M-CSF and RANKL treatment, many large, multinucleated cells could be seen, some with the ruffled-border morphology that is characteristic of osteoclasts (*Figure 36C*).

Osteoclasts highly express the TRAP enzyme, therefore TRAP staining was used to identify osteoclasts as cells that were TRAP-stained and multinucleated, containing 3 or more nuclei, according to the literature (Arai *et al.*, 1999; Tevlin *et al.*, 2014). The percentage of osteoclast-like cells was determined from the total cell number in order to normalise osteoclast count against the total cell number. CD14-positive cells that had been treated with M-CSF and RANKL contained a higher percentage of osteoclasts compared to controls which were CD14-positive but not treated. Additionally, cells that were CD14-negative did not contain any osteoclasts

when treated with M-CSF and RANKL (*Figure 36C-D*). These results suggested that hBMCs contained a population of cells that could differentiate into osteoclast-like cells. Other osteoclast markers such as OSCAR or Calcitonin were not analysed, neither was the functionality of these cells, for instance by looking at their ability to resorb bone or dentine. This would have provided more concrete evidence, however the presence of TRAP-positive multinucleated cells is often used in the literature to determine the presence of osteoclast-like cells, and was therefore sufficient for the purpose of determining the hBMCs and the osteoclast differentiation protocol were appropriate for this work.

5.3.2 Determining the effects of LPS on Osteoclast Differentiation

On considering the effect of LPS tolerance on osteoclast differentiation, there were broadly two avenues that could have been pursued: firstly, that LPS tolerance affected osteoclast precursors themselves, and secondly in LPS tolerance affecting other cells that would then cross-talk with osteoclast precursors. In the context of periodontal disease, either scenario could have been relevant as *P.gingivalis* has been shown to activate monocytes which then circulate in the bloodstream to cause chronic inflammation systemically (Hayashi *et al.*, 2010).

However, the hBMCs used as the osteoclast precursors were found not to differentiate into osteoclasts after LPS treatment (*Figure 37*), most likely because LPS encourages HSC and monocyte differentiation to M1 inflammatory macrophages (Martinez and Gordon, 2014; Murray *et al.*, 2014). This is corroborated in the literature which states that M1 macrophages cannot typically differentiate into osteoclasts (Jeganathan *et al.*, 2014); one paper showed osteoclasts formed after M1 macrophages were treated with RANKL, however these were deemed to be a population of M1 macrophages distinct from those classically induced by LPS and IFN γ (Huang *et al.*, 2017).

Therefore, the latter scenario was explored in the context of this thesis, considering whether LPS tolerance affects cells surrounding osteoclast precursors. THP1 cells were used to represent the peripheral monocytes that would likely come into contact with LPS and circulate to cause

systemic inflammation. THP1s are a pre-monocyte human cell line from a leukaemia patient, and have been established to be tolerised to LPS treatment in the literature (Xiong *et al.*, 2011). While THP1 cells have been shown to be able to differentiate into osteoclasts, this is an arduous process with many additional steps and factors involved than is the case with primary bone marrow cells; one paper demonstrated osteoclast differentiation from THP1s after treatment with high concentrations of PMA (100ng/ml) alongside M-CSF and RANKL treatment. Our LPS tolerance protocol included 24 hour PMA treatment prior to treatment with M-CSF and RANKL, to stimulate the pre-monocytes to differentiate into macrophages. However, the paper describing osteoclast differentiation from THP1s found that simply treating with PMA for 48 hours prior to M-CSF and RANKL did not yield osteoclasts from THP1 cells, and that PMA was required throughout to ensure osteoclast formation (Li *et al.*, 2017). Additionally, the majority of THP1 cells that were treated with the osteoclast differentiation protocol did not attach to the plate surface and no osteoclast-like cells were observed via TRAP staining (*Figure 48*). Therefore, THP1 cells were unable to differentiate into osteoclasts using our osteoclast differentiation protocol, and were an appropriate cell choice for determining the effects of LPS tolerance in this model.

5.3.3 LPS Tolerance

LPS tolerance is achieved by multiple exposures of the cell to LPS, and has been related to chronic inflammation in the literature (Muthukuru, Jotwani and Cutler, 2005; Collins and Carmody, 2015). LPS tolerance was first thought to be a beneficial adaptive response, however it may also be the result of a dysregulated immune system (Biswas and Lopez-Collazo, 2009). It was hypothesised that LPS tolerance could play a role in osteoclast differentiation in relation to the severity of periodontal disease.

Models of LPS tolerance broadly follow three main avenues in the literature; *in vivo* studies where animal models are given subsequent injections of LPS, *in vitro* work where cells are treated with LPS and washed before further treatments, and studies where cells are extracted

from patients with various inflammatory conditions and LPS challenge is carried out *ex vivo* (Cavaillon and Adib-Conquy, 2006; López-Collazo, Fresno and del Fresno, 2013). While the *in vivo* work was essential in the discovery of tolerance and the initial experiments in this field, it is not as desirable today due to monetary factors and in attempts to comply with the 3Rs of animal research (Bayne *et al.*, 2015; Sneddon, Halsey and Bury, 2017). In addition, the injection of LPS or its derivatives directly into the animal produces a sudden systemic infection which is not representative of the majority of infections that would ultimately lead to tolerance (Munford, 2010). Therefore, for this work, *in vitro* studies were sufficient for the study of LPS tolerance, and also allowed for the investigation of cross-talk between THP1 cells that had been exposed to LPS multiple times (2x) and osteoclast precursors.

The LPS tolerance protocol used in this thesis was based on several in the literature that involve LPS exposure, washing, followed by a rest period, then re-exposure to LPS. The periods of LPS exposure ranged from 1-24 hours, however many papers demonstrated successful cytokine upregulation after 4 hours, and the intervals between the first and second exposures ranged from 24 hours to 5 days (Sly *et al.*, 2004; Koons *et al.*, 2008; West and Koons, 2008; López-Collazo, Fresno and del Fresno, 2013; Xu *et al.*, 2018). In our protocol, THP1 cells were first treated with PMA for 24 hours to stimulate differentiation to macrophages and prime them for LPS treatment (Park *et al.*, 2007; Lund *et al.*, 2016). This can be measured by an upregulation in the production of TNF α , an early marker of inflammation, which was observed in this model with PMA-treated THP1 cells compared to un-treated controls (*Figure 38B*). Cells then had their media changed and were placed in fresh media without PMA to rest for 24 hours before LPS treatment. To tolerate cells, LPS treatment was given for 4 hours before cells were washed and placed in fresh media for 24 hours. The second LPS treatment was then given for 4 hours before cells were washed again and placed in fresh media. 1x cells were only given LPS at the second treatment stage, while control cells were simply given culture media throughout (*Figure 38A*).

The LPS tolerance protocol was tested using both *E.coli* and *P.gingivalis* LPS. *E.coli* LPS is well established for use in endotoxin tolerance work, and as such is often used as a positive control when testing LPS tolerance with other strains. It is also clinically relevant to sepsis, pneumonia, meningitis and urinary tract infections. While these may not seem relevant to bone biology, osteoclast differentiation is known to be affected by inflammation, and many of these conditions cause inflammation which is not localised to the infection site (Cafiero *et al.*, 2018; Souza and Lerner, 2019). *P.gingivalis* LPS is significant in terms of periodontal disease as it is the bacteria most implicated in periodontitis. Therefore, *P.gingivalis* was of interest to the initial aims of this thesis and the experiments using this LPS provided some preliminary results. However, variability in the results obtained through repeat experiments mean that extensive work would be required to establish their reliability. It was determined that uncovering the mechanisms at play in this model was more important and a better use of the time that was available, hence *E.coli* LPS was used as the focus for the LPS tolerance work.

5.3.3.1 *E.coli* LPS Tolerance of Inflammatory Pre-Monocytes

Tolerance can be identified by a reduction in cytokine expression compared to that of 1x cells that have only been exposed to LPS once (Raetz *et al.*, 1991; Medvedev, Kopydlowski and Vogel, 2000). THP1s exposed to the tolerance protocol with *E.coli* LPS had a reduction in *IL1 β* , *IL6* and *TNF α* gene expression at 4 hours and 24 hours after the second LPS treatment, compared to 1x cells. *TNF α* protein expression was decreased in 2x cells compared to 1x cells at 24 hours.

1x cells had an increase in all inflammatory cytokine gene expression compared to the untreated controls, at 4 and 24 hours-post LPS treatment. There was also an increase of *IL1 β* , *IL6* and *IL8* expression at 72 hours, and *TNF α* protein was highly expressed at 24 and 72 hours (Figure 39). This demonstrates that the LPS treatment had the expected results of stimulating an inflammatory response in the 1x cell population.

Overall, these indicated that THP1 cells could be tolerised to *E.coli* LPS at 24 hours after the second LPS treatment, at both RNA and protein levels.

5.3.3.2 Investigating *E.coli* LPS Tolerance and the expression of Hyaluronan Synthases

HA signalling was considered as a mechanism at play in this model due to several papers in the literature linking HA signalling to both LPS tolerance regulation and osteoclast differentiation.

THP1s that had undergone the LPS tolerance protocol were analysed for their expression of HAS genes. *HAS3* gene expression was found to be upregulated at 4 and 24 hours after the second LPS treatment (*Figure 40A*). However, immunofluorescence showed *HAS3* protein was decreased in 2x cells, while it was upregulated in 1x cells (*Figure 40B*). *HAS3* is the enzyme linked to the production of LMW HA. Although there is more research published concerning HMW HA and its effect on osteoclasts, LMW HA is associated with inflammation and is thought of as more pathogenic, so may be more relevant to the situation seen in diseases of chronic inflammation such as periodontitis. In fact, a paper that was published after the conclusion of this work put forward the theory that the destruction of the periodontium as seen in periodontitis results in fragmentation of HA in the ECM resulting in higher levels of LMW HA (Monasterio *et al.*, 2019). This provides a credible reason as to why levels of LMW HA may be increased in diseases of chronic inflammation, however this thesis has also shown that cells exposed to LPS once (the 1x population) have increased expression of *HAS3*, the enzyme that produces LMW HA.

The discrepancy between *HAS3* RNA and protein expression in the 2x cells could have been due to microRNAs or ubiquitination, as *HAS2* has been demonstrated to undergo ubiquitination (Karousou *et al.*, 2010). However, with the time points used in this experiment being 4 and 24 hours, the speed at which the reduction of *HAS3* protein expression occurred led to the consideration of autophagy as a potential mechanism.

5.3.3.3 Investigating *E.coli* LPS Tolerance and Autophagy Expression

Autophagy has been demonstrated to rapidly tag, capture and degrade proteins, and has been found to regulate many molecular processes. Additionally, while HA is usually produced extracellularly, due to the positioning of the HAS enzymes in the plasma membrane, *HAS3* localisation to the plasma membrane is inhibited in times of glucose deprivation, a condition

which is also associated with autophagy activation (Tammi *et al.*, 2011). Activation of autophagy has also been shown after intracellular synthesis of HA (A. Wang *et al.*, 2011; Wang *et al.*, 2014). Autophagy has also been linked to intracellular synthesis of AMPK, which regulates the autophagy pathway by inhibiting mTOR, and has also been linked to the regulation of HAS2 expression (Vigetti *et al.*, 2011; Vigetti, Viola, *et al.*, 2014). Therefore, a link between HA production and autophagy has already been established, if not fully explored. Autophagy levels have also been shown to be higher in periodontitis patients, the PDL of which had increased expression of LC3, p62 and Beclin compared to the PDL of those without the disease (An *et al.*, 2016).

Therefore, THP1 cells that had undergone the LPS tolerance protocol were analysed for their expression of key autophagy genes including p62, ATG5 and LC3 (*Figure 41*). A major protein involved in the tagging of molecules for capture by autophagosomes, p62, was upregulated at 4 hours post-second LPS treatment in 2x cells. Conversely, p62 was downregulated at 24 hours in 1x cells. ATG5 and LC3, keys to the formation of the autophagosome, were upregulated in 2x cells at 4 and 24 hours, compared to controls (*Figure 41*). These results would suggest that the autophagy pathway was active in 2x cells at 4 and 24 hours, which coincides with the upregulation of HAS3 and the tolerance effect on cytokine expression (*Figures 39-41*). Expression of LC3 and LAMP1 proteins were increased in 2x THP1s compared to 1x or control cells, and these markers seemed to be co-localised, which would be expected in the formation of autolysosomes. Additionally, LC3 puncta staining was increased in 2x cells, suggesting increased formation of autophagosomes and autophagy activation (*Figure 41B,42B*).

If time and resources had allowed, it would have been interesting to carry out *ex vivo* work on monocytes and peripheral macrophages isolated from patients with periodontitis, to investigate whether they exhibited tolerance when exposed to LPS challenge, and whether they had similar patterns of HAS and autophagy marker expression, as was seen in the THP1 cells. However, as the data stands it indicates that there is a link between autophagy and the tolerance condition

of pre-monocytes which coincides with the upregulation of HAS3 gene, but not protein, expression.

Overall, it was determined that THP1 cells that had multiple exposures to *E.coli* LPS exhibited tolerance 24 hours after the second exposure, along with an increase in *HAS3* gene but not protein expression and an activated autophagy pathway.

5.3.3.4 *P.gingivalis* LPS Tolerance of Inflammatory Pre-Monocytes

THP1s were treated with the same LPS tolerance protocol as before but using *P.gingivalis* LPS, due to this strain's clinical relevance to periodontitis. Within the body of work undertaken for this thesis, the response of cells to *P.gingivalis* LPS varied greatly. The results were therefore not reproducible, however these experiments are still worth discussing with an understanding of their limitations.

The 1x cells did not show the expected inflammatory cytokine expression after exposure to the LPS (*Figure 43*). Several papers demonstrate a weaker inflammatory response to *P.gingivalis* LPS compared to that of other bacterial strains, however these papers do demonstrate upregulated expression of IL1 β , IL6, IL8 and TNF α , while our results only showed increased *IL1 β* , *IL8*, and *TNF α* expression in 1x cells at 4 hours (Zaric *et al.*, 2010; Holden *et al.*, 2014). Therefore, based on the literature we would expect that THP1 cells exposed to *P.gingivalis* LPS once would also have upregulation of *IL6*, and that inflammatory cytokine gene expression would be increased at 24 hours. An interesting point to consider here is in the ability of the inflammatory response to cause osteoclast differentiation; inflammation is a known stimulant to osteoclast differentiation, however some papers have recently shown that the combination of IL6 and TNF α successfully stimulates osteoclasts to differentiate, while treatment with TNF α alone is insufficient (Novack, 2016; O'Brien *et al.*, 2017). The results shown in this work demonstrate an upregulation of *TNF α* but not *IL6* by *P.gingivalis* exposure (*Figure 43*). In the context of the aforementioned paper, this could indicate that the inflammatory response produced by *P.gingivalis* exposure would not be sufficient to stimulate osteoclast differentiation.

Based on the TNF α gene and protein expression, it could be interpreted that tolerance to *P.gingivalis* LPS was observed at 9 days in our model (Figure 43). However, all other inflammatory cytokines either showed increased expression in 2x cells compared to 1x cells, or there was no inflammatory response in 1x cells at all. Tolerance has been observed with *P.gingivalis* LPS in other models, which also found that TNF α and IL1 β were downregulated in 2x cells while IL8 expression was not affected (Zaric *et al.*, 2010; Lu *et al.*, 2018). This could indicate that tolerance with *P.gingivalis* LPS does not follow the same patterns as that with *E.coli* LPS, supporting our results indicating tolerance at 9 days based on TNF α expression. However, this experiment was attempted several times and no repeat demonstrated consistent tolerance across several inflammatory cytokines. Therefore, while TNF α seemed to show tolerance at 9 days, this would need to be verified more robustly in order to be deemed a reliable result. Repeating this experiment with purified *P.gingivalis* LPS rather than the synthetic LPS used in this thesis may have been worth exploring to try and overcome the issues in batch variability and more robustly validate the data.

While the study of *P.gingivalis* LPS within this work was preferred, the issues with batch variance and unreliable activation of the expected inflammatory response was a limit to the work. Nevertheless, it was decided that it was worth investigating whether the THP1 cells that had shown some tolerance effect to *P.gingivalis* LPS had the same downstream effects on HAS and autophagy gene expression as seen in the *E.coli* model.

5.3.3.5 Investigating *P.gingivalis* LPS Tolerance and the expression of Autophagy and Hyaluronan Synthases

THP1 cells that had undergone the tolerance protocol with *P.gingivalis* LPS were also analysed for their expression of *HAS3* and autophagy-related genes (Figure 44A-B). *HAS3* expression was upregulated at 4 hours in 2x cells, but there was little change at 9 days which is the time point most relevant to *P.gingivalis* LPS tolerance based on the previous figure (Figure 43). In contrast to the *E.coli* results, 1x cells did not have upregulated *HAS3* expression at 24 hours. High

magnification staining demonstrated an increase in HAS3 expression in 1x cells but a reduction of HAS3 in 2x cells at 4 hours after the second LPS treatment (*Figure 44C*). Therefore, the results obtained for 2x cells show an increase in *HAS3* gene expression but a decrease in HAS3 protein, the same pattern of expression as was seen in samples treated with *E.coli* LPS. However, 1x cells show a decrease in *HAS3* gene expression but an increase in HAS3 protein at 4 hours compared to controls, which is dissimilar to the results observed with *E.coli* LPS treatment.

LC3 and *ATG5* gene expression were increased, LC3 puncta staining was upregulated and puncta were larger in 2x cells than in control and 1x cells at 4 hours (*Figure 44B-C*). These results are similar to what was seen in the samples treated with *E.coli* LPS. Autophagy gene expression was also measured at 24 and 72 hour samples, however the Q-PCR results provided no Ct values for these samples. This could be because expression levels were so low that they were indistinguishable to the background noise and therefore could not be measured before the end of the last cycle of the PCR. Alternatively, the cell number could have been too low in these samples in order to achieve a signal for measurement. As mentioned previously, this *P.gingivalis* LPS tolerance experiment was repeated several times however an inflammatory response in the 1x population was not always seen, therefore the number of samples able to be used for further analysis was limited. Some papers in the literature have also mentioned variability in results using synthetic *P.gingivalis* LPS even within the same batch (Kumada *et al.*, 2008; Liu *et al.*, 2008).

This is clearly an issue for this work, and therefore while the experiments using *P.gingivalis* LPS for tolerance supplied some preliminary data, further study would be required to verify these results and overcome the issues with result variability and reliability. For this reason it was decided that the focus for the subsequent experiments would be on the more reliable *E.coli* LPS to attempt to establish the mechanism at work.

5.3.4 Determining the effect of Hyaluronan on the Differentiation of Osteoclast Precursors

In order to investigate the effect HA may have on osteoclast differentiation, hBMCs were treated with either low (LMW) or high molecular weight (HMW) HA alongside the osteoclast differentiation protocol. HA was added at an 'early' stage, at the time M-CSF was added, or at a 'late' stage, when RANKL was added alongside M-CSF treatment.

In general, HA treatment alongside the osteoclast differentiation protocol resulted in more osteoclasts than the osteoclast differentiation protocol alone, regardless of the molecular weight used (*Figure 45*). In the literature there has been some investigation into the effects of HMW HA on osteoclasts, with this either being thought of as inhibitory to their differentiation or having no effect on osteoclast differentiation at all (Ariyoshi *et al.*, 2005; Chang *et al.*, 2007). This was not what was observed in our experiment, as even HMW HA treatment enhanced osteoclast differentiation compared to controls (*Figure 45*). In our system however treatment with LMW HA at the early differentiation stage had the most profound effect on the number of osteoclasts observed. This condition produced the highest number of osteoclasts, and also seemed to produce osteoclasts that were larger. Osteoclasts' resorptive activity is correlated to cell size and multinucleation, therefore these results may represent a highly resorptive state (Piper, Boyde and Jones, 1992; Boissy *et al.*, 2002). One option for confirming that the osteoclasts being produced were active would have been to culture these cells on a slice of dentine and measure the resorptive pit formed (Rumpler *et al.*, 2013); without this data we are unable to confirm whether the osteoclasts produced with LMW HA treatment were more active than with other conditions, however the presence of more osteoclasts is still a significant observation. Additionally, this result was particularly significant as LMW HA is produced by HAS3, which was the enzyme that had altered expression in the LPS tolerance condition.

Ultimately, this experiment led to the hypothesis that LMW HA could have a role in enhancing osteoclast differentiation, which corroborates the results of a paper demonstrating increased functionality of osteoclasts formed with LMW HA treatment (Ariyoshi *et al.*, 2005).

5.3.5 Determining the effects of LPS and Hyaluronan treatment on the Differentiation of Osteoclast Precursors

In order to determine whether LPS tolerance was affecting osteoclast precursors directly, or other cells that may interact with osteoclast precursors, it was decided to investigate the effects of LPS treatment on the success of the osteoclast differentiation of hBMCs. As discussed previously, hBMCs were not suitable for tolerance to LPS, therefore repeated exposure was used in order to mimic chronic inflammation, as would be seen in periodontitis.

hBMCs that were treated with LPS alongside the osteoclast differentiation protocol had a decrease in the number of osteoclasts observed compared to controls (*Figure 46*). Instead, the majority of cells were small, round cells or long and spindly, similar to the morphology of M1 macrophages (Zajac *et al.*, 2013; Zhang *et al.*, 2015). While some papers state that osteoclast differentiation shouldn't be inhibited by LPS treatment, the literature generally demonstrates that hBMCs do not differentiate into osteoclasts immediately after LPS exposure (Hayashi *et al.*, 2003), therefore these results fit with the current understanding. There was also a decrease in the number of osteoclasts produced from hBMCs that were treated with HA and LPS, alongside the osteoclast differentiation protocol (*Figure 46A*). While LMW HA and LPS treatment produced more osteoclasts than HMW HA and LPS treatment or LPS alone, it was still significantly less than the number of osteoclasts produced in the control condition. These results indicated to us that LPS exposure was unlikely to be directly causing the osteoclast precursors to differentiate, therefore we investigated the potential of cross-talk between cells of the inflammatory monocyte/macrophage lineage and osteoclast precursors.

5.3.6 Co-culturing Inflammatory Monocytes and Osteoclast Precursors

In order to investigate the hypothesis of cross-talk between inflammatory monocytes and osteoclast precursors, hBMCs undergoing the osteoclast differentiation protocol were co-cultured with THP1 cells that had undergone the LPS tolerance protocol (*Figure 47A*). The timings for the co-culture were carefully considered; at the time of co-culture 2x THP1 cells had been exposed to the second *E.coli* LPS treatment for 24 hours as this was the timepoint where tolerance was established in this model (*Figure 39*). Whereas the hBMCs were at the 'early' differentiation stage at the time of co-culture, that being when cells were first treated with M-CSF as previous experiments showed that intervention with HA at this timepoint had the most profound effect on osteoclasts number (*Figure 45*).

Overall, the conditions where hBMCs were co-cultured with control or 1x THP1 cells had an increased number of osteoclasts compared to the hBMC-alone control. The co-culture of hBMCs and 2x THP1s produced a slight increase in the number of osteoclasts produced compared to the hBMC control, however this was a marked decrease on the number produced from the co-culture of hBMCs with control or 1x THP1 cells. The same number of hBMC cells were used in each condition, as it had already been established that THP1 cells could not differentiate into osteoclasts using our osteoclast differentiation protocol (*Figure 48*). Therefore, any changes in osteoclast number in the co-culture conditions was not explained by a change in the starting cell number of osteoclast precursors. Therefore, the addition of THP1 cells increased hBMC differentiation to osteoclasts, however this effect was reduced when the THP1 cells were tolerised to *E.coli* LPS (the 2x THP1s; *Figure 47*). Overall, this experiment corroborated and linked the results of the previous figures showing that LPS tolerance of inflammatory monocytes decreases their HAS3 protein expression and treatment with LMW HA, the product of HAS3, increased osteoclast differentiation of precursor cells. While this experiment alone is not conclusive proof that a cross-talk mechanism is at play between inflammatory monocytes and osteoclast precursors in an LPS tolerance scenario, it provides a sound argument for consideration.

In contemplating the clinical situation, the hypothesis resulting from this thesis is that LPS tolerance of inflammatory monocytes, which can be the result of chronic inflammation, activates the autophagy pathway which targets and degrades HAS3 protein. This results in a net decrease in the amount of LMW HA produced into the ECM, negating the stimulus of LPS-induced HA production on osteoclast differentiation. This may infer that autophagy levels and HA signalling are important factors determining bone loss in periodontal disease, and should be investigated further *in vivo*.

5.3.7 Future Work

The results from this work produced many questions that would require answers in order to fully understand the mechanisms at play. Some of these would involve repeating experiments or further optimising protocols, as discussed in previous sections. Additionally, the concepts and theories put forward in this work would require verification by other means, whether that be using different methods of analysis or *in vivo* studies.

For example, one experiment that was attempted was to isolate the plasma membrane of THP1 cells that had undergone the LPS tolerance protocol, in order to confirm the absence of HAS3 protein. Two methods were trialled to isolate the plasma membrane; one was a plasma membrane isolation kit, and the other was a centrifugation-based method. The first method seemed to produce an acceptable concentration of protein according to BCA measurement, however western blotting revealed no bands for these samples unlike a total protein control, even with a ponceau stain. The centrifugation method was a lot more energy-intensive, however the protein concentration produced at the end was insufficient for further study. This may have been the result of sample being lost in each centrifugation step as the solutions were transferred to different tubes. Increasing the starting material was trialled, however this made minimal difference. If time and resources had allowed, further optimisation of these methods may have been successful and provided more quantitative proof that HAS3 protein was not present in the plasma membrane in 2x THP1s. Instead, this thesis had to rely on immunofluorescence images

to display the presence of HAS3 protein on the plasma membrane of control and 1x cells, and its absence in 2x cells. Immunofluorescence also provides data on the co-localisation of different markers, although this data is also not quantitative.

Another future experiment that would further elucidate the mechanisms used in this system would be to investigate the receptor being activated by LMW HA on the osteoclast precursors. There are many receptors for HA, however the best known and most investigated are CD44 and TLR4. Interestingly, another paper showed HA treatment protected against LPS-induced injury by acting through TLR4 (Xu *et al.*, 2015), however this may be due to HA competing with LPS to bind to TLR4 resulting in less LPS binding and therefore a decreased downstream inflammatory response. It is unclear whether this is the mechanism seen in our model, as LPS treatment was found to reduce osteoclast differentiation. Regardless, it was decided to first test whether TLR4 was the receptor activated by LMW HA. This was initially trialled using an antibody to inhibit TLR4 and block its activation on hBMCs. The competency of the method was tested by treating cells with LPS and measuring TNF α secretion, as there would be no change if the antibody had successfully blocked the TLR4 receptor (Pérez-Figueroa *et al.*, 2016). Cells treated with IgG2a blocking and anti-TLR4 were found to have little to no change in TNF α secretion 24 hours after LPS treatment, unlike the increase in TNF α seen in controls. The half-life of the antibody was unknown therefore cell secretions were also analysed 5 days after LPS treatment; however, these samples did have an increase in TNF α secretion therefore the TLR4 neutralisation was not prolonged to 5 days. This method was used to neutralise TLR4 in hBMCs 24 hours prior to treatment with HA and the osteoclast differentiation protocol. The neutralisation was then repeated 24 hours prior to every treatment with M-CSF and RANKL and/or HA. The samples treated with LMW HA after TLR4 blocking did have a reduction in the number of osteoclasts produced, however the results from this experiment were highly variable with large standard deviations. Not only that, but the samples treated with IgG and anti-TLR4 but no HA also had a decrease in the number of osteoclasts produced compared to controls, therefore this decrease may be related to the anti-TLR4 treatment itself rather than the blocking of the receptor.

Because of this, no real conclusions could be made from these results. One option for optimising this method would be to increase the antibody concentration or alter the blocking solution used. Other papers describe internalisation of antibodies which may have been a factor in the outcome of this experiment (Stefansson *et al.*, 1995). A simpler method of neutralising TLR4 would be to use antagonists such as LPS-RS, which blocks the binding domain of the receptor, or TAK-242 which inhibits the binding of TIRAP and TRAM on the intracellular domain of TLR4 (Matsunaga *et al.*, 2011; Abdelmageed *et al.*, 2016). Alternatively, siRNAs specific to TLR4 or CD44 mRNA sequences could be used to prevent protein production, although this would not prevent the activation of receptors already at the cell membrane (Xu *et al.*, 2007). Ultimately, it would also have been interesting to inhibit TLR4 on hBMCs directly before co-culture with 2x THP1s, to see if the effects seen in the co-culture experiment could be negated. This would provide further proof of the receptor activated by LMW HA in this mechanism.

Finally, there are many potential experiments that would allow for the translation of this work to a clinical scenario. In this model, THP1 cells were used to represent peripheral monocytes not only for ease of use, as these cells grow more rapidly and survive for more passages than bone marrow-derived monocytes in culture, but also because they are well established in inflammation and LPS tolerance research. However, THP1 cells are a cell line derived from leukemic monocytes and their malignant nature is not directly comparable to that of normal human monocytes (Chanput, Mes and Wichers, 2014). It would therefore have been interesting to obtain blood samples from patients with different stages of periodontitis and analyse the peripheral monocytes' autophagy levels and expression of HAS3. Challenging these monocytes with LPS *ex vivo* could also allow for the study of tolerance in these samples, and co-culturing these cells with osteoclast precursors could help to verify the results presented in this work.

5.4 Concluding Remarks

Controlled alveolar bone remodelling is key to maintaining the integrity of the periodontium. This thesis explored two disease states where alveolar bone remodelling is altered in order to elucidate the role of autophagy and the molecular mechanisms at play.

In both *in vivo* and *in vitro* models of orthodontic tooth movement, autophagy levels were found to be increased prior to the onset of osteogenesis. Additionally, modulating autophagy prior to the onset of constant tensile strain altered the expression of osteogenesis markers, suggesting that autophagy may have roles in regulating early signals for osteogenic differentiation. Other papers have previously demonstrated that autophagy is activated in cells exposed to mechanical strain, however before this work there was little research investigating the effects of constant tensile strain, which is relevant to the clinical scenario of orthodontic tooth movement. When taking the results demonstrated in this thesis alongside the current understanding in the literature, it would suggest that autophagy activation is an initial response to mechanical strain as a protective mechanism, after which osteogenesis may occur.

Using *in vitro* models of LPS tolerance in order to investigate periodontitis, inflammatory monocytes were found to have increased expression of HAS3, responsible for LMW HA production, in response to a single exposure to *E.coli* LPS which resulted in enhanced differentiation of osteoclast precursors. However, inflammatory monocytes that were tolerised to *E.coli* LPS had a reduction in LMW HA synthesis which was found to reduce differentiation of osteoclast precursors. These tolerised cells also had an upregulation of proteins involved in the autophagy pathway, which is suggested as the potential mechanism of rapid HAS3 removal. The results obtained using this model suggest that LPS tolerance alters the response of cells to inflammatory cues and may begin to explain why some people do not develop periodontal disease with the associated alveolar bone loss.

Autophagy is difficult to target pharmaceutically with minimal risks due to its prevalence in many different tissues and the relative newness of the field. However, there is some evidence to

suggest that drugs that affect the autophagy pathway are tolerable for short-term use. Furthermore, due to the ease of accessing the periodontium, compared to other areas of the body, it is plausible that topical pharmaceutical application of autophagy modulators to the periodontium could be possible. With this in mind, future research into modulating autophagy in this system and its effect on alveolar bone remodelling may result in suitable targets for future therapeutics that could improve clinical outcomes both in orthodontic tooth movement and the treatment of periodontal disease.

6 References

- Abdelmageed, M. E. *et al.* (2016) 'LPS-RS attenuation of lipopolysaccharide-induced acute lung injury involves NF- κ B inhibition', *Canadian Journal of Physiology and Pharmacology*, 94(2), pp. 140–146. doi: 10.1139/cjpp-2015-0219.
- Abrams, M. B. *et al.* (2009) 'Multipotent mesenchymal stromal cells attenuate chronic inflammation and injury-induced sensitivity to mechanical stimuli in experimental spinal cord injury', *Restorative Neurology and Neuroscience*, 27(4), pp. 307–321. doi: 10.3233/RNN-2009-0480.
- Adib-Conquy, M. and Cavaillon, J.-M. (2009) 'Compensatory anti-inflammatory response syndrome.', *Thrombosis and haemostasis*, 101(1), pp. 36–47.
- Ahmed, W. W. *et al.* (2010) 'Myoblast morphology and organization on biochemically micro-patterned hydrogel coatings under cyclic mechanical strain', *Biomaterials*, 31(2), pp. 250–258. doi: 10.1016/j.biomaterials.2009.09.047.
- Akira, S. and Kishimoto, T. (1992) 'IL-6 and NF-IL6 in acute-phase response and viral infection.', *Immunological reviews*, 127, pp. 25–50.
- Akira, S. and Takeda, K. (2004) 'Toll-like receptor signalling', *Nature Reviews Immunology*, 4(7), pp. 499–511. doi: 10.1038/nri1391.
- Al-Qutub, M. N. *et al.* (2006) 'Hemin-Dependent Modulation of the Lipid A Structure of *Porphyromonas gingivalis* Lipopolysaccharide', *Infection and Immunity*, 74(8), pp. 4474–4485. doi: 10.1128/IAI.01924-05.
- Alihemmati, Z. *et al.* (2017) 'Computational simulation of static/cyclic cell stimulations to investigate mechanical modulation of an individual mesenchymal stem cell using confocal microscopy', *Materials Science and Engineering C*, 70(Pt 1), pp. 494–504. doi: 10.1016/j.msec.2016.09.026.
- Almeida, M. (2012) 'Aging mechanisms in bone', *BoneKEy Reports*, 1(7). doi: 10.1038/bonekey.2012.102.
- Alpagot, T. *et al.* (1996) 'Risk indicators for periodontal disease in a racially diverse urban population.', *Journal of clinical periodontology*, 23(11), pp. 982–8.
- Altman, G. *et al.* (2002) 'Cell differentiation by mechanical stress', *The FASEB Journal*, 16(2), pp. 270–272. doi: 10.1096/fj.01-0656fje.
- An, Y. *et al.* (2016) 'Increased autophagy is required to protect periodontal ligament stem cells from apoptosis in inflammatory microenvironment', *Journal of Clinical Periodontology*. doi: 10.1111/jcpe.12549.
- Anderson, D. E. and Johnstone, B. (2017) 'Dynamic Mechanical Compression of Chondrocytes for Tissue Engineering: A Critical Review.', *Frontiers in bioengineering and biotechnology*. Frontiers Media SA, 5, p. 76. doi: 10.3389/fbioe.2017.00076.
- Aomatsu, E. *et al.* (2014) 'Cell-cell adhesion through N-cadherin enhances VCAM-1 expression via PDGFR β in a ligand-independent manner in mesenchymal stem cells', *International Journal of Molecular Medicine*, 33(3), pp. 565–572. doi: 10.3892/ijmm.2013.1607.
- Aonuma, T. *et al.* (2020) 'Delayed tooth movement in Runx2+/- mice associated with mTORC2 in stretch-induced bone formation', *Bone Reports*. doi: 10.1016/j.bonr.2020.100285.
- Arai, F. *et al.* (1999) 'Commitment and Differentiation of Osteoclast Precursor Cells by the

- Sequential Expression of C-Fms and Receptor Activator of Nuclear Factor kb (Rank) Receptors', *The Journal of Experimental Medicine*. The Rockefeller University Press, 190(12), pp. 1741–1754. doi: 10.1084/jem.190.12.1741.
- Arango Duque, G. and Descoteaux, A. (2014) 'Macrophage Cytokines: Involvement in Immunity and Infectious Diseases', *Frontiers in Immunology*, 5, p. 491. doi: 10.3389/fimmu.2014.00491.
- Ariyoshi, W. *et al.* (2005) 'Mechanisms involved in enhancement of osteoclast formation and function by low molecular weight hyaluronic acid', *Journal of Biological Chemistry*. doi: 10.1074/jbc.M412740200.
- Aruffo, A. *et al.* (1990) 'CD44 is the principal cell surface receptor for hyaluronate', *Cell*. Cell Press, 61(7), pp. 1303–1313. doi: 10.1016/0092-8674(90)90694-A.
- Asagiri, M. *et al.* (2005) 'Autoamplification of NFATc1 expression determines its essential role in bone homeostasis.', *The Journal of experimental medicine*. The Rockefeller University Press, 202(9), pp. 1261–9. doi: 10.1084/jem.20051150.
- Ashford, T. P. and Porter, K. R. (1962) 'Cytoplasmic components in hepatic cell lysosomes.', *The Journal of cell biology*, 12(1), pp. 198–202. doi: 10.1083/jcb.12.1.198.
- Awad, H. A. *et al.* (2004) 'Chondrogenic differentiation of adipose-derived adult stem cells in agarose, alginate, and gelatin scaffolds', *Biomaterials*, 25(16), pp. 3211–3222. doi: 10.1016/j.biomaterials.2003.10.045.
- Bainbridge, B. W., Coats, S. R. and Darveau, R. P. (2002) 'Porphyromonas gingivalis Lipopolysaccharide Displays Functionally Diverse Interactions With the Innate Host Defense System', *Annals of Periodontology*, 7(1), pp. 29–37. doi: 10.1902/annals.2002.7.1.29.
- Bajorath, J. *et al.* (1998) 'Identification of CD44 residues important for hyaluronan binding and delineation of the binding site.', *The Journal of biological chemistry*. American Society for Biochemistry and Molecular Biology, 273(1), pp. 338–43. doi: 10.1074/jbc.273.1.338.
- Banerji, S. *et al.* (1999) 'LYVE-1, a New Homologue of the CD44 Glycoprotein, Is a Lymph-specific Receptor for Hyaluronan', *The Journal of Cell Biology*. Rockefeller University Press, 144(4), pp. 789–801. doi: 10.1083/JCB.144.4.789.
- Bayne, K. *et al.* (2015) 'The evolution of animal welfare and the 3Rs in Brazil, China, and India.', *Journal of the American Association for Laboratory Animal Science : JAALAS*. American Association for Laboratory Animal Science, 54(2), pp. 181–91.
- Beertsen, W. *et al.* (1984) 'Microtubules in periodontal ligament cells in relation to tooth eruption and collagen degradation', *Journal of Periodontal Research*. doi: 10.1111/j.1600-0765.1984.tb01304.x.
- Belfield, L. A. *et al.* (2017) 'Exposure to Porphyromonas gingivalis LPS during macrophage polarisation leads to diminished inflammatory cytokine production', *Archives of Oral Biology*. doi: 10.1016/j.archoralbio.2017.04.021.
- Belstrøm, D. *et al.* (2012) 'Does a causal relation between cardiovascular disease and periodontitis exist?', *Microbes and Infection*. Elsevier Masson, 14(5), pp. 411–418. doi: 10.1016/J.MICINF.2011.12.004.
- Berendsen, A. D. and Olsen, B. R. (2015) 'Bone development.', *Bone*. NIH Public Access, 80, pp. 14–18. doi: 10.1016/j.bone.2015.04.035.
- Berman, J. W. and Basch, R. S. (1985) 'Thy-1 antigen expression by murine hematopoietic precursor cells.', *Experimental hematology*, 13(11), pp. 1152–6.
- Beutler, B. and Rietschel, E. T. (2003) 'Innate immune sensing and its roots: the story of

- endotoxin', *Nature Reviews Immunology*, 3(2), pp. 169–176. doi: 10.1038/nri1004.
- Beveridge, T. J. (1999) 'Structures of gram-negative cell walls and their derived membrane vesicles.', *Journal of bacteriology*, 181(16), pp. 4725–33.
- Bi, W. *et al.* (1999) 'Sox9 is required for cartilage formation', *Nature Genetics*, 22(1), pp. 85–89. doi: 10.1038/8792.
- Bialek, P. *et al.* (2004) 'A twist code determines the onset of osteoblast differentiation.', *Developmental cell*, 6(3), pp. 423–35.
- Birbrair, A. and Frenette, P. S. (2016) 'Niche heterogeneity in the bone marrow', *Annals of the New York Academy of Sciences*. NIH Public Access, 1370(1), p. 82. doi: 10.1111/NYAS.13016.
- Biswas, S. K. and Lopez-Collazo, E. (2009) *Endotoxin tolerance: new mechanisms, molecules and clinical significance*, *Trends in Immunology*. Elsevier Current Trends. doi: 10.1016/j.it.2009.07.009.
- Blitz, E. *et al.* (2009) 'Bone Ridge Patterning during Musculoskeletal Assembly Is Mediated through SCX Regulation of Bmp4 at the Tendon-Skeleton Junction', *Developmental Cell*. Cell Press, 17(6), pp. 861–873. doi: 10.1016/J.DEVCEL.2009.10.010.
- Böhrer, H. *et al.* (1997) 'Role of NFkappaB in the mortality of sepsis.', *The Journal of clinical investigation*. American Society for Clinical Investigation, 100(5), pp. 972–85. doi: 10.1172/JCI119648.
- Boissy, P. *et al.* (2002) 'Transcriptional activity of nuclei in multinucleated osteoclasts and its modulation by calcitonin', *Endocrinology*. doi: 10.1210/endo.143.5.8813.
- Boland, G. M. *et al.* (2004) 'Wnt 3a promotes proliferation and suppresses osteogenic differentiation of adult human mesenchymal stem cells', *Journal of Cellular Biochemistry*, 93(6), pp. 1210–1230. doi: 10.1002/jcb.20284.
- Bone, R. C., Grodzin, C. J. and Balk, R. A. (1997) 'Sepsis: A New Hypothesis for Pathogenesis of the Disease Process', *Chest*, 112(1), pp. 235–243. doi: 10.1378/chest.112.1.235.
- Boone, D. L. *et al.* (2004) 'The ubiquitin-modifying enzyme A20 is required for termination of Toll-like receptor responses', *Nature Immunology*, 5(10), pp. 1052–1060. doi: 10.1038/ni1110.
- van den Bos, T. *et al.* (2005) 'Cementum and Dentin in Hypophosphatasia', *Journal of Dental Research*, 84(11), pp. 1021–1025. doi: 10.1177/154405910508401110.
- Bosshardt, D. D. (2005) 'Are cementoblasts a subpopulation of osteoblasts or a unique phenotype?', *Journal of Dental Research*. doi: 10.1177/154405910508400501.
- Boudin, E. and Van Hul, W. (2017) 'Genetics of human bone formation', *European Journal of Endocrinology*. doi: 10.1530/EJE-16-0990.
- Boyle, W. J., Simonet, W. S. and Lacey, D. L. (2003) 'Osteoclast differentiation and activation', *Nature*, pp. 337–342. doi: 10.1038/nature01658.
- van der Bruggen, T. *et al.* (1999) 'Lipopolysaccharide-induced tumor necrosis factor alpha production by human monocytes involves the raf-1/MEK1-MEK2/ERK1-ERK2 pathway.', *Infection and immunity*. American Society for Microbiology (ASM), 67(8), pp. 3824–9.
- Bruno, S., Chiabotto, G. and Camussi, G. (2014) 'Concise review: different mesenchymal stromal/stem cell populations reside in the adult kidney.', *Stem cells translational medicine*. Wiley-Blackwell, 3(12), pp. 1451–5. doi: 10.5966/sctm.2014-0142.
- Bucay, N. *et al.* (1998) 'osteoprotegerin-deficient mice develop early onset osteoporosis and arterial calcification.', *Genes & development*, 12(9), pp. 1260–8.

Bullon, P. *et al.* (2012) 'Autophagy in periodontitis patients and gingival fibroblasts: Unraveling the link between chronic diseases and inflammation', *BMC Medicine*. doi: 10.1186/1741-7015-10-122.

Burgess, T. L. *et al.* (1999) 'The ligand for osteoprotegerin (OPGL) directly activates mature osteoclasts.', *The Journal of cell biology*, 145(3), pp. 527–38.

Burr, D. B. *et al.* (1989) 'The effects of altered strain environments on bone tissue kinetics', *Bone*. doi: 10.1016/8756-3282(89)90056-2.

Cafiero, C. *et al.* (2018) 'Inflammation induces osteoclast differentiation from peripheral mononuclear cells in chronic kidney disease patients: Crosstalk between the immune and bone systems', *Nephrology Dialysis Transplantation*, 33(1), pp. 65–75. doi: 10.1093/ndt/gfx222.

Cano, J. *et al.* (2006) 'Osteogenic alveolar distraction: A review of the literature', *Oral Surgery, Oral Medicine, Oral Pathology, Oral Radiology, and Endodontology*, 101(1), pp. 11–28. doi: 10.1016/j.tripleo.2005.04.015.

Caramés, B. *et al.* (2012) 'Mechanical injury suppresses autophagy regulators and pharmacologic activation of autophagy results in chondroprotection.', *Arthritis and rheumatism*, 64(4), pp. 1182–1192. doi: 10.1002/art.33444.

Cavaillon, J.-M. and Adib-Conquy, M. (2006) 'Bench-to-bedside review: Endotoxin tolerance as a model of leukocyte reprogramming in sepsis', *Critical Care*. BioMed Central, 10(5), p. 233. doi: 10.1186/CC5055.

Chang, E. J. *et al.* (2007) 'Hyaluronan inhibits osteoclast differentiation via Toll-like receptor 4', *J Cell Sci*, 120(Pt 1), pp. 166–176. doi: 10.1242/jcs.03310.

Chang, M. Y. *et al.* (2014) 'A rapid increase in macrophage-derived versican and hyaluronan in infectious lung disease.'

Chanmee, T. *et al.* (2015) 'Key Roles of Hyaluronan and Its CD44 Receptor in the Stemness and Survival of Cancer Stem Cells', *Frontiers in Oncology*. Frontiers, 5, p. 180. doi: 10.3389/fonc.2015.00180.

Chanput, W., Mes, J. J. and Wichers, H. J. (2014) 'THP-1 cell line: An in vitro cell model for immune modulation approach', *International Immunopharmacology*. doi: 10.1016/j.intimp.2014.08.002.

Chaubaroux, C. *et al.* (2015) 'Cell Alignment Driven by Mechanically Induced Collagen Fiber Alignment in Collagen/Alginate Coatings', *Tissue Engineering. Part C, Methods*. Mary Ann Liebert, Inc., 21(9), p. 881. doi: 10.1089/TEN.TEC.2014.0479.

Chen, C. S. (2008) 'Mechanotransduction - a field pulling together?', *Journal of Cell Science*, 121(20), pp. 3285–3292. doi: 10.1242/jcs.023507.

Chen, G., Deng, C. and Li, Y.-P. (2012) 'TGF- β and BMP signaling in osteoblast differentiation and bone formation.', *International journal of biological sciences*. Ivyspring International Publisher, 8(2), pp. 272–88. doi: 10.7150/ijbs.2929.

Chen, L., Mo, S. and Hua, Y. (2019) 'Compressive force-induced autophagy in periodontal ligament cells downregulates osteoclastogenesis during tooth movement', *Journal of Periodontology*. doi: 10.1002/JPER.19-0049.

Chen, Q. *et al.* (2016) 'Fate decision of mesenchymal stem cells: adipocytes or osteoblasts?', *Cell Death and Differentiation*. Nature Publishing Group, 23(7), pp. 1128–1139. doi: 10.1038/cdd.2015.168.

Chen, X. *et al.* (2014) 'Isolation of autophagosome subpopulations after induction of

- autophagy by calcium', *Biochemistry and Cell Biology*. doi: 10.1139/bcb-2014-0115.
- Chen, X. *et al.* (2018) 'Osteoblast–osteoclast interactions', *Connective Tissue Research*, 59(2), pp. 99–107. doi: 10.1080/03008207.2017.1290085.
- Cheng, X.-T. *et al.* (2015) 'Axonal autophagosomes recruit dynein for retrograde transport through fusion with late endosomes.', *The Journal of cell biology*. Rockefeller University Press, 209(3), pp. 377–86. doi: 10.1083/jcb.201412046.
- Cheung, W.-F., Cruz, T. F. and Turley, E. A. (1999) 'Receptor for hyaluronan-mediated motility (RHAMM), a hyaladherin that regulates cell responses to growth factors', *Biochemical Society Transactions*, 27(2), pp. 135–141. doi: 10.1042/bst0270135.
- Chi, L. *et al.* (2019) 'Increased cortical infarction and neuroinflammation in ischemic stroke mice with experimental periodontitis', *NeuroReport*, 30(6), pp. 428–433. doi: 10.1097/WNR.0000000000001220.
- Chomczynski, P. and Sacchi, N. (1987) 'Single-step method of RNA isolation by acid guanidinium thiocyanate-phenol-chloroform extraction', *Analytical Biochemistry*, 162(1), pp. 156–159. doi: 10.1016/0003-2697(87)90021-2.
- Choudhary, M. *et al.* (2007) 'Putative Role of Hyaluronan and Its Related Genes, *HAS2* and *RHAMM*, in Human Early Preimplantation Embryogenesis and Embryonic Stem Cell Characterization', *Stem Cells*, 25(12), pp. 3045–3057. doi: 10.1634/stemcells.2007-0296.
- Chung, Y.-H. *et al.* (2012) 'Microtubule-associated protein light chain 3 regulates Cdc42-dependent actin ring formation in osteoclast', *The International Journal of Biochemistry & Cell Biology*. Pergamon, 44(6), pp. 989–997. doi: 10.1016/J.BIOCEL.2012.03.007.
- Clarke, B. (2008) 'Normal bone anatomy and physiology.', *Clinical journal of the American Society of Nephrology : CJASN*. American Society of Nephrology, 3 Suppl 3(Suppl 3), pp. S131-9. doi: 10.2215/CJN.04151206.
- Cochran, D. L. (2008) 'Inflammation and Bone Loss in Periodontal Disease', *Journal of Periodontology*. John Wiley & Sons, Ltd, 79(8s), pp. 1569–1576. doi: 10.1902/jop.2008.080233.
- Cody, J. J. *et al.* (2011) 'A simplified method for the generation of human osteoclasts in vitro.', *International journal of biochemistry and molecular biology*. e-Century Publishing Corporation, 2(2), pp. 183–189.
- Collins, P. E. and Carmody, R. J. (2015) 'The regulation of endotoxin tolerance and its impact on macrophage activation', *Critical Reviews in Immunology*.
- Collinsworth, A. M. *et al.* (2000) 'Orientation and length of mammalian skeletal myocytes in response to a unidirectional stretch.', *Cell and tissue research*, 302(2), pp. 243–51.
- Colter, D. C. *et al.* (2000) 'Rapid expansion of recycling stem cells in cultures of plastic-adherent cells from human bone marrow', *Proceedings of the National Academy of Sciences*, 97(7), pp. 3213–3218. doi: 10.1073/pnas.070034097.
- Conceição, R. A. *et al.* (2012) 'Human sepsis-associated *Escherichia coli* (SEPEC) is able to adhere to and invade kidney epithelial cells in culture.', *Brazilian journal of medical and biological research = Revista brasileira de pesquisas medicas e biologicas*. Associação Brasileira de Divulgação Científica, 45(5), pp. 417–24. doi: 10.1590/s0100-879x2012007500057.
- Cowin, S. C. and Cardoso, L. (2015) 'Blood and interstitial flow in the hierarchical pore space architecture of bone tissue', *Journal of Biomechanics*, 48(5), pp. 842–854. doi: 10.1016/j.jbiomech.2014.12.013.
- Crockett, J. C. *et al.* (2011) 'Bone remodelling at a glance', *Journal of Cell Science*, 124(7), pp.

991–998. doi: 10.1242/jcs.063032.

Curtale, G., Rubino, M. and Locati, M. (2019) 'MicroRNAs as Molecular Switches in Macrophage Activation.', *Frontiers in immunology*. Frontiers Media SA, 10, p. 799. doi: 10.3389/fimmu.2019.00799.

Cyphert, J. M., Trempus, C. S. and Garantziotis, S. (2015) 'Size Matters: Molecular Weight Specificity of Hyaluronan Effects in Cell Biology', *International Journal of Cell Biology*. Hindawi, 2015, pp. 1–8. doi: 10.1155/2015/563818.

Dalagiorgou, G. *et al.* (2013) 'Mechanical stimulation of polycystin-1 induces human osteoblastic gene expression via potentiation of the calcineurin/NFAT signaling axis', *Cellular and Molecular Life Sciences*. doi: 10.1007/s00018-012-1164-5.

Darveau, R. P. *et al.* (2004) 'Porphyromonas gingivalis Lipopolysaccharide Contains Multiple Lipid A Species That Functionally Interact with Both Toll-Like Receptors 2 and 4', *Infection and Immunity*, 72(9), pp. 5041–5051. doi: 10.1128/IAI.72.9.5041-5051.2004.

Day, A. J. and Prestwich, G. D. (2002) *Hyaluronan-binding proteins: Tying up the giant*, *Journal of Biological Chemistry*. American Society for Biochemistry and Molecular Biology. doi: 10.1074/jbc.R100036200.

Deed, R. *et al.* (1997) 'Early-response gene signalling is induced by angiogenic oligosaccharides of hyaluronan in endothelial cells. Inhibition by non-angiogenic, high-molecular-weight hyaluronan', *International Journal of Cancer*. John Wiley & Sons, Ltd, 71(2), pp. 251–256. doi: 10.1002/(SICI)1097-0215(19970410)71:2<251::AID-IJC21>3.0.CO;2-J.

Denes, B. J. *et al.* (2018) 'A longitudinal study on timing and velocity of rat molar eruption: Timing of rat molar eruption', *Laboratory Animals*, 52(4), pp. 394–401. doi: 10.1177/0023677217750410.

DeSelm, C. J. *et al.* (2011) 'Autophagy Proteins Regulate the Secretory Component of Osteoclastic Bone Resorption', *Developmental Cell*, 21(5), pp. 966–974. doi: 10.1016/j.devcel.2011.08.016.

Detert, J. *et al.* (2010) 'The association between rheumatoid arthritis and periodontal disease', *Arthritis Research & Therapy*. BioMed Central, 12(5), p. 218. doi: 10.1186/ar3106.

Doherty, W. J. *et al.* (1995) 'The effect of glucocorticoids on osteoblast function. The effect of corticosterone on osteoblast expression of beta 1 integrins.', *The Journal of bone and joint surgery. American volume*, 77(3), pp. 396–404. doi: 10.2106/00004623-199503000-00009.

Dominici, M. *et al.* (2006) 'Minimal criteria for defining multipotent mesenchymal stromal cells. The International Society for Cellular Therapy position statement', *Cytotherapy*, 8(4), pp. 315–317. doi: 10.1080/14653240600855905.

Dong, Y. *et al.* (2016) 'Endotoxin free hyaluronan and hyaluronan fragments do not stimulate TNF- α , interleukin-12 or upregulate co-stimulatory molecules in dendritic cells or macrophages', *Scientific Reports*, 6(1), p. 36928. doi: 10.1038/srep36928.

Dougados, M. *et al.* (1993) 'High molecular weight sodium hyaluronate (hyalectin) in osteoarthritis of the knee: a 1 year placebo-controlled trial.', *Osteoarthritis and cartilage*, 1(2), pp. 97–103.

Dougall, W. C. *et al.* (1999) 'RANK is essential for osteoclast and lymph node development.', *Genes & development*, 13(18), pp. 2412–24.

Dower, C. M. *et al.* (2018) *Mechanisms and context underlying the role of autophagy in cancer metastasis*, *Autophagy*. doi: 10.1080/15548627.2018.1450020.

- Du, J. and Li, M. (2017) 'Functions of Periostin in dental tissues and its role in periodontal tissues' regeneration', *Cellular and Molecular Life Sciences*, 74(23), pp. 4279–4286. doi: 10.1007/s00018-017-2645-3.
- Ducy, P. *et al.* (1997) 'Osf2/Cbfa1: A Transcriptional Activator of Osteoblast Differentiation', *Cell*, 89(5), pp. 747–754. doi: 10.1016/S0092-8674(00)80257-3.
- de Duve, C. and Wattiaux, R. (1966) 'Functions of Lysosomes', *Annual Review of Physiology*, 28(1), pp. 435–492. doi: 10.1146/annurev.ph.28.030166.002251.
- Eastwood, M. *et al.* (1998) 'Effect of precise mechanical loading on fibroblast populated collagen lattices: Morphological changes', *Cell Motility and the Cytoskeleton*, 40(1), pp. 13–21. doi: 10.1002/(SICI)1097-0169(1998)40:1<13::AID-CM2>3.0.CO;2-G.
- Eaves, C. J. (2015) 'Hematopoietic stem cells: concepts, definitions, and the new reality.', *Blood*. American Society of Hematology, 125(17), pp. 2605–13. doi: 10.1182/blood-2014-12-570200.
- Eisenstein, B. I. and Jones, G. W. (1988) 'The spectrum of infections and pathogenic mechanisms of Escherichia coli.', *Advances in internal medicine*, 33, pp. 231–52.
- Ek-Rylander, B. *et al.* (1994) 'Dephosphorylation of osteopontin and bone sialoprotein by osteoclastic tartrate-resistant acid phosphatase. Modulation of osteoclast adhesion in vitro.', *The Journal of biological chemistry*, 269(21), pp. 14853–6.
- Engin, F. *et al.* (2008) 'Dimorphic effects of Notch signaling in bone homeostasis.', *Nature medicine*. NIH Public Access, 14(3), pp. 299–305. doi: 10.1038/nm1712.
- Engler, A. J. *et al.* (2006) 'Matrix Elasticity Directs Stem Cell Lineage Specification', *Cell*, 126(4), pp. 677–689. doi: 10.1016/j.cell.2006.06.044.
- Faas, M. M. *et al.* (2014) 'Porphyromonas Gingivalis and E-coli Induce Different Cytokine Production Patterns in Pregnant Women', *PLoS ONE*. Edited by A. Kumar. Public Library of Science, 9(1), p. e86355. doi: 10.1371/journal.pone.0086355.
- Fan, H. and Cook, J. A. (2004) 'Molecular mechanisms of endotoxin tolerance', *Journal of Endotoxin Research*, 10(2), pp. 71–84. doi: 10.1179/096805104225003997.
- Farhat, K. *et al.* (2008) 'Heterodimerization of TLR2 with TLR1 or TLR6 expands the ligand spectrum but does not lead to differential signaling', *Journal of Leukocyte Biology*, 83(3), pp. 692–701. doi: 10.1189/jlb.0807586.
- Fekete, T. *et al.* (2012) 'Constraints for monocyte-derived dendritic cell functions under inflammatory conditions', *European Journal of Immunology*, 42(2), pp. 458–469. doi: 10.1002/eji.201141924.
- Fink, D. F. and Smith, R. J. (1992) 'The duration of orthodontic treatment', *American Journal of Orthodontics and Dentofacial Orthopedics*, 102(1), pp. 45–51. doi: 10.1016/0889-5406(92)70013-Z.
- Fischer, A. H. *et al.* (2008) 'Hematoxylin and Eosin Staining of Tissue and Cell Sections', *Cold Spring Harbor Protocols*, 2008(6), p. pdb.prot4986-pdb.prot4986. doi: 10.1101/pdb.prot4986.
- Foster, B. L. (2012) 'Methods for studying tooth root cementum by light microscopy.', *International journal of oral science*. Nature Publishing Group, 4(3), pp. 119–28. doi: 10.1038/ijos.2012.57.
- Foster, S. L., Hargreaves, D. C. and Medzhitov, R. (2007) 'Gene-specific control of inflammation by TLR-induced chromatin modifications', *Nature*, 447(7147), pp. 972–978. doi: 10.1038/nature05836.

- Fresno, C. del *et al.* (2005) 'Tumor Cells Deactivate Human Monocytes by Up-Regulating IL-1 Receptor Associated Kinase-M Expression via CD44 and TLR4', *The Journal of Immunology*. American Association of Immunologists, 174(5), pp. 3032–3040. doi: 10.4049/JIMMUNOL.174.5.3032.
- del Fresno, C. *et al.* (2008) 'Monocytes from Cystic Fibrosis Patients Are Locked in an LPS Tolerance State: Down-Regulation of TREM-1 as Putative Underlying Mechanism', *PLoS ONE*. Edited by O. Eickelberg. Public Library of Science, 3(7), p. e2667. doi: 10.1371/journal.pone.0002667.
- del Fresno, C. *et al.* (2009) 'Potent Phagocytic Activity with Impaired Antigen Presentation Identifying Lipopolysaccharide-Tolerant Human Monocytes: Demonstration in Isolated Monocytes from Cystic Fibrosis Patients', *The Journal of Immunology*, 182(10), pp. 6494–6507. doi: 10.4049/jimmunol.0803350.
- Friedenstein, A. J., Chailakhjan, R. K. and Lalykina, K. S. (1970) 'The development of fibroblast colonies in monolayer cultures of guinea-pig bone marrow and spleen cells.', *Cell and tissue kinetics*, 3(4), pp. 393–403.
- Friedenstein, A. J., Gorskaja, J. F. and Kulagina, N. N. (1976) 'Fibroblast precursors in normal and irradiated mouse hematopoietic organs.', *Experimental hematology*, 4(5), pp. 267–74.
- Fuchs, E., Tumber, T. and Guasch, G. (2004) 'Socializing with the neighbors: stem cells and their niche.', *Cell*, 116(6), pp. 769–78.
- Fujioka-Kobayashi, M. *et al.* (2017) 'In vitro effects of hyaluronic acid on human periodontal ligament cells', *BMC Oral Health*. doi: 10.1186/s12903-017-0341-1.
- Fukushima, O., Bekker, P. J. and Gay, C. V. (1991) 'Characterization of the functional stages of osteoclasts by enzyme histochemistry and electron microscopy', *The Anatomical Record*, 231(3), pp. 298–315. doi: 10.1002/ar.1092310303.
- Galluzzi, L. *et al.* (2017) 'Pharmacological modulation of autophagy: Therapeutic potential and persisting obstacles', *Nature Reviews Drug Discovery*. doi: 10.1038/nrd.2017.22.
- Ganley, I. G. *et al.* (2011) 'Distinct Autophagosomal-Lysosomal Fusion Mechanism Revealed by Thapsigargin-Induced Autophagy Arrest', *Molecular Cell*, 42(6), pp. 731–743. doi: 10.1016/j.molcel.2011.04.024.
- Gardel, M. L. *et al.* (2008) 'Mechanical response of cytoskeletal networks.', *Methods in cell biology*. NIH Public Access, 89, pp. 487–519. doi: 10.1016/S0091-679X(08)00619-5.
- La Gatta, A. *et al.* (2010) 'A complete hyaluronan hydrodynamic characterization using a size exclusion chromatography–triple detector array system during in vitro enzymatic degradation', *Analytical Biochemistry*. Academic Press, 404(1), pp. 21–29. doi: 10.1016/J.AB.2010.04.014.
- GBD 2015 Disease and Injury Incidence and Prevalence Collaborators, G. 2015 D. and I. I. and P. (2016) 'Global, regional, and national incidence, prevalence, and years lived with disability for 310 diseases and injuries, 1990–2015: a systematic analysis for the Global Burden of Disease Study 2015.', *Lancet (London, England)*. Elsevier, 388(10053), pp. 1545–1602. doi: 10.1016/S0140-6736(16)31678-6.
- Gee, K. *et al.* (2002) 'Differential regulation of CD44 expression by lipopolysaccharide (LPS) and TNF-alpha in human monocytic cells: distinct involvement of c-Jun N-terminal kinase in LPS-induced CD44 expression.', *Journal of immunology (Baltimore, Md. : 1950)*, 169(10), pp. 5660–5672. doi: 10.4049/jimmunol.169.10.5660.
- Gefen, A. and Weihs, D. (2016) 'Mechanical cytoprotection: A review of cytoskeleton-protection approaches for cells', *Journal of Biomechanics*. doi:

10.1016/j.jbiomech.2015.10.030.

Gelb, B. D. *et al.* (1996) 'Pycnodysostosis, a lysosomal disease caused by cathepsin K deficiency.', *Science (New York, N.Y.)*, 273(5279), pp. 1236–8.

Gelman, A. and Elazar, Z. (2011) 'Autophagic Factors Cut to the Bone', *Developmental Cell*. Cell Press, 21(5), pp. 808–810. doi: 10.1016/J.DEVCEL.2011.10.021.

Gerber, J. S. and Mosser, D. M. (2001) 'Reversing lipopolysaccharide toxicity by ligating the macrophage Fc gamma receptors.', *Journal of immunology (Baltimore, Md. : 1950)*. American Association of Immunologists, 166(11), pp. 6861–8. doi: 10.4049/jimmunol.166.11.6861.

Gerecht, S. *et al.* (2007) 'The effect of actin disrupting agents on contact guidance of human embryonic stem cells', *Biomaterials*, 28(28), pp. 4068–4077. doi: 10.1016/j.biomaterials.2007.05.027.

Gerlach, J. C. *et al.* (2012) 'Perivascular Mesenchymal Progenitors in Human Fetal and Adult Liver', *Stem Cells and Development*. Mary Ann Liebert, Inc. 140 Huguenot Street, 3rd Floor New Rochelle, NY 10801 USA , 21(18), pp. 3258–3269. doi: 10.1089/scd.2012.0296.

Girish, K. S. and Kemparaju, K. (2007) 'The magic glue hyaluronan and its eraser hyaluronidase: A biological overview', *Life Sciences*, 80(21), pp. 1921–1943. doi: 10.1016/j.lfs.2007.02.037.

Goa, K. L. and Benfield, P. (1994) 'Hyaluronic Acid: A Review of its Pharmacology and Use as a Surgical Aid in Ophthalmology, and its Therapeutic Potential in Joint Disease and Wound Healing', *Drugs*, 47(3), pp. 536–566. doi: 10.2165/00003495-199447030-00009.

Goessler, U. R. *et al.* (2008) 'Integrin expression in stem cells from bone marrow and adipose tissue during chondrogenic differentiation.', *International journal of molecular medicine*, 21(3), pp. 271–9.

Goodship, A. E. *et al.* (1998) 'Bone loss during long term space flight is prevented by the application of a short term impulsive mechanical stimulus', *Acta Astronautica*, 43(3–6), pp. 65–75. doi: 10.1016/S0094-5765(98)00144-1.

Grandfield, K. *et al.* (2015) 'Strain-guided mineralization in the bone–PDL–cementum complex of a rat periodontium', *Bone Reports*. Elsevier, 3, pp. 20–31. doi: 10.1016/J.BONR.2015.04.002.

Graves, D. T., Jiang, Y. and Valente, A. J. (1999) 'The expression of monocyte chemoattractant protein-1 and other chemokines by osteoblasts.', *Frontiers in bioscience : a journal and virtual library*, 4, pp. D571-80.

Greenwald, R. A. and Moy, W. W. (1980) 'Effect of oxygen-derived free radicals on hyaluronic acid.', *Arthritis and rheumatism*, 23(4), pp. 455–63.

Griffen, A. L. *et al.* (1998) 'Prevalence of Porphyromonas gingivalis and periodontal health status.', *Journal of clinical microbiology*. American Society for Microbiology (ASM), 36(11), pp. 3239–42.

Groeger, S. and Meyle, J. (2019) 'Oral Mucosal Epithelial Cells.', *Frontiers in immunology*. Frontiers Media SA, 10, p. 208. doi: 10.3389/fimmu.2019.00208.

Gronthos, S. *et al.* (2000) 'Postnatal human dental pulp stem cells (DPSCs) in vitro and invivo', *Proceedings of the National Academy of Sciences*, 97(25), pp. 13625–13630. doi: 10.1073/pnas.240309797.

Grossi, S. G. *et al.* (1994) 'Assessment of Risk for Periodontal Disease. I. Risk Indicators for Attachment Loss', *Journal of Periodontology*, 65(3), pp. 260–267. doi: 10.1902/jop.1994.65.3.260.

- Guilak, F. *et al.* (2009) 'Control of Stem Cell Fate by Physical Interactions with the Extracellular Matrix', *Cell Stem Cell*, 5(1), pp. 17–26. doi: 10.1016/j.stem.2009.06.016.
- Günther, J. *et al.* (2017) 'TLR ligands, but not modulators of histone modifiers, can induce the complex immune response pattern of endotoxin tolerance in mammary epithelial cells', *Innate Immunity*, 23(2), pp. 155–164. doi: 10.1177/1753425916681076.
- Guo, F.-X. *et al.* (2017) 'Shear Stress in Autophagy and Its Possible Mechanisms in the Process of Atherosclerosis.', *DNA and cell biology*. Mary Ann Liebert, Inc., 36(5), pp. 335–346. doi: 10.1089/dna.2017.3649.
- Gutierrez, J. A., Suzara, V. V. and Dobbs, L. G. (2003) 'Continuous Mechanical Contraction Modulates Expression of Alveolar Epithelial Cell Phenotype', *American Journal of Respiratory Cell and Molecular Biology*, 29(1), pp. 81–87. doi: 10.1165/rcmb.2002-0135OC.
- Haapasalo, H. *et al.* (2000) 'Exercise-induced bone gain is due to enlargement in bone size without a change in volumetric bone density: A peripheral quantitative computed tomography study of the upper arms of male tennis players', *Bone*, 27(3), pp. 351–357. doi: 10.1016/S8756-3282(00)00331-8.
- Hackett, C. H., Flaminio, M. J. B. F. and Fortier, L. A. (2011) 'Analysis of CD14 expression levels in putative mesenchymal progenitor cells isolated from equine bone marrow.', *Stem cells and development*. Mary Ann Liebert, Inc., 20(4), pp. 721–35. doi: 10.1089/scd.2010.0175.
- Hajishengallis, G., Darveau, R. P. and Curtis, M. A. (2012) 'The keystone-pathogen hypothesis', *Nature Reviews Microbiology*, 10(10), pp. 717–725. doi: 10.1038/nrmicro2873.
- Hale, A. N. *et al.* (2013) 'Autophagy: Regulation and role in development', *Autophagy*, 9(7), pp. 951–972. doi: 10.4161/auto.24273.
- Hall, B. K. and Miyake, T. (1992) 'The membranous skeleton: the role of cell condensations in vertebrate skeletogenesis.', *Anatomy and embryology*, 186(2), pp. 107–24.
- Halldorsson, S. *et al.* (2015) 'Advantages and challenges of microfluidic cell culture in polydimethylsiloxane devices', *Biosensors and Bioelectronics*. Elsevier, 63, pp. 218–231. doi: 10.1016/J.BIOS.2014.07.029.
- Hamant, O. *et al.* (2019) 'Are microtubules tension sensors?', *Nature Communications*. doi: 10.1038/s41467-019-10207-y.
- Hamey, F. K. *et al.* (2017) 'Reconstructing blood stem cell regulatory network models from single-cell molecular profiles.', *Proceedings of the National Academy of Sciences of the United States of America*. National Academy of Sciences, 114(23), pp. 5822–5829. doi: 10.1073/pnas.1610609114.
- Harada, H. and Takahashi, M. (2007) 'CD44-dependent Intracellular and Extracellular Catabolism of Hyaluronic Acid by Hyaluronidase-1 and -2', *Journal of Biological Chemistry*. American Society for Biochemistry and Molecular Biology, 282(8), pp. 5597–5607. doi: 10.1074/JBC.M608358200.
- Harris, J. (2011) 'Autophagy and cytokines', *Cytokine*. doi: 10.1016/j.cyto.2011.08.022.
- Harshad, K. *et al.* (2016) 'An electromagnetic cell-stretching device for mechanotransduction studies of olfactory ensheathing cells', *Biomedical Microdevices*, 18(3), p. 45. doi: 10.1007/s10544-016-0071-1.
- Hascall, V. C. *et al.* (2004) 'Intracellular hyaluronan: A new frontier for inflammation?', *Biochimica et Biophysica Acta - General Subjects*, 1673(1–2), pp. 3–12. doi: 10.1016/j.bbagen.2004.02.013.

- Hascall, V. C. *et al.* (2014) 'The dynamic metabolism of hyaluronan regulates the cytosolic concentration of UDP-GlcNAc', *Matrix Biology*, 35, pp. 14–17. doi: 10.1016/j.matbio.2014.01.014.
- Hass, R. *et al.* (2011) 'Different populations and sources of human mesenchymal stem cells (MSC): A comparison of adult and neonatal tissue-derived MSC.', *Cell communication and signaling : CCS*. BioMed Central, 9, p. 12. doi: 10.1186/1478-811X-9-12.
- Hayashi, C. *et al.* (2010) 'Pathogen-induced inflammation at sites distant from oral infection: bacterial persistence and induction of cell-specific innate immune inflammatory pathways', *Molecular Oral Microbiology*. John Wiley & Sons, Ltd (10.1111), 25(5), pp. 305–316. doi: 10.1111/j.2041-1014.2010.00582.x.
- Hayashi, S.-I. *et al.* (1997) 'Osteoclast precursors in bone marrow and peritoneal cavity', *Journal of Cellular Physiology*, 170(3), pp. 241–247. doi: 10.1002/(SICI)1097-4652(199703)170:3<241::AID-JCP4>3.0.CO;2-O.
- Hayashi, S.-I. *et al.* (2003) 'Distinct osteoclast precursors in the bone marrow and extramedullary organs characterized by responsiveness to Toll-like receptor ligands and TNF-alpha.', *Journal of immunology (Baltimore, Md. : 1950)*. American Association of Immunologists, 171(10), pp. 5130–9. doi: 10.4049/jimmunol.171.10.5130.
- Hayman, A. R. (2008) 'Tartrate-resistant acid phosphatase (TRAP) and the osteoclast/immune cell dichotomy', *Autoimmunity*, 41(3), pp. 218–223. doi: 10.1080/08916930701694667.
- Helfrich, M. H. (2005) 'Osteoclast diseases and dental abnormalities', *Archives of Oral Biology*, 50(2), pp. 115–122. doi: 10.1016/j.archoralbio.2004.11.016.
- Henderson, J. H. and Carter, D. R. (2002) 'Mechanical induction in limb morphogenesis: the role of growth-generated strains and pressures.', *Bone*, 31(6), pp. 645–53.
- Henderson, L., Lim, C. and Zambon, A. (2014) *A live-cell reporter that differentiates between quiescent and cycling cells*, *The FASEB Journal*.
- Heppner, G. and Weiss, D. W. (1965) 'High Susceptibility of Strain A Mice to Endotoxin and Endotoxin-Red Blood Cell Mixtures.', *Journal of bacteriology*, 90(3), pp. 696–703.
- Herber, R.-P. *et al.* (2012) 'Imaging an Adapted Dentoalveolar Complex', *Anatomy Research International*. Hindawi Limited, 2012. doi: 10.1155/2012/782571.
- Heremans, H. *et al.* (1990) 'Interferon gamma, a mediator of lethal lipopolysaccharide-induced Shwartzman-like shock reactions in mice.', *The Journal of experimental medicine*. The Rockefeller University Press, 171(6), pp. 1853–69. doi: 10.1084/jem.171.6.1853.
- Heymann, D. (2006) 'Autophagy: A protective mechanism in response to stress and inflammation.', *Current opinion in investigational drugs (London, England : 2000)*. Inserm, 7(5), pp. 443–50.
- Hienz, S. A., Paliwal, S. and Ivanovski, S. (2015) 'Mechanisms of Bone Resorption in Periodontitis', *Journal of Immunology Research*, 2015, pp. 1–10. doi: 10.1155/2015/615486.
- Hikida, T. *et al.* (2016) 'Comparisons of orthodontic root resorption under heavy and jiggling reciprocating forces during experimental tooth movement in a rat model.', *Korean journal of orthodontics*. Korean Association of Orthodontists, 46(4), pp. 228–41. doi: 10.4041/kjod.2016.46.4.228.
- Hill, T. P. *et al.* (2005) 'Canonical Wnt/ β -Catenin Signaling Prevents Osteoblasts from Differentiating into Chondrocytes', *Developmental Cell*, 8(5), pp. 727–738. doi: 10.1016/j.devcel.2005.02.013.

- Hirschfeld, M. *et al.* (2001) 'Signaling by Toll-Like Receptor 2 and 4 Agonists Results in Differential Gene Expression in Murine Macrophages', *Infection and Immunity*, 69(3), pp. 1477–1482. doi: 10.1128/IAI.69.3.1477-1482.2001.
- Hirt, J. and Liton, P. B. (2017) 'Autophagy and mechanotransduction in outflow pathway cells', *Experimental Eye Research*, 158, pp. 146–153. doi: 10.1016/j.exer.2016.06.021.
- Hocking, L. J. *et al.* (2004) 'Novel UBA Domain Mutations of SQSTM1 in Paget's Disease of Bone: Genotype Phenotype Correlation, Functional Analysis, and Structural Consequences', *Journal of Bone and Mineral Research*, 19(7), pp. 1122–1127. doi: 10.1359/JBMR.0403015.
- Holden, J. A. *et al.* (2014) 'Porphyromonas gingivalis lipopolysaccharide weakly activates M1 and M2 polarized mouse macrophages but induces inflammatory cytokines', *Infection and Immunity*. doi: 10.1128/IAI.02325-14.
- Holliday, L. *et al.* (2009) 'Osteoclast polarization and orthodontic tooth movement', *Orthodontics & Craniofacial Research*, 12(2), pp. 105–112. doi: 10.1111/j.1601-6343.2009.01443.x.
- Horwitz, E. M. *et al.* (1999) 'Transplantability and therapeutic effects of bone marrow-derived mesenchymal cells in children with osteogenesis imperfecta', *Nature Medicine*, 5(3), pp. 309–313. doi: 10.1038/6529.
- Høyer-Hansen, M., Nordbrandt, S. P. S. and Jäätelä, M. (2010) 'Autophagy as a basis for the health-promoting effects of vitamin D', *Trends in Molecular Medicine*, 16(7), pp. 295–302. doi: 10.1016/j.molmed.2010.04.005.
- Hoyte, D. A. (1960) 'Alizarin as an indicator of bone growth.', *Journal of anatomy*. Wiley-Blackwell, 94(Pt 3), pp. 432–42.
- Huang, L. *et al.* (2019) 'Experimental mechanical strain measurement of tissues.', *PeerJ*. PeerJ, Inc, 7, p. e6545. doi: 10.7717/peerj.6545.
- Huang, R. *et al.* (2017) 'RANKL-induced M1 macrophages are involved in bone formation', *Bone Research*. Nature Publishing Group, 5(1), p. 17019. doi: 10.1038/boneres.2017.19.
- Huang, Y. and Nguyen, N.-T. (2013) 'A polymeric cell stretching device for real-time imaging with optical microscopy', *Biomedical Microdevices*, 15(6), pp. 1043–1054. doi: 10.1007/s10544-013-9796-2.
- Huh, D. *et al.* (2010) 'Reconstituting Organ-Level Lung Functions on a Chip', *Science*, 328(5986), pp. 1662–1668. doi: 10.1126/science.1188302.
- Ibrahim, A. Y. *et al.* (2017) 'Resolving differences between animal models for expedited orthodontic tooth movement', *Orthodontics & Craniofacial Research*. John Wiley & Sons, Ltd (10.1111), 20, pp. 72–76. doi: 10.1111/ocr.12175.
- Ingber, D E (1997) 'Integrins, tensegrity, and mechanotransduction', *Gravit Space Biol Bull*, 10(2), pp. 49–55.
- Ingber, D. E. (1997) 'Tensegrity: the Architectural Basis of Cellular Mechanotransduction', *Annual Review of Physiology*, 59(1), pp. 575–599. doi: 10.1146/annurev.physiol.59.1.575.
- Ingber, D. E. (2006) 'Cellular mechanotransduction: putting all the pieces together again', *The FASEB Journal*, 20(7), pp. 811–827. doi: 10.1096/fj.05-5424rev.
- Ingber, D. E. (2008) 'Tensegrity and mechanotransduction', *Journal of Bodywork and Movement Therapies*, 12(3), pp. 198–200. doi: 10.1016/j.jbmt.2008.04.038.
- Ingber, D. E., Wang, N. and Stamenović, D. (2014) 'Tensegrity, cellular biophysics, and the

- mechanics of living systems', *Reports on Progress in Physics*, 77(4), p. 046603. doi: 10.1088/0034-4885/77/4/046603.
- Itano, N. (2008) 'Simple Primary Structure, Complex Turnover Regulation and Multiple Roles of Hyaluronan', *Journal of Biochemistry*. Narnia, 144(2), pp. 131–137. doi: 10.1093/jb/mvn046.
- Izadpanah, R. *et al.* (2006) 'Biologic properties of mesenchymal stem cells derived from bone marrow and adipose tissue', *Journal of Cellular Biochemistry*, 99(5), pp. 1285–1297. doi: 10.1002/jcb.20904.
- Jaalouk, D. E. and Lammerding, J. (2009) 'Mechanotransduction gone awry', *Nature Reviews Molecular Cell Biology*, 10(1), pp. 63–73. doi: 10.1038/nrm2597.
- Jacobson, A. *et al.* (2000) 'Expression of human hyaluronan synthases in response to external stimuli.', *The Biochemical journal*, 348 Pt 1, pp. 29–35.
- Jaiswal, N. *et al.* (1997) 'Osteogenic differentiation of purified, culture-expanded human mesenchymal stem cells in vitro.', *Journal of cellular biochemistry*, 64(2), pp. 295–312.
- Jakubzick, C. V., Randolph, G. J. and Henson, P. M. (2017) 'Monocyte differentiation and antigen-presenting functions', *Nature Reviews Immunology*. Nature Publishing Group, 17(6), pp. 349–362. doi: 10.1038/nri.2017.28.
- Jeanes, A., Gottardi, C. J. and Yap, A. S. (2008) 'Cadherins and cancer: how does cadherin dysfunction promote tumor progression?', *Oncogene*, 27(55), pp. 6920–6929. doi: 10.1038/onc.2008.343.
- Jeganathan, S. *et al.* (2014) 'Modulation of Osteoclastogenesis with Macrophage M1- and M2-Inducing Stimuli', *PLoS ONE*. Edited by G. P. Bansal. Public Library of Science, 9(8), p. e104498. doi: 10.1371/journal.pone.0104498.
- Jentsch, H. *et al.* (2003) 'Treatment of gingivitis with hyaluronan.', *Journal of clinical periodontology*, 30(2), pp. 159–64.
- Jiang, D. *et al.* (2005) 'Regulation of lung injury and repair by Toll-like receptors and hyaluronan', *Nature Medicine*. Nature Publishing Group, 11(11), pp. 1173–1179. doi: 10.1038/nm1315.
- Jiang, M., Li, Z. and Zhu, G. (2020) 'The role of autophagy in the pathogenesis of periodontal disease', *Oral Diseases*. doi: 10.1111/odi.13045.
- Jiang, P. *et al.* (2014) 'The HOPS complex mediates autophagosome-lysosome fusion through interaction with syntaxin 17.', *Molecular biology of the cell*. American Society for Cell Biology, 25(8), pp. 1327–37. doi: 10.1091/mbc.E13-08-0447.
- Jiang, Y. *et al.* (2002) 'Multipotent progenitor cells can be isolated from postnatal murine bone marrow, muscle, and brain.', *Experimental hematology*, 30(8), pp. 896–904.
- Jiang, Z. *et al.* (2005) 'CD14 is required for MyD88-independent LPS signaling', *Nature Immunology*, 6(6), pp. 565–570. doi: 10.1038/ni1207.
- Joiner, K. *et al.* (1983) 'Studies on the mechanism of bacterial resistance to complement-mediated killing. III. C5b-9 deposits stably on rough and type 7 *S. pneumoniae* without causing bacterial killing.', *Journal of immunology (Baltimore, Md. : 1950)*, 130(2), pp. 845–9.
- Jones, D. C. (2006) 'Regulation of Adult Bone Mass by the Zinc Finger Adapter Protein Schnurri-3', *Science*, 312(5777), pp. 1223–1227. doi: 10.1126/science.1126313.
- de Jong, T. *et al.* (2017) 'The intricate anatomy of the periodontal ligament and its development: Lessons for periodontal regeneration', *Journal of Periodontal Research*. doi:

10.1111/jre.12477.

Jordan, A. R. *et al.* (2015) 'The Role of CD44 in Disease Pathophysiology and Targeted Treatment', *Frontiers in Immunology*, 6, p. 182. doi: 10.3389/fimmu.2015.00182.

Jørgensen, N. R. *et al.* (2003) 'Activation of L-type Calcium Channels Is Required for Gap Junction-mediated Intercellular Calcium Signaling in Osteoblastic Cells', *Journal of Biological Chemistry*, 278(6), pp. 4082–4086. doi: 10.1074/jbc.M205880200.

Kagan, J. C. *et al.* (2008) 'TRAM couples endocytosis of Toll-like receptor 4 to the induction of interferon- β ', *Nature Immunology*, 9(4), pp. 361–368. doi: 10.1038/ni1569.

Kaipatur, N. *et al.* (2015) 'Impact of selective alveolar decortication on bisphosphonate burdened alveolar bone during orthodontic tooth movement', *Archives of Oral Biology*, 60(11), pp. 1681–1689. doi: 10.1016/j.archoralbio.2015.08.008.

Kamble, H. *et al.* (2016) 'Cell stretching devices as research tools: engineering and biological considerations', *Lab on a Chip*. The Royal Society of Chemistry, 16(17), pp. 3193–3203. doi: 10.1039/C6LC00607H.

Kamotani, Y. *et al.* (2008) 'Individually programmable cell stretching microwell arrays actuated by a Braille display', *Biomaterials*, 29(17), pp. 2646–2655. doi: 10.1016/j.biomaterials.2008.02.019.

Kanayama, T. *et al.* (2008) 'Application of elastic salmon collagen gel to uniaxial stretching culture of human umbilical vein endothelial cells', *Journal of Bioscience and Bioengineering*. Elsevier, 105(5), pp. 554–557. doi: 10.1263/JBB.105.554.

Kania, E. *et al.* (2017) 'Verapamil treatment induces cytoprotective autophagy by modulating cellular metabolism', *The FEBS Journal*, 284(9), pp. 1370–1387. doi: 10.1111/febs.14064.

Karousou, E. *et al.* (2010) 'The activity of hyaluronan synthase 2 is regulated by dimerization and ubiquitination', *Journal of Biological Chemistry*, 285(31), pp. 23647–23654. doi: 10.1074/jbc.M110.127050.

Karp, N. S. *et al.* (1992) 'Membranous bone lengthening: a serial histological study.', *Annals of plastic surgery*, 29(1), pp. 2–7.

Karsenty, G., Kronenberg, H. M. and Settembre, C. (2009) 'Genetic Control of Bone Formation', *Annual Review of Cell and Developmental Biology*, 25(1), pp. 629–648. doi: 10.1146/annurev.cellbio.042308.113308.

Kasulanati, S. and Venkatesan, V. (2018) 'Understanding pluripotency under folic acid deficiency using embryonic stem cells as an in vitro model', *Medical Hypotheses*, 111, pp. 24–26. doi: 10.1016/j.mehy.2017.12.019.

Katsianou, M. A. *et al.* (2018) 'The role of transient receptor potential polycystin channels in bone diseases', *Annals of Translational Medicine*. doi: 10.21037/atm.2018.04.10.

Katz, J. *et al.* (2009) 'Localization of P. gingivalis in Preterm Delivery Placenta', *Journal of Dental Research*. SAGE Publications, 88(6), pp. 575–578. doi: 10.1177/0022034509338032.

Kawamoto, H. *et al.* (2010) 'A map for lineage restriction of progenitors during hematopoiesis: the essence of the myeloid-based model', *Immunological Reviews*, 238(1), pp. 23–36. doi: 10.1111/j.1600-065X.2010.00959.x.

Kawane, T. *et al.* (2014) 'Dlx5 and Mef2 Regulate a Novel Runx2 Enhancer for Osteoblast-Specific Expression', *Journal of Bone and Mineral Research*, 29(9), pp. 1960–1969. doi: 10.1002/jbmr.2240.

- Kearney, E. M., Prendergast, P. J. and Campbell, V. a (2008) 'Mechanisms of strain-mediated mesenchymal stem cell apoptosis.', *Journal of biomechanical engineering*, 130(6), p. 061004. doi: 10.1115/1.2979870.
- Kearns, A. E., Khosla, S. and Kostenuik, P. J. (2008) 'Receptor Activator of Nuclear Factor κ B Ligand and Osteoprotegerin Regulation of Bone Remodeling in Health and Disease', *Endocrine Reviews*, 29(2), pp. 155–192. doi: 10.1210/er.2007-0014.
- Kiel, M. J. *et al.* (2005) 'SLAM family receptors distinguish hematopoietic stem and progenitor cells and reveal endothelial niches for stem cells.', *Cell*. Elsevier, 121(7), pp. 1109–21. doi: 10.1016/j.cell.2005.05.026.
- Kim, E.-J. *et al.* (2013) 'Ihh and Runx2/Runx3 Signaling Interact to Coordinate Early Chondrogenesis: A Mouse Model', *PLoS ONE*. Edited by G. Stein. Public Library of Science, 8(2), p. e55296. doi: 10.1371/journal.pone.0055296.
- Kim, J. H. and Kim, N. (2016) 'Signaling Pathways in Osteoclast Differentiation.', *Chonnam medical journal*. Chonnam National University Medical School, 52(1), pp. 12–7. doi: 10.4068/cmj.2016.52.1.12.
- Kim, K. *et al.* (2005) 'Nuclear Factor of Activated T Cells c1 Induces Osteoclast-associated Receptor Gene Expression during Tumor Necrosis Factor-related Activation-induced Cytokine-mediated Osteoclastogenesis', *Journal of Biological Chemistry*, 280(42), pp. 35209–35216. doi: 10.1074/jbc.M505815200.
- Kim, N. *et al.* (2002) 'A novel member of the leukocyte receptor complex regulates osteoclast differentiation.', *The Journal of experimental medicine*. The Rockefeller University Press, 195(2), pp. 201–9. doi: 10.1084/JEM.20011681.
- Kim, S. *et al.* (2003) 'Stat1 functions as a cytoplasmic attenuator of Runx2 in the transcriptional program of osteoblast differentiation', *Genes & Development*, 17(16), pp. 1979–1991. doi: 10.1101/gad.1119303.
- Kim, Y. *et al.* (2005) 'Contribution of Nuclear Factor of Activated T Cells c1 to the Transcriptional Control of Immunoreceptor Osteoclast-associated Receptor but Not Triggering Receptor Expressed by Myeloid Cells-2 during Osteoclastogenesis', *Journal of Biological Chemistry*, 280(38), pp. 32905–32913. doi: 10.1074/jbc.M505820200.
- King, J. S., Veltman, D. M. and Insall, R. H. (2011) 'The induction of autophagy by mechanical stress', *Autophagy*, 7(12), pp. 1490–1499. doi: 10.4161/auto.7.12.17924.
- Kirikae, T. *et al.* (1999) 'Lipopolysaccharides (LPS) of oral black-pigmented bacteria induce tumor necrosis factor production by LPS-refractory C3H/HeJ macrophages in a way different from that of Salmonella LPS.', *Infection and immunity*, 67(4), pp. 1736–42.
- Kitaura, H. *et al.* (2014) 'Effect of cytokines on osteoclast formation and bone resorption during mechanical force loading of the periodontal membrane', *The Scientific World Journal*, 2014, p. 617032. doi: 10.1155/2014/617032.
- Kjær, I. and Bagheri, A. (1999) 'Prenatal Development of the Alveolar Bone of Human Deciduous Incisors and Canines', *Journal of Dental Research*. doi: 10.1177/00220345990780020601.
- Klein-Nulend, J. *et al.* (2003) 'Microgravity and bone cell mechanosensitivity', *Advances in Space Research*, 32(8), pp. 1551–1559. doi: 10.1016/S0273-1177(03)90395-4.
- Klein-Nulend, J., Bacabac, R. G. and Bakker, A. D. (2012) 'Mechanical loading and how it affects bone cells: the role of the osteocyte cytoskeleton in maintaining our skeleton.', *European cells & materials*, 24, pp. 278–91.

- Kleinhans, C. *et al.* (2015) 'Comparison of osteoclastogenesis and resorption activity of human osteoclasts on tissue culture polystyrene and on natural extracellular bone matrix in 2D and 3D', *Journal of Biotechnology*, 205, pp. 101–110. doi: 10.1016/j.jbiotec.2014.11.039.
- Koga, T. *et al.* (2005) 'NFAT and Osterix cooperatively regulate bone formation', *Nature Medicine*, 11(8), pp. 880–885. doi: 10.1038/nm1270.
- Kolf, C. M., Cho, E. and Tuan, R. S. (2007) 'Mesenchymal stromal cells. Biology of adult mesenchymal stem cells: regulation of niche, self-renewal and differentiation.', *Arthritis research & therapy*. BioMed Central, 9(1), p. 204. doi: 10.1186/ar2116.
- Komori, T. *et al.* (1997) 'Targeted disruption of Cbfa1 results in a complete lack of bone formation owing to maturational arrest of osteoblasts.', *Cell*, 89(5), pp. 755–64. doi: 10.1016/s0092-8674(00)80258-5.
- Kondo, M. *et al.* (2003) 'Biology of hematopoietic stem cells and progenitors: implications for clinical application', *Annual Review of Immunology*, 21(1), pp. 759–806. doi: 10.1146/annurev.immunol.21.120601.141007.
- Koons, A. *et al.* (2008) 'Even ephemeral endotoxin exposure establishes endotoxin tolerance', *Journal of Trauma - Injury, Infection and Critical Care*. doi: 10.1097/TA.0b013e318166b7f3.
- Kornak, U. and Mundlos, S. (2003) 'Genetic disorders of the skeleton: A developmental approach', *American Journal of Human Genetics*. doi: 10.1086/377110.
- Koseki, H. *et al.* (2019) 'Two Diverse Hemodynamic Forces, a Mechanical Stretch and a High Wall Shear Stress, Determine Intracranial Aneurysm Formation', *Translational Stroke Research*. Springer US, pp. 1–13. doi: 10.1007/s12975-019-0690-y.
- Kramann, R. *et al.* (2016) 'Adventitial MSC-like Cells Are Progenitors of Vascular Smooth Muscle Cells and Drive Vascular Calcification in Chronic Kidney Disease.', *Cell stem cell*. NIH Public Access, 19(5), pp. 628–642. doi: 10.1016/j.stem.2016.08.001.
- Krishnan, V. and Davidovitch, Z. (2006) 'Cellular, molecular, and tissue-level reactions to orthodontic force', *American Journal of Orthodontics and Dentofacial Orthopedics*, 129(4), pp. 1–32. doi: 10.1016/j.ajodo.2005.10.007.
- Krishnan, V. and Davidovitch, Z. (2009) 'On a Path to Unfolding the Biological Mechanisms of Orthodontic Tooth Movement', *Journal of Dental Research*, 88(7), pp. 597–608. doi: 10.1177/0022034509338914.
- Kuipers, H. F. *et al.* (2016) 'Hyaluronan synthesis is necessary for autoreactive T-cell trafficking, activation, and Th1 polarization', *Proceedings of the National Academy of Sciences*, 113(5), pp. 1339–1344. doi: 10.1073/pnas.1525086113.
- Kulms, D. *et al.* (2002) 'Apoptosis induced by disruption of the actin cytoskeleton is mediated via activation of CD95 (Fas/APO-1)', *Cell Death and Differentiation*. doi: 10.1038/sj.cdd.4401002.
- Kultti, A. *et al.* (2006) 'Hyaluronan Synthesis Induces Microvillus-like Cell Surface Protrusions', *Journal of Biological Chemistry*. American Society for Biochemistry and Molecular Biology, 281(23), pp. 15821–15828. doi: 10.1074/JBC.M512840200.
- Kumada, H. *et al.* (1995) 'Structural study on the free lipid A isolated from lipopolysaccharide of *Porphyromonas gingivalis*.', *Journal of Bacteriology*, 177(8), pp. 2098–2106. doi: 10.1128/jb.177.8.2098-2106.1995.
- Kumada, H. *et al.* (2008) 'Biological properties of the native and synthetic lipid a of *Porphyromonas gingivalis* lipopolysaccharide', *Oral Microbiology and Immunology*. doi:

10.1111/j.1399-302X.2007.00392.x.

Kurazumi, H. *et al.* (2011) 'The effects of mechanical stress on the growth, differentiation, and paracrine factor production of cardiac stem cells', *PLoS ONE*, 6(12), p. e28890. doi: 10.1371/journal.pone.0028890.

Kwon, D. *et al.* (2016) 'The Effect of Fetal Bovine Serum (FBS) on Efficacy of Cellular Reprogramming for Induced Pluripotent Stem Cell (iPSC) Generation', *Cell Transplantation*. SAGE PublicationsSage CA: Los Angeles, CA, 25(6), pp. 1025–1042. doi: 10.3727/096368915X689703.

Lacey, D. L. *et al.* (1994) 'Interleukin 4 enhances osteoblast macrophage colony-stimulating factor, but not interleukin 6, production.', *Calcified tissue international*, 55(1), pp. 21–8.

Lakschevitz, F. *et al.* (2011) 'Diabetes and periodontal diseases: interplay and links.', *Current diabetes reviews*, 7(6), pp. 433–9.

Langenbach, F. and Handschel, J. (2013) 'Effects of dexamethasone, ascorbic acid and beta-glycerophosphate on the osteogenic differentiation of stem cells in vitro', *Stem Cell Res Ther*, 4(5), p. 117. doi: 10.1186/scrt328.

Laurent, T. C. and Fraser, J. R. (1992) 'Hyaluronan.', *FASEB journal : official publication of the Federation of American Societies for Experimental Biology*, 6(7), pp. 2397–404. doi: 10.1096/FASEBJ.6.7.1563592.

Lecuit, T. (2010) 'α-catenin mechanosensing for adherens junctions', *Nature Cell Biology*, 12(6), pp. 522–524. doi: 10.1038/ncb2066.

Lee, J. D. *et al.* (1992) 'Transfection of CD14 into 70Z/3 cells dramatically enhances the sensitivity to complexes of lipopolysaccharide (LPS) and LPS binding protein.', *The Journal of experimental medicine*, 175(6), pp. 1697–705.

Lee, J. E. and Lee, D. R. (2011) 'Human embryonic stem cells: derivation, maintenance and cryopreservation.', *International journal of stem cells*. Korean Society for Stem Cell Research, 4(1), pp. 9–17.

Lee, S. K., Goldring, S. R. and Lorenzo, J. A. (1995) 'Expression of the calcitonin receptor in bone marrow cell cultures and in bone: a specific marker of the differentiated osteoclast that is regulated by calcitonin.', *Endocrinology*, 136(10), pp. 4572–4581. doi: 10.1210/endo.136.10.7664679.

Lefebvre, V. and Bhattaram, P. (2010) 'Vertebrate skeletogenesis.', *Current topics in developmental biology*. NIH Public Access, 90, pp. 291–317. doi: 10.1016/S0070-2153(10)90008-2.

Lesley, J. *et al.* (1997) 'CD44 in inflammation and metastasis', *Glycoconjugate Journal*. Kluwer Academic Publishers, 14(5), pp. 611–622. doi: 10.1023/A:1018540610858.

Lesley, J. *et al.* (2000) 'Hyaluronan Binding by Cell Surface CD44', *Journal of Biological Chemistry*, 275(35), pp. 26967–75. doi: 10.1074/jbc.M002527200.

Levine, B., Packer, M. and Codogno, P. (2015) 'Development of autophagy inducers in clinical medicine', *Journal of Clinical Investigation*. doi: 10.1172/JCI73938.

Li, J. *et al.* (2000) 'RANK is the intrinsic hematopoietic cell surface receptor that controls osteoclastogenesis and regulation of bone mass and calcium metabolism.', *Proceedings of the National Academy of Sciences of the United States of America*. National Academy of Sciences, 97(4), pp. 1566–71.

Li, P. *et al.* (2016) 'Endotoxin Tolerance Inhibits Degradation of Tumor Necrosis Factor

Receptor–Associated Factor 3 by Suppressing Pellino 1 Expression and the K48 Ubiquitin Ligase Activity of Cellular Inhibitor of Apoptosis Protein 2', *Journal of Infectious Diseases*, 214(6), pp. 906–915. doi: 10.1093/infdis/jiw279.

Li, Y. *et al.* (2007) 'Hyaluronan in limb morphogenesis.' NIH Public Access, 305(2). doi: 10.1016/j.ydbio.2007.02.023.

Li, Z. H. *et al.* (2017) 'High-dose PMA with RANKL and MCSF induces THP-1 cell differentiation into human functional osteoclasts in vitro', *Molecular Medicine Reports*. Spandidos Publications, 16(6), pp. 8380–8384. doi: 10.3892/mmr.2017.7625.

Lien, E. *et al.* (1999) 'Toll-like receptor 2 functions as a pattern recognition receptor for diverse bacterial products.', *The Journal of biological chemistry*, 274(47), pp. 33419–25.

Lin, N.-Y. *et al.* (2016) 'Inactivation of autophagy ameliorates glucocorticoid-induced and ovariectomy-induced bone loss', *Annals of the Rheumatic Diseases*, 75(6), pp. 1203–1210. doi: 10.1136/annrheumdis-2015-207240.

Lin, S. *et al.* (2014) 'Constitutive Nuclear Expression of Dentin Matrix Protein 1 Fails to Rescue the Dmp1 -null Phenotype', *Journal of Biological Chemistry*, 289(31), pp. 21533–21543. doi: 10.1074/jbc.M113.543330.

Little, R. M., Riedel, R. A. and Artun, J. (1988) 'An evaluation of changes in mandibular anterior alignment from 10 to 20 years postretention', *American Journal of Orthodontics and Dentofacial Orthopedics*. doi: 10.1016/0889-5406(88)90102-3.

Littlewood, S. J., Kandasamy, S. and Huang, G. (2017) 'Retention and relapse in clinical practice', *Australian Dental Journal*. doi: 10.1111/adj.12475.

Litwiniuk, M. *et al.* (2016) 'Hyaluronic Acid in Inflammation and Tissue Regeneration.', *Wounds : a compendium of clinical research and practice*, 28(3), pp. 78–88.

Liu, C. *et al.* (2014) 'Effect of Static Pre-stretch Induced Surface Anisotropy on Orientation of Mesenchymal Stem Cells', *Cellular and Molecular Bioengineering*. NIH Public Access, 7(1), pp. 106–121. doi: 10.1007/s12195-013-0300-0.

Liu, F. *et al.* (2010) 'FIP200 is required for the cell-autonomous maintenance of fetal hematopoietic stem cells', *Blood*, 116(23), pp. 4806–4814. doi: 10.1182/blood-2010-06-288589.

Liu, G. *et al.* (2015) 'ROS activates JNK-mediated autophagy to counteract apoptosis in mouse mesenchymal stem cells in vitro.', *Acta pharmacologica Sinica*. Nature Publishing Group, 36(12), pp. 1473–9. doi: 10.1038/aps.2015.101.

Liu, Y. *et al.* (2008) 'Periodontal Ligament Stem Cell-Mediated Treatment for Periodontitis in Miniature Swine', *Stem Cells*. NIH Public Access, 26(4), pp. 1065–1073. doi: 10.1634/stemcells.2007-0734.

Liu, Y. S. *et al.* (2015) 'Mechanosensitive TRPM7 mediates shear stress and modulates osteogenic differentiation of mesenchymal stromal cells through Osterix pathway', *Scientific Reports*. doi: 10.1038/srep16522.

Long, F. (2012) 'Building strong bones: molecular regulation of the osteoblast lineage', *Nature Reviews Molecular Cell Biology*, 13(1), pp. 27–38. doi: 10.1038/nrm3254.

López-Collazo, E., Fresno, C. del and del Fresno, C. (2013) 'Pathophysiology of endotoxin tolerance: mechanisms and clinical consequences', *Critical Care*. BioMed Central, 17(6), p. 242.

Lu, W. *et al.* (2018) 'Tolerance induced by porphyromonas gingivalis may occur independently of TLR2 and TLR4', *PLoS ONE*. doi: 10.1371/journal.pone.0200946.

- Lu, Y. *et al.* (2012) 'An overview of tubulin inhibitors that interact with the colchicine binding site', *Pharmaceutical Research*. doi: 10.1007/s11095-012-0828-z.
- Lu, Y. C., Yeh, W. C. and Ohashi, P. S. (2008) 'LPS/TLR4 signal transduction pathway', *Cytokine*, pp. 145–151. doi: 10.1016/j.cyto.2008.01.006.
- Lum, L. *et al.* (1999) 'Evidence for a role of a tumor necrosis factor-alpha (TNF-alpha)-converting enzyme-like protease in shedding of TRANCE, a TNF family member involved in osteoclastogenesis and dendritic cell survival.', *The Journal of biological chemistry*, 274(19), pp. 13613–8.
- Lumeng, C. N., Bodzin, J. L. and Saltiel, A. R. (2007) 'Obesity induces a phenotypic switch in adipose tissue macrophage polarization', *Journal of Clinical Investigation*, 117(1), pp. 175–184. doi: 10.1172/JCI29881.
- Lund, M. E. *et al.* (2016) 'The choice of phorbol 12-myristate 13-acetate differentiation protocol influences the response of THP-1 macrophages to a pro-inflammatory stimulus', *Journal of Immunological Methods*. Elsevier, 430, pp. 64–70. doi: 10.1016/j.jim.2016.01.012.
- Luo, Z.-J. and Seedhom, B. B. (2007) 'Light and low-frequency pulsatile hydrostatic pressure enhances extracellular matrix formation by bone marrow mesenchymal cells: An *in-vitro* study with special reference to cartilage repair', *Proceedings of the Institution of Mechanical Engineers, Part H: Journal of Engineering in Medicine*, 221(5), pp. 499–507. doi: 10.1243/09544119JEIM199.
- Mabuchi, Y. *et al.* (2013) 'LNGFR+THY-1+VCAM-1hi+ Cells Reveal Functionally Distinct Subpopulations in Mesenchymal Stem Cells', *Stem Cell Reports*, 1(2), pp. 152–165. doi: 10.1016/j.stemcr.2013.06.001.
- Madeo, F. *et al.* (2019) 'Spermidine: a physiological autophagy inducer acting as an anti-aging vitamin in humans?', *Autophagy*. Taylor & Francis, 15(1), p. 165. doi: 10.1080/15548627.2018.1530929.
- Magara, J. *et al.* (2012) 'Alterations in intermediate filaments expression in disc cells from the rat temporomandibular joint following exposure to continuous compressive force', *Journal of Anatomy*. Wiley-Blackwell, 220(6), pp. 612–621. doi: 10.1111/j.1469-7580.2012.01501.x.
- Maitra, U. *et al.* (2012) 'Molecular Mechanisms Responsible for the Selective and Low-Grade Induction of Proinflammatory Mediators in Murine Macrophages by Lipopolysaccharide', *The Journal of Immunology*, 189(2), pp. 1014–1023. doi: 10.4049/jimmunol.1200857.
- Mammoto, A. *et al.* (2009) 'A mechanosensitive transcriptional mechanism that controls angiogenesis', *Nature*. Nature Publishing Group, 457(7233), pp. 1103–1108. doi: 10.1038/nature07765.
- Mammoto, T. and Ingber, D. E. (2010) 'Mechanical control of tissue and organ development', *Development*, 137(9), pp. 1407–1420. doi: 10.1242/dev.024166.
- Mandl, M. *et al.* (2014) 'Characterization of the CD14++CD16+ monocyte population in human bone marrow.', *PloS one*. Public Library of Science, 9(11), p. e112140. doi: 10.1371/journal.pone.0112140.
- Mantovani, A. *et al.* (2004) 'The chemokine system in diverse forms of macrophage activation and polarization', *Trends in Immunology*, 25(12), pp. 677–686. doi: 10.1016/j.it.2004.09.015.
- Marinković, M. *et al.* (2018) 'Autophagy modulation in cancer: Current knowledge on action and therapy', *Oxidative Medicine and Cellular Longevity*. doi: 10.1155/2018/8023821.
- Marino, S. *et al.* (2014) 'Generation and culture of osteoclasts', *BoneKEy Reports*. Nature

Publishing Group, 3, p. 570. doi: 10.1038/bonekey.2014.65.

Marrie, T. J. *et al.* (1998) 'Community-acquired pneumonia due to *Escherichia coli*.', *Clinical microbiology and infection : the official publication of the European Society of Clinical Microbiology and Infectious Diseases*, 4(12), pp. 717–723.

Martinez, F. O. and Gordon, S. (2014) 'The M1 and M2 paradigm of macrophage activation: time for reassessment.', *F1000prime reports*. Faculty of 1000 Ltd, 6, p. 13. doi: 10.12703/P6-13.

Martino, F. *et al.* (2018) *Cellular mechanotransduction: From tension to function*, *Frontiers in Physiology*. doi: 10.3389/fphys.2018.00824.

Matsumoto, M. *et al.* (2004) 'Essential role of p38 mitogen-activated protein kinase in cathepsin K gene expression during osteoclastogenesis through association of NFATc1 and PU.1.', *The Journal of biological chemistry*. American Society for Biochemistry and Molecular Biology, 279(44), pp. 45969–79. doi: 10.1074/jbc.M408795200.

Matsunaga, K. *et al.* (2009) 'Two Beclin 1-binding proteins, Atg14L and Rubicon, reciprocally regulate autophagy at different stages', *Nature Cell Biology*, 11(4), pp. 385–396. doi: 10.1038/ncb1846.

Matsunaga, N. *et al.* (2011) 'TAK-242 (Resatorvid), a Small-Molecule Inhibitor of Toll-Like Receptor (TLR) 4 Signaling, Binds Selectively to TLR4 and Interferes with Interactions between TLR4 and Its Adaptor Molecules', *Molecular Pharmacology*, 79(1), pp. 34–41. doi: 10.1124/mol.110.068064.

Matsuoka, K. *et al.* (2014) 'Osteoclast-Derived Complement Component 3a Stimulates Osteoblast Differentiation', *Journal of Bone and Mineral Research*, 29(7), pp. 1522–1530. doi: 10.1002/jbmr.2187.

Matsuzaki, K. *et al.* (1998) 'Osteoclast Differentiation Factor (ODF) Induces Osteoclast-like Cell Formation in Human Peripheral Blood Mononuclear Cell Cultures', *Biochemical and Biophysical Research Communications*, 246(1), pp. 199–204. doi: 10.1006/bbrc.1998.8586.

Mauthe, M. *et al.* (2018) 'Chloroquine inhibits autophagic flux by decreasing autophagosome-lysosome fusion', *Autophagy*. doi: 10.1080/15548627.2018.1474314.

Mavreas, D. and Athanasiou, A. E. (2008) 'Factors affecting the duration of orthodontic treatment: a systematic review', *European Journal of Orthodontics*. Narnia, 30(4), pp. 386–395. doi: 10.1093/ejo/cjn018.

McBeath, R. *et al.* (2004) 'Cell shape, cytoskeletal tension, and RhoA regulate stem cell lineage commitment', *Developmental Cell*, 6(4), pp. 483–495. doi: 10.1016/S1534-5807(04)00075-9.

McCall, C. E. *et al.* (1993) 'Tolerance to endotoxin-induced expression of the interleukin-1 beta gene in blood neutrophils of humans with the sepsis syndrome.', *Journal of Clinical Investigation*, 91(3), pp. 853–861. doi: 10.1172/JCI116306.

McCarthy, J. G. *et al.* (2001) 'Distraction Osteogenesis of the Craniofacial Skeleton', *Plastic and Reconstructive Surgery*, 107(7), pp. 1812–1824. doi: 10.1097/00006534-200106000-00029.

McKee, C. M. *et al.* (1996) 'Hyaluronan (HA) fragments induce chemokine gene expression in alveolar macrophages. The role of HA size and CD44.', *Journal of Clinical Investigation*, 98(10), pp. 2403–2413. doi: 10.1172/JCI119054.

Meazzini, M. C. *et al.* (1998) 'Osteoblast cytoskeletal modulation in response to mechanical strain In Vitro', *Journal of Orthopaedic Research*. doi: 10.1002/jor.1100160204.

Medvedev, A. E. *et al.* (2007) 'Role of TLR4 tyrosine phosphorylation in signal transduction and

- endotoxin tolerance.', *The Journal of biological chemistry*. NIH Public Access, 282(22), pp. 16042–53. doi: 10.1074/jbc.M606781200.
- Medvedev, A. E., Kopydlowski, K. M. and Vogel, S. N. (2000) 'Inhibition of Lipopolysaccharide-Induced Signal Transduction in Endotoxin-Tolerized Mouse Macrophages: Dysregulation of Cytokine, Chemokine, and Toll-Like Receptor 2 and 4 Gene Expression', *The Journal of Immunology*, 164(11), pp. 5564–5574. doi: 10.4049/jimmunol.164.11.5564.
- Medvedev, A. E. and Vogel, S. N. (2003) 'Overexpression of CD14, TLR4, and MD-2 in HEK 293T cells does not prevent induction of in vitro endotoxin tolerance', *Journal of Endotoxin Research*, 9(1), pp. 60–64. doi: 10.1179/096805103125001360.
- Medvinsky, A. and Dzierzak, E. (1996) 'Definitive hematopoiesis is autonomously initiated by the AGM region.', *Cell*. Elsevier, 86(6), pp. 897–906. doi: 10.1016/S0092-8674(00)80165-8.
- Mehrpour, M. *et al.* (2010) 'Overview of macroautophagy regulation in mammalian cells', *Cell Research*, 20(7), pp. 748–762. doi: 10.1038/cr.2010.82.
- Meikle, M. C. (2005) 'The tissue, cellular, and molecular regulation of orthodontic tooth movement: 100 years after Carl Sandstedt', *The European Journal of Orthodontics*. Narnia, 28(3), pp. 221–240. doi: 10.1093/ejo/cjl001.
- Mendichi, R., Šoltés, L. and Giacometti Schieron, A. (2003) 'Evaluation of radius of gyration and intrinsic viscosity molar mass dependence and stiffness of hyaluronan', *Biomacromolecules*. American Chemical Society, 4(6), pp. 1805–1810. doi: 10.1021/bm0342178.
- Meng, Y. *et al.* (2018) 'Nicotinamide Promotes Cell Survival and Differentiation as Kinase Inhibitor in Human Pluripotent Stem Cells', *Stem Cell Reports*, 11(6), pp. 1347–1356. doi: 10.1016/j.stemcr.2018.10.023.
- Merrild, D. M. *et al.* (2015) 'Pit- and trench-forming osteoclasts: a distinction that matters.', *Bone research*. Nature Publishing Group, 3, p. 15032. doi: 10.1038/boneres.2015.32.
- Meyer, J. *et al.* (2005) 'Tonic mechanosensitivity of outer hair cells after loss of tip links', *Hearing Research*, 202(1–2), pp. 97–113. doi: 10.1016/j.heares.2004.11.013.
- Millan, C. *et al.* (2018) 'Mesenchymal Stem Cells and Calcium Phosphate Bioceramics: Implications in Periodontal Bone Regeneration', in *Advances in experimental medicine and biology*, pp. 91–112. doi: 10.1007/5584_2018_249.
- Misra, S. *et al.* (2015) 'Interactions between Hyaluronan and Its Receptors (CD44, RHAMM) Regulate the Activities of Inflammation and Cancer.', *Frontiers in immunology*. Frontiers Media SA, 6, p. 201. doi: 10.3389/fimmu.2015.00201.
- Mizushima, N., Yoshimori, T. and Levine, B. (2010) 'Methods in Mammalian Autophagy Research', *Cell*, 140(3), pp. 313–326. doi: 10.1016/j.cell.2010.01.028.
- Monasterio, G. *et al.* (2019) 'Immunostimulatory activity of low-molecular-weight hyaluronan on dendritic cells stimulated with *Aggregatibacter actinomycetemcomitans* or *Porphyromonas gingivalis*', *Clinical Oral Investigations*. doi: 10.1007/s00784-018-2641-5.
- Moraes, C. *et al.* (2010) 'Microfabricated arrays for high-throughput screening of cellular response to cyclic substrate deformation.', *Lab on a chip*, 10(2), pp. 227–34. doi: 10.1039/b914460a.
- Moreau, K., Renna, M. and Rubinsztein, D. C. (2013) 'Connections between SNAREs and autophagy.', *Trends in biochemical sciences*. Elsevier, 38(2), pp. 57–63. doi: 10.1016/j.tibs.2012.11.004.

- Moreno, J. L. *et al.* (2003) 'IL-4 suppresses osteoclast development and mature osteoclast function by a STAT6-dependent mechanism: irreversible inhibition of the differentiation program activated by RANKL', *Blood*, 102(3), pp. 1078–1086. doi: 10.1182/blood-2002-11-3437.
- Moretto, P. *et al.* (2015) 'Regulation of Hyaluronan Synthesis in Vascular Diseases and Diabetes', *Journal of Diabetes Research*. Hindawi, 2015, pp. 1–9. doi: 10.1155/2015/167283.
- Morioka, M. *et al.* (2011) 'Microtubule dynamics regulate cyclic stretch-induced cell alignment in human airway smooth muscle cells', *PLoS ONE*. doi: 10.1371/journal.pone.0026384.
- Mortensen, M. *et al.* (2011) 'The autophagy protein Atg7 is essential for hematopoietic stem cell maintenance', *The Journal of Experimental Medicine*, 208(3), pp. 455–467. doi: 10.1084/jem.20101145.
- Mosser, D. M. and Edwards, J. P. (2008) 'Exploring the full spectrum of macrophage activation', *Nature Reviews Immunology*. Nature Publishing Group, 8(12), pp. 958–969. doi: 10.1038/nri2448.
- Motiur Rahman, M. *et al.* (2015) 'Proliferation-coupled osteoclast differentiation by RANKL: Cell density as a determinant of osteoclast formation', *Bone*. Elsevier, 81, pp. 392–399. doi: 10.1016/j.BONE.2015.08.008.
- Muhamed, I., Chowdhury, F. and Maruthamuthu, V. (2017) 'Biophysical Tools to Study Cellular Mechanotransduction.', *Bioengineering (Basel, Switzerland)*. Multidisciplinary Digital Publishing Institute (MDPI), 4(1). doi: 10.3390/bioengineering4010012.
- Müllegger, J. *et al.* (2003) "'Piggy-Back" Transport of Xenopus Hyaluronan Synthase (XHAS1) via the Secretory Pathway to the Plasma Membrane', *Biological Chemistry*, 384(1), pp. 175–82. doi: 10.1515/BC.2003.019.
- Müller, A. M. *et al.* (1994) 'Development of hematopoietic stem cell activity in the mouse embryo.', *Immunity*. Elsevier, 1(4), pp. 291–301. doi: 10.1016/1074-7613(94)90081-7.
- Müller, P. *et al.* (2007) 'Calcium phosphate surfaces promote osteogenic differentiation of mesenchymal stem cells', *Journal of Cellular and Molecular Medicine*, 12(1), pp. 281–291. doi: 10.1111/j.1582-4934.2007.00103.x.
- Munford, R. S. (2010) 'Murine responses to endotoxin: another dirty little secret?', *The Journal of infectious diseases*. NIH Public Access, 201(2), pp. 175–7. doi: 10.1086/649558.
- Munoz, C. *et al.* (1991) 'Dysregulation of in vitro cytokine production by monocytes during sepsis.', *The Journal of clinical investigation*. American Society for Clinical Investigation, 88(5), pp. 1747–54. doi: 10.1172/JCI115493.
- Murad, S. *et al.* (1981) 'Regulation of collagen synthesis by ascorbic acid.', *Proceedings of the National Academy of Sciences*, 78(5), pp. 2879–2882. doi: 10.1073/pnas.78.5.2879.
- Murray, P. J. *et al.* (2014) 'Macrophage Activation and Polarization: Nomenclature and Experimental Guidelines', *Immunity*. NIH Public Access, pp. 14–20. doi: 10.1016/j.immuni.2014.06.008.
- Murshed, M. (2018) 'Mechanism of Bone Mineralization', *Cold Spring Harbor Perspectives in Medicine*, 8(12), p. a031229. doi: 10.1101/cshperspect.a031229.
- Muthukuru, M., Jotwani, R. and Cutler, C. W. (2005) 'Oral mucosal endotoxin tolerance induction in chronic periodontitis', *Infection and Immunity*. doi: 10.1128/IAI.73.2.687-694.2005.
- Myeku, N. and Figueiredo-Pereira, M. E. (2011) 'Dynamics of the Degradation of Ubiquitinated

- Proteins by Proteasomes and Autophagy', *Journal of Biological Chemistry*, 286(25), pp. 22426–22440. doi: 10.1074/jbc.M110.149252.
- Na, S. *et al.* (2008) 'Rapid signal transduction in living cells is a unique feature of mechanotransduction', *Proceedings of the National Academy of Sciences*, 105(18), pp. 6626–6631. doi: 10.1073/pnas.0711704105.
- Nagano, O. and Saya, H. (2004) 'Mechanism and biological significance of CD44 cleavage', *Cancer Science*, 95(12), pp. 930–935. doi: 10.1111/j.1349-7006.2004.tb03179.x.
- Nagy, N. *et al.* (2015) 'Inhibition of hyaluronan synthesis restores immune tolerance during autoimmune insulinitis', *Journal of Clinical Investigation*. doi: 10.1172/JCI79271.
- Nahid, M. A. *et al.* (2009) 'miR-146a Is Critical for Endotoxin-induced Tolerance', *Journal of Biological Chemistry*, 284(50), pp. 34590–34599. doi: 10.1074/jbc.M109.056317.
- Naito, M. *et al.* (1991) 'Abnormal differentiation of tissue macrophage populations in "osteopetrosis" (op) mice defective in the production of macrophage colony-stimulating factor.', *The American journal of pathology*, 139(3), pp. 657–67.
- Nakagawa, I. *et al.* (2004) 'Autophagy defends cells against invading group A Streptococcus', *Science*. doi: 10.1126/science.1103966.
- Nakamura, H. *et al.* (2004) 'Immunolocalization of matrix metalloproteinase-13 on bone surface under osteoclasts in rat tibia.', *Bone*, 34(1), pp. 48–56.
- Nakamura, H. (2007) 'Morphology, Function, and Differentiation of Bone Cells', *Journal of Hard Tissue Biology*. THE SOCIETY FOR HARD TISSUE REGENERATIVE BIOLOGY, 16(1), pp. 15–22. doi: 10.2485/jhtb.16.15.
- Nakano, T. *et al.* (2014) 'Effects of different types of tooth movement and force magnitudes on the amount of tooth movement and root resorption in rats', *Angle Orthodontist*, 84(6), pp. 1079–1085. doi: 10.2319/121913-929.1.
- Nakashima, K. *et al.* (2002) 'The novel zinc finger-containing transcription factor osterix is required for osteoblast differentiation and bone formation.', *Cell*, 108(1), pp. 17–29.
- Nanci, A. (1999) 'Content and Distribution of Noncollagenous Matrix Proteins in Bone and Cementum: Relationship to Speed of Formation and Collagen Packing Density', *Journal of Structural Biology*. Academic Press, 126(3), pp. 256–269. doi: 10.1006/JSBI.1999.4137.
- Narayanan, K. *et al.* (2003) 'Dual Functional Roles of Dentin Matrix Protein 1', *Journal of Biological Chemistry*, 278(19), pp. 17500–17508. doi: 10.1074/jbc.M212700200.
- Natrel, B. *et al.* (2017) 'Porphyromonas gingivalis lipopolysaccharides act exclusively through TLR4 with a resilience between mouse and human', *Scientific Reports*. Nature Publishing Group, 7(1), p. 15789. doi: 10.1038/s41598-017-16190-y.
- Natu, S. S. *et al.* (2014) 'The biology of distraction osteogenesis for correction of mandibular and craniomaxillofacial defects: A review.', *Dental research journal*, 11(1), pp. 16–26.
- Neidlinger-Wilke, C. *et al.* (1994) 'Cyclic stretching of human osteoblasts affects proliferation and metabolism: A new experimental method and its application', *Journal of Orthopaedic Research*, 12(1), pp. 70–78. doi: 10.1002/jor.1100120109.
- Ng TC, Chiu KW, Rabie AB, H. U. *et al.* (2006) 'Repeated Mechanical Loading Enhances the Expression of Indian Hedgehog in Condylar Cartilage', *Frontiers in Bioscience*, 11(1), p. 943. doi: 10.2741/1850.
- Nguyen, C. M. *et al.* (2015) 'Periodontal associations in cardiovascular diseases: The latest

- evidence and understanding', *Journal of Oral Biology and Craniofacial Research*. Elsevier, 5(3), pp. 203–206. doi: 10.1016/J.JOBCR.2015.06.008.
- Nobuto, T. *et al.* (2003) 'Microvascular Response in the Periodontal Ligament Following Mucoperiosteal Flap Surgery', *Journal of Periodontology*. doi: 10.1902/jop.2003.74.4.521.
- Nollet, M. *et al.* (2014) 'Autophagy in osteoblasts is involved in mineralization and bone homeostasis', *Autophagy*. Taylor & Francis, 10(11), pp. 1965–1977. doi: 10.4161/auto.36182.
- Nombela-Arrieta, C. *et al.* (2013) 'Quantitative imaging of haematopoietic stem and progenitor cell localization and hypoxic status in the bone marrow microenvironment', *Nature Cell Biology*, 15(5), pp. 533–543. doi: 10.1038/ncb2730.
- Nombela-Arrieta, C., Ritz, J. and Silberstein, L. E. (2011) 'The elusive nature and function of mesenchymal stem cells', *Nature Reviews Molecular Cell Biology*, 12(2), pp. 126–131. doi: 10.1038/nrm3049.
- Novack, D. V. (2016) 'Inflammatory Osteoclasts: A Different Breed of Bone Eaters?', *Arthritis and Rheumatology*. doi: 10.1002/art.39835.
- O'Brien, E. A., Williams, J. H. H. and Marshall, M. J. (2000) 'Osteoprotegerin Ligand Regulates Osteoclast Adherence to the Bone Surface in Mouse Calvaria', *Biochemical and Biophysical Research Communications*, 274(2), pp. 281–290. doi: 10.1006/bbrc.2000.3129.
- O'Brien, M. *et al.* (2017) 'A bioluminescent caspase-1 activity assay rapidly monitors inflammasome activation in cells', *Journal of Immunological Methods*, 447, pp. 1–13. doi: 10.1016/j.jim.2017.03.004.
- Oami, T. *et al.* (2017) 'Suppression of T Cell Autophagy Results in Decreased Viability and Function of T Cells Through Accelerated Apoptosis in a Murine Sepsis Model', *Critical Care Medicine*. doi: 10.1097/CCM.0000000000002016.
- Ogawa, H. *et al.* (2003) 'Mechanisms of Endotoxin Tolerance in Human Intestinal Microvascular Endothelial Cells', *The Journal of Immunology*, 170(12), pp. 5956–5964. doi: 10.4049/jimmunol.170.12.5956.
- Oguchi, T. and Ishiguro, N. (2004) 'Differential Stimulation of Three Forms of Hyaluronan Synthase by TGF- β , IL-1 β , and TNF- α ', *Connective Tissue Research*, 45(4–5), pp. 197–205. doi: 10.1080/03008200490523031.
- Ohbayashi, N. *et al.* (2002) 'FGF18 is required for normal cell proliferation and differentiation during osteogenesis and chondrogenesis', *Genes & Development*, 16(7), pp. 870–879. doi: 10.1101/gad.965702.
- Okaji, M. *et al.* (2003) 'The regulation of bone resorption in tooth formation and eruption processes in mouse alveolar crest devoid of cathepsin k.', *Journal of pharmacological sciences*, 91(4), pp. 285–94.
- Oksayan, R., Sokucu, O. and Ucuncu, N. (2014) 'Effects of bite-jumping appliances on mandibular advancement in growing rats: A radiographic study.', *European journal of dentistry*. Dental Investigations Society, 8(3), pp. 291–5. doi: 10.4103/1305-7456.137624.
- Oliveira-Nascimento, L., Massari, P. and Wetzler, L. M. (2012) 'The Role of TLR2 in Infection and Immunity.', *Frontiers in immunology*. Frontiers Media SA, 3, p. 79. doi: 10.3389/fimmu.2012.00079.
- Oliver, L. *et al.* (2012) 'Basal Autophagy Decreased During the Differentiation of Human Adult Mesenchymal Stem Cells', *Stem Cells and Development*, 21(15), pp. 2779–2788. doi: 10.1089/scd.2012.0124.

- Orr, A. W. *et al.* (2006) 'Matrix-specific Suppression of Integrin Activation in Shear Stress Signaling', *Molecular Biology of the Cell*. Edited by R. Hynes, 17(11), pp. 4686–4697. doi: 10.1091/mbc.e06-04-0289.
- Osathanon, T. *et al.* (2013) 'Notch signaling is involved in neurogenic commitment of human periodontal ligament-derived mesenchymal stem cells', *Stem Cells and Development*. doi: 10.1089/scd.2012.0430.
- Otto, F. *et al.* (1997) 'Cbfa1, a candidate gene for cleidocranial dysplasia syndrome, is essential for osteoblast differentiation and bone development.', *Cell*, 89(5), pp. 765–71.
- Page, R. C. *et al.* (1997) 'Advances in the pathogenesis of periodontitis: summary of developments, clinical implications and future directions.', *Periodontology 2000*, 14, pp. 216–48.
- Pan, H. *et al.* (2013) 'Autophagic control of cell "stemness".' , *EMBO molecular medicine*. Wiley-Blackwell, 5(3), pp. 327–31. doi: 10.1002/emmm.201201999.
- Parada, C. and Chai, Y. (2015) 'Mandible and Tongue Development', in *Current Topics in Developmental Biology*. NIH Public Access, pp. 31–58. doi: 10.1016/bs.ctdb.2015.07.023.
- Park, D. *et al.* (2016) 'Resveratrol induces autophagy by directly inhibiting mTOR through ATP competition', *Scientific Reports*. Nature Publishing Group, 6(1), p. 21772. doi: 10.1038/srep21772.
- Park, E. K. *et al.* (2007) 'Optimized THP-1 differentiation is required for the detection of responses to weak stimuli', *Inflammation Research*. Birkhäuser-Verlag, 56(1), pp. 45–50. doi: 10.1007/s00011-007-6115-5.
- Passlick, B., Flieger, D. and Ziegler-Heitbrock, H. W. (1989) 'Identification and characterization of a novel monocyte subpopulation in human peripheral blood.', *Blood*, 74(7), pp. 2527–34.
- Pearson, O. M. and Lieberman, D. E. (2004) 'The aging of "Wolff's law": Ontogeny and responses to mechanical loading in cortical bone', *American Journal of Physical Anthropology*, 125(S39), pp. 63–99. doi: 10.1002/ajpa.20155.
- Pekovic, V. and Hutchison, C. J. (2008) 'Adult stem cell maintenance and tissue regeneration in the ageing context: the role for A-type lamins as intrinsic modulators of ageing in adult stem cells and their niches', *Journal of Anatomy*, 213(1), pp. 5–25. doi: 10.1111/j.1469-7580.2008.00928.x.
- Pelaez, D. *et al.* (2017) 'Cardiomyogenesis of periodontal ligament-derived stem cells by dynamic tensile strain', *Cell and Tissue Research*. doi: 10.1007/s00441-016-2503-x.
- Peled, T. *et al.* (2012) 'Nicotinamide, a SIRT1 inhibitor, inhibits differentiation and facilitates expansion of hematopoietic progenitor cells with enhanced bone marrow homing and engraftment', *Experimental Hematology*. Elsevier, 40(4), pp. 342-355.e1. doi: 10.1016/J.EXPHEM.2011.12.005.
- Pérez-Figueroa, E. *et al.* (2016) 'Activation of NLRP3 inflammasome in human neutrophils by *Helicobacter pylori* infection', *Innate Immunity*, 22(2), pp. 103–112. doi: 10.1177/1753425915619475.
- Persson, M. (2005) 'A 100th anniversary: Sandstedt's experiments on tissue changes during tooth movement', *Journal of Orthodontics*, 32(1), pp. 27–28. doi: 10.1179/146531205225020760.
- Peter, S. J. *et al.* (1998) 'Osteoblastic phenotype of rat marrow stromal cells cultured in the presence of dexamethasone, beta-glycerolphosphate, and L-ascorbic acid.', *Journal of cellular*

biochemistry, 71(1), pp. 55–62.

Piao, W. *et al.* (2009) 'Endotoxin tolerance dysregulates MyD88- and Toll/IL-1R domain-containing adapter inducing IFN-beta-dependent pathways and increases expression of negative regulators of TLR signaling.', *Journal of leukocyte biology*. The Society for Leukocyte Biology, 86(4), pp. 863–75. doi: 10.1189/jlb.0309189.

Pietras, E. M. (2017) 'Inflammation: a key regulator of hematopoietic stem cell fate in health and disease', *Blood*. American Society of Hematology, 130(15), pp. 1693–1698. doi: 10.1182/BLOOD-2017-06-780882.

Piper, K., Boyde, A. and Jones, S. J. (1992) 'The relationship between the number of nuclei of an osteoclast and its resorptive capability in vitro', *Anatomy and Embryology*. doi: 10.1007/BF00185977.

Pittenger, M. F. *et al.* (1999) 'Multilineage potential of adult human mesenchymal stem cells.', *Science (New York, N.Y.)*, 284(5411), pp. 143–7.

Plotkin, L. I. *et al.* (2005) 'Bisphosphonates and Estrogens Inhibit Osteocyte Apoptosis via Distinct Molecular Mechanisms Downstream of Extracellular Signal-regulated Kinase Activation', *Journal of Biological Chemistry*, 280(8), pp. 7317–7325. doi: 10.1074/jbc.M412817200.

Ponnaiyan, D. and Jegadeesan, V. (2014) 'Comparison of phenotype and differentiation marker gene expression profiles in human dental pulp and bone marrow mesenchymal stem cells.', *European journal of dentistry*. Dental Investigations Society, 8(3), pp. 307–13. doi: 10.4103/1305-7456.137631.

Ponta, H., Sherman, L. and Herrlich, P. A. (2003) *CD44: From adhesion molecules to signalling regulators*, *Nature Reviews Molecular Cell Biology*. Nature Publishing Group. doi: 10.1038/nrm1004.

Porter, K. M., Jeyabalan, N. and Liton, P. B. (2014) 'MTOR-independent induction of autophagy in trabecular meshwork cells subjected to biaxial stretch', *Biochimica et Biophysica Acta (BBA) - Molecular Cell Research*, 1843(6), pp. 1054–1062. doi: 10.1016/j.bbamcr.2014.02.010.

Poulin, A. *et al.* (2016) 'Dielectric elastomer actuator for mechanical loading of 2D cell cultures', *Lab Chip*, 16(19), pp. 3788–3794. doi: 10.1039/C6LC00903D.

Povea-Cabello, S. *et al.* (2017) 'Dynamic reorganization of the cytoskeleton during apoptosis: The two coffins hypothesis', *International Journal of Molecular Sciences*. doi: 10.3390/ijms18112393.

Powell, J. D. and Horton, M. R. (2005) 'Threat Matrix: Low-Molecular-Weight Hyaluronan (HA) as a Danger Signal', *Immunologic Research*, 31(3), pp. 207–218. doi: 10.1385/IR:31:3:207.

Qi, D., Hoelzle, D. J. and Rowat, A. C. (2012) 'Probing single cells using flow in microfluidic devices', *The European Physical Journal Special Topics*. Springer-Verlag, 204(1), pp. 85–101. doi: 10.1140/epjst/e2012-01554-x.

Qi, M. *et al.* (2017) 'Autophagy Maintains the Function of Bone Marrow Mesenchymal Stem Cells to Prevent Estrogen Deficiency-Induced Osteoporosis', *Theranostics*, 7(18), pp. 4498–4516. doi: 10.7150/thno.17949.

Quan, J. *et al.* (2018) 'Characterization of different osteoclast phenotypes in the progression of bone invasion by oral squamous cell carcinoma', *Oncology Reports*. Spandidos Publications, 39(3), pp. 1043–1051. doi: 10.3892/or.2017.6166.

Qureshi, N. *et al.* (1998) 'Natural and synthetic LPS and lipid a analogs or partial structures that

antagonize or induce tolerance to LPS.', *Progress in clinical and biological research*, 397, pp. 289–300.

Raetz, C. R. *et al.* (1991) 'Gram-negative endotoxin: an extraordinary lipid with profound effects on eukaryotic signal transduction.', *The FASEB Journal*, 5(12), pp. 2652–2660. doi: 10.1096/fasebj.5.12.1916089.

Raetz, C. R. H. and Whitfield, C. (2002) 'Lipopolysaccharide endotoxins.', *Annual review of biochemistry*. NIH Public Access, 71, pp. 635–700. doi: 10.1146/annurev.biochem.71.110601.135414.

Ravikumar, B. *et al.* (2004) 'Inhibition of mTOR induces autophagy and reduces toxicity of polyglutamine expansions in fly and mouse models of Huntington disease', *Nature Genetics*, 36(6), pp. 585–595. doi: 10.1038/ng1362.

Rayahin, J. E. *et al.* (2015) 'High and low molecular weight hyaluronic acid differentially influence macrophage activation.', *ACS biomaterials science & engineering*. NIH Public Access, 1(7), pp. 481–493. doi: 10.1021/acsbiomaterials.5b00181.

Reife, R. A. *et al.* (2006) 'Porphyromonas gingivalis lipopolysaccharide lipid A heterogeneity: differential activities of tetra- and penta-acylated lipid A structures on E-selectin expression and TLR4 recognition', *Cellular Microbiology*, 8(5), pp. 857–868. doi: 10.1111/j.1462-5822.2005.00672.x.

Ren, C. *et al.* (2017) 'Autophagy: A potential therapeutic target for reversing sepsis-induced immunosuppression', *Frontiers in Immunology*. doi: 10.3389/fimmu.2017.01832.

Rens, E. G. and Merks, R. M. H. (2017) 'Cell Contractility Facilitates Alignment of Cells and Tissues to Static Uniaxial Stretch.', *Biophysical journal*. The Biophysical Society, 112(4), pp. 755–766. doi: 10.1016/j.bpj.2016.12.012.

Rietschel, E. T. *et al.* (1994) 'Bacterial endotoxin: molecular relationships of structure to activity and function.', *FASEB journal : official publication of the Federation of American Societies for Experimental Biology*, 8(2), pp. 217–25.

Rietschel, E. T. and Cavaillon, J.-M. (2003) 'Richard Pfeiffer and Alexandre Besredka: creators of the concept of endotoxin and anti-endotoxin.', *Microbes and infection*, 5(15), pp. 1407–14.

Riggs, B. L. (2000) 'The mechanisms of estrogen regulation of bone resorption.', *The Journal of clinical investigation*. American Society for Clinical Investigation, 106(10), pp. 1203–4. doi: 10.1172/JCI11468.

Rilla, K. *et al.* (2005) 'Plasma membrane residence of hyaluronan synthase is coupled to its enzymatic activity', *Journal of Biological Chemistry*, 280(36), pp. 31890–31897. doi: 10.1074/jbc.M504736200.

Rilla, K. *et al.* (2013) 'Hyaluronan Synthase 1 (HAS1) Requires Higher Cellular UDP-GlcNAc Concentration than HAS2 and HAS3', *Journal of Biological Chemistry*. American Society for Biochemistry and Molecular Biology, 288(8), pp. 5973–5983. doi: 10.1074/JBC.M112.443879.

Rios, H. F. *et al.* (2008) 'Periostin Is Essential for the Integrity and Function of the Periodontal Ligament During Occlusal Loading in Mice', *Journal of Periodontology*, 79(8), pp. 1480–1490. doi: 10.1902/jop.2008.070624.

Robling, A. G., Castillo, A. B. and Turner, C. H. (2006) 'Biomechanical and molecular regulation of bone remodeling', *Annual Review of Biomedical Engineering*, 8(1), pp. 455–498. doi: 10.1146/annurev.bioeng.8.061505.095721.

Rocksén, D. *et al.* (2004) 'Lung effects during a generalized Shwartzman reaction and

- therapeutic intervention with dexamethasone or vitamin E.', *Shock (Augusta, Ga.)*, 22(5), pp. 482–90.
- Rodda, S. J. and McMahon, A. P. (2006) 'Distinct roles for Hedgehog and canonical Wnt signaling in specification, differentiation and maintenance of osteoblast progenitors.', *Development (Cambridge, England)*, 133(16), pp. 3231–44. doi: 10.1242/dev.02480.
- Rumpler, M. *et al.* (2013) 'Osteoclasts on bone and dentin in vitro: Mechanism of trail formation and comparison of resorption behavior', *Calcified Tissue International*. doi: 10.1007/s00223-013-9786-7.
- Rutkovskiy, A., Stensløkken, K.-O. and Vaage, I. J. (2016) 'Osteoblast Differentiation at a Glance.', *Medical science monitor basic research*. International Scientific Information, Inc., 22, pp. 95–106. doi: 10.12659/MSMBR.901142.
- Ryter, S. W., Mizumura, K. and Choi, A. M. K. (2014) 'The impact of autophagy on cell death modalities', *International Journal of Cell Biology*, 2014, p. 502676. doi: 10.1155/2014/502676.
- Ryu, J.-K. *et al.* (2017) 'Reconstruction of LPS Transfer Cascade Reveals Structural Determinants within LBP, CD14, and TLR4-MD2 for Efficient LPS Recognition and Transfer.', *Immunity*. Elsevier, 46(1), pp. 38–50. doi: 10.1016/j.immuni.2016.11.007.
- Saari, H. (1991) 'Oxygen derived free radicals and synovial fluid hyaluronate.', *Annals of the Rheumatic Diseases*, 50(6), pp. 389–392. doi: 10.1136/ard.50.6.389.
- Saitoh, T. *et al.* (2008) 'Loss of the autophagy protein Atg16L1 enhances endotoxin-induced IL-1 β production', *Nature*, 456(7219), pp. 264–268. doi: 10.1038/nature07383.
- Sakamoto, S. and Sakamoto, M. (1982) 'Biochemical and immunohistochemical studies on collagenase in resorbing bone in tissue culture. A novel hypothesis for the mechanism of bone resorption.', *Journal of periodontal research*, 17(5), pp. 523–6.
- van der Schaft, D. W. J. *et al.* (2011) 'Mechanoregulation of vascularization in aligned tissue-engineered muscle: a role for vascular endothelial growth factor.', *Tissue engineering. Part A*, 17(21–22), pp. 2857–65. doi: 10.1089/ten.TEA.2011.0214.
- Schieber, M. and Chandel, N. S. (2014) 'ROS Function in Redox Signaling and Oxidative Stress', *Current biology : CB*. NIH Public Access, 24(10), p. R453. doi: 10.1016/J.CUB.2014.03.034.
- Schlegel, P. G. *et al.* (2000) 'Characterization of osteoclast precursors in human blood.', *British journal of haematology*. Blackwell Science Ltd, 111(2), pp. 501–12. doi: 10.1046/j.1365-2141.2000.02379.x.
- Schuelke, J. *et al.* (2018) 'Intramembranous bone formation after callus distraction is augmented by increasing axial compressive strain', *PLOS ONE*. Edited by J. M. Garcia Aznar. Public Library of Science, 13(4), p. e0195466. doi: 10.1371/journal.pone.0195466.
- Sen, B. *et al.* (2015) 'Intranuclear Actin Regulates Osteogenesis', *Stem Cells*. doi: 10.1002/stem.2090.
- Sen, B. *et al.* (2017) 'Intranuclear Actin Structure Modulates Mesenchymal Stem Cell Differentiation', *Stem Cells*. doi: 10.1002/stem.2617.
- Sengupta, P. (2013) 'The Laboratory Rat: Relating Its Age With Human's.', *International journal of preventive medicine*. Wolters Kluwer -- Medknow Publications, 4(6), pp. 624–30.
- Seo, B. M. *et al.* (2004) 'Investigation of multipotent postnatal stem cells from human periodontal ligament', *Lancet*. doi: 10.1016/S0140-6736(04)16627-0.
- Serluca, F. C., Drummond, I. A. and Fishman, M. C. (2002) 'Endothelial Signaling in Kidney

- Morphogenesis: A Role for Hemodynamic Forces', *Current Biology*. Cell Press, 12(6), pp. 492–497. doi: 10.1016/S0960-9822(02)00694-2.
- Sfyroeras, G. S. *et al.* (2012) 'Association between periodontal disease and stroke', *Journal of Vascular Surgery*. Elsevier, 55(4), pp. 1178–1184. doi: 10.1016/j.jvs.2011.10.008.
- Shaker, J. L. (2009) 'Paget's Disease of Bone: A Review of Epidemiology, Pathophysiology and Management.', *Therapeutic advances in musculoskeletal disease*. SAGE Publications, 1(2), pp. 107–25. doi: 10.1177/1759720X09351779.
- Shapiro, F. (1988) 'Cortical bone repair. The relationship of the lacunar-canalicular system and intercellular gap junctions to the repair process.', *The Journal of bone and joint surgery. American volume*, 70(7), pp. 1067–81.
- Shapiro, I. M. *et al.* (2014) 'Boning up on autophagy :The role of autophagy in skeletal biology', *Autophagy*. Taylor & Francis, pp. 7–19. doi: 10.4161/auto.26679.
- Sharir, A. *et al.* (2011) 'Muscle force regulates bone shaping for optimal load-bearing capacity during embryogenesis.', *Development*. Oxford University Press for The Company of Biologists Limited, 138(15), pp. 3247–3259. doi: 10.1242/dev.063768.
- Sharma, Y., Astle, C. M. and Harrison, D. E. (2007) 'Heterozygous Kit Mutants with Little or No Apparent Anemia Exhibit Large Defects in Overall Hematopoietic Stem Cell Function', *Experimental Hematology*, 35(2), pp. 214.e1-214.e9. doi: 10.1016/j.exphem.2006.10.001.
- Shen, G. (2005) 'The role of type X collagen in facilitating and regulating endochondral ossification of articular cartilage', *Orthodontics and Craniofacial Research*, 8(1), pp. 11–17. doi: 10.1111/j.1601-6343.2004.00308.x.
- Shin, J. (1998) 'P62 and the sequestosome, a novel mechanism for protein metabolism.', *Archives of pharmacal research*, 21(6), pp. 629–33.
- Shizuru, J. A., Negrin, R. S. and Weissman, I. L. (2005) 'Hematopoietic Stem and Progenitor Cells: Clinical and Preclinical Regeneration of the Hematolymphoid System', *Annual Review of Medicine*, 56(1), pp. 509–538. doi: 10.1146/annurev.med.54.101601.152334.
- Shui, C., Riggs, B. L. and Khosla, S. (2002) 'The Immunosuppressant Rapamycin, Alone or with Transforming Growth Factor- β , Enhances Osteoclast Differentiation of RAW264.7 Monocyte-Macrophage Cells in the Presence of RANK-Ligand', *Calcified Tissue International*, 71(5), pp. 437–446. doi: 10.1007/s00223-001-1138-3.
- Shum, L. *et al.* (2003) 'Morphogenesis and dysmorphogenesis of the appendicular skeleton', *Birth Defects Research Part C: Embryo Today: Reviews*, 69(2), pp. 102–122. doi: 10.1002/bdrc.10012.
- Shwartz, Y., Blitz, E. and Zelzer, E. (2013) 'One load to rule them all: Mechanical control of the musculoskeletal system in development and aging', *Differentiation*, 86(3), pp. 104–111. doi: 10.1016/j.diff.2013.07.003.
- Sieburg, H. B. *et al.* (2006) 'Deterministic regulation of hematopoietic stem cell self-renewal and differentiation', *Blood*. American Society of Hematology, 100(4), pp. 1302–1309. doi: 10.1182/blood-2005-07-2970.
- Siffert, R. S. (1951) 'The role of alkaline phosphatase in osteogenesis.', *The Journal of experimental medicine*. The Rockefeller University Press, 93(5), pp. 415–26. doi: 10.1084/jem.93.5.415.
- da Silva Correia, J. *et al.* (2001) 'Lipopolysaccharide Is in Close Proximity to Each of the Proteins in Its Membrane Receptor Complex', *Journal of Biological Chemistry*, 276(24), pp. 21129–

21135. doi: 10.1074/jbc.M009164200.

Siminovitch, L., McCulloch, E. A. and Till, J. E. (1963) 'The Distribution of Colony-Forming Cells Among Spleen Colonies.', *Journal of cellular and comparative physiology*, 62, pp. 327–36.

Simmons, C. S. *et al.* (2011) 'Integrated strain array for cellular mechanobiology studies', *Journal of Micromechanics and Microengineering*, 21(5), p. 054016. doi: 10.1088/0960-1317/21/5/054016.

Simmons, P. J. and Torok-Storb, B. (1991) 'Identification of stromal cell precursors in human bone marrow by a novel monoclonal antibody, STRO-1.', *Blood*, 78(1), pp. 55–62.

Singh, S., Kumar, D. and Sharma, N. R. (2014) 'Role of hyaluronic Acid in early diagnosis of knee osteoarthritis.', *Journal of clinical and diagnostic research : JCDR*. JCDR Research & Publications Private Limited, 8(12), pp. LC04-7. doi: 10.7860/JCDR/2014/11732.5342.

Siyam, A. *et al.* (2012) 'Nuclear localization of DMP1 proteins suggests a role in intracellular signaling', *Biochemical and Biophysical Research Communications*. NIH Public Access, 424(3), pp. 641–646. doi: 10.1016/j.bbrc.2012.07.037.

Sly, L. M. *et al.* (2004) 'LPS-Induced Upregulation of SHIP Is Essential for Endotoxin Tolerance', *Immunity*, 21(2), pp. 227–239. doi: 10.1016/j.immuni.2004.07.010.

Smith, E. J. *et al.* (2004) 'Transient Retention of Endochondral Cartilaginous Matrix With Bisphosphonate Treatment in a Long-Term Rabbit Model of Distraction Osteogenesis', *Journal of Bone and Mineral Research*, 19(10), pp. 1698–1705. doi: 10.1359/JBMR.040709.

Sneddon, L. U., Halsey, L. G. and Bury, N. R. (2017) 'Considering aspects of the 3Rs principles within experimental animal biology', *Journal of Experimental Biology*. The Company of Biologists Ltd, 220(17), pp. 3007–3016. doi: 10.1242/JEB.147058.

Sniadecki, N. J. *et al.* (2008) 'Magnetic microposts for mechanical stimulation of biological cells: fabrication, characterization, and analysis.', *The Review of scientific instruments*. American Institute of Physics, 79(4), p. 044302. doi: 10.1063/1.2906228.

Solitro, A. R. and Mackeigan, J. P. (2016) 'Leaving the lysosome behind: Novel developments in autophagy inhibition', *Future Medicinal Chemistry*. doi: 10.4155/fmc.15.166.

Šoltés, L. *et al.* (2006) 'Degradative action of reactive oxygen species on hyaluronan', *Biomacromolecules*, 7(3), pp. 659–668. doi: 10.1021/bm050867v.

Song, I.-H., Caplan, A. I. and Dennis, J. E. (2009) 'In vitro dexamethasone pretreatment enhances bone formation of human mesenchymal stem cells in vivo.', *Journal of orthopaedic research : official publication of the Orthopaedic Research Society*, 27(7), pp. 916–21. doi: 10.1002/jor.20838.

Sørensen, M. G. *et al.* (2007) 'Characterization of osteoclasts derived from CD14+ monocytes isolated from peripheral blood', *Journal of Bone and Mineral Metabolism*. Springer-Verlag, 25(1), pp. 36–45. doi: 10.1007/s00774-006-0725-9.

Souza, P. P. C. and Lerner, U. H. (2019) 'Finding a Toll on the Route: The Fate of Osteoclast Progenitors After Toll-Like Receptor Activation', *Frontiers in Immunology*. doi: 10.3389/fimmu.2019.01663.

Spangrude, G., Heimfeld, S. and Weissman, I. (1988) 'Purification and characterization of mouse hematopoietic stem cells', *Science*. American Association for the Advancement of Science, 241(4861), pp. 58–62. doi: 10.1126/science.2898810.

Stanley, E. R., Chen, D.-M. and Lin, H.-S. (1978) 'Induction of macrophage production and proliferation by a purified colony stimulating factor', *Nature*. Nature Publishing Group,

274(5667), pp. 168–170. doi: 10.1038/274168a0.

Stark, R. J. *et al.* (2016) 'Endothelial cell tolerance to lipopolysaccharide challenge is induced by monophosphoryl lipid A', *Clinical Science*, 130(6), pp. 451–461. doi: 10.1042/CS20150592.

Stefansson, S. *et al.* (1995) 'gp330 on type II pneumocytes mediates endocytosis leading to degradation of pro-urokinase, plasminogen activator inhibitor-1 and urokinase-plasminogen activator inhibitor-1 complex.', *Journal of cell science*, 108 (Pt 6), pp. 2361–8.

Stern, R., Asari, A. A. and Sugahara, K. N. (2006) 'Hyaluronan fragments: An information-rich system', *European Journal of Cell Biology*. Urban & Fischer, 85(8), pp. 699–715. doi: 10.1016/J.EJCB.2006.05.009.

Strydom, H. *et al.* (2012) 'The oxytalan fibre network in the periodontium and its possible mechanical function', *Archives of Oral Biology*. doi: 10.1016/j.archoralbio.2012.06.003.

Su, P. *et al.* (2018) 'Mesenchymal Stem Cell Migration during Bone Formation and Bone Diseases Therapy', *International Journal of Molecular Sciences*, 19(8), p. 2343. doi: 10.3390/ijms19082343.

Sumanasinghe, R. D., Bernacki, S. H. and Lobo, E. G. (2006) 'Osteogenic Differentiation of Human Mesenchymal Stem Cells in Collagen Matrices: Effect of Uniaxial Cyclic Tensile Strain on Bone Morphogenetic Protein (BMP-2) mRNA Expression', *Tissue Engineering*, 12(12), pp. 3459–3465. doi: 10.1089/ten.2006.12.3459.

Sun, W. *et al.* (2019) 'The mechanosensitive Piezo1 channel is required for bone formation', *eLife*. doi: 10.7554/eLife.47454.

Sun, Y.-L. *et al.* (2004) 'Stretching type II collagen with optical tweezers', *Journal of Biomechanics*, 37(11), pp. 1665–1669. doi: 10.1016/j.jbiomech.2004.02.028.

Swift, J. *et al.* (2013) 'Nuclear Lamin-A Scales with Tissue Stiffness and Enhances Matrix-Directed Differentiation', *Science*, 341(6149), pp. 1240104–1240104. doi: 10.1126/science.1240104.

Swirski, F. K. *et al.* (2009) 'Identification of splenic reservoir monocytes and their deployment to inflammatory sites.', *Science (New York, N.Y.)*. NIH Public Access, 325(5940), pp. 612–6. doi: 10.1126/science.1175202.

Szilvassy, S. J. *et al.* (1990) 'Quantitative assay for totipotent reconstituting hematopoietic stem cells by a competitive repopulation strategy.', *Proceedings of the National Academy of Sciences of the United States of America*. National Academy of Sciences, 87(22), pp. 8736–40.

Takahashi, M. *et al.* (2017) 'Magnetic Separation of Autophagosomes from Mammalian Cells Using Magnetic-Plasmonic Hybrid Nanobeads', *ACS Omega*. doi: 10.1021/acsomega.7b00929.

Takahashi, N. *et al.* (1988) 'Osteoclast-Like Cell Formation and its Regulation by Osteotropic Hormones in Mouse Bone Marrow Cultures*', *Endocrinology*, 122(4), pp. 1373–1382. doi: 10.1210/endo-122-4-1373.

Takahashi, W. *et al.* (2013) 'Kinetics and protective role of autophagy in a mouse cecal ligation and puncture-induced sepsis', *Critical Care*. doi: 10.1186/cc12839.

Takayanagi, H. *et al.* (2002) 'Induction and activation of the transcription factor NFATc1 (NFAT2) integrate RANKL signaling in terminal differentiation of osteoclasts.', *Developmental cell*, 3(6), pp. 889–901.

Tammi, R. H. *et al.* (2011) 'Transcriptional and post-translational regulation of hyaluronan synthesis', *FEBS Journal*, 278(9), pp. 1419–1428. doi: 10.1111/j.1742-4658.2011.08070.x.

- Tanabe, F. *et al.* (2011) 'Accumulation of p62 in degenerated spinal cord under chronic mechanical compression', *Autophagy*, 7(12), pp. 1462–1471. doi: 10.4161/auto.7.12.17892.
- Tanida, I. *et al.* (2005) 'Lysosomal Turnover, but Not a Cellular Level, of Endogenous LC3 is a Marker for Autophagy', *Autophagy*, 1(2), pp. 84–91. doi: 10.4161/auto.1.2.1697.
- Tare, R. S. *et al.* (2008) 'Skeletal stem cells: Phenotype, biology and environmental niches informing tissue regeneration', *Molecular and Cellular Endocrinology*, 288(1–2), pp. 11–21. doi: 10.1016/j.mce.2008.02.017.
- Tearney, G. J. *et al.* (2003) 'Quantification of macrophage content in atherosclerotic plaques by optical coherence tomography.', *Circulation*, 107(1), pp. 113–9.
- Termeer, C. *et al.* (2002) 'Oligosaccharides of Hyaluronan activate dendritic cells via toll-like receptor 4.' Rockefeller University Press, 195(1), pp. 99–111.
- Termeer, C., Sleeman, J. P. and Simon, J. C. (2003) 'Hyaluronan – magic glue for the regulation of the immune response?', *Trends in Immunology*. Elsevier Current Trends, 24(3), pp. 112–114. doi: 10.1016/S1471-4906(03)00029-2.
- Tevlin, R. *et al.* (2014) 'Osteoclast Derivation from Mouse Bone Marrow', *Journal of Visualized Experiments*. MyJoVE Corporation, (93), p. e52056. doi: 10.3791/52056.
- 'The number of adults seeking orthodontic treatment in the UK continues to rise' (2018) *British dental journal*. NLM (Medline), p. 847. doi: 10.1038/sj.bdj.2018.455.
- Tichomirowa, M. *et al.* (2005) 'Bacterial Endotoxin (lipopolysaccharide) Stimulates Interleukin-6 Production and Inhibits Growth of Pituitary Tumour Cells Expressing the Toll-Like Receptor 4', *Journal of Neuroendocrinology*, 17(3), pp. 152–160. doi: 10.1111/j.1365-2826.2005.01286.x.
- Till, J. E. and McCulloch, E. A. (1961) 'A Direct Measurement of the Radiation Sensitivity of Normal Mouse Bone Marrow Cells', *Radiation Research*. Radiation Research Society, 14(2), p. 213. doi: 10.2307/3570892.
- Tobias, P. S., Soldau, K. and Ulevitch, R. J. (1986) 'Isolation of a lipopolysaccharide-binding acute phase reactant from rabbit serum.', *The Journal of experimental medicine*, 164(3), pp. 777–93.
- Toma, C. D. *et al.* (1997) 'Signal Transduction of Mechanical Stimuli Is Dependent on Microfilament Integrity: Identification of Osteopontin as a Mechanically Induced Gene in Osteoblasts', *Journal of Bone and Mineral Research*, 12(10), pp. 1626–1636. doi: 10.1359/jbmr.1997.12.10.1626.
- Tomokiyo, A., Wada, N. and Maeda, H. (2019) 'Periodontal Ligament Stem Cells: Regenerative Potency in Periodontium', *Stem Cells and Development*, 28(15), pp. 974–985. doi: 10.1089/scd.2019.0031.
- Tondon, A. and Kaunas, R. (2014) 'The direction of stretch-induced cell and stress fiber orientation depends on collagen matrix stress.' Public Library of Science, 9(2), p. e89592.
- Toole, B. P. (2001) 'Hyaluronan in morphogenesis', *Seminars in Cell & Developmental Biology*, 12(2), pp. 79–87. doi: 10.1006/scdb.2000.0244.
- Toole, B. P. *et al.* (2005) 'Hyaluronan: A Critical Component of Epithelial-Mesenchymal and Epithelial-Carcinoma Transitions', *Cells Tissues Organs*, 179(1–2), pp. 66–72. doi: 10.1159/000084510.
- Toole, B. P., Ghatak, S. and Misra, S. (2008) 'Hyaluronan oligosaccharides as a potential anticancer therapeutic.', *Current pharmaceutical biotechnology*, 9(4), pp. 249–52.

- Törrönen, K. *et al.* (2014) 'Tissue distribution and subcellular localization of hyaluronan synthase isoenzymes', *Histochemistry and Cell Biology*, 141(1), pp. 17–31. doi: 10.1007/s00418-013-1143-4.
- Toyosawa, S. *et al.* (2004) 'mRNA expression and protein localization of dentin matrix protein 1 during dental root formation', *Bone*. doi: 10.1016/j.bone.2003.08.010.
- Treiser, M. D. *et al.* (2010) 'Cytoskeleton-based forecasting of stem cell lineage fates', *Proceedings of the National Academy of Sciences of the United States of America*. doi: 10.1073/pnas.0909597107.
- Triantafilou, M., Triantafilou, K. and Fernandez, N. (2000) 'Rough and smooth forms of fluorescein-labelled bacterial endotoxin exhibit CD14/LBP dependent and independent binding that is influenced by endotoxin concentration.', *European journal of biochemistry*, 267(8), pp. 2218–26.
- Trubiani, O. *et al.* (2019) 'Periodontal Ligament Stem Cells: Current Knowledge and Future Perspectives', *Stem Cells and Development*, 28(15), pp. 995–1003. doi: 10.1089/scd.2019.0025.
- Tsuda, H. *et al.* (2010) 'Butyrate, a bacterial metabolite, induces apoptosis and autophagic cell death in gingival epithelial cells', *Journal of Periodontal Research*. doi: 10.1111/j.1600-0765.2010.01277.x.
- Tsutsumi, S. *et al.* (2001) 'Retention of Multilineage Differentiation Potential of Mesenchymal Cells during Proliferation in Response to FGF', *Biochemical and Biophysical Research Communications*, 288(2), pp. 413–419. doi: 10.1006/bbrc.2001.5777.
- Uchida, N. *et al.* (1993) 'Heterogeneity of hematopoietic stem cells.', *Current opinion in immunology*, 5(2), pp. 177–84.
- Valenti, M. T., Dalle Carbonare, L. and Mottes, M. (2016) 'Role of autophagy in bone and muscle biology.', *World journal of stem cells*. Baishideng Publishing Group Inc, 8(12), pp. 396–398. doi: 10.4252/wjsc.v8.i12.396.
- Vázquez, P. *et al.* (2012) 'Atg5 and Ambra1 differentially modulate neurogenesis in neural stem cells', *Autophagy*, 8(2), pp. 187–199. doi: 10.4161/auto.8.2.18535.
- Vergadi, E., Vaporidi, K. and Tsatsanis, C. (2018) 'Regulation of Endotoxin Tolerance and Compensatory Anti-inflammatory Response Syndrome by Non-coding RNAs', *Frontiers in Immunology*, 9. doi: 10.3389/fimmu.2018.02705.
- Verreck, F. A. W. *et al.* (2004) 'Human IL-23-producing type 1 macrophages promote but IL-10-producing type 2 macrophages subvert immunity to (myco)bacteria', *Proceedings of the National Academy of Sciences*, 101(13), pp. 4560–4565. doi: 10.1073/pnas.0400983101.
- Vesprey, A. and Yang, W. (2016) 'Pit Assay to Measure the Bone Resorptive Activity of Bone Marrow-derived Osteoclasts.', *Bio-protocol*. NIH Public Access, 6(12). doi: 10.21769/BioProtoc.1836.
- Vessoni, A. T., Muotri, A. R. and Okamoto, O. K. (2012) 'Autophagy in Stem Cell Maintenance and Differentiation', *Stem Cells and Development*, 21(4), pp. 513–520. doi: 10.1089/scd.2011.0526.
- Vidoni, C. *et al.* (2019) 'Autophagy drives osteogenic differentiation of human gingival mesenchymal stem cells', *Cell Communication and Signaling*. doi: 10.1186/s12964-019-0414-7.
- Vigetti, D. *et al.* (2010) 'Proinflammatory Cytokines Induce Hyaluronan Synthesis and Monocyte Adhesion in Human Endothelial Cells through Hyaluronan Synthase 2 (HAS2) and the Nuclear Factor- κ B (NF- κ B) Pathway', *Journal of Biological Chemistry*, 285(32), pp. 24639–

24645. doi: 10.1074/jbc.M110.134536.

Vigetti, D. *et al.* (2011) 'Hyaluronan synthesis is inhibited by adenosine monophosphate-activated protein kinase through the regulation of HAS2 activity in human aortic smooth muscle cells', *Journal of Biological Chemistry*. doi: 10.1074/jbc.M110.193656.

Vigetti, D., Karousou, E., *et al.* (2014) 'Hyaluronan: Biosynthesis and signaling', *Biochimica et Biophysica Acta (BBA) - General Subjects*, 1840(8), pp. 2452–2459. doi: 10.1016/j.bbagen.2014.02.001.

Vigetti, D., Viola, M., *et al.* (2014) 'Metabolic control of hyaluronan synthases', *Matrix Biology*. doi: 10.1016/j.matbio.2013.10.002.

Viti, F. *et al.* (2016) 'Osteogenic Differentiation of MSC through Calcium Signaling Activation: Transcriptomics and Functional Analysis.', *PloS one*. Public Library of Science, 11(2), p. e0148173. doi: 10.1371/journal.pone.0148173.

Wada, N. *et al.* (2009) 'Immunomodulatory properties of human periodontal ligament stem cells', *Journal of Cellular Physiology*. doi: 10.1002/jcp.21710.

Wada, S. *et al.* (2017) 'Novel device for application of continuous mechanical tensile strain to mammalian cells', *Biology Open*, 6(4), pp. 518–524. doi: 10.1242/bio.023671.

Wan, S. X. *et al.* (2016) 'Ghrelin protects small intestinal epithelium against sepsis-induced injury by enhancing the autophagy of intestinal epithelial cells', *Biomedicine and Pharmacotherapy*. doi: 10.1016/j.biopha.2016.08.048.

Wang, A. *et al.* (2011) *Hyaluronan matrices in pathobiological processes*, *FEBS Journal*. doi: 10.1111/j.1742-4658.2011.08069.x.

Wang, A. *et al.* (2014) 'Heparin prevents intracellular hyaluronan synthesis and autophagy responses in hyperglycemic dividing mesangial cells and activates synthesis of an extensive extracellular monocyte-adhesive hyaluronan matrix after completing cell division', *Journal of Biological Chemistry*. doi: 10.1074/jbc.M113.541441.

Wang, K. *et al.* (2011) 'Osteoclast precursor differentiation by MCP1P via oxidative stress, endoplasmic reticulum stress, and autophagy', *Journal of Molecular Cell Biology*. doi: 10.1093/jmcb/mjr021.

Wang, N. *et al.* (2001) 'Mechanical behavior in living cells consistent with the tensegrity model', *Proceedings of the National Academy of Sciences*, 98(14), pp. 7765–7770. doi: 10.1073/pnas.141199598.

Wang, N., Liang, H. and Zen, K. (2014) 'Molecular Mechanisms That Influence the Macrophage M1 to M2 Polarization Balance', *Frontiers in Immunology*, 5, p. 614. doi: 10.3389/fimmu.2014.00614.

Wang, T. *et al.* (2019) 'Autophagy: A Promising Target for Age-related Osteoporosis', *Current Drug Targets*, 20(3), pp. 354–365. doi: 10.2174/1389450119666180626120852.

Wani, M. R. *et al.* (1999) 'Prostaglandin E2 cooperates with TRANCE in osteoclast induction from hemopoietic precursors: Synergistic activation of differentiation, cell spreading, and fusion', *Endocrinology*. Oxford University Press, 140(4), pp. 1927–1935. doi: 10.1210/endo.140.4.6647.

Warshawsky, H. *et al.* (1981) 'The development of enamel structure in rat incisors as compared to the teeth of monkey and man', *The Anatomical Record*, 200(4), pp. 371–399. doi: 10.1002/ar.1092000402.

Watanabe, M. *et al.* (2005) 'Progressive degeneration of stereocilia in cochlear hair cells in

hearing-impaired kuru2 mice', *In Vivo*, 19(4), pp. 675–682.

Watson, J. and Riblet, R. (1974) 'Genetic control of responses to bacterial lipopolysaccharides in mice. I. Evidence for a single gene that influences mitogenic and immunogenic responses to lipopolysaccharides.', *The Journal of experimental medicine*, 140(5), pp. 1147–61.

Watson, J. and Riblet, R. (1975) 'Genetic control of responses to bacterial lipopolysaccharides in mice. II. A gene that influences a membrane component involved in the activation of bone marrow-derived lymphocytes by lipopolysaccharides.', *Journal of immunology (Baltimore, Md. : 1950)*, 114(5), pp. 1462–8.

Weigel, P. H. and Baggenstoss, B. A. (2017) 'What is special about 200 kDa hyaluronan that activates hyaluronan receptor signaling?', *Glycobiology*. Narnia, 27(9), pp. 868–877. doi: 10.1093/glycob/cwx039.

Wentowski, C., Mewada, N. and Nielsen, N. D. (2019) 'Sepsis in 2018: a review', *Anaesthesia & Intensive Care Medicine*. Elsevier, 20(1), pp. 6–13. doi: 10.1016/J.MPAIC.2018.11.009.

West, D. *et al.* (1985) 'Angiogenesis induced by degradation products of hyaluronic acid', *Science*. American Association for the Advancement of Science, 228(4705), pp. 1324–1326. doi: 10.1126/SCIENCE.2408340.

West, M. A. and Koons, A. (2008) 'Endotoxin Tolerance in Sepsis: Concentration-Dependent Augmentation or Inhibition of LPS-Stimulated Macrophage TNF Secretion by LPS Pretreatment', *The Journal of Trauma: Injury, Infection, and Critical Care*, 65(4), pp. 893–900. doi: 10.1097/TA.0b013e3181877fde.

Wheeler-Jones, C. P. D., Farrar, C. E. and Pitsillides, A. A. (2010) 'Targeting hyaluronan of the endothelial glycocalyx for therapeutic intervention.', *Current opinion in investigational drugs (London, England : 2000)*, 11(9), pp. 997–1006.

Whitfield, C., Amor, P. A. and Köplin, R. (1997) 'Modulation of the surface architecture of gram-negative bacteria by the action of surface polymer:lipid A-core ligase and by determinants of polymer chain length.', *Molecular microbiology*, 23(4), pp. 629–38.

Widdrington, J. D. *et al.* (2018) 'Exposure of Monocytic Cells to Lipopolysaccharide Induces Coordinated Endotoxin Tolerance, Mitochondrial Biogenesis, Mitophagy, and Antioxidant Defenses', *Frontiers in immunology*. doi: 10.3389/fimmu.2018.02217.

Wiebe, S. H. *et al.* (1996) 'Osteoclast activation in inflammatory periodontal diseases.', *Oral diseases*, 2(2), pp. 167–80.

Wiktor-Jedrzejczak, W. and Gordon, S. (1996) 'Cytokine regulation of the macrophage (M phi) system studied using the colony stimulating factor-1-deficient op/op mouse', *Physiological Reviews*, 76(4), pp. 927–947. doi: 10.1152/physrev.1996.76.4.927.

Wilson, C. S. *et al.* (1997) 'In Vivo Endotoxin Tolerance: Impaired LPS-Stimulated TNF Release of Monocytes from Patients with Sepsis, but Not SIRS', *Journal of Surgical Research*, 69(1), pp. 101–106. doi: 10.1006/jsre.1997.5040.

Wise, G. (2009) 'Cellular and molecular basis of tooth eruption', *Orthodontics & Craniofacial Research*, 12(2), pp. 67–73. doi: 10.1111/j.1601-6343.2009.01439.x.

Wise, G. E. and King, G. J. (2008) 'Mechanisms of tooth eruption and orthodontic tooth movement.', *Journal of dental research*, 87(5), pp. 414–34. doi: 10.1177/154405910808700509.

Wishney, M. (2017) 'Potential risks of orthodontic therapy: a critical review and conceptual framework', *Australian Dental Journal*. doi: 10.1111/adj.12486.

- Wittkowske, C. *et al.* (2016) 'In Vitro Bone Cell Models: Impact of Fluid Shear Stress on Bone Formation.', *Frontiers in bioengineering and biotechnology*. Frontiers Media SA, 4, p. 87. doi: 10.3389/fbioe.2016.00087.
- Wongkhantee, S., Yongchaitrakul, T. and Pavasant, P. (2007) 'Mechanical Stress Induces Osteopontin Expression in Human Periodontal Ligament Cells Through Rho Kinase', *Journal of Periodontology*, 78(6), pp. 1113–1119. doi: 10.1902/jop.2007.060433.
- Wright, S. D. *et al.* (1990) 'CD14, a receptor for complexes of lipopolysaccharide (LPS) and LPS binding protein.', *Science (New York, N.Y.)*, 249(4975), pp. 1431–3.
- Wu, Q. and Chen, Q. (2000) 'Mechanoregulation of Chondrocyte Proliferation, Maturation, and Hypertrophy: Ion-Channel Dependent Transduction of Matrix Deformation Signals', *Experimental Cell Research*, 256(2), pp. 383–391. doi: 10.1006/excr.2000.4847.
- Wu, Y. T. *et al.* (2010) 'Dual role of 3-methyladenine in modulation of autophagy via different temporal patterns of inhibition on class I and III phosphoinositide 3-kinase', *Journal of Biological Chemistry*. American Society for Biochemistry and Molecular Biology, 285(14), pp. 10850–10861. doi: 10.1074/jbc.M109.080796.
- Wu, Y. T. and Adnan, A. (2018) 'Damage and Failure of Axonal Microtubule under Extreme High Strain Rate: An In-Silico Molecular Dynamics Study', *Scientific Reports*. doi: 10.1038/s41598-018-29804-w.
- Xaus, J. *et al.* (2000) 'LPS induces apoptosis in macrophages mostly through the autocrine production of TNF-alpha.', *Blood*, 95(12), pp. 3823–31.
- Xiong, Y. *et al.* (2011) 'Endotoxin tolerance impairs IL-1 receptor-associated kinase (IRAK) 4 and TGF-beta-activated kinase 1 activation, K63-linked polyubiquitination and assembly of IRAK1, TNF receptor-associated factor 6, and IkappaB kinase gamma and increases A20 expression.', *The Journal of biological chemistry*. American Society for Biochemistry and Molecular Biology, 286(10), pp. 7905–16. doi: 10.1074/jbc.M110.182873.
- Xiong, Y. and Medvedev, A. E. (2011) 'Induction of endotoxin tolerance in vivo inhibits activation of IRAK4 and increases negative regulators IRAK-M, SHIP-1, and A20', *Journal of Leukocyte Biology*. The Society for Leukocyte Biology, 90(6), pp. 1141–1148. doi: 10.1189/jlb.0611273.
- Xu, C. *et al.* (2015) 'Hyaluronan ameliorates LPS-induced acute lung injury in mice via Toll-like receptor (TLR) 4-dependent signaling pathways', *International Immunopharmacology*. doi: 10.1016/j.intimp.2015.08.021.
- Xu, H. *et al.* (2014) 'Autophagy protects end plate chondrocytes from intermittent cyclic mechanical tension induced calcification', *Bone*, 66, pp. 232–239. doi: 10.1016/j.bone.2014.06.018.
- Xu, H. *et al.* (2018) 'PKR inhibition mediates endotoxin tolerance in macrophages through inactivation of PI3K/AKT signaling', *Molecular Medicine Reports*, 17(6), pp. 8548–8556. doi: 10.3892/mmr.2018.8869.
- Xu, J., Tseng, Y. and Wirtz, D. (2000) 'Strain hardening of actin filament networks: Regulation by the dynamic cross-linking protein α -actinin', *Journal of Biological Chemistry*. doi: 10.1074/jbc.M002377200.
- Xu, L. *et al.* (2017) 'Tissue source determines the differentiation potentials of mesenchymal stem cells: a comparative study of human mesenchymal stem cells from bone marrow and adipose tissue', *Stem Cell Research & Therapy*. BioMed Central, 8(1), p. 275. doi: 10.1186/s13287-017-0716-x.

- Xu, Z. *et al.* (2007) 'Toll-like receptor 4 siRNA attenuates LPS-induced secretion of inflammatory cytokines and chemokines by macrophages', *Journal of Infection*, 55(1), pp. e1–e9. doi: 10.1016/j.jinf.2007.01.003.
- Xue, Z. *et al.* (2013) 'Increased mechanical strain imposed on murine lungs during ventilation in vivo depresses airway responsiveness and activation of protein kinase Akt', *Journal of Applied Physiology*, 114(11), pp. 1506–1510. doi: 10.1152/jappphysiol.01460.2012.
- Yamada, M. *et al.* (2019) 'p62/SQSTM1 and Nrf2 are essential for exercise-mediated enhancement of antioxidant protein expression in oxidative muscle', *The FASEB Journal*, 33(7), pp. 8022–8032. doi: 10.1096/fj.201900133R.
- Yamamoto, Tsuneyuki *et al.* (2016) 'Histology of human cementum: Its structure, function, and development', *Japanese Dental Science Review*. doi: 10.1016/j.jdsr.2016.04.002.
- Yan, K. *et al.* (2020) 'A20 inhibits osteoclastogenesis via TRAF6-dependent autophagy in human periodontal ligament cells under hypoxia', *Cell Proliferation*. doi: 10.1111/cpr.12778.
- Yang, R., Yu, T. and Zhou, Y. (2017) 'Interplay between craniofacial stem cells and immune stimulus', *Stem Cell Research & Therapy*. BioMed Central, 8(1), p. 147. doi: 10.1186/S13287-017-0607-1.
- Yang, X. *et al.* (2004) 'ATF4 is a substrate of RSK2 and an essential regulator of osteoblast biology; implication for Coffin-Lowry Syndrome.', *Cell*, 117(3), pp. 387–98.
- Yang, X. and Karsenty, G. (2004) 'ATF4, the Osteoblast Accumulation of Which Is Determined Post-translationally, Can Induce Osteoblast-specific Gene Expression in Non-osteoblastic Cells', *Journal of Biological Chemistry*, 279(45), pp. 47109–47114. doi: 10.1074/jbc.M410010200.
- Yang, Z. and Klionsky, D. J. (2010) 'Eaten alive: a history of macroautophagy.', *Nature cell biology*. NIH Public Access, 12(9), pp. 814–22. doi: 10.1038/ncb0910-814.
- Yao, S. *et al.* (2008) 'Differentiation of stem cells in the dental follicle', *Journal of Dental Research*. doi: 10.1177/154405910808700801.
- Ye, L. *et al.* (2008) 'Periodontal breakdown in the Dmp1 null mouse model of hypophosphatemic rickets', *Journal of Dental Research*. doi: 10.1177/154405910808700708.
- Yin, C. *et al.* (2019) 'ApoE attenuates unresolvable inflammation by complex formation with activated C1q', *Nature Medicine*. Nature Publishing Group, 25(3), pp. 496–506. doi: 10.1038/s41591-018-0336-8.
- Yourek, G., Hussain, M. A. and Mao, J. J. (2007) 'Cytoskeletal changes of mesenchymal stem cells during differentiation', *ASAIO Journal*. doi: 10.1097/MAT.0b013e31802deb2d.
- Ypey, D. L. *et al.* (1992) 'Voltage, calcium, and stretch activated ionic channels and intracellular calcium in bone cells', *Journal of Bone and Mineral Research*, 7(S2), pp. S377–S387. doi: 10.1002/jbmr.5650071404.
- Yuasa, M. *et al.* (2015) 'Dexamethasone enhances osteogenic differentiation of bone marrow- and muscle-derived stromal cells and augments ectopic bone formation induced by bone morphogenetic protein-2.', *PloS one*. Public Library of Science, 10(2), p. e0116462. doi: 10.1371/journal.pone.0116462.
- Zajac, E. *et al.* (2013) 'Angiogenic capacity of M1- and M2-polarized macrophages is determined by the levels of TIMP-1 complexed with their secreted proMMP-9.', *Blood*. American Society of Hematology, 122(25), pp. 4054–67. doi: 10.1182/blood-2013-05-501494.
- Zambon, A. C. (2010) 'Use of the Ki67 promoter to label cell cycle entry in living cells', *Cytometry Part A*, 77(6), pp. 564–570. doi: 10.1002/cyto.a.20890.

- Zanoni, I. *et al.* (2011) 'CD14 controls the LPS-induced endocytosis of toll-like receptor 4', *Cell*. NIH Public Access, 147(4), pp. 868–880. doi: 10.1016/j.cell.2011.09.051.
- Zaric, S. *et al.* (2010) 'Impaired immune tolerance to *Porphyromonas gingivalis* lipopolysaccharide promotes neutrophil migration and decreased apoptosis', *Infection and Immunity*. doi: 10.1128/IAI.00600-10.
- Zhang, G., Liu, W. and Wang, R. (2020) 'Retraction: The role of tantalum nanoparticles in bone regeneration involves the bmp2/smad4/runx2 signaling pathway (Int J Nanomedicine. 2020, 15, (2419–2435)', *International Journal of Nanomedicine*. doi: 10.2147/IJN.S261824.
- Zhang, J. *et al.* (2003) 'Identification of the haematopoietic stem cell niche and control of the niche size', *Nature*, 425(6960), pp. 836–841. doi: 10.1038/nature02041.
- Zhang, J. *et al.* (2012) 'FRS2 α -Mediated FGF Signals Suppress Premature Differentiation of Cardiac Stem Cells Through Regulating Autophagy Activity', *Circulation Research*, 110(4). doi: 10.1161/CIRCRESAHA.111.255950.
- Zhang, Q. *et al.* (2013) 'DAMPs and autophagy: Cellular adaptation to injury and unscheduled cell death', *Autophagy*. doi: 10.4161/auto.23691.
- Zhang, Y. *et al.* (2015) 'Inflamed macrophage microvesicles induce insulin resistance in human adipocytes', *Nutrition & Metabolism*, 12(1), p. 21. doi: 10.1186/s12986-015-0016-3.
- Zhao, N. *et al.* (2016) *Effect of hyaluronic acid in bone formation and its applications in dentistry*, *Journal of Biomedical Materials Research - Part A*. Wiley-Blackwell. doi: 10.1002/jbm.a.35681.
- Zhou, B. *et al.* (2000) 'Identification of the hyaluronan receptor for endocytosis (HARE).', *The Journal of biological chemistry*. American Society for Biochemistry and Molecular Biology, 275(48), pp. 37733–41. doi: 10.1074/jbc.M003030200.
- Zhou, T. *et al.* (2020) 'Piezo1/2 mediate mechanotransduction essential for bone formation through concerted activation of NFAT-YAP1- β -catenin', *eLife*. doi: 10.7554/eLife.52779.
- Zhou, Z. *et al.* (2018) 'Autophagy activation facilitates mechanical stimulation-promoted osteoblast differentiation and ameliorates hindlimb unloading-induced bone loss.', *Biochemical and biophysical research communications*. Academic Press, 498(3), pp. 667–673. doi: 10.1016/j.bbrc.2018.03.040.
- Zhu, W. and Liang, M. (2015) 'Periodontal ligament stem cells: Current status, concerns, and future prospects', *Stem Cells International*. doi: 10.1155/2015/972313.
- Zwolaneck, D. *et al.* (2015) ' β 1 Integrins Mediate Attachment of Mesenchymal Stem Cells to Cartilage Lesions', *BioResearch Open Access*. Mary Ann Liebert, Inc., 4(1), p. 39. doi: 10.1089/BIORES.2014.0055.